Gene expression profiling in primary rat hepatocytes for the prediction of hepatotoxicity

Vom Fachbereich Biologie der Technischen Universität Darmstadt

zur

Erlangung des akademischen Grades

eines Doctor rerum naturalium

genehmigte Dissertation von

Dipl. Ing. (FH) Birthe Lauer

aus Worms

Berichterstatter (1. Referent): Prof. Dr. Paul Layer

Mitberichterstatter (2. Referent): Prof. Dr. Bodo Laube

Externer Referent: PD Dr. Stefan O. Müller

Tag der Einreichung: 27. September 2011

Tag der mündlichen Prüfung: 10. Februar 2012

Darmstadt 2012

D17

“Word of honor”

I assure herewith on my word of honor, that I wrote this thesis by myself. All quotes, whether word by word, or in my own words, have been put in quotation marks or otherwise identified as such. The thesis has not been published any where else or has been presented to any other examination board.

Darmstadt, 27 September 2011,.....

CONTENT

ACKNOWLEDGEMENTS

First I would like to thank Dr. Klaus Krauser, Dr. Stefan O. Müller, and Dr. Phil G. Hewitt for giving me the opportunity to work on this exciting project in the laboratories of Merck Serono Research and to attend scientific conferences and advanced training courses.

My heartfelt thanks to Prof. Dr. P. Layer, Prof. Dr. B. Laube, and the faculty for Biology of the Technische Universität Darmstadt for being open to supervise the graduation of an engineer as well as for intensive discussions and the interest in my work.

I would like to thank Dr. Stefan O. Müller for his scientific support, helpful discussions and for encouraging me to work independently.

I am deeply grateful to Dr. Phil G. Hewitt for his guidance throughout the project, his support and emphathy during frustrating times, and his aversion to the German language which helped me to improve my command of English.

Special thanks to Dr. Gillian Wallace and Dr. Nicky Hewitt for their support during problems with the cell culture and for sharing their enormous knowledge of hepatocytes.

I would like to thank Margret Kling, Yvonne Walter, Bettina von Eiff, and Johanna Sebbel for their technical support in the lab, Claudia Klement for performing the hepatocyte isolation and Jörg Hiller for solving nearly all my computer problems.

I am deeply grateful to Tobias Fuchs, Yasmin Dietz, Christina Schmitt, Germaine Truisi, as well as all previous PhD students for their boundless help and friendship in good times and bad, Gregor Tuschl for introducing me into the world of hepatocytes and Kathleen Boehme and Christina Schmitt for their support of the performance and analysis of gene expression studies. Special thanks to Germaine for laughing and joking even after endless hours in the lab, for her hard work and for dancing with me in the lab on Sunday evenings.

Most of all, I want to thank my parents, my sister, and my grandmother Apollonia for their implicit support and belief in me, Berit for reviewing my thesis, and Andreas for his love, understanding, and boundless encouragement.

ABBREVIATIONS[1]

%	Percentage
ALT	Alanine aminotransferase
AST	Aspartate aminotransferase
(c)DNA	(complementary) Deoxyribonucleic acid
(c)RNA	(complementary) Ribonucleic acid
°C	Centigrade
µ	Micro
3D	Three dimensional
3R's	Reduce, refine, replace
APAP	Acetaminophen
ATP	Adenosine triphosphate
BCRP	Breast cancer resistance protein
BH-Q-value	False discovery rate defined by Benjamini and Hochberg
BSA	Bovine serum albumin
BSEP	Bile salt export pump
Ca	Calcium
c_{max}	Maximum plasma concentration
CO_2	Carbon dioxide
CYP	Cytochrome P-450-dependent monooxygenase
DMSO	Dimethyl sulfoxide
EMA	European Medicines Agency
ER	Endoplasmic reticulum
FA	Free fatty acids
FCS	Fetal calve serum
FDA	Food and Drug Administration
FF	Fenofibrate
g	Gram
GSH	Glutathione
GST	Glutathione-S-transferase
h	Hour
HD	High dose
ICH	International Conference of Harmonization of Technical Requirements for Registration of Pharmaceuticals for Human Use
IPA®	Ingenuity Pathway Analysis
kDa	Kilodaltons
kg	Kilogram
l	Litre
LD	Low dose

[1] Gene symbols and the appropriate gene names are listed in the text or in the gene tables in the appendix and not in the list of appreviations.

M	Molarity
MDR	Multi drug resistance protein
Met	Metformin
min	Minute
ML	Monolayer
MOS	Margin of Safety
mRNA	Messenger Ribonucleic acid
MRP	Multi drug resistance protein
mtDNA	Mitochondrial Deoxyribonucleic acid
MW	Molecular weight
Na	Sodium
NOAEL	No observed adverse effect level
NOEC	No observed effect concentration
NTCP	Sodium/taurocholate cotransporting polypeptide
OAT	Organic anion transporter
OATP	Organic anion transporting protein
OCT	Organic cation transporter
OECD	Organisation for Economic Co-operation and Development
OST	Organic solute transporter
PB1	Perfusion buffer one
PB2	Perfusion buffer two
PBPK	Physiologically based pharmacokinetic
PBS	Phosphate buffered saline
PCA	Principal Components Analysis
PPARα	Peroxisome proliferator-activated receptor alpha
PPARγ	Peroxisome proliferator-activated receptor gamma
ROS	Reactive oxygen species
Rosi	Rosiglitazone
rpm	Rounds per minute
RT	Room temperature
sec	Second
SNP	Single nucleotide polymorphism
SULT	Sulfotransferase
TC10	Toxic concentration killing 10 % of the treated cells
Tro	Troglitazone
TZDs	Thiazolidinediones
UGT	UDP-glucuronosyltransferase
US$	United States of America dollar
VA	Valproic acid
WB	Washing buffer
x g	Times gravity

ABSTRACT

New human pharmaceuticals are required by law to be tested in pre-clinical studies in order to predict any potential drug side effects. However, during the last decade the number of new drug approvals has markedly decreased while the cost of drug development has increased. The reasons for this are twofold: firstly, due to adverse effects in humans which are not predicted by animal studies, leading to the compound's failure in late phases of the development process, and secondly because some drug candidates never reach clinical trials due to intolerable toxic effects in animals. Thus, a need exists for new in vitro assays to be developed which enable the detection of a compound's toxicity prior to animal studies. A better pre-selection of drug candidates could increase the success rate during preclinical trials since very toxic compounds could be excluded from animal tests. Furthermore in vitro tests also provide mechanistic information which supports the interpretation of in vivo observations, as well as play a role in human safety assessment, since these tests could be performed in both animal and human cells.

The present study describes one part of the research activities associated with the project Predict-IV financed by the European Commission. Predict-IV's aim is the development of a non-animal based prediction system for the toxicity of new drugs related to the organs kidney and liver as well as the central nervous system. In the liver work package primary human and rat hepatocytes as well as the human hepatoma cell line HepaRG were treated for 14 days with toxic and non-toxic doses of eleven pharmaceutical reference substances of known in vivo toxicity. After one, three and 14 days, respectively, samples for proteomic, metabolomic, genomic and kinetic analyses were collected.

The genomic endpoint was investigated by performing a whole-genome gene expression analysis with Illumina BeadChips. In the present study the global gene expression profiles of primary rat hepatocytes were interpreted biologically after treatment with seven of the eleven reference compounds to investigate the potential of drug-treated rat primary hepatocytes to reflect the in vivo effects noted in the literature. In this study the pharmaceutical mode of action was distinguished from off-target mechanisms which were discussed in relation to hepatotoxic effects in vivo. In accordance with its pharmaceutical mode of action, the PPARα-agonist Fenofibrate increased the expression of genes involved in lipid metabolism. In addition, genes

were also induced which indicated the formation of oxidative stress and the depletion of glutathione which was considered to be a basic mechanism of Fenofibrate's hepatotoxicity. Similar results were found for EMD335823, supporting the assumption that this withdrawn drug candidate is also a PPARα-agonist. However, the small number of genes deregulated by Valproic acid and Acetaminophen was insufficient to reflect any in vivo effects probably related to cellular treatment with too small doses.

The PPARγ-agonists Troglitazone and Rosiglitazone induced genes which coded for drug-metabolizing enzymes known to oxidize these substances, especially Troglitazone, into reactive potentially cytotoxic metabolites. Additional genes involved in the metabolism of glutathione and the response to oxidative stress, a major toxic mechanism of Troglitazone and Rosiglitazone, were upregulated. Since both compounds pharmacologically act on muscle cells their mode of action could not be reconstructed. Metformin which acts on the liver without causing severe adverse effects was used as negative control. It deregulated a large number of genes but its gene expression profile clearly differed from that of the hepatotoxic compounds.

In the last chapter of this study the genes commonly deregulated by Fenofibrate, EMD335823, Troglitazone, Rosiglitazone and Metformin were discussed. The major part of these genes was involved in lipid metabolism which seemed to be related to the mode of action of the tested compounds since PPARα- and PPARγ-agonists regulate lipid and glucose homeostasis.

In conclusion the whole-genome gene expression profile of drug treated primary rat hepatocytes reflected cellular mechanisms which could explain hepatotoxic effects in vivo. During the next phases of Predict-IV the gene expression profiles of rat and human primary hepatocytes and HepaRG cells treated with all of the eleven reference compounds will be compared. The gene expression profiles of the four reference compounds not discussed in this study will be compared with their protein expression profiles. Additionally, the real cellular concentration of the test compounds and the kinetic of their metabolism will be calculated. Furthermore, species-specific effects as well as the responsiveness of the cell line compared to primary cells will be investigated in order to define the cell system best suited for an early predictive screening system. Finally, genomic and proteomic markers should be defined and validated which could enable the early prediction of new drugs' hepatotoxic potential in future.

ZUSAMMENFASSUNG

Die Prüfung neuer Arzneimittel in präklinischen Studien zur Voraussage potentieller Nebenwirkungen ist gesetzlich vorgeschrieben. In den letzten zehn Jahren sank die Anzahl an neu zugelassenen Wirkstoffen jedoch merklich, während die Kosten für deren Entwicklung anstiegen. Die Gründe hierfür sind zum einen Nebenwirkungen am Menschen, die durch Tierstudien nicht vorhergesagt werden konnten und zum Scheitern der Substanz in späten Entwicklungsphasen führten. Zum anderen gelangten einige Wirkstoffkandidaten aufgrund nicht tolerierbarer toxischer Effekte im Tier erst gar nicht in die klinischen Studien. Daher ist es notwending, in vitro-Tests zu entwickeln, die es ermöglichen, die Toxizität neuer Wirkstoffe vor dem Beginn der Tierstudien zu erkennen. Denn eine bessere Vorauswahl von Wirkstoffkandidaten für die präklinischen Studien könnte deren Erfolgsquote erhöhen, da sehr toxische Stoffe erst gar nicht am Tier getestet würden. Zudem liefern in vitro-Tests mechanistische Informationen, die die Interpretation von Beobachtungen in präklinischen und klinischen Studien unterstützen, da diese Tests mit tierischen und humanen Zellen durchgeführt werden können.

Die vorliegende Dissertation beschreibt einen Teil der Forschungsarbeiten, die im Rahmen des von der Europäischen Union geförderten Projektes Predict-IV durchgeführt wurden. Das Ziel von Predict-IV ist die Entwicklung eines tierversuchs-freien Prädiktionsmodells für die Toxizität neuer pharmazeutischer Wirkstoffe für die Organe Niere und Leber sowie das Zentrale Nervensystem. Im Bereich der Leber wurden primäre Human- und Rattenhepatozyten sowie die humane Hepatomazelllinie HepaRG über 14 Tage mit einer toxischen und einer nicht-toxischen Dosis von elf pharamazeutischen Referenzsubstanzen mit bekannter in vivo Toxizität behandelt. Nach einem, drei bzw. 14 Tagen erfolgte die Probennahme für Proteom- und Metabolomanalysen bzw. genetische und kinetische Untersuchungen.

Die genetischen Analysen wurden mit Hilfe einer globalen Genexpressionsanalyse mit Illumina BeadChips durchgeführt. In der vorliegenden Arbeit wurden die globalen Genexpressionsprofile von primären Rattenhepatozyten biologisch interpretiert, die mit sieben der elf Referenzsubstanzen behandelt worden waren. Das Ziel der Arbeit war, zu untersuchen, inwieweit wirkstoffbehandelte Rattenhepatozyten in der Literatur beschriebene in vivo-Effekte widerspiegeln. Dabei wurde der

pharmakologische Wirkprozess von solchen Effekten abgegrenzt, die im Bezug zu in vivo-Toxizitäten diskutiert wurden.

Der PPARα-Agonist Fenofibrat erhöhte in Korrelation zu dessen pharmakologischen Wirkmechanismus die Expression von Genen, die für Enzyme des Lipidmetabolismus codieren. Zudem wurden Gene induziert, die im Zusammenhang mit oxidativem Stress und Glutathiondepletion stehen, den grundlegenden Mechanismen der Hepatotoxizität von Fenofibrat. Ähnliche Ergebnisse wurden für EMD335823 erzielt, was die Annahme stützt, dass auch dieser gestoppte Wirkstoffkandidat ein PPARα-Agonist ist. Valproinsäure und Acetaminophen deregulierten eine sehr geringe Anzahl von Genen, wodurch eine Rekonstruktion der in vivo-Effekte nicht möglich war. Dies schien in der Behandlung der Zellen mit einer zu geringen Dosis begründet gewesen zu sein.

Die PPARγ-Agonisten Troglitazon und Rosiglitazon induzierten Gene, die für arzneimittel-metabolisierende Enzyme codieren, die speziell Troglitazon zu einem potentiell zytotoxischen Metaboliten oxidieren. Zusätzlich wurde die Expression von Genen erhöht, die in den Glutathionmetabolismus und die Antwort auf oxidativen Stress als Hauptmechanismus der Toxizität von Troglitazon und Rosiglitazon involviert sind. Da beide Substanzen pharmakologisch hauptsächlich in Muskelzellen agieren, konnte ihr Wirkmechanismus nicht rekonstruiert werden. Metformin, das pharmakologisch in der Leber wirkt ohne schwere Nebenwirkungen zu verursachen, wurde als Negativkontrolle benutzt. Es deregulierte eine große Anzahl von Genen. Das Genexpressionsprofil unterschied sich jedoch deutlich von dem der hepatotoxischen Substanzen.

Im letzten Kapitel der vorliegenden Arbeit wurden die durch Fenofibrat, EMD335823, Troglitazon, Rosiglitazon und Metformin gemeinsam deregulierten Gene diskutiert. Der größte Teil dieser Gene war in den Lipidmetabolismus involviert, was mit dem Wirkmechanismus der untersuchten Substanzen zusammenzuhängen schien, da PPARα- und PPARγ-Agonisten den Lipid- und Glucosehaushalt regulieren.

Abschließend kann gesagt werden, dass die globalen Genexpressionsprofile der wirkstoffbehandelten primären Rattenhepatozyten zelluläre Mechanismen widerspiegelten, mit Hilfe derer hepatotoxische in vivo-Effekte erklärt werden können. Innerhalb der nächsten Schritte von Predict-IV werden die Genexpressionsprofile von

primären Ratten- und Humanhepatozyten sowie HepaRG-Zellen verglichen, die mit allen elf Referenzsubstanzen behandelt wurden. Des Weiteren werden die Genexpressionsprofile der vier Substanzen, die in der vorliegenden Arbeit nicht diskutiert wurden, mit den Proteinexpressionsprofilen der behandelten Zellen verglichen werden. Zusätzlich werden die wahren Substanzkonzentrationen in der Zelle sowie die Kinetik des Substanzabbaus gemessen werden. Abschließend werden Speziesunterschiede sowie die Responsivität der HepaRG-Zellen im Vergleich zu den Primärzellen untersucht werden, um herauszufinden, welches Zellkultursystem am besten für den Aufbau eines frühen Screening-Tests geeignet ist. Zudem sollen Marker auf Gen- und Proteinebene gefunden und validiert werden, die in Zukunft die frühe Vorhersage der Hepatotoxizität neuer Wirkstoffkandidaten ermöglichen könnten.

1 Introduction

1.1 Toxicology

The term toxicology has its origin in the Greek words *toxicon* (toxin) and *logos* (science). Modern toxicology is a science which investigates adverse effects of (agro)chemicals, pharmaceuticals, environmental pollutants, additives in food and everyday objects as well as cosmetics on humans and the environment based on the principle that the effect is dependent on the concentration (dose) of the substance acting on. The physician Theophrastus Bombastus von Hohenheim called Paracelsus (1493-1541) was the first one who postulated dose-effect-correlations: *"Was ist das nit gifft ist, alle ding sind gifft, und nichts ohn gifft. Allein die Dosis macht, dass ein ding gifft ist."* [Marquardt 2004] (What is not a poison, all things are poisons and nothing is without poison. Only the dose renders a thing to be a poison.)

With the help of animal studies as well as biochemical and cellular assays experimental toxicologists define the test compound's mode of action and the side effects in correlation to the exposed doses. Parameters like general condition, chemico-clinical markers, organ pathology and lethality are investigated. Then the task of regulatory toxicologists is to estimate the compound's hazard towards chemical workers, consumers, patients and the environment by considering the exposed dose and the risk of exposure. Based on these data (agro)chemicals, food additives, cosmetics and drugs are approved and doses, working concentrations and limits for the daily uptake or emissions are determined [Marquardt 2004].

However, a number of ethical and technical issues arise from the dependence of substance development on animal studies. Firstly, traditional toxicological methods need a large number of animals; therefore, the pharmaceutical industry has acted on the 3R's principle in order to *reduce, refine and replace* animal studies where possible [Russel and Burch 1959]. In this context the total number of used animals is *reduced*, e.g., by an optimized combination of endpoints in one study. *Refinement* includes techniques diminishing pain and stress in the test animals, improved strategies for data analysis and interpretation as well as new biomarkers and test methods providing additional information. Finally, *replacement* means alternative test methods which completely replace animal experiments. Secondly, species-specificity

can decrease the predictive power of animal studies. Some compounds cause human adverse effects which could not be predicted by animal tests and lead to failures of drug candidates in late phases of the drug development process [Olson 1998, Xu 2004, Uetrecht 2008]. Lastly, the European Commission prohibits trading of cosmetics containing compounds which were tested on animals after 11th March 2013 and the new chemical regulation for "Registration, Evaluation and Authorisation of Chemicals" (REACH) dictated the re-testing of thousands of chemicals [ECHA 2011]. In order to conform to these new regulations for an increased number of compounds, the chemical and pharmaceutical industry is forced to develop new non-animal based test strategies for the prediction of human toxicities.

1.2 Drug discovery and development

Hundreds of new drug candidates are tested during the drug discovery phase with biochemical and cellular screening methods. Here the relevant pharmaceutical effects like target binding but also off-target effects like inhibition of necessary physiological functions or induction of drug metabolizing enzymes are investigated. Finally, one definite candidate reaches the first phase of drug development (phase 0; Figure 1.1) where preclinical tests in animals are conducted. Every pharmaceutical compound which is approved for human use has to pass animal and human regulatory tests which are well-defined and required by law. These tests should estimate the risk of the new drug, determine a safe dosage for human treatment and identify drug side effects as well as interactions with other drugs or food very clearly [Kola 2004, Preziosi 2004, Butcher 2005].

During animal studies, the drug candidate's potential to cause acute and chronic toxicity, dermal or ocular sensitization or irritation, adverse effects of the respiratory and cardiovascular system, as well as mutagenicity, teratogenicity and carcinogenicity, is tested. The pharmacokinetic profile is investigated which describes how the drug is taken up (bioavailability), distributed, metabolized and eliminated in an animal's body. Finally the optimal dosage and formulation for the first-in-man studies is determined by extrapolation of the animal data with additional safety factors. Traditional endpoints in preclinical animal tests are histopathological evaluations to detect adverse modifications in different tissues and the measurement

of different parameters in blood and urine like elevated plasma level of liver enzymes [ICH-M3 2009].

Drug candidates which successfully pass the preclinical studies are further tested in healthy human volunteers (phase 1 of clinical trials, Figure 1.1), with a few exceptions; for example in the case of anti-cancer therapies phase 1 trials are directly conducted in cancer patients. Here, the drug effects on the basic functions of the organism (safety) and the human pharmacokinetics are used to determine the maximum tolerable dose.

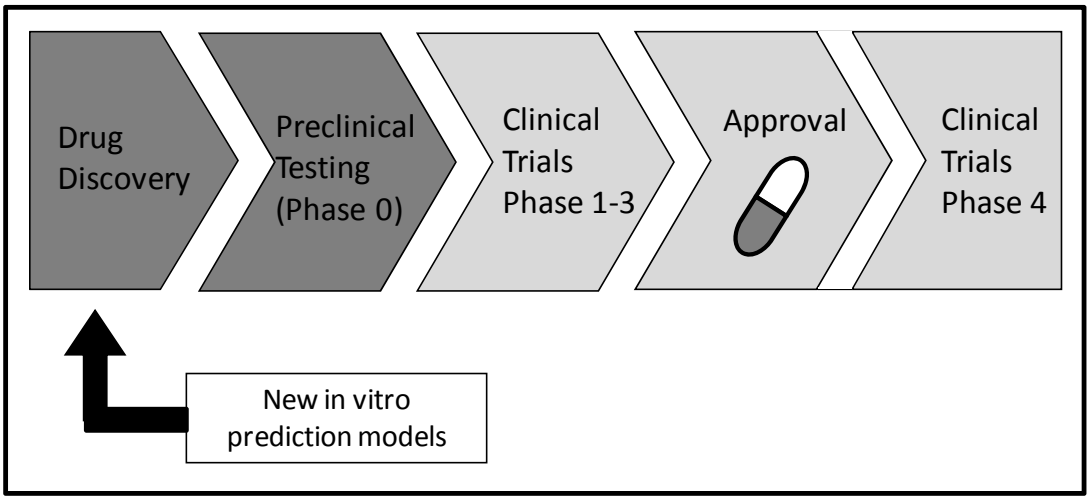

Figure 1.1: The process of drug discovery and development is divided into different phases.
New non-animal based test strategies should support drug discovery to enhance pre-selection of drug candidates for the preclinical phase followed by three clinical trials, drug approval and clinical phase 4.

During clinical phase 2 a small group of patients is treated with the drug candidate in order to validate the expected pharmacological efficacy. Phase 3 clinical studies are performed in comparison to the current standard therapy to show the superiority of the new drug candidate while treatment of a larger population of patients is necessary for statistical reasons [NIH 2011]. Based on the results of these tests, the new drug is approved if its risk-benefit ratio is deemed to be acceptable. Finally, after this long testing process which lasts on average 15 years and costs about US$ 880 million per drug, the new drug is further observed during clinical phase 4 [DiMasi 2003]. Rare clinical side effects are often not seen until this phase when a huge population is treated and can lead to the withdrawal of the drug. The major reasons for withdrawal of already approved drugs are cardiovascular and hepatic adverse effects [Watkins 2011].

Preclinical testing strategies are not always successful in extrapolating animal to human data and in predicting human toxicity which can result in attrition of drug candidates in the late phases of the drug development process [Olson 1998, Xu 2004]. This is especially true for idiosyncratic effects - very rare side effects observed only in a small, susceptible portion of the human population - which are not detected until clinical phase 3 or 4 in most cases [Uetrecht 2008]. As a result, the amount of new drug approvals is decreasing while the costs of drug development are increasing [Mullard 2011]. Much of this attrition happens in the later phases of the drug development process, because earlier tests were not able to fully predict human toxicity. Therefore pharmaceutical companies have reinforced their research in the field of in vitro screening methods to enable a better pre-selection of drug candidates for preclinical studies and to detect a candidate's toxic potential much earlier in the drug development process [Kola 2004, Preziosi 2004, Rawlins 2004, Watkins 2011].

1.3 New testing strategies for non-clinical drug development

Traditional toxicological methods describe changes of organ morphology and measures serum and urine parameter indicating organ damage [Marquardt 2004]. Some of these parameters possess limited organ specificity and sensitivity and are elevated only after a large part of the appropriate organ is already damaged [Muller 2009]. For example, alanine aminotransferase (ALT) and aspartate aminotransferase (AST) are routinely measured serum markers for hepatocellular damage, while alkaline phosphatase (AP) and γ-glutamyl transpeptidase (GGT) are used to detect cholestasis. However, elevated plasma levels of these enzymes can also be caused by extra-hepatic injuries. Other common markers include total bilirubin (hepatobiliary injury) and serum bile acids (general liver damage) which are also influenced by hemolysis and diet, respectively [Ozer 2008].

The US Food and Drug Administration (FDA) and the European Medicines Agency (EMA) recently approved seven urinary protein biomarkers for kidney injury in the rat which were submitted by the Predictive Safety Testing Consortium (PSTC) lead by the non-profit Critical Path Institute (C-Path). These biomarkers can improve renal safety assessment during non-clinical studies due to their higher sensitivity and specificity compared to traditional urine parameters. However, this non-invasive

method refines but does not replace or reduce animal studies. Their use is recommended by the FDA on a voluntary base and the validation for the use in human clinical studies is discussed [C-Path 2008]. Several research groups and consortia including the PSTC [Goodsaid 2007] also work on the establishment of novel biomarkers for hepatotoxicity which are more sensitive and liver specific than traditional ones. The major goal is the discovery of minimally-invasive biomarkers for preclinical and clinical use, which indicate liver injuries before they become irreversible [Halegoua-De Marzio 2008, Amacher 2010]. Therefore new 'omics technologies are used to compare the changes in gene expression (genomics), protein expression (proteomics) and the products of cellular metabolism (metabolomics) to traditional toxicological endpoints [Dieterle 2008]. In the context of the EU-funded project PredTox, the kidneys, livers, blood and urine of drug treated rats were investigated according to this scheme [Suter 2011]. Nevertheless, not a single novel biomarker for hepatotoxicity has been approved by regulatory agencies, so far.

Another current goal of biomarker discovery is the development of novel in vitro-screening methods which enable the elucidation of a compound's mode of action and the prediction of organ-specific toxicities prior to animal tests. These tests can enhance the selection of the best drug candidate for preclinical trials, increase the success rate of regulatory studies and reduce the time and costs of drug development [Butcher 2005, Ukelis 2008, Dash 2009, Schoonen 2009]. The methods performed in the phase of drug discovery (Figure 1.1) prior to animal studies are up to each company's discretion and not required by law. Here, different in vitro animal and human cell-based methods are performed which investigate a compound's potential to induce stress markers (NFκB signaling), DNA damage (p53 signaling), proliferation, GSH- or ATP-depletion, drug transporters, nuclear receptors or CYP-enzymes as indicators of potential for drug-drug interactions [Mueller 2007]. The study in hand, as part of the EU-funded project Predict-IV, (chapter 1.7) supports this field of research in order to refine and reduce animal tests in terms of the 3 R's principle.

1.4 Status quo of alternative methods

Regulatory approved alternative methods for the replacement of animal tests are described in guidelines of the International Conference of Harmonization of Technical Requirements for Registration of Pharmaceuticals for Human Use (ICH) or the Organisation for Economic Co-operation and Development (OECD). ICH and OECD release guidelines for the international preclinical safety testing of pharmaceuticals and the toxicological testing of chemicals, respectively. These regulations are edited permanently related to the necessity of single studies and endpoints. Thus, lethality is no longer a desired endpoint and acute toxicity should not be tested in standalone studies if this information can be derived from other studies [ICH-M3 2009].

ICH has approved different in vitro studies for the testing of genotoxicity; such as the mutation test in bacteria (Ames test) which is predictive for rodent mutagens, the chromosome aberration and micronucleus test (incorrect incorporation of chromosomes or fragments during cell cycle) in mammalian cells and the in vitro gene mutation assay in mouse lymphoma cells. These in vitro tests are approved if they are combined with an in vivo genotoxicity test which is recommended to be integrated into other studies, again to avoid standalone studies which increase the number of animals used. In vitro genotoxicity tests provide additional mechanistical data but they are not sufficient to completely replace in vivo tests since parameters like absorption, distribution, metabolism, and excretion by the animal or human body are missing [ICH-S2 2008].

The Hen's Egg Test - Chorio-Allantoic Membrane (HET-CAM) test - is approved in the European Union for the detection of severe eye irritation. Here, the membrane of a fertilized chicken egg which is rich in blood vessels serves as a surrogate for an eye. Only substances with negative test results have to be re-tested in vivo (Draize test, rabbit eye) for a clear classification [ZEBET25]. OECD has also approved an in vitro test for severe eye irritation using isolated chicken eyes [OECD 438]. But again, substances with negative results also have to be re-tested in vivo.

The OECD validated multi-layer human skin models (EpiDerm™, EPISKIN™) for the testing of skin corrosion [OECD 431] as an alternative to in vivo tests. Reconstructed human epidermis was also approved for the testing of skin irritation [OECD 439]. Furthermore, the 3T3 NRU assay was also accepted for the testing of phototoxicity as a possible drug side effect. During this test, the increased toxic potential of

compounds in UV-light is estimated via the vitality of a treated mouse fibroblast cell line with and without UV-light exposure [OECD 432]. Drugs not administrated orally have to be tested for endotoxins which can cause infections. The appropriate in vivo test was replaced by an in vitro test using an aqueous extract of horseshoe crab blood cells which forms a gel after incubation with endotoxins [ZEBET133]. Other fields of toxicology where the establishment of alternative methods is being fostered include embryotoxicity and teratogenicity. A few non-animal based methods have been validated and regulatory acceptance is pending. One approach monitors the suppression of the differentiation of mouse embryonic stem cells by embryotoxic compounds [ZEBET169].

1.5 Hepatotoxicity

The liver is one of the main target organs of drug-induced toxicities. The physiological principles as well as the major mechanisms of hepatotoxicity are explained in the following.

1.5.1 Morphology and physiology of the liver

The liver is the main organ of the metabolism of endogenous and xenobiotic substances, as well as the largest gland found in vertebrates. The liver contains a complex system of enzymes to produce and secrete proteins like albumin, coagulation factors, apolipoproteins, transferrin, acute phase proteins, and hormones (1) to maintain the xenobiotic metabolism (phase-I, -II, and - III enzymes), (2) to manage large parts of lipid catabolism and (3) to synthesize cholesterol. Furthermore the liver breaks down amino acids and synthesizes urea to detoxify amino acid-derived ammonia. Another essential function of the liver is the production of bile which helps absorb lipids via the intestine and eliminate bilirubin, a product of hemoglobin catabolism which cannot be reused. The liver also stores iron, copper, and vitamins, especially Vitamin A, and stabilizes the blood glucose level by the synthesis and catabolism of glucose and glycogen [Schmidt 2005].

In vertebrates, the liver is divided into four lobes which can be further divided into lobules. Nutrient-laden blood from the intestine reaches the liver via the portal vein.

Endogenous metabolic substances, proteins and, lipoproteins for breakdown enter the liver via the hepatic artery which also provides oxygenated blood. The liver is flushed with 1.5 l blood per minute while ¾ derives from the portal vein which fuses with the hepatic artery after entering the liver (Figure 1.2). The blood flows through the liver capillaries called sinusoids along the hepatocytes, the liver parenchymal cells, which are arranged into cords so that each hepatocyte comes in contact with two sinusoids [Marquardt 2004]. Besides the hepatocytes which build up 78% of the liver's mass and the endothelial (2.8%) cells the organ contains three types of sinusoidal cells: The Kupffer cells (2.1%) are resident macrophages which secrete inflammatory factors and phagocytize bacteria and other substances. Pit cells have an anti-tumor activity and Ito cells (also called stellate cells, 1.4%) store Vitamin A and lipids and play a major role in the development of liver cirrhoses and fibrosis by producing collagen [Blouin 1977, Friedmann 1997]. The blood from all the sinusoids is collected in the liver vein which joins the vena cava (Figure 1.2). The bile produced by the hepatocytes is secreted into intercellular channels called bile canaliculi which fuse to bile ducts that lead the bile into the gall bladder [Marquardt 2004].

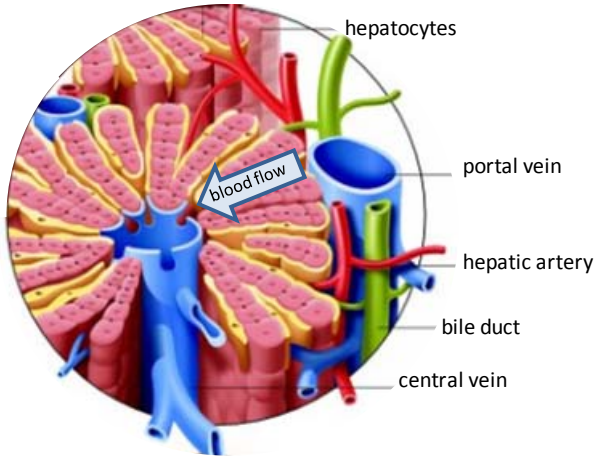

Figure 1.2: Structure of the liver.
In the liver the hepatocytes are arranged into cords. The blood coming from the portal vein flows along the beams into central vein while several substrates are exchanged with the cells. The bile is secreted into bile canaliculi located between the hepatocytes which join in bile ducts [© wissenmedia in the inmedia ONE] GmbH, Gütersloh/Germany, modified].

1.5.2 Hepatocytes and xenobiotic metabolism

The major task of hepatocytes is the maintenance of the liver's metabolic activity. Compared to other cell types in vertebrates hepatocytes contain the same cell organelles like the endoplasmic reticulum (ER) and the Golgi apparatus for protein

biosynthesis including a well-marked rough ER as residence of the Cytochrome-P450-dependent-monooxygenases (CYP), the peroxisomes for the breakdown of long chain fatty acids and mitochondria for the energy production and the breakdown of shorter fatty acids. Hepatocytes are differentiated and therefore highly specialized cells which proliferate very rarely. Around 20% of them contain two nuclei and a fourfold set of chromosomes. Hepatocytes abut on the bile canaliculi (apical/canalicular) with 15% and to the sinusoids (basolateral/sinusoidal) with 70% of their surface. The endothelium of the sinusoids lack a basement membrane and has many pores which allow molecules < 250 kDa to directly diffuse from the blood to the space of Disse, the interstitial space between the endothelium and the hepatocytes. Here an extensive exchange of metabolic products is enabled by passive diffusion via the cell membrane and water pores, pinocytosis, and receptor-mediated endocytosis as well as carrier-mediated diffusion and active transport [Marquardt 2004].

The metabolic activity of the liver enables the elimination of endogenous metabolic products as well as xenobiotica which cannot be used as educts or for energy production to prevent their accumulation in the body. Therefore these substances have to be transformed into a biologically non-reactive and hydrophilic form to facilitate their excretion via bile or urine without damaging endogenous material. The liver holds a broad spectrum of different enzymes covering a wide range of substrate specificities to be able to metabolize new and unknown compounds. The xenobiotic metabolism is divided into three phases: functionalisation (phase-I), conjugation (phase-II) and excretion (phase-III).

Table 1.1: Overview of the major classes of xenobiotic metabolizing enzymes.
Phase-I enzymes activate their substrates for the conjugation reaction in phase-II where water soluble endogenous compounds are covalently bound to the phase-I-metabolite [Marquardt 2004].

Phase-I enzymes	Phase-II enzymes
Cytochrome-P450-dependent monooxygenases (CYP)	Glutathiontransferases (GST)
Flavin-dependent monooxygenases	UDP-glucuronosyltransferases (UGT)
Monoaminoxidases	Sulfotransferases (SULT)
Cyclooxygenases	Acetyltransferases
Alcohol- and Aldehyde dehydrogenases (ADH, ALDH)	Aminoacyltransferases
Esterases	Methyltransferases
Epoxidhydrolases	
Hydrolases	

Phase-I enzymes (Table 1.1) transform apolar, lipophilic substances into more polar and hydrophilic ones. By oxidation, reduction or hydrolysis the appropriate enzyme introduces new chemically functional groups into the molecule which act as targets during phase-II reactions. The major group of phase-I enzymes are the CYPs which are related to their amino acid sequence organized into different families (ongoing numbered starting with one) and subfamilies (named with capitals from A-Z) while the different isoenzymes of one subfamiliy are again ongoing numbered starting with one. The major human CYPs involved in xenobiotic metabolism are CYP1A2, CYP2A6, CYP2B6, CYP2C8, CYP2C9, CYP2C19, CYP2D6, CYP2E1, CYP3A4 [FDA 2004]. CYPs of different species are evolutionarily related and their sequences are very similar. Therefore most human CYPs have orthologs in other species like, e.g., rodents and inducers, inhibitors as well as substrates are often but not always comparable (Table 1.2).

Table 1.2: Inducers and substrates of the major CYPs in human and rat.
CYP-inducers and -substrates are often comparable between human and rat [Hewitt 2007].
BNF = β-Naphthoflavone, Dex = Dexamethasone, 3MC = 3-Methylcholantrene, OM = Omeprazole, Pac = Paclitaxal, PB = Phenobarbitone, Rif = Rifampicine, Testo = Testosterone, Tol = Tolbutamide

CYP-family		Human	Rat
1A	CYP-isoform:	1A1/2	1A1/2
	Inducer:	OM, BNF, 3MC	PB, BNF, 3MC
	Substrate:	Phenacetin	Phenacetin
2C	CYP-isoform:	2C8/9/18/19	2C6/11
	Inducer:	Rif, PB	Dex
	Substrate:	Pac, Tol, Diclo	Diclo, Testo
3A	CYP-isoform:	3A4/5	3A1/2
	Inducer:	Rif	Dex, PB
	Substrate:	Testo, Midazolam	Testo, Midazolam
4A	CYP-isoform:	4A9/11	4A1/2/3/8
	Inducer:	Clofibrate	Clofibrate
	Substrate:	Lauric acid	Lauric acid

Phase-I biotransformation carries the risk of generating strong electrophilic metabolites which react with endogen nucleophiles like proteins or nucleic acids before they can be further metabolized in phase-II (Figure 1.3). So per se non toxic and chemically inert drugs could be transformed into very reactive hepatotoxic metabolites. Phase-I metabolites are conjugated by phase-II enzymes (Table 1.1) with endogenous water soluble components like glutathione (GSH), glucuronic acid or sulfonyl groups to increase their water solubility. The resulting phase-II metabolites

are then excreted into the bile canaliculi for the elimination via the bile or into the blood for the elimination via the kidney [Marquardt 2004].

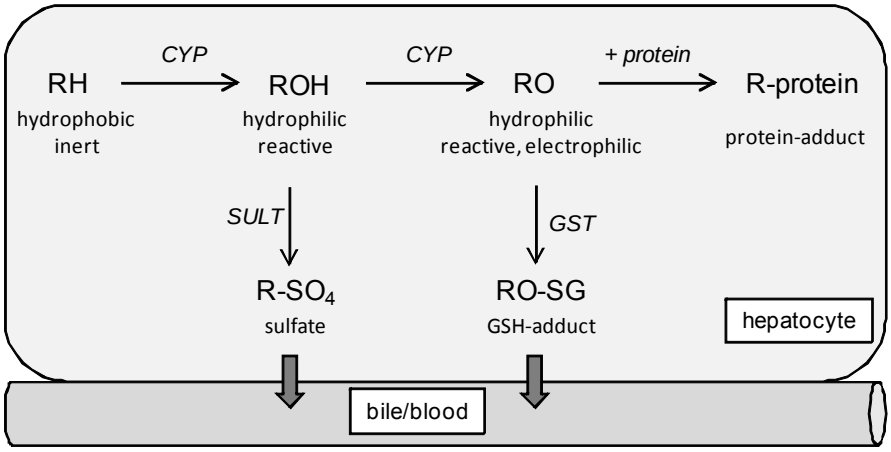

Figure 1.3: Scheme of xenobiotic metabolism.
More or less chemically inert, hydrophobic substances are oxidized by phase-I enzymes, conjugated with endogenous molecules by phase-II enzymes, and excreted into bile or blood. Very reactive metabolites may bind covalently to cellular components like proteins. R = residual.

This excretion process is often called phase-III of the xenobiotic metabolism. The basolateral membrane of the hepatocytes is rich in transporters (Figure 1.4, Table 1.3) for the uptake and the export of organic cations and anions, bile salts, different metabolic products, and xenobiotica. The apical surface of hepatocytes expresses transporters for the export of bile salts, endogenous products and xenobiotics and their metabolites into the bile canaliculi [Giacomini 2010, Klaassen 2010].

Table 1.3: Hepatic transporters.
Hepatocytes express in their basolateral membrane transporters for the exchange of products with the blood. On their apical side efflux transporters transfer bile salts and metabolic products into the bile. [Giacomini 2010]

Uptake transporters	Efflux transporters
Organic cation transporter (OCT)	Multi drug resistance protein (MDR, MRP)
Organic anion transporter (OAT)	Breast cancer resistance protein (BCRP)
Organic anion transporting protein (OATP)	Bile salt export pump (BSEP)
Na+/taurocholate cotransporting polypeptide (NTCP)	Organic solute transporter (OST)
Organic solute transporter (OST)	

NTCP is a sodium dependent cotransporter which takes up bile salts from the portal blood before they are again excreted into the bile by BSEP. So most of the bile acids are recycled rather than newly synthesized which becomes important during cholestasis where the expression of NTCP was found to be decreased in animals and humans [Hagenbuch 2003]. OATPs are symporters which exchange bile salts

and organic anions for intracellular bicarbonate and play a major role in the hepatic clearance of drugs while they were found to be downregulated in cholestatic animal models [Hagenbuch 2003]. MDR1, BCRP and MRP1 were found to be responsible for the resistance of tumors to chemotherapeutics and several studies showed that their overexpression in vitro make cells resistant to cytotoxic drugs. For the major human hepatic transporters rat orthologs with similar substrate specificity do exist [Giacomini 2010, Klaassen 2010].

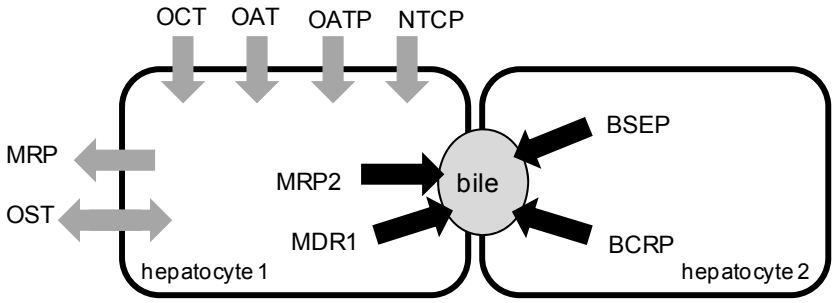

Figure 1.4: Hepatic transporters.
Hepatocytes express different transporters on their basolateral membrane for the exchange of metabolic educts and products as well as bile salts with the blood. The apical membrane contains transporters for the excretion of bile salts and metabolites into the bile [Giacomini 2010, modified].

The xenobiotic metabolism is regulated by four basic mechanisms: (1) Increase or (2) decrease of an enzyme's (3) expression or its (4) activity. Especially CYPs are often induced by their substrate which allows a quick response to new xenobiotics. Thereby substrates often induce different enzymes of all three phases of the xenobiotic metabolism by a cascade starting from one of the following nuclear receptors:

* Peroxisome proliferation-activated receptor (PPAR)
* Farnesoid X receptor (FXR)
* Pregnane X receptor (PXR)
* Liver X receptor (LXR)
* Constitutive androstane receptor (CAR)

These receptors are located in the cytoplasm and are translocated into the nucleus after they were activated by a substrate. There they heterodimerise with the Retinoid X receptor (RXR) which is also activated by a cofactor. This heterodimer binds to a response element of the DNA and initiates the expression of transcription factors for

several enzymes of the xenobiotic metabolism. The helix-loop-helix receptor aryl-hydrocarbon receptor (AhR) also binds its ligand in the cytoplasm, translocates to the nucleus and heterodimerizes with the AhR nuclear translocator (Arnt) in order to bind to a responsive element in the DNA and activate the transcription of several target genes [Waxman 1999, Patel 2007]. Nuclear receptors have an overlapping field of target genes (Figure 1.5) and crosstalk with each other [Xie 2004].

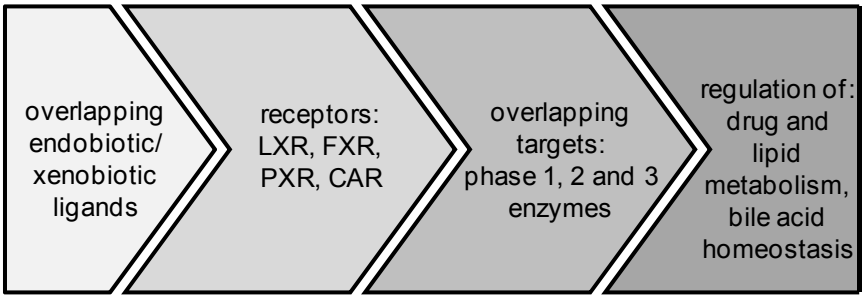

Figure 1.5: Regulation of the xenobiotic metabolism.
The enzymes of the xenobiotic metabolism are regulated by nuclear receptors which act as transcription factors for a wide field of target genes after they were activated by a ligand. Overlapping fields of target genes and ligands make the system flexible for new xenobiotics [Xie 2004, modified].

The drug related induction and inhibition of various enzymes of the xenobiotic metabolism can result in drug-drug interactions which often cause drug side effects as explained in the next chapter [Guengerich 2008, Walsky 2008].

1.5.3 Drug induced hepatotoxicity

Hepatotoxicity is the most frequent reason for the failure of new pharmaceutical compounds during the process of drug development or for the withdrawal of drugs after they have been marketed [Lee 2003, Lee 2005, Halegoua-De Marzio 2008]. Several drugs cause idiosyncratic adverse effects [Lee 2003, Daly 2010] which are not dose-dependent, show variable latencies, occur very seldom (one in every 1000 to one in every 100.000 patients) and are not predictable by regulatory studies in most cases. Idiosyncrasy seems to be related to the hypersensitivity of individuals which may be related inter alia to single nucleotide polymorphisms (SNPs) in enzymes of the xenobiotic metabolism. Thus, severe adverse effects which can lead to acute liver failure and the death of patients often occur not until a larger population is treated with these drugs after the approval [Li 2002, Kaplowitz 2004, Uetrecht 2008, Hussaini 2007]. Some drugs show well predictable hepatotoxicity with dose-

dependent effects which can be divided into cytotoxic effects (necrosis, apoptosis), cholestasis (dysfunction of bile secretion), steatosis (fatty liver), fibrosis (increased production of connective tissue), cirrhosis (increased production of connective tissue in consequence of steatosis or hepatitis), hepatitis (inflammation), and liver tumors [Lee 2003, Marquardt 2004]. Drug induced hepatotoxic effects can be caused by different mechanisms:

a) *Reactive metabolites*: Phase-I enzymes biotransform drugs to metabolites with a higher solubility in water. Such biotransformations sometimes result in very reactive electrophiles which bind to proteins or other cellular components. This can lead to cellular dysfunctions like loss in ionic gradients and the intracellular calcium homeostasis followed by a decreased ATP-level, cell swelling and rupture or the activation of apoptosis. Furthermore protein adducts presented on the cell surface can cause immune reactions [Li 2002, Lee 2003, Kaplowitz 2004 and 2005, Uetrecht 2008, Guengerich 2008]. Reactive metabolites can also bind to the DNA which is a key event of genotoxicity [Boehme 2010, Hashizume 2010].

b) *Apoptosis*: Immune reactions as well as drugs and their metabolites can activate apoptosis pathways in the hepatocytes which lead to programmed cell death if protective survival pathways cannot rescue the cell [Kaplowitz 2000, Lee 2003].

c) *Oxidative stress*: Reactive oxygen species (ROS) like oxygen ions and hydrogen peroxide are produced during normal cell functions like fatty acid oxidation or the electron transport in the mitochondrial respiratory chain. Under normal conditions they are detoxified by enzymes like dismutases, catalases and glutathione (GSH) transferases. Reactive metabolites of drugs can trigger oxidative stress by for example disturbing the electron transport in the respiratory chain. ROS and reactive metabolites can be detoxified, e.g., by conjugation with GSH. However, intensive production of ROS leads to GSH depletion when the cellular antioxidant mechanisms are exhausted. Then several cellular components including the DNA can be damaged. Finally oxidative stress can result in cell death if too many cellular functions are diminished [Kaplowitz 2000, Jaeschke 2000, Lee 2003, Guengerich 2008,

Avery 2011]. Oxidative stress is furthermore discussed as a key mechanism of non-genotoxic carcinogens [Hernández 2009].

d) *Immune reactions*: Adducts of covalently bound metabolites to enzymes or other cellular components are transported in vesicles to the cell surface and presented to immune cells. Thus, the immunological cascade starts to eliminate the foreign compound and trigger inflammation, formation of antibodies or cytolytic reactions. Furthermore inflammation can be induced by drugs causing necrosis as a result of reactive metabolites or oxidative stress [Lee 2003, Ganey 2004, Kaplowitz 2004 and 2005].

e) *Transporter inhibition*: Drugs like Cyclosporine A inhibit the bile salt export pump (BSEP). The disturbed secretion of bile salts from the hepatocyte into the bile canaliculi causes cholestasis. The block of transporters for bilirubin or organic ions causes a backlog of these substances in the hepatocytes and later in the blood which for example can lead to jaundice [Lee 2003, Tang 2007, Giacomini 2010].

f) *Enzyme inhibition and induction*: A reactive phase-I metabolites can covalently bind to its biotransforming CYP enzyme. This can result in irreversibly blocked enzymes and protein adducts which potentially activate the immune system. Other drugs block enzymes time-dependently and reversibly. If a compound inhibits a major CYP of its own catabolism the clearance of this drug may be decreased. Consequently, the drug's plasma level and half life could be increased as well as its pharmacological and may be toxic effect. Against that the plasma level of the appropriate drug could be decreased if this CYP is induced and the drug metabolism is accelerated. This may lower the drug's efficacy but also enhance the production of reactive metabolites with the consequences explained before. Enzyme inhibition and induction play a major role in drug-drug interactions which can trigger adverse effects while one drug inhibits or induces a CYP involved in the metabolism of a coadministered drug. A prominent example is Acetaminophen which is transformed by CYP2E1 into a reactive metabolite. The co-consumption of alcohol which induces CYP2E1 results in the rapid formation of a large amount of this metabolite and can cause oxidative stress, liver necrosis and acute liver failure [Lee 2003, Walsky 2008, Zhou 2008]. Since the inhibition and induction of

CYPs as well as the drug-drug interaction play a major role in drug induced hepatotoxicity the FDA demands the in vitro and in vivo testing of the major human CYPs [FDA 2004].

g) *Damage of mitochondria*: The mitochondria can be affected directly or indirectly by drugs via many different ways. Since mitochondria are essential for energy production of the cell mitochondrial damage commonly leads to cell death by apoptosis or necrosis. Drugs like Acetaminophen can directly open the mitochondrial permeability transition (MPT) pore which results in loss of the mitochondrial transmembrane potential, rupture of the mitochondria due to water influx and the release of proapoptotic factors into the cytosol. These mechanisms can cause hepatitis and acute liver failure. Some drugs inhibit the mitochondrial DNA (mtDNA) transcription machinery and cause mtDNA depletion or block enzymes of the mitochondrial respiratory chain (e.g. Troglitazone) or the fatty acid catabolism (e.g. Valproic acid) which diminish the mitochondrial function and can result in the formation of ROS and oxidative stress. Modifications in the fatty acid metabolism can cause steatosis and hepatitis as a result of lipid accumulation. Cationic amphiphilic substances can dissipate the transmembrane potential via passing the inner membrane after they were protonated in the intermembrane space. These drugs act as uncoupling agents and inhibit the energy production. Furthermore glycolysis is induced in order to produce ATP in the cytosol when the mitochondrial ATP production is inhibited by mitochondrial damage. The incidental pyruvate which is usually further metabolized in the mitochondria is transformed into lactate and secreted into the blood. The protons produced during increased glycolysis and ATP hydrolysis as well as the increased plasma level of lactate lead to lactic acidoses (e.g. Metformin) [Lee 2003, Kaplowitz 2004, Lee 2005, Dykens 2007, Labbe 2008].

Although hepatocytes are the major target of hepatotoxicity other hepatic cell types can be affected as well. Kupffer cells, the immune cells of the liver, can activate cytokine signaling and inflammation reactions. The fat storing and collagen producing Ito cells are involved in the development of fibrosis and cirrhosis. Furthermore the canaliculi and the bile ducts can be damaged by drugs and metabolites excreted into the bile [Friedmann 1997, Marquardt 2004].

1.5.4 In vitro liver models for the prediction of human hepatotoxicity

For the investigation of human toxic effects human material seems to be the best device but also animal models can provide substantial information about a drug's metabolism, biological target and toxic effects. Generally more complex models better reflect the in vivo situation than less complex models but these are easier to standardize, manipulate and interpret [Tuschl 2008]. Commonly used in vitro systems for the investigation of hepatotoxicity are isolated perfused livers, liver slices, primary hepatocytes in an adherent cell culture or as suspension culture, liver cell lines and transgenic cells, as well as subcellular fractions like microsomes or S9 mix (Figure 1.6).

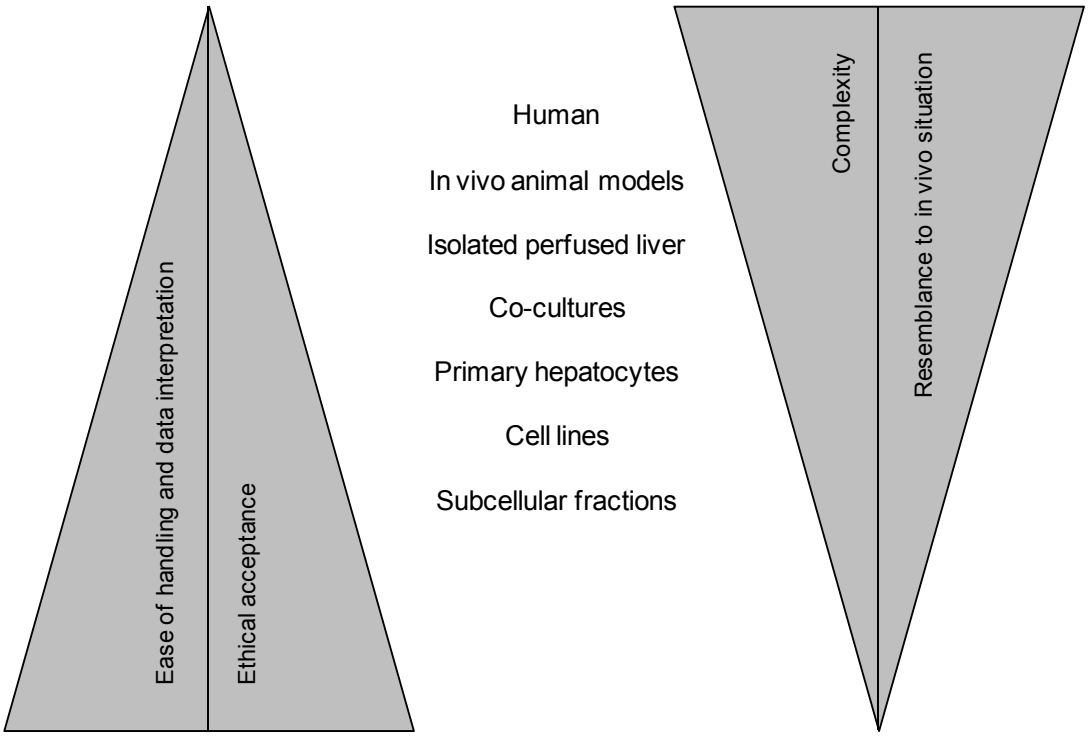

Figure 1.6: In vivo and in vitro models for the study and prediction of human hepatotoxicity.
More complex models reflect the human in vivo situation better but complicate handling, data interpretation and ethical acceptance [Tuschl 2008, modified].

Isolated perfused livers provide the complete set of liver cell types in their original three-dimensional architecture and function including the vascular and the biliary system, cell-cell and cell-matrix interactions, signaling, and regulation [Gordon 1972]. However, isolated livers are difficult to handle and maintain their function for only a few hours while the reproducibility of different experiments is quite low. Furthermore the availability of human organs is low and difficult to plan, the amount of animals is not reduced and only one compound can be tested per liver.

Liver slices are produced by cutting livers in thin slices which can be cultured for up to 72h in culture media. The optimal thickness of these slices is between 150µm and 225µm to guarantee an optimal exchange of oxygen and nutrients and to keep the ratio of functional cells to cells damaged via the cutting process at an optimal balance. Liver slices possess all cell types in their original three-dimensional architecture as well as cell-cell and cell-matrix interactions, signaling, and regulation. Therefore they enable studies of drug metabolism and excretion into the bile in the same way like isolated livers. In addition a lot of slices can be produced out of one organ, so several different compounds can be tested which significantly decreases the amount of animals used. Another advantage of liver slices is the possibility to perform biochemical tests and histopathological examinations in parallel [Lupp 2001, Vickers 2004, Barth 2006]. Nevertheless, a big disadvantage is the short culture time of 72h.

Liver cell cultures can be used in flexible formats and applications. Furthermore culture conditions are easy to standardize and experiments can be performed with a high reproducibility. Hepatic cell cultures are based on primary hepatocytes, transfected hepatocytes, hepatic cell lines or co-cultures of different cell types which are explained below in more detail.

Co-cultures of hepatocytes and non-parenchymal liver cells enable intercellular signaling. Hence, effects on different liver cell types could be investigated in a minor complex system compared to isolated livers or liver slices. So sinusoidal endothelial cells co-cultured with hepatocytes stabilize each other and enable the detection of adverse effects in the liver's vascular system [Hwa 2007, Dash 2009]. Kupffer cells as hepatic immune cells are involved in inflammatory processes and influence CYP activities in vivo and in vitro [Hoebe 2001, Sunman 2004]. 3D perfused liver bioreactors are built up by seeding different liver cell types onto scaffolds that mimic the vascular system and enables more complex studies for drug clearance, metabolite assessment and inflammatory adverse effects [Dash 2009]. These culture systems are currently used for special questions and are not suited for screening methods due to their complex handling. In another 3D-system better suited for high troughput approaches all cell types of the native liver are seeded onto an interconnecting porous scaffold in multiwell plates. This organotypic cell culture

system provides activity and inducibility of phase-II, -II, and -III enzymes for up to 70 days near the in vivo level [Vidales 2011].

Primary hepatocytes are the major in vitro system for early prediction of hepatotoxicity [Soars 2007, Hewitt 2007, Schoonen 2009, Gómez-Lechón 2010, Li 2010]. Primary hepatocytes are freshly isolated out of animal or human livers by organ perfusion. During this process the liver is flushed via its vascular system with a buffer containing collagenases and/or proteinases which digest the vessels and the extracellular matrix to be able to isolate vital hepatocytes after organ homogenization and centrifugation. For the isolation of human primary hepatocytes several life science companies have cooperations with medical centers to receive organ parts removed during surgeries or livers of dead patients [Seglen 1976, Richert 2004]. Primary hepatocytes are highly differentiated cells which do not proliferate. Therefore they have to be isolated freshly for every experiment while the use of cryopreserved cells makes the investigator more flexible. Optimized protocols for cryopreservation and thawing guaranty the metabolic activity of thawed cells [Gómez-Lechón 2006, Hewitt 2007].

Short time studies for drug transport and drug clearance are often performed with hepatocyte suspension cultures. In this culture system the cells are incubated on a shaker and remain vital for only a few hours due to the lack of cell-cell and cell-matrix contacts [Jouin 2006, Hewitt 2007]. In monolayer cultures the cells adhere onto cell culture plates coated with extracellular matrix proteins (Collagen I or Matrigel™) and form close cell-cell and cell-matrix contacts assuming the polygonal hepatocyte-like shape with clear cytoplasm. Since they do not proliferate the cells are plated with a confluence of 100% and form a cell monolayer. After three to five days the cells look like fibroblasts and detach [Tuschl 2006, Sahu 2007]. Thus, monolayer cultured hepatocytes are used for short term studies like acute cytotoxicity and CYP-induction as a hint for drug-drug interactions [Hewitt 2007, Gómez-Lechón 2010].

Cultured between two layers of gelled collagen or in monolayer culture overlaid by a film of Matrigel™ (extracellular matrix derived from Engelbreth-Holm-Swarm mouse sarcoma) primary hepatocytes additionally form bile canaliculi-like structures (Figure 1.7) and maintain their characteristical shape at least for ten days. The functional activity of the canaliculi was proven by incubating the cells with a fluorescent dye which is known to be transported by MRP2 into the bile canaliculi where its

accumulation was detected. The so called sandwich cultured hepatocytes (Figure 1.7), the cell culture system used for the present study, reorganize themselves during the first three days in culture and after that maintain a stable expression and inducibility of the major CYPs, phase II enzymes, transporters, nuclear receptors, transcription factors, as well as liver functions like albumin production near the in vivo level [Tuschl 2006, Tuschl 2009]. Thereby the culture conditions dramatically influence the vitality and functionality of hepatocytes. Cells cultured with fetal calf serum lose their characteristical shape and the expression of major enzymes of the xenobiotic metabolism much earlier than serum-free cultured cells [Tuschl 2006, Tuschl 2009].

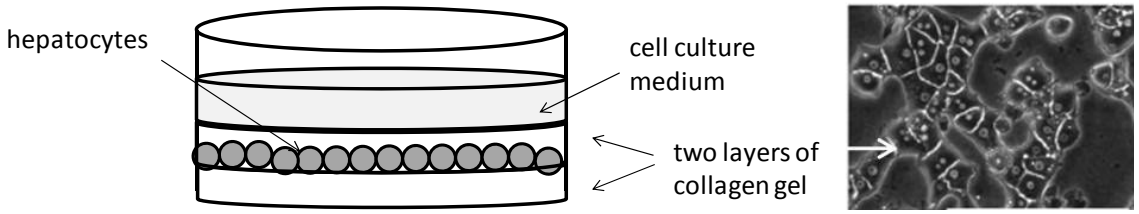

Figure 1.7: Scheme of the sandwich culture system.
In the sandwich culture the cells are cultured between two layers of gelled collagen I. Cultured this way the hepatocytes maintain their function and morphology for at least ten days and build canaliculi-like structures (white arrow).

Cell lines are immortal and grow constantly for an almost unlimited life-span [Donato 2008]. Therefore their use enables long term studies of high reproducibility [Schmitz 2007]. In contrast to primary cells cell lines are permanently available and make cell culture studies more flexible. However, nearly all hepatoma derived cell lines express enzymes of the xenobiotic metabolism to a lesser extent than primary cells [Donato 2008, Fujimura 2010, Lin 2011]. HepG2 is a human liver hepatoma cell line with a very small basal expression and inducibility of nuclear receptors [Westerink 2007] and nearly all the major CYP enzymes as well as of some phase-II enzymes and transporters [Rodríguez-Antona 2002, Boehme 2010, Guo 2011]. Thus, they are often less sensitive towards hepatotoxic agents than primary hepatocytes and are only used for selected studies [Westerink 2007] or used with S9-mix to mimik the metabolic activity of the cells [Otto 2008, Boehme 2010]. HepaRG cells derive from a human hepatocarcinoma and differentiate during four weeks in culture into cells comparable to primary hepatocytes based on morphology, expression of major phase-I, -II, and -III enzymes and several liver functions which remain stable for at

least four weeks [Aninat 2006, Jossé 2008, Anthérieu 2010]. The application capabilities of this cell line for predicting liver toxicity of new drugs is tested in the EU-project Predict-IV in comparison to human and rat primary hepatocytes. The non-tumorigenic cell line Fa2N-4 originates from human primary hepatocytes immortalized by stable transfection. The inducibility of CYP1A2 and CYP3A4 is comparable to primary hepatocytes while CYP2B6 is less inducible and several hepatic transporters are expressed on lower level [Kenny 2008]. Lin et al. [Lin 2011] investigated the activities of major phase-I and phase-II enzymes in the five human hepatoma cell lines HepG2, Hep3B, HCC-T, HCC-M, and Huh-7. In conclusion the activities of all tested enzymes were lower than in human primary hepatocytes and varied over the ten assayed passages while Huh-7 showed the highest activities. The THLE-2 cell line is based on human adult liver epithelial cells immortalized by the introduction of a recombinant simian virus 40 large T antigen gene. These cells express different phase-II and antioxidant enzymes and activate different chemical carcinogens [Pfeifer 1993]. Their poor CYP activity was successfully stocked up by transfection [Bort 1999, Donato 2008]. H4IIE and FAO are rat hepatoma cell lines. Compared to rat primary hepatocytes they lack the expression of some genes coding for drug metabolizing enzymes or express them at a lower level while not all expressed CYPs are inducible [Clayton 1985, Fujimura 2010]. Therefore the results of studies performed in hepatic cell lines should be interpreted with respect to the differences in gene expression, enzyme activity, and inducibility of hepatic cell lines compared to primary hepatocytes.

Subcellular fractions are commercially available and prepared by homogenization of the liver followed by specific centrifugation steps. Microsomes are one class of subcellular fractions which is often used in toxicology. These membrane surrounded vesicles containing fragments of the endoplasmatic reticulum and the thereon bound CYPs. A further commonly used class are S9-mixtures, supernatants which result from the centrifugation of liver homogenate at 9,000 x g and contain all enzymes of the xenobiotic metabolism. To increase the activity of these enzymes the donor animal is treated with CYP inducers before the liver is isolated to produce microsomes and S9-mixtures. These are used for short-time experiments with limited applications like CYP inhibition, CYP induction or drug metabolism studies [Callander 1995]. S9-mixes are routinely used as an activation system for compounds tested with the Ames assay for their genotoxic potential [Ames 1973]. Furthermore they

provide a metabolic system for hepatic cell lines which often express enzymes of the xenobiotic metabolism very limited [Otto 2008, Boehme 2010 and 2011].

1.6 Toxicogenomics can sustain drug discovery and development

Genomics methods used in the field of toxicology are called toxicogenomics [Lord 2006]. Compared to traditional studies toxicogenomics can detect drug induced toxicities before these effects become adverse and are observed histopathologically [Van Hummelen 2010]. Kier et al. could correlate gene expression changes in the liver tissue of rats 24 h after drug treatment with histopathological findings after 72 h [Kier 2004] while Hirode et al. describe early marker genes for phospholipidosis [Hirode 2008]. Zidek et al. identified 64 potential marker genes for hepatotoxicity in rat livers after single dose treatment and built a prediction model which classifies toxic and non-toxic compounds related to their gene expression changes before histopathological changes can be detected [Zidek 2007]. These changes can be investigated related to specific target genes (e.g. branched-DNA, qRT-PCR, Nothern Blotting) or genome wide (whole genome gene expression analysis) where tens of thousands of genes can be analyzed in parallel in one sample. Genomics tests can be performed in various matrices like tissue and body fluids or cultured cells and are therefore well suited for the discovery of novel early biomarkers [Van Hummelen 2010]. Proteins which are in vivo secreted into urine, feces, or blood where they act as biomarkers for organ toxicity or a specific disease can be linked to altered genes in organs of drug treated animals. After the correlation between biomarker release, histopathology findings and changes in gene expression had been proven diagnostic kits and novel biomarkers are established for the support of preclinical and clinical studies. These in vivo findings can be also compared with genomic data of drug treated cells in order to define marker genes for the prediction of drug toxicity in vitro [Pennie 2000, Fielden 2006, Hewitt 2008, Mendrick 2008, Van Hummelen 2010]. Furthermore genomics enable the profiling of single nucleotide polymorphisms (SNPs) in individual patients. A large number of SNPs has been detected in the human genome while several SNPs are postulated to be disease relevant or involved in toxic side effects of drugs. Especially SNPs of CYPs are often involved in drug induced toxicity [Koo 2006]. Therefore the test kit AmpliChip™ was worldwide

approved to detect several SNPs of CYP2D6 which is involved in the metabolism of approximately 25% of the marketed drugs and triggers predispositions for adverse effects [Mendrick 2008].

Toxicogenomics methods are well suited for the development of early prediction models for specific organ toxicities. In vitro screenings in different cell types performed prior to animal studies have the potential to prioritize less toxic drug candidates which are further developed while the toxic ones are stopped before they are tested in animals [Pennie 2000, Fielden 2006, Hewitt 2008, Menderick 2008, Van Hummelen 2010]. Thus, these early screening methods can help to reduce the amount of animals used for regulatory studies during drug development. These tests can furthermore give first information about target organs as well as species differences related to toxic effects and represent a giant stride towards the 3R's principle [Russel 1959]. A prediction model is based on a database filled with gene expression data of as many as possible reference compounds with well known mode of action and in vivo toxicity where gene alterations are correlated with. Using the appropriate software a set of genes can be found which enables the classification of new drug candidates as toxic or non toxic [Lord 2006, Zidek 2007, Hrach 2011].

During the last decade several public consortia and international initiatives have been founded in order to facilitate the application of toxicogenomics methods, investigate molecular mechanisms, establish genomic biomarkers, or to create reference databases for different fields of toxicology [Mattes 2008]:

* International Life Science Institute Health and Environmental Science Institute Committee (ILSI HESI; international; academic, industrial and governmental partners)
* Toxicogenomics Research Consortium (TRC; USA; academic)
* Predictive Safety Testing Consortium (PTSC; USA; FDA, EMA, industrial partners)
* InnoMed PredTox Consortium (EU, academic and industrial partners)
* Toxicogenomics Project (Japan) [TGPJ 2011]
* National Centre for Toxicogenomics (NCT) founded by the National Institute of Environmental Health Science (NIEHS; USA) [Tennant 2002].

Furthermore FDA and EMA perceived the potential of genomics methods to support clinical studies and encourage their establishment and application [Menderick 2008]. Therefore the FDA released the “Guidance for Industry Pharmacogenomics data submission” [FDA 2005] and enabled genomics data to be part of the approval package. Currently these data are assumed to be additional information and its submission is optional on a voluntary base. The EMA founded the Innovation Task Force to also integrate genomics into the drug development process and therefore published the “Reflection paper on co-development of pharmacogenomic biomarkers and assays in the context of drug development” [EMA 2010].

The timeframe of toxicogenomic studies is very variable and strongly depends on the study design. In vitro screening models measuring a defined gene set followed by a standardized data analysis usually last a few days. The big advantage of in vitro models compared to animal studies is the possibility to test several different compounds and doses with the cells of one donor including the vehicle control. During preclinical trials one animal can only be treated with one dose of one specific compound while for the vehicle control a further animal is used [ICH-M3 2009]. However, the reagents, technical equipment and softwares required for genomics studies are relatively expensive [Farkas 2010]. Especially the establishment of screening models is cost-intensive and time-consuming since several biological replicates of cells treated with a large number of reference compounds have to be analyzed in order to obtain statistically significant results [Elashoff 2008]. Here the time points of sample collection have to be chosen carefully so as not to miss the critical time window of cellular changes. Furthermore during the first step of the development of a screening system whole-genome gene expression analyses are often perfomed. These methods usually include different working steps like cell or tissue lysis, RNA isolation and purification, cDNA or cRNA synthesis and purification, as well as the hybridization of the targets onto the gene chips, chip processing and scanning [Pennie 2000, Lord 2006]. Such multi-step operations take their time and always involve the danger of accumulating errors. Whole genome gene expression analyses detecting more than 20,000 different genes per sample produce large amounts of data whose biological interpretation is very complex [Hewitt 2008]. Therefore bioinformatic softwares like Genedata’s Expressionist™ have been developed providing tools for the normalization of raw data, the performance of statistical tests as well as the calculation of fold changes and the statistical

significance of gene expression changes [Genedata 2011]. Additionally a variety of software tools (IPA® [Ingenuity 2011], MetaTox™ [GeneGo 2011], ArrayTrack/FDA [Van Hummelen 2010]) supporting the biological data interpretation are commercially available. These tools access databases filled with information about the interaction of biological molecules like transcription factors, transporters, enzymes, and receptors with each other as well as with chemicals or drugs. After whole genome gene expression data were uploaded into these softwares a list of affected canonical pathways and physiological functions are shown. With the help of this information the molecular mechanisms of toxic effects, the mode of action of drugs, molecular targets, as well as changes in specific cell signaling or gene regulation pathways can be elucidated. However, drawing the right conclusions based on a long list of deregulated functions and pathways is anything but trivial and requires a keen scientific knowledge and experience [Hewitt 2008, Van Hummelen 2010]. Furthermore these informations are based on the current understanding and maybe not complete since several pathways and mechanisms have not been fully described yet. During analysis it is essential to verify if the gene probes of necessary target genes were contained on the processed array.

Due to their complex performance and data analysis whole genome gene expression methods are less suited as routinely used screening models. Nevertheless, they enable the definition of predictive gene sets by correlation of the gene expression data with in vivo findings or by application of specific bioinformatic calculations. After that the resulting gene set need to be validated by another genomics method. Finally a standardized high throughput in vitro system can be established for the prediction of new drugs' organ toxicities. Ideally this model is based on a cell culture system which is easy to handle and a fast genomics method measuring the gene expression changes of a defined gene set without the need of multiple working steps and complex data interpretation [Zidek 2007, Hrach 2011].

1.7 EU-project Predict-IV

The study in hand is part of Predict-IV a collaborative project funded by the European Commission's Seventh Framework Programme (FP7). FP7 is a financial tool to support the research and development of several scientific areas, while the full

project title is ‘Profiling the toxicity of new drugs: a non animal-based approach integrating toxico-dynamics and biokinetics’ (grant agreement no.: 202222). The project has started on May 1st 2008 for the duration of 60 months and includes 21 partners from industry and academia. The overall goal is to develop in vitro testing strategies for a better prediction of drug safety during the phase of drug discovery or early stages of drug development. With the help of different ‘omics technologies (metabolomics, proteomics and genomics) as well as high content imaging (HCI) and kinetics novel and early in vitro biomarkers should be defined which may enable the prediction of human toxicities. Thus, a predictive in vitro screening battery could enable the identification of drug candidates which are potentially toxic in humans before they are tested in animals in future. This better pre-selection of drug candidates could reduce late stage failures resulting in decreased costs and duration of drug development and represents a major improvement towards the 3R’s principle [Predict-IV 2011].

As part of Predict-IV the three organ systems liver and kidney as major target organs for drug-induced toxicities as well as the central nervous system (CNS) as a target of undesired side effects are tested. Different culture models of primary cells and cell lines from human, rat, mouse, and cow are treated with reference compounds of well known toxicity and kinetics in animals and human. These reference compounds were selected due to their organ specific toxicity in order to cover different molecular mechanisms and toxic phenotypes. After a dose finding study the cells were treated with two doses: A toxic dose around the TC10 (toxic concentration; concentration which kills 10% of the cells) and a non-toxic dose which was fixed at 1/10 of the toxic dose. The effect of the treatment was measured at different endpoints: Metabolomics (NMR, MS), proteomics (MS), genomics (global gene expression analysis), kinetics (HPLC), and HCI. Metabolomics methods detect changes in endogenous metabolites while with proteomics and genomics changes in the global protein and gene expression, respectively, are investigated. With the help of kinetics the in vitro catabolism rates of the reference compounds are determined. In addition the real intracellular concentrations of the substances are calculated as well as the amount of compound sticking to the cell culture plates since these data are essential for the correct extrapolation of the in vitro data to the in vivo situation and for the comparison with in vivo plasma concentrations.

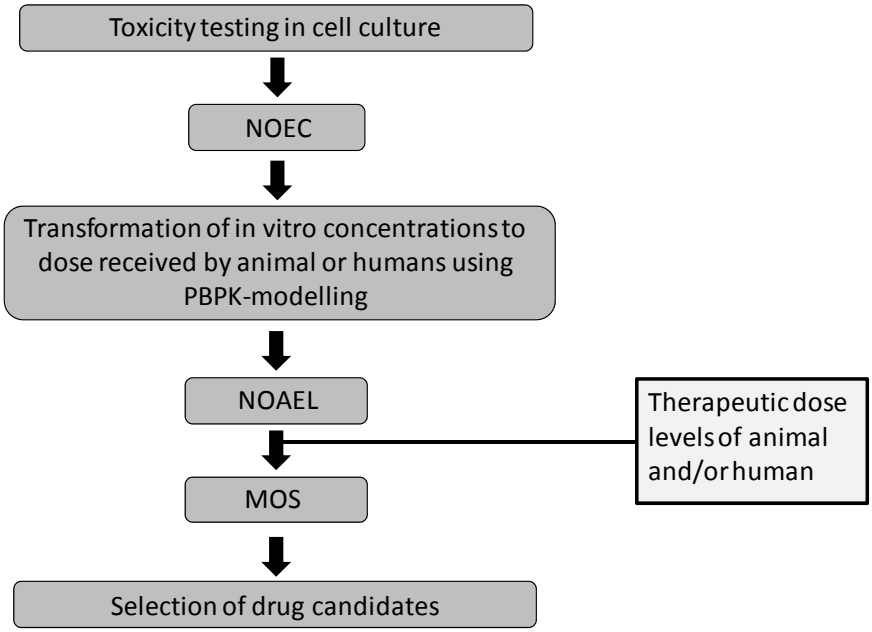

Figure 1.8: Proposed Predict-IV approach for the use of in vitro data in drug safety assessment.
NOEC = no observed effect concentration; PBPK = physiologically based pharmacokinetic; NOAEL = no observed adverse effect level; MOS = margin of safety [Predict-IV 2011]

HCI enables the measurement of cellular changes via, e.g., fluorescent dyes. At time of writing the cell culture work was nearly completed while the measurement of the different endpoints was pending. The results of all these endpoints will be correlated with in vivo data from the literature in order to define novel biomarkers which predict human toxicities correctly. Thereby the concentration of a compound which does not change these biomarkers is called the no observed effect concentration (NOEC) (Figure 1.8). The NOEC calculated in vitro will be transformed into in vivo doses using physiologically based pharmacokinetic (PBPK) modeling, a mathematical tool which predicts the absorption, distribution, metabolism, and elimination of a compound in a living organism. Based on these calculated in vivo doses the so called no observed adverse effect level (NOAEL, dose which does not cause any adverse effects) for human and animals is estimated. In routine preclinical studies the calculation of human start doses is based on the animal NOAEL. The NOAEL estimated in our model is then compared with the NOAEL once measured in preclinical trials. Finally the difference between both NOAELs is used to calculate margins of safety (MOS) which enable the extrapolation from the in vitro data to safe human doses.

Table 1.4: Overview of the Predict-IV reference compounds for hepatotoxicity.
[a: Miyamoto 2009, b: Robin 2008, c: Pollak 2004, d: Vassallo 2007, e: Boehmer 2011, f: Kassianides 1990, g: Suzuki 2008, h: unpublished internal data, i: Rainsford 2009, j: Sandimmune 2011, k: James 2003, l: RX-FF 2011, m: Willson 2000, p: Yokoi 2010, q: Smith 2003, r: Floyd 2009, s: press release 11/10 BfArM, t: Lebovitz 2002, u: Chang 2006], ALT: Alanine transferase as serum marker for liver damage, ULNR: upper limit of normal range, KC: kinetic compound, BfArM: Bundesinstitut für Arzneimittel und Medizinprodukte

Compound	Therapeutic area	Human hepatotoxicity	Rodent hepatotoxicity	Incidence of human hepatotoxicity
Acetaminophen	pain	apoptosis, necrosis and inflammation[k]	apoptoses, necrosis and inflammation[k]	toxic at very high doses (overdosage, abuse)[k]
Amiodarone (KC)	arrhythmics	phospholipidosis[a], steatohepatitis[b], hepatitis[cd], cirrhosis[d]	phospholipidosis [a]	toxic at high doses and long-term usage[c]
Chlorpromazine (KC)	psychotic disorders	cholestasis[g]	cholestasis[g]	--
Cyclosporine A (KC for liver, kidney, CNS)	Immuno-suppressant	cholestasis[t]	ox. Stress, necrosis[e]	4-7%(all hepatotoxic effects)[j]
EMD 335823	diabetic complications	stopped prior to clinical trials	bile duct and liver cell necrosis[h]	Unacceptable animal hepatotoxicity
Fenofibrate	dislipidemia, hypercholes-terolemia	cholestatic hepatitis[l]	non-genotoxic hepatocarcinogen, peroxisome proliferation[m]	7.5% (abnormal liver function test)[l]
Ibuprofen (KC)	pain, arthritis	--	--	0.7%(liver and biliary effects)[i]
Metformin	non-insulin dependent diabetes mellitus	--	--	--
Rosiglitazone	non-insulin dependent diabetes mellitus	--	--	ALT >3x ULNR[t] in 0.17%, withdrawn due to cardiotoxicity[s]
Troglitazone	non-insulin dependent diabetes mellitus	cholestasis[p], acute liver failure[q]	apoptosis, necrosis, steatosis[q]	idiosyncratic, ALT >3x ULNR in 1.9%, 94 cases of acute liver failure, 65 deaths[rt], withdrawn due to hepatotoxicity[r]
Valproic acid	epilepsy	steatosis[u]	steatosis[u]	elevated ALT in 30-50% of patients, idiosyncratic[u]

In the liver workpackage the human hepatoma-derived cell line HepaRG will be compared with primary human and rat hepatocytes. Each cell system is treated under its optimized conditions with the same eleven reference compounds. These

compounds cover a range of toxic phenotypes and cause in vivo hepatotoxic effects of variable severity (Table 1.4). Samples for the same endpoint measurement at equal time points are prepared for all of the three cell culture systems. Furthermore a SNP analysis is performed for each donor since some SNPs are known to influence drugs' toxicities [Koo 2006]. Thus, differences of the toxic effects of the various biological replicates could be possibly correlated with donor-specific variations in drug metabolizing enzymes. Furthermore the activity of the major drug-metabolizing CYPs is measured for every donor since the metabolic activity of the cells influences drug-induced toxicity and the kinetic of the drug's catabolism.

Primary rat hepatocytes have to be freshly isolated for every study. Therefore it is not planned to integrate these cells into the final model since the project's goal is the development of a non-animal based prediction model. However, the data derived from human cells will be compared to the rat data in order to elucidate species-specific effects which play a major role in terms of extrapolation of animal to human dosage and the prediction of human adverse effects.

1.8 Aim of the study

The work in hand describes the endpoint genomics for seven of the eleven reference compounds tested in rat primary hepatocytes. For statistical reasons cells of one biological replicate were planned to be treated with all the eleven compounds in one study. This study design was feasible for the dose finding studies but not for the final studies which included more endpoints and therefore had to be performed in a larger cell culture format and with more technical replictates. Hence, the eleven reference compounds were devided into the seven non-kinetic and the four kinetic compounds since the Predict-IV consortium agreed that the endpoint kinetics is only measured for Amiodarone, Chlorpromazine, Cyclosporine A and Ibuprofen.

The first major task was the establishment of the sampling for the different endpoints. Therefore preliminary studies with variable preparations of the cell culture samples were performed in order to optimize the sampling for the metabolomic, proteomic, genomic and kinetic analysis conducted by other project members. Furthermore the protocol of the cell treatment for the CYP activity assay was established. After that the TC10s of the eleven reference compounds were determined and validated during

a multi-step dose finding study. Finally three biological replicates of primary rat hepatocytes were treated for 14 days with the seven non-kinetic compounds including sample preparation for the different endpoints on day one, three and 14. In the course of the cell culture experiments it was declared that the metabolomics samples are not analyzed due to a capacity bottleneck of the appropriate project partner. Additionally the measurement of the proteomics samples was limited to the four kinetic compounds for the same reason.

Hence, the present study describes the whole genome gene expression analysis of the non-kinetic compounds. Since the data of seven compounds is not sufficient for the establishment of a prediction model the gene expression profiles of the test compounds were mechanistically analyzed. Thereby it was focused on the reconstruction of the pharmaceutical mode of action of the different compounds as well as the detection of off-target effects and the mechanistical understanding of the drugs' side effects. The biological interpretation of the genomics results was performed in comparison to in vivo literature data of the well known reference compounds in order to estimate the predictivity of sandwich cultured primary rat hepatocytes for rodent in vivo hepatotoxicity. The rodent gene expression results were also compared to human in vivo and in vitro literature data in order to estimate species-specific effects and the predictivity of primary rat hepatocytes for human in vivo hepatotoxicity.

2 Material

2.1 Chemicals and reagents for hepatocyte isolation

4-(2-hydroxyethyl)-1-piperazineethanesulfonic acid (HEPES)	Merck KGaA, Darmstadt/Germany
Bovine serum albumin (BSA)	Merck KGaA, Darmstadt/Germany
Calcium chloride dihydrate ($CaCl_2 \times 2$ H2O)	Sigma-Aldrich, Steinheim/Germany
D-glucose	Merck KGaA, Darmstadt/Germany
Ethylene glycol tetraacetic acid (EGTA)	Merck KGaA, Darmstadt/Germany
Liberase TM	Roche Applied Science, Mannheim/Germany
Magnesium sulfate hepatahydrate ($MgSO_4 \times 7\ H_2O$)	Merck KGaA, Darmstadt/Germany
Potassium chloride (KCl)	Merck KGaA, Darmstadt/Germany
Potassium dihydrogen phosphate (KH_2PO_4)	Merck KGaA, Darmstadt/Germany
Sodium chloride (NaCl)	Merck KGaA, Darmstadt/Germany
Sodium hydrogen carbonate ($NaHCO_3$)	Merck KGaA, Darmstadt/Germany
Sodium hydroxide solution 1N (NaOH)	Sigma-Aldrich, Steinheim/Germany

2.2 Chemicals and reagents for cell culture work

Acetaminophen	Sigma-Aldrich, Steinheim/Germany
Acetic acid	Merck KGaA, Darmstadt/Germany
Albumin solution 35%	Sigma-Aldrich, Steinheim/Germany
Ammonium bicarbonate	Sigma-Aldrich, Steinheim/Germany
α-Naphthoflavone	Sigma-Aldrich, Steinheim/Germany
CellTiter-Glo® Luminescent Cell Viability Assay	Promega Corporation, Madison/USA
Collagen I (rat tail tendon)	Roche Applied Science, Mannheim/Germany
Dexamethasone	Sigma-Aldrich, Steinheim/Germany
Dimethylsulfoxyd (DMSO) HYBRI-MAX®	Sigma-Aldrich, Steinheim/Germany
D-MEM/F-12 (1:1) liquid - with GlutaMAX™ I	Invitrogen, Karlsruhe/Germany
D-MEM/F-12 (1:1) powder	Invitrogen, Karlsruhe/Germany
EMD335823	Merck KGaA, Darmstadt/Germany
Fenofibrate	Sigma-Aldrich, Steinheim/Germany
Fetal bovine serum	HyClone, South Logan/USA
Insulin solution 10 mg/ml	Sigma-Aldrich, Steinheim/Germany
Insulin Transferrin Selenium (ITS)	Invitrogen, Karlsruhe/Germany
Ketokonazol	Sigma-Aldrich, Steinheim/Germany
Metformin	Calbiochem, Darmstadt/Germany
Methanol	Merck KGaA, Darmstadt/Germany
3-Methylcholanthrene	Sigma-Aldrich, Steinheim/Germany
Midazolam	Sigma-Aldrich, Steinheim/Germany
PBS Dulbeccos w/o Ca, Mg	Invitrogen, Karlsruhe/Germany
Penicillin (10.000 U/ml) -Streptomycin (10 mg/ml) solution	Sigma-Aldrich, Steinheim/Germany
Phenacetin	Sigma-Aldrich, Steinheim/Germany
Phenobarbital	Sigma-Aldrich, Steinheim/Germany
Pregnane carbonitrile	Sigma-Aldrich, Steinheim/Germany
Quant-iT™ PicoGreen® dsDNA Kit	Invitrogen, Karlsruhe/Germany
Rosiglitazone	Cayman Chemical Company, Michigan/USA
Sodium hydroxide solution 1N (NaOH)	Sigma-Aldrich, Steinheim/Germany
Sodium pyruvate 100 mM	Invitrogen, Karlsruhe/Germany

Testosterone	Sigma-Aldrich, Steinheim/Germany
Troglitazone	Cayman Chemical Company, Michigan/USA
Trypan Blue 0.5% (w/v) in PBS	Biochrome AG, Berlin/Germany
Valproic acid sodium salt	Sigma-Aldrich, Steinheim/Germany

2.3 Chemicals and reagents for molecularbiological methods

Agencourt® RNAClean™	Agencourt/Beckham Coulter, Beverly/USA
Block E1 buffer	Illumina Inc., San Diego/USA
β-mercaptoethanol	Sigma-Aldrich, Taufkirchen/Germany
Cy3™ labelled streptavidin (1mg/ml)	Amersham Bioscience/GE Healthcare, Buckinghamshire/UK
DEPC water	Ambion/ Applied Biosystems, Austin/USA
E1BC buffer	Illumina Inc., San Diego/USA
Ethanol LiChrosolv™	Merck KGaA, Darmstadt/Germany
GEX-HCB buffer	Illumina Inc., San Diego/USA
GEX-HYB buffer	Illumina Inc., San Diego/USA
High Temperature Wash buffer	Illumina Inc., San Diego/USA
HybE1 buffer	Illumina Inc., San Diego/USA
Illumina® TotalPrep™-96 RNA Amplification Kit	Ambion, Austin/USA
Nuclease free water	Ambion, Austin/USA
QuantiGene® Plex 2.0 Assay	Affymetrix, Santa Clara/USA
QIAshredder columns	Qiagen, Hilden/Germany
RNA 6000 Nano Kit	Agilent Technologies, Waldbronn/Germany
RNA 6000 Pico Kit	Agilent Technologies, Waldbronn/Germany
RNAprotect cell reagent	Qiagen, Hilden/Germany
RNeasy Plus Mini Kit	Qiagen, Hilden/Germany

2.4 Technical equipment and auxiliary material

Agilent 2100 Bioanalyzer	Agilent Technologies, Waldbronn/Germany
Agilent 2100 Bioanalyzer Priming Station	Agilent Technologies, Waldbronn/Germany
ART® BioRobotix™ Tips	Molecular BioProducts, San Diego/USA
Autoclave	H&P Labortechnik, Oberschleißheim/Germany
BeadChip® Hyb Cartrige (hybridisation chamber)	Illumina Inc., San Diego/USA
Bottle-top filter 0.2µm	Nalge Nunc International, Rochester/USA
Cell scraper	IWAKI, Japan
chemiluminometer lumistar Galaxy	BMG Lab Technologies, Offenburg/Germany
Combitips plus (1, 2.5, 5, 10 ml)	Eppendorf, Hamburg/Germany
Digital camera CC 12	Olympus, Hamburg/Germany
Fuchs-Rosenthal-Chamber	Paul Marienfeld GmbH & Co., Lauda-Königshofen/Germany
Glass ware	Schott Glas, Mainz/Germany
Heat block Thermo Stat Plus	Eppendorf, Hamburg/Germany
Hybridization Oven 650	Affymetrix, Santa Clara/USA
Illumina BeadArray Reader	Illumina Inc., San Diego/USA
Illumina Sentrix® RatRef-12 v1 Expression BeadChip Arrays	Illumina Inc., San Diego/USA
Incubator Hera Cell	Heraeus GmbH, Hanau/Germany
Little Dipper™ Microarray Processor Model 650c	SciGene Corporation, Sunnyvale/USA
Megafuge 1.0 R	Heraeus (Thermo Fisher Scientific),

	Langenselbold/Germany
Microcentrifuge 5415R	Eppendorf, Hamburg/Germany
Microscope Olympus IX70	Olympus, Hamburg/Germany
Microtiter plate 96 well, white	Nunc (Thermo Fisher Scientific), Langenselbold/Germany
Microtiter plates (96/24/6 well)	Nalge Nunc International, Rochester/USA
Microtiter plates 96 well, sterile, white with clear bottom	Becton Dickinson Labware, Franklin Lakes/USA
Multifuge® 3S-R	Heraeus (Thermo Fisher Scientific), Langenselbold/Germany
NanoDrop ND-1000	NanoDrop Technologies, München/Germany
Peristaltic pump 313S	Watson-Marlow, Birmingham/UK
pH meter 766 calimatic	Knick GmbH & Co. KG, Berlin/Germany
Pipet tips, sterile and Rnase free (10, 20, 100, 200, 1000 µl)	MolecularBioProducts, San Diego/USA
Pipets (2-1000 µl)	Eppendorf, Hamburg/Germany
Pipets, serological (5, 10, 25, 50 ml)	Nunc (Thermo Fisher Scientific), Langenselbold/Germany
Pipettboy	Hirschmann Laborgeräte, Eberstadt/Germany
Plastic tubes (15/50 ml)	Greiner Bio-One, Frickenhausen/Germany
QIAcube	Qiagen, Hilden/Germany
Reaction cups nuclease free (1.5/ 2 ml)	Eppendorf, Hamburg/Germany
Rotor adapters	Qiagen, Hilden/Germany
Round bottom plates 96 well	Bilatec AG, Viernheim/Germany
Scale Navigator	Ohaus, Giessen/Germany
Scale Sartorius BP211D	Sartorius, Göttingen/Germany
Sonoplus HD 3100	BANDELIN electronic GmbH & Co. KG, Berlin/Germany
Sterile work bench Herasafe	Heraeus GmbH, Hanau/Germany
Surgical instruments	Braun, Melsungen/Germany
Syringes	MT Braun, Melsungen/Germany
Theonyx Liquid Performer	AVISO, Jena/Germany
Thermosprint® PCR plates 96 well	Bilatec AG, Viernheim/Germany
Ultra pure water processing system Pure Lab Plus	ELGA, Celle/Germany
U-RFL-T Power SupplyUnit	Olympus, Hamburg/Germany
Vortex for Agilent Chips	IKA™ Werke GmbH, Staufen/Germany
Vortex Genie 2	Scientific Industries, Bohemia/USA
Water bath Julabo SW22	Julabo GmbH, Seelbach/Germany

2.5 Softwares

2100 Expert Software	Agilent Technologies, Waldbronn/Germany
BeadScan	Illumina Inc., San Diego/USA
Expressionist™ Analyst Pro 6.1	Genedata AG, Basel/Suisse
GenomeStudio V2009.1	Illumina Inc., San Diego/USA
IPA®	Ingenuity Systems, Inc., Redwood City/USA

3 Methods

3.1 Cell culture methods

3.1.1 Isolation of fresh primary rat hepatocytes

Primary hepatocytes were isolated using a modificated protocol of the two-step perfusion method described by Seglen [Seglen 1976]. During this in situ perfusion, the liver remaining in the anesthetized rat is flushed with two different buffers. The buffers are piped into the portal vein via a syringe which is connected to a peristaltic pump via flexible tubes. The connection of the pumping system with the organ is a very critical point since the original blood pressure of the organism should be sustained and pressure peaks must be prevented. Variations of the pressure in the organ disturb the physiology and especially high pressure can damage the hepatocytes since the organ is enclosed by a relatively stable capsule. In order to maintain the physiological pressure in the organ the syringe is connected with the pumping system at a very small flow rate and the inferior vena cava is opened shortly afterwards to let out the blood and the buffers. Then the flow rate is raised carefully.

The first buffer removes the blood from the vascular system of the liver. It is Ca^{2+} free and the containing ethylene glycol tetraacetic acid (EGTA) complexes the Ca^{2+}-ions remaining in the vascular system in order to loosen the intercellular adhesion since many cell-cell-adhesion molecules like Cadherins, Integrins and Selectins need Ca^{2+} as Co-factor. At the second step of perfusion the liver is flushed with a solution of Liberase TM (contains a medium concentration of Thermolysine). This enzyme is a blend of Collagenase I, Collagenase II and Thermolysine, a neutral protease, which digest the extracellular matrix of the liver tissue to release individual cells. Liberase blends are manufactured with different amounts of Thermolysine. A medium amount of this neutral protease (Liberase TM) resulted in a higher viability and functionality of the isolated cells than the usage of Liberase with a high concentration of Thermolysine (Liberase TH). Highly purified Liberase enzyme blends replaced the traditionally used collagenases since isoforms of highly specific activity combined with specific neutral proteases can be manufactured reproducibly without appreciable batch to batch variations.

The components for the perfusion buffers 1 and 2 (PB1, BP2) and the washing buffer (WB) were weighed according to Table 3.1 in 1l-beakers and solved in 800ml of

distilled water. The pH = 7.4 was justified with 1M NaOH using a pH meter. The neutralized buffers were sterile filtered and stored up to four weeks at 4°C.

Table 3.1: Components of perfusion buffer 1, perfusion buffer 2 and washing buffer.

Stock solution for PB1, PB2 and WB	
6.30 g	NaCl
0.32 g	KCl
0.27 g	$MgSO_4 \cdot 7\ H_20$
0.15 g	KH_2PO_4
1.81 g	$NaHCO_3$
3.58 g	HEPES
1.50 g	D-Glucose

Supplements		
PB1	0.038 g	EGTA
PB2	0.58 g	$CaCl_2$•2
WB	0.58 g	$CaCl_2$•2
	20.00 g	BSA

Male Wistar-rats were kept according to animal welfare regulations (Deutsches Tierschutzgesetz) and the perfusion was done with authorization from the local authorities (Approval-Nr. v54-19c20/15, DA4/Anz271E). The rats had free access to food and water and were kept at a constant temperature of 20°C and a light dark circle of 12h each. Rats with a body weight between 200g to 300g were anesthetized by a mixture of Ketanest S (10%) and Rompun 2% at a concentration of 100mg/kg body weight and 15mg/kg bodyweight, respectively. The anesthesized rats were fastened supine, the abdominal wall was opened and a syringe was inserted into the portal vein and fixed with a clamp. After that the syringe was connected to a pumping system and the liver was flushed with perfusion buffer 1 (PB1) with a flow rate of 50ml/min for two minutes and afterwards with a flow rate of 40ml/min for another three minutes to remove all the blood from the liver. The inferior vena cava was opened to enable the perfusion buffers to drain off. During this first step of liver perfusion the colour of the rat liver changes from reddish brown to gray.

At the second step the liver was rinsed with perfusion buffer 2 (PB2) containing Liberase TM (10mg/ 300ml) at a flow rate of 50ml/min for two minutes following five minutes at 40ml/min. The time needed for digestion of the extracellular matrix highly depends on the individual rat and is therefore to be controlled carefully. The perfusion was stopped after a fine network on the surface of the liver appeared and dents remained on the organ's surface when it was squeezed carefully with a finger. The liver was transferred into an ice cold washing buffer (WB), the liver capsule was opened and the separated cells were released. The washing buffer contained 2%

BSA which stops the enzyme activity of the Liberase blend to protect the isolated cells from digestion. The cell suspension was filtered through a coarse gaze to remove bigger cell clumps. To remove non-parenchymal and dead cells as well as the Liberase the cell suspension was centrifuged three times (43 x g, 4°C, 2min) while the hepatocyte pellet was resuspened very carefully in fresh ice-cold washing buffer to inhibit endogen proteases released from dead cells.

3.1.2 Trypan Blue exclusion test

Cell viability and cell number of isolated primary hepatocytes were assessed using the trypan blue exclusion test. Viable cells exclude trypan blue due to their intact cell membranes and appear uncolored, whereas dead cells are colored blue after the dye diffused into them.

25µl cell suspension was incubated with 1ml trypan blue solution (100µl trypan blue 0.5% + 900µl PBS) for three minutes at RT. After that viable and dead cells were counted in a Fuchs-Rosenthal-Chamber and the viability, the number of living cells per ml, as well as the total amount of viable cells were calculated. Cell suspensions with a viability greater than 85% were used for further studies.

$$Cells/ml = Cells_{Viable} \bullet D \bullet 5000 \qquad \%_{(Viability)} = \frac{Cells_{Viable}}{Cells_{Dead}} \bullet 100$$

D = Dilution Factor = 41

Figure 3.1: Formula for the calculation of vital cell concentration and cell viability.

3.1.3 Preparation of culture dishes

Primary rat hepatocytes are adherent cells which do not adhere optimally onto uncoated cell culture surfaces. They were cultured in two different culture systems: monolayer or sandwich culture. In the monolayer culture the cells are cultured onto a dried Collagen I layer. In this culture system the cellular functions remain stable for up to five days. After that the cells dedifferentiate, die and detach. In the sandwich culture the cells are cultured in between two layers of gelled collagen I which mimic the three dimensional structure of the liver tissue and the cell morphology and

function as well as the expression of main enzymes of the xenobiotic metabolism remain stable and near the in vivo level for up to four weeks.

3.1.3.1 Monolayer culture

The dishes for the monolayer cultures (ML) were coated by adding an acidic collagen I solution which was dried under sterile conditions over night (ON) or longer (Table 3.2).

Table 3.2: Coating scheme of culture dishes for monolayer culture.

Cell culture plate	Volume	Concentration	Time to dry
96 well plate	110 µl	20 µg/ml	2 d
24 well plate	125 µl	100 µg/ml	ON
6 well plate	600 µl	100 µg/ml	ON

3.1.3.2 Sandwich culture

In sandwich cultures (SW) cells were seeded onto a layer of gelled collagen. Therefore an ice-cold acidic solution of collagen I (1 mg/ml) was mixed with 10x DMEM-F12 media resulting in a final collagen-concentration of 900µg/ml and was then neutralized to a pH of 7.2 to 7.4 with a 1M sodium hydroxide solution. Cell culture plates were immediately coated with this neutralized collagen I solution (Table 3.3) and incubated in an incubator at 37°C for at least one hour to gelatinize the collagen.

Table 3.3: Volume of collagen I solution used for bottom and top layer of sandwich cultures.

Cell culture plate	Volume for bottom layer	Volume for top layer
24 well plate	75 µl	100 µl
6 well plate	250 µl	400 µl

3.1.4 Plating of cells

Freshly isolated and counted primary hepatocytes were mixed with plating media (DMEM/F12 medium supplemented with 10% (v/v) FBS, sodium pyruvate (100X), antibiotics (100X) and 5µg/ml insulin) and seeded onto the collagen I coated cell

culture plates (Table 3.4). The amount of cells is linked to the used plate format and did not vary between sandwich and monolayer cultures.

Table 3.4: Media volumes and amounts of cells used for cell seeding in monolayer and sandwich cultures.

Cell culture plate	Cells/ ml	Volume	Total number of cells
96 well plates	500 *10^3	80 µl	40 *10^3
24 well plates	500 *10^3	0.5 ml	250 *10^3
6 well plates	1 *10^6	1.5 ml	1.5 *10^6

Cells were allowed to attach to the culture surfaces at 37°C and 5% CO_2 in a humidified atmosphere for four hours. After that the cell culture media was changed. 24 hours after cell seeding the cell culture medium of the monolayer cultures was replaced by FBS-free medium (DMEM/F12 medium supplemented with sodium pyruvate (100X), antibiotics (100X), ITS (100X) and 100nM dexamethasone), cells were cultured in an incubator (37°C, 5% CO_2, humidified atmosphere) and experiments were started.

24 hours after seeding sandwich cultures were washed with ice-cold PBS and overlaid with a second layer of collagen I (Table 3.3). The collagen was allowed to gelatinize for one and a half up to two hours in the incubator before FBS-free cell culture medium was given on top of the collagen. Cells were cultured in an incubator (37°C, 5% CO_2, humidified atmosphere) and medium was changed every second day until experiments started at day three after cell seeding.

3.2 CellTiter-Glo® Luminescent Cell Viability assay

The CellTiter-Glo® Luminescent Cell Viability Assay was used to determine the viability of the cells after treatment with pharmaceutical substances. This test enables the quantitation of ATP in metabolically active cells based on a luciferase reaction (Figure 3.2) since the luminescence signal is proportional to the amount of cellular ATP. The amount of ATP is directly proportional to the amount of viable cells because they lose their ability to synthesize ATP soon after, e.g., loss of membrane integrity or other cytotoxic events. The protocol originally written for the use in the 96-well plate format was adapted to 24- and 6-well plates. The cells were incubated at

RT for ten minutes on a shaker with a 1:1 mixture of CellTiter-Glo® Reagent and DMEM-F12 medium without supplements. Three times 50µl cell lysate was transferred into a white 96-well plate to eliminate stray light, and the bioluminescence was measured. The cell viability was calculated as percentage related to the vehicle treated control.

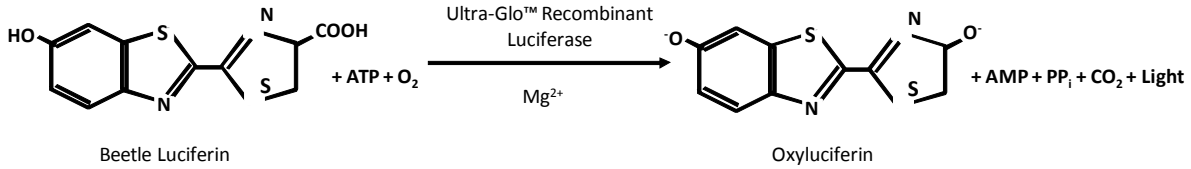

Figure 3.2: Chemical reaction of the CellTiter-Glo® Luminescent Cell Viability Assay.
The reagent contains recombinant luciferase that uses the likewise contained luciferin as a substrate and reacts under the consumption of cellular ATP with the release of luminescence [CellTiter 2009].

3.3 Molecular biological methods

3.3.1 RNA isolation

The RNA was isolated using the RNeasy Plus Mini Kit and the QIAcube from Qiagen (Figure 3.3). This kit enables a selective removal of double-stranded DNA via gDNA Eliminator Mini Spin Columns without the need of DNase digestion. After that the total RNA binds to RNeasy Mini Spin Column and contaminants are washed away efficiently which results in very pure RNA samples. The RNA isolation was run fully automated on the QIAcube to reduce error-proneness. Primary hepatocytes were treated for one, three or 14 days, respectively, with pharmaceutical substances in 6-well plate collagen I sandwich cultures. Then the cells were washed two times with ice-cold PBS and scraped in 3ml of RNAprotect Cell Reagent. The RNAprotect Cell Reagent stabilizes the RNA during cell harvesting and enables the separation of the RNA from the cells and the extracellular matrix by two additional centrifugation steps. The scraped cells were transferred to a 15ml centrifuge tube and centrifuged at RT for five minutes at 5,000 x g. The supernatant was aspirated, the pellet was resuspended in 5ml RNAprotect Cell Reagent by vortexing and centrifuged again for five minutes at 5,000 x g. The supernatant was aspirated and the pellet was loosened by flicking the tube. 350µl RLT Buffer Plus including 10µl β-Mercaptoethanol (β-ME) per 1ml were added and the pellet was dissolved by vortexing. The cell lysate was pipetted into a QIAshredder spin column and centrifuged two minutes at 16,000 x g at RT to homogenize the sample. During this

step high-molecular-weight cellular components and genomic DNA was sheared to reduce the viscosity of the sample and enable an efficient binding of the RNA to the RNeasy Mini Spin Column membrane since a high viscosity of the sample could reduce the resulting RNA yield. The eluate was stored at -80°C. Frozen lysates were incubated at 37°C for five minutes and all the further steps (gDNA elimination, RNA binding and washing) were performed using the QIAcube. The rotor adapters were filled with gDNA Eliminator Mini Spin Columns, RNeasy Mini Spin Columns and empty collection tubes. The concentrate of Buffer RPE was filled up with 44ml of 100% Ethanol.

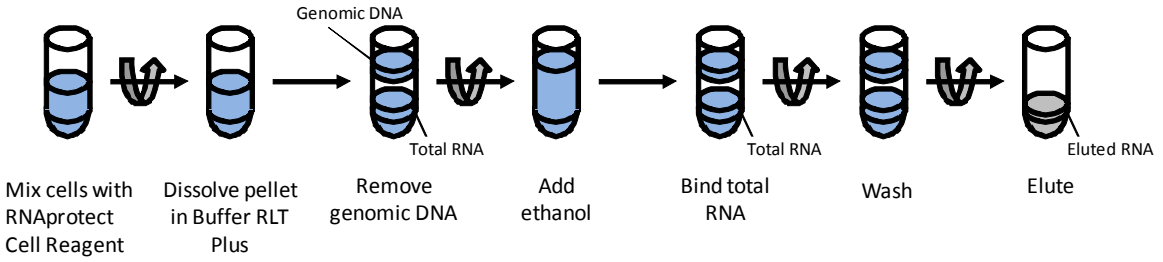

Figure 3.3: Workflow of the RNeasy protect cell mini kit. [RNAprotect 2010]

The QIAcube was loaded with the buffers RPE and RW1 as well as nuclease-free water, the samples, and the filled rotor adapters according to the manufacturer's recommendations. The RNeasy Plus Mini Kit protocol was started, the RNA was eluted in 40µl of nuclease-free water and stored at -80°C [RNAprotect 2010].

3.3.2 RNA quantification and quality check

The quantification of the RNA and cRNA was performed with the UV-spectrophotometer NanoDrop ND-1000. Therefore 1µl of the sample was given onto the measuring pedestal (Figure 3.4). After the instrument was closed two class fiber cables were connected by the sample and the absorption of a Xenon lamp's light during the passage of the sample was measured. The ratio between the absorbance at 260nm and 280nm is a dimensionless parameter for RNA purity while pure RNA yields a ratio of 2. Contaminations with protein and phenol decrease this ratio. The concentration of the sample was calculated using the absorption at 260nm and the modified Lambert-Beer-Law together with the molar extinction-coefficient [NanoDrop 2008]:

$$c = (A*e)/b$$

c: concentration of nucleic acid in ng/µl

A: absorbance in absorbance units (AU)

e: wavelength-dependent extinction coefficient in ng-cm/µl (RNA: e = 40)

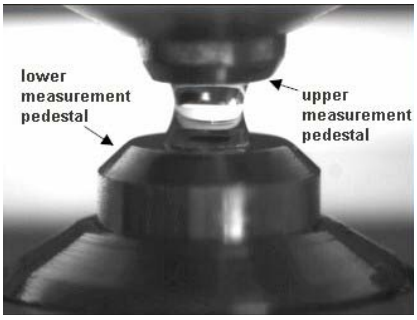

Figure 3.4: RNA quantification with the NanoDrop ND-1000.
The RNA is measured in 1µl sample which forms a drop of controlled thickness without the need of a cuvette [NanoDrop 2008].

The quality of the RNA and the cRNA was checked using the Lab-on-a-Chip technology from Agilent Technologies. This technology is based on capillary electrophoresis of up to twelve different samples in capillaries arranged onto a plastic chip. The RNA or cRNA is fractioned according to their length and detected by a fluorescent dye which is applicated in combination with the gel matrix. The 2100 Expert Software enables the visualization of the results as electropherograms or gel like pictures. A typical electropherogram of total RNA shows two peaks: the 18s and the 28s rRNA. The ratio of the 28s and the 18s is 2.0 or higher for RNA of high quality. The concentration of the samples is calculated based on the area under the curve of a RNA ladder. Furthermore the RNA Integrity Number (RIN) was automatically determined for each sample. The RIN is calculated based on the complete electropherogram and is therefore much better reproducible compared to the 28s/18s ratio. The RIN is ranged from one to ten while high quality RNA shows a RIN of ten and most degraded RNA a RIN of one, respectively (Figure 3.5) [Agilent 2011].

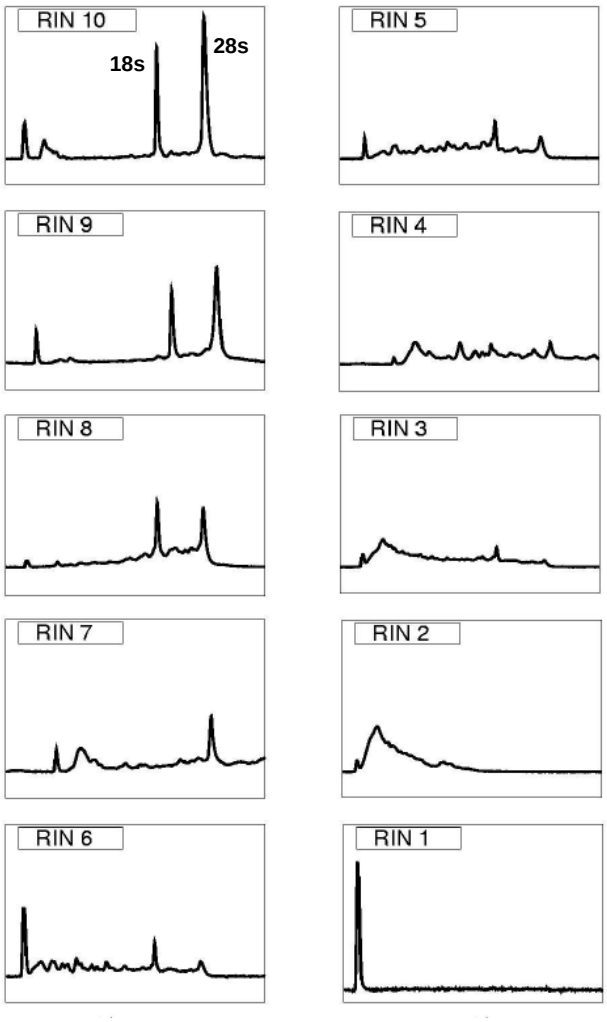

Figure 3.5: Reference electropherogrames for the different RNA integrity categories.

The RIN categories reach from ten (high quality) to one (completely degradated). A decrease in quality results in a shift towards shorter nucleotide fragment. X-axis = time, Y-axis = fluorescence [Schroeder 2006].

The quality check of the samples was performed using the Agilent RNA 6000 Nano Chip and the Agilent RNA 6000 Nano Kit which allows the parallel measurement of twelve samples. 550µl Agilent RNA 6000 Nano Gelmatrix were spun for ten minutes at 1,500 x g and RT in a centrifugation filter tube. 65µl of the filtered gel were mixed with 1µl RNA 6000 Nano dye concentrate, vortexed, and centrifuged for ten minutes at RT and 13,000 x g. 9µl of the gel-dye-mixture were added to the well named with "G" at the bottom of an Agilent 6000 RNA Nano Chip. The capillaries of the chip were filled with the gel-dye-mixture with the help of the Priming station for 30sec. After that both top wells named with "G" were filled with 9µl of the gel-dye-mixture and 5µl of RNA 6000 Nano Marker were given to every sample well as well as to the ladder well. The samples and the ladder were denatured for two minutes at 70°C and 1µl per sample or ladder, respectively, was added to the appropriate wells. The chip was vortexed for 60sec at 2,400rpm and measured with the Agilent Bioanalyzer [Agilent 2006].

Biotinylated cRNA shows a very different electropherogram (Figure 3.6) since the amplification process results in a mixture of fragments of various lengths over a wide region with a peak between 1,000 to 1,500nt.

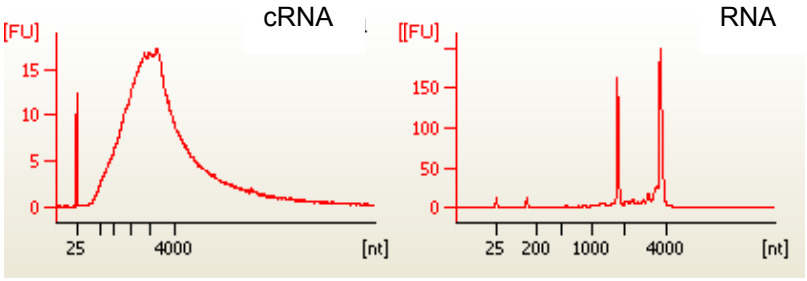

Figure 3.6: Electropherograms of cRNA and total RNA.
The electropherograms differ from each other since during the amplification process a mixture of fragments is processed.

3.3.3 The Illumina Technology

The Illumina Sentrix® BeadChip technology was used to perform whole gene expression analyses. Therefore the isolated total RNA was transcribed by a first and a second strand synthesis step into cDNA followed by an in vitro transcription amplification that incorporates biotin-labeled nucleotides. The labeled cRNA was then hybridized to gene specific probes onto an Illumina Sentrix® RatRef-12 Expression BeadChip (Figure 3.7). Twelve samples could be measured in parallel per chip and each chip contains 21,910 probes of the rat genome which was chosen with the help of the National Centre for Biotechnology Information (NCBI) Reference Sequence Database and UniGene based on parameters like inequality to other gene sequences and lack of repetitive genomic sequences.

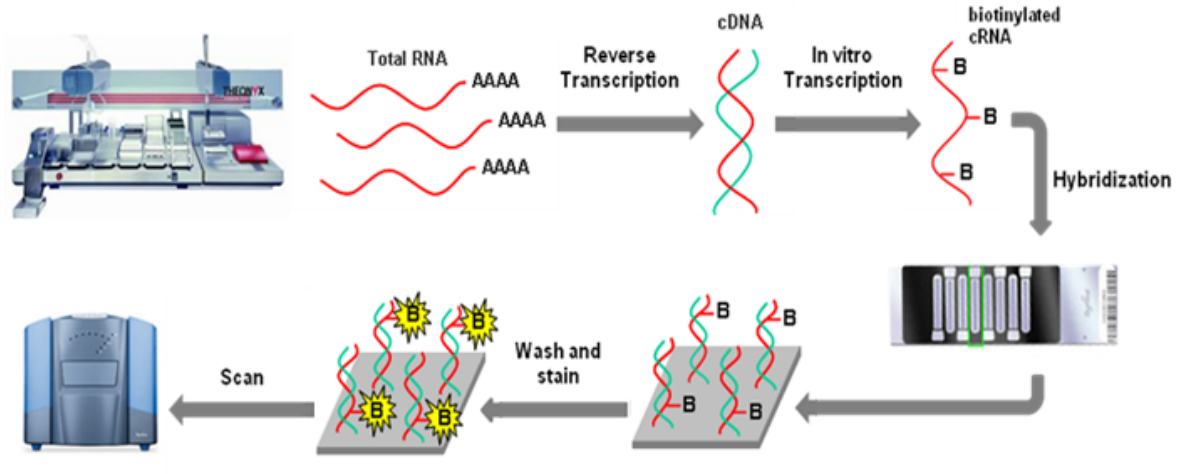

Figure 3.7: The different steps of gene expression analysis with Illumina Sentrix® BeadChips.

The 50-mer gene specific probes are linked to a 29-mer address sequence which is covalently bound to a bead (Figure 3.8). Each bead type contains approximately 10^8 copies of the gene-specific sequence and is present 30 times per array. The high amount of copies of the gene-specific sequences as well as the high abundance of the various bead types are internal technical replicates and guarantee a high reproducibility and good stability of the system.

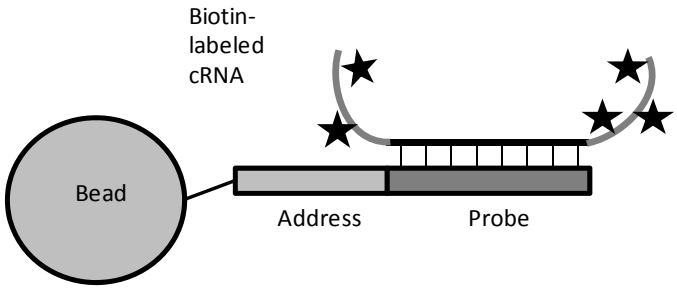

Figure 3.8: The Direct Hybridization Assay from Illumina.
Beads are immobilized onto glass chips and bound to an address sequence which is linked with a 50-base gene-specific probe where the sample derived biotinylated cRNA is hybridized to [Illumina 2011].

The beads are arranged randomly in small plasma etched wells onto silica slides and held there by Van der Waals forces and hydrostatic interactions with the well (Figure 3.9). Because of that every array must be decoded by an individual algorithm which identifies the position of every bead or transcript, respectively, based on the specific address sequence [Gunderson 2004].

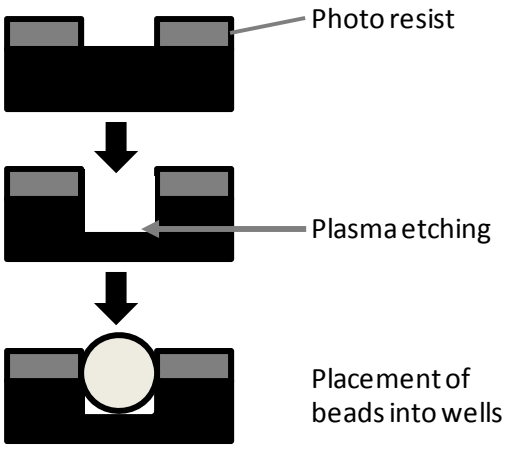

Figure 3.9: Manufacturing of Illumina Sentrix® BeadChips.
The beads are placed into wells which were etched into the chip's surface [Illumina 2011].

3.3.3.1 cRNA Synthesis from total RNA

The isolated total RNA was transformed into biotinylated cRNA during different steps with the Illumina®TotalPrep™-96 RNA Amplification Kit from Ambion (Figure 3.10). The reactions were performed fully automated in 96-well plates with adapted volumes using the Theonyx Liquid Performer robot to standardize the process optimally including magnetic-bead based purification of both the cDNA and the cRNA which reduces the elution volumes and enables sample processing in 96-well plates. 500ng total RNA per sample were reverse transcribed into first strand cDNA. Therefore the RNA was diluted with nuclease-free water to a concentration of 45.45ng/µl and 11µl of the diluted RNA per well were given to a thermosprint 96 well plate and placed onto the cooled pipeting station of the robot. The master mixes for the first and second strand cDNA synthesis were set into the appropriate cooled positions. The robot added 9µl of the first strand master mix (Table 3.5) to each sample, mixed the solution and incubated the plate for two hours at 42°C in a thermocycler. After that 80µl of the cDNA second strand master mix (Table 3.5) was given to each sample and the plate was incubated another two hours in the thermocycler at 16°C. The double stranded cDNA was purified using magnetic beads which bind the cDNA. Therefore the samples are transferred to a round bottom 96-well plate and 180µl of the magnetic bead solution were added. The magnetic beads sink to the bottom of the multiwell reaction plate attracted by a magnet and build a ring around the middle of the well so that the supernatant could be aspirated completely by pipetting into the centre of the well. The beads were washed three times with 200µl ethanol 70%. The cDNA was released from the beads by adding 20µl of nuclease free water and shaking at 1,500 rpm and was transferred into a fresh thermosprint plate. The master mix for the in vitro transcription (IVT) (Table 3.5) was given to the appropriate cooled position, the robot added 7.5µl of this master mix to every sample and incubated the plate for 14h at 37°C in the thermocycler to synthesize biotinylated cRNA using biotinylated UTP nucleotides. The cRNA is purified the same way like the cDNA using magnetic beads but ethanol 80% and eluted with 40µl of nuclease-free water by shaking at 1,500 rpm. The quality of the cRNA was checked using the Agilent RNA 6000 Nano Kit. The cRNA was quantified with the NanoDrop 1000 and stored until the next working step at -80°C.

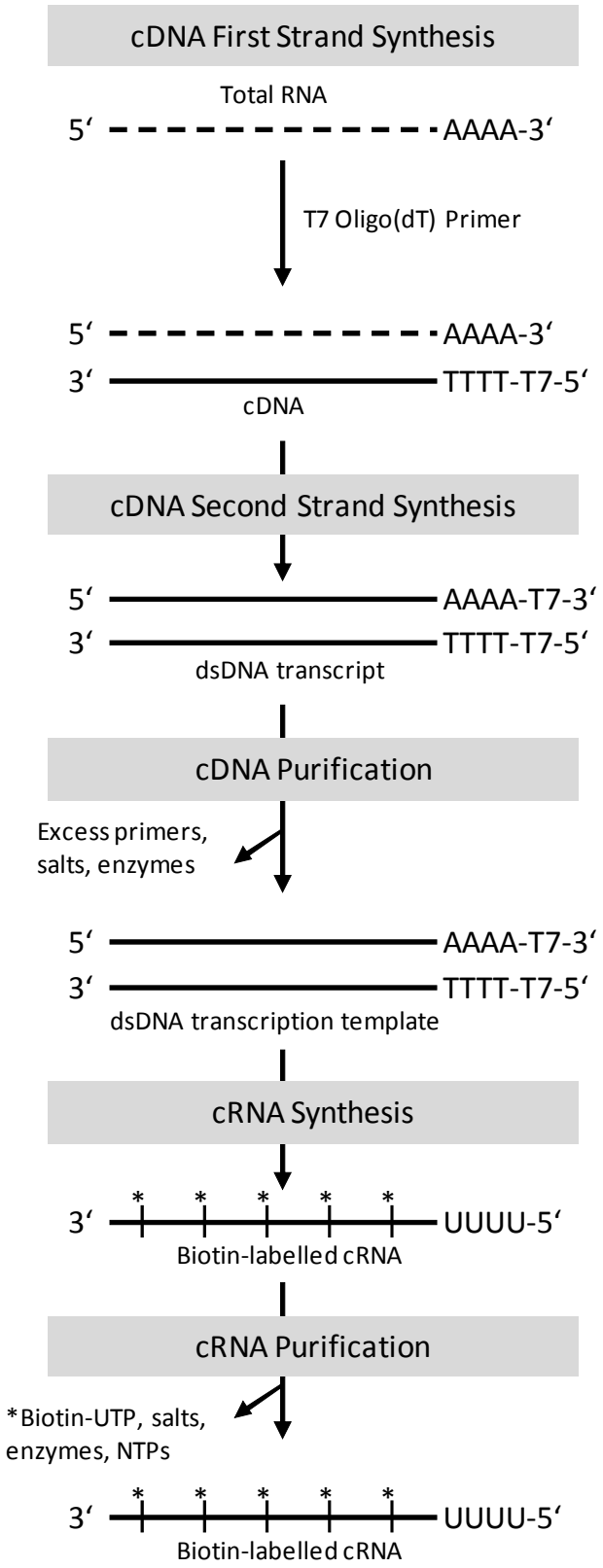

Figure 3.10: Workflow of the Illumina® TotalPrep™-96 RNA Amplification Kit from Ambion to synthesize biotinylated cRNA from total RNA [Illumina 2010].

Table 3.5: Composition of the master mixes and purification solutions used for the cRNA synthesis .[Illumina 2010]

Master mix	Component	Volume/sample (µl)
1st strand	T7 Oligo(dT) Primer	1.1
	10x 1st Strand Buffer	2.2
	dNTP mix	4.4
	RNase Inhibitor	1.1
	Reverse Transcriptase	1.1
2nd strand	10x 2nd Strand Buffer	11.0
	dNTP mix	4.4
	DNA Polymerase	2.2
	Rnase H	1.1
	nuclease-free H_2O	69.3
IVT	10x Reaction Buffer	2.75
	Biotin-NTP Mix	2.75
	T7 Enzyme Mix	2.75

Master mix	Component	Volume
cDNA purification	magnetic beads	7ml + 220µl/sample
	nuclease-free H_2O	3ml + 60µl/sample
	70% Ethanol	3ml + 800µl/sample
cRNA purification	magnetic beads	7 ml + 120µl/sample
	nuclease-free H_2O	3 ml + 135µl/sample
	80% Ethanol	3 ml + 800µl/sample

3.3.3.2 Hybridization of cRNA to Illumina® BeadChips

For the hybridization the biotinylated cRNA is diluted with nuclease-free water to a concentration of 750ng in 5µl and mixed with 10µl of hybridization buffer (GEX-HYB buffer) in a 96-well thermosprint plate and incubated at 65°C for five minutes to denaturate the cRNA. The reservoirs of the hybridization chambers were filled with 200µl of humidifying buffer (GEX-HCB) and 15µl of each sample were pipeted into the sample port of the appropriate array. The chips were placed into the hybridization chambers and incubated for 20 hours at 58°C in the hybridization oven with rocker speed at five. After that the chips were transferred into a bath of E1BC Buffer, their plastic coverseals were removed carefully under the liquid's surface and the chips were collected into a chip rack standing in the same buffer (Table 3.6).

Table 3.6: Preparation of the different buffers used for hybridization of cRNA onto Illumina® BeadChips.

Working solution	Compound 1	Compound 2
High Temperature Wash Buffer	70ml 10X Stock	630ml RNAse-free water
E1BC Buffer	2.4ml Stock	800ml RNAse-free water
Streptavidin-Cy3 Stain	200µl Stock (1mg/ml)	200ml Block E1 Buffer

The following washing and dying steps were performed with the Little Dipper® Processor for Illumina® BeadChips. The robot's different bathes were filled according to the scheme in Table 3.7, the magnetic stirrers of all the bathes were set to a speed forming a vigorous vortex, bath one was heated to 55°C and the centrifuge was balanced with eight reference chips. Running the Bead2 protocol the robot dipped eight chips at a time standing in a chip rack for a fixed time at a specific frequency in turn into different washing solutions (High Temp Buffer, E1BC Buffer, Ethanol 100%), blocking buffer (Block E1), Streptavidin- Cy3 staining solution and a final washing step with E1BC Buffer. The robot dried the stained chips by centrifuging. After that the chips were stored in the dark at RT.

Table 3.7: Overview of the buffers and parameters of the different steps of the Little Dipper's™ Bead2 Protocol for processing of Illumina® BeadChips after the sample hybridization.
[Little Dipper 2008]

Step	Buffer	Temperature	Agitation (cycles/min)	Time (sec)
1	High Temp	55°C	250	600
2	E1BC	RT	250	300
3	Ethanol	RT	250	600
4	E1BC	RT	250	120
5	Block E1	RT	50	600
6	Strep-Cy3	RT	50	600
7	E1BC	RT	250	300
8	Centrifuge	RT	-	300

3.4 Gene expression analysis

3.4.1 Quality control of microarray data

After BeadArray chips are scanned first of all the quality of the data must be checked. Therefore Illumina included six different internal controls for each chip which can be analyzed using the software GenomeStudio from Illumina. These controls contain sample-independent features using oligonucleotides as part of the hybridization

buffer which indicate general problems during the process of hybridization, washing and staining as well sample-dependent features which indicate problems with the sample itself or the labeling process.

For the control of the hybridization process each chip contains two different sets of probes. The first set bind special oligonucleotides in the hybridization buffer with high stringency (perfect match, PM) while the other set binds them with very low stringency (mismatch, MM) due to a slightly modified sequence and should therefore show a lower signal intensity than the PM. The staining process is checked via biotin-controls in the hybridization buffer which show a high signal after a successful staining. Furthermore the control set includes negative controls which should not bind to any probes and are used to define the level of the background signal and the limit of detection. The sample-dependent controls are based on the signal of different species-specific housekeeping genes which are contained in every sample independent from the used tissue or cell type. The signal intensity of these housekeepers should always be higher than the signal of all the other genes.

GenomeStudio provides different tools for a more detailed quality control. The visualization of the total number of detected genes or the signal-to-noise ratio of every single array enables the detection of outliers. Further possibilities for the search of outliers are box and scatter plots which visualize the data distribution. [Illumina-TN 2010]

3.4.2 Normalization of microarray data

For the comparison and the common analysis of a number of chips the data have to be normalized. In this way systematic errors, differences during the synthesis of the cRNA, the hybridization, the washing and staining of the chips which could be caused by processing of the chips at different time points could be compensated. The normalization and further statistical analysis of the gene expression data was performed with the software Expressionist providing several methods. The normalization method has to be adapted to the property of the data. Therefore the distribution of the data is visualized (Figure 3.11) using log-log-plots (scatter plots).

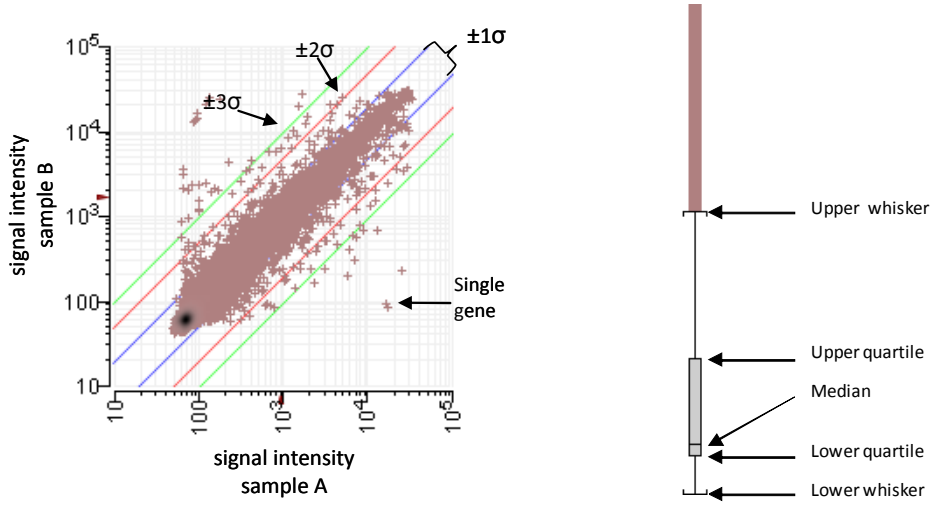

Figure 3.11: Visualization of the data distribution with scatter and box plots.
Scatter plots (left) plot the signal intensity of every single gene of two different samples against each other and show the standard deviation of resulting data cloud. Box plots visualize the median and the quartiles for a single sample.

If these plots show a shift of the data's cloud parallel to the central line linear methods like the Central Tendency normalization could be used which shifts the median of each array to a common target value. Thereby the distances between the single gene's signals are not altered so that this normalization makes the data of different chips comparable without influencing the individual data or the results. If the data's cloud is curved non-linear methods like LOWESS (Locally Weighted Polynominal Regression) have to be used for normalization. LOWESS normalizes the data to a reference data set using a complex algorithm and should be performed with pre-normalized data (linear method) since the method is sensitive towards outliers [Expressionist 2011].

3.4.3 Fold change calculation and statistics

The change of the gene expression level of treated cells relative to the vehicle control is expressed via the fold change. The fold change was calculated using the Relative Normalization while each sample was compared to its time-matched control which is set equal to one. The statistical significance of the gene expression changes was calculated using a paired Student's t-test. This test calculates the p-value as the probability of the difference between the gene expression level of the sample and the control. Genes with $p \leq 0.05$ were used for further analyses which means a probability of ≥ 95% that the gene expression of the sample differs from the control's

expression level [Engesser 1991]. A second evaluation criterion for the statistical significance was the false discovery rate described by Benjamini and Hochberg (BH-Q-value) which estimates the proportion of false discoveries in the given test set of discoveries [Benjamini 2001]. A BH-Q = 0.3 for example describes a probability of 30% that the given discovery is false positive.

3.4.4 Data visualization with Expressionist™

The software Expressionist™ provides several tools for the visualization of the results of gene expression analyses. The Principal Component Analysis (PCA) exhibits a multivariate statistical technique displaying each single experiment as one spot in a three-dimensional diagram (Figure 3.12). Therefore underlying algorithms reduce the dimensionality of the data set to three new variables (principal component 1 to 3) regarding the most dominant differences of the single experiments. Each principal component is a linear combination of the original variables and the three principal components together account for as much of the variance in the original amount of variables as possible. The PCA visualizes samples of very similar expression profiles closer together than samples of more different expression profiles. So the PCA is well suited for a first overview of a data set, for the detection of outliers, and furthermore indicates experimental conditions, e.g. compound, dose, and time of treatment, which affected the gene expression profile of the appropriate samples [Expressionist 2011, Raychaudhuri 2000].

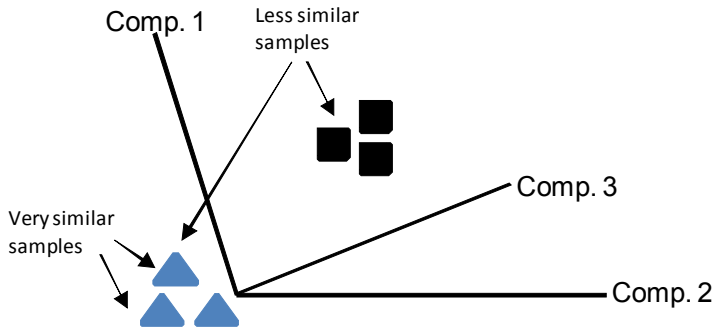

Figure 3.12: The Principal Component Analysis (PCA).
The PCA clusters samples based on their differences in gene expression in a three-dimensional space while very similar samples clusters closer together than samples of different expression levels.

Gene expression changes can be further visualized using the Heat Map where the fold changes are encoded with the colors black, red and green. The color depth increases with the fold change while green codes for downregulation, red for upregulation and black for non-deregulated expression levels [Expressionist 2011].

3.4.5 Biological data interpretation

The lists of significantly deregulated genes ($p \leq 0.05$) were transferred from Expressionist into the software Ingenuity Pathway Analysis (IPA). The background of IPA is a database including information about genes, proteins, RNA and chemicals (including pharmaceuticals), their interaction with each other and alterations during diseases or treatment with pharmaceuticals or chemicals as well as several detailed physiological pathways like, e.g., lipid metabolism. This information is available for several species and is updated weekly to the state of the art in science. Therefore Ingenuity cooperates among others with the FDA, leading journals and databases like Entrez Gene, KEGG, Clinicaltrials.gov and many more. Based on this information the uploaded gene expression data (fold changes) is matched with biological (= physiological, e.g., carbohydrate metabolism) and toxic (= adverse effects, e.g., hepatocellular carcinoma) functions as well as canonical pathways (e.g. carbohydrate metabolism). Complete pathways can be visualized including the deregulated genes which are colored red or green when they are up- or downregulated, respectively. The functions and pathways are ranked related to the number of genes which can be matched with.

IPA furthermore calculates a ratio for pathways by dividing the number of matched genes by the total number of genes making up the pathway. This enables a detection of the pathways most affected by the appropriate data set. Additionally IPA calculates a p-value for pathways and functions taking into consideration the total number of genes and associated functions or pathways in a reference set. The p-value describes the probability of a target's association with a pathway or function while a small p-value implies a high probability [IPA 2011].

4 Results and discussion

4.1 Establishment of sample processing for metabolomics, proteomics, genomics and kinetics

The final studies could not be performed until the sample preparation protocols for the different analytical methods had been established. With the exception of the whole genome gene expression protocol, well-described in the methods chapter, all the analyses were performed by other project partners. Since these analyses had not been finished at time of writing and the results are not part of the present study, only the challenges in establishing the sample preparation are discussed in this chapter.

A common problem for all the analytical laboratories was the high content of collagen I in the samples. Heidebrecht et al. [Heidebrecht 2009] developed a method which enables the separation of collagen from sandwich cultured cells by centrifugation. However, this method could not be established during the present study. Despite varying the centrifugation time and g-force of the original protocol, the resulting cell pellet always was stuck to a cord of collagen. The pellet had to be cut from the collagen string manually, a procedure not suited to the parallel processing of the large number of samples expected in the final studies of the present work. A further idea, the enzymatic digestion of the collagen followed by the separation from the living cells, was also considered. However, this procedure was never tested due to various issues. Firstly, a similar method was performed during another in house project resulting in traces of the digesting enzyme and remaining collagen during gel electrophoresis. Secondly, the enzyme activity and time of digestion for this procedure is very critical since the cells could also be enzymatically attacked. Finally, the method was too labor intensive in the context of the present project.

During proteomics analysis it was not feasible to distinguish if the Collagen I peptide identified was from the cellular protein or from the collagen I applied to the cell culture plate. This had a direct consequence on the validity of data interpretation since aliquots were taken for total protein content determination for the normalisation of the Omics data. In addition, especially for MS and HPLC analysis, sample spectra contained huge peaks representing components of the collagen gel, such as phenol red and acetate. In the end, most of the measurement procedures were optimized such that these peaks did not mask other essential peaks.

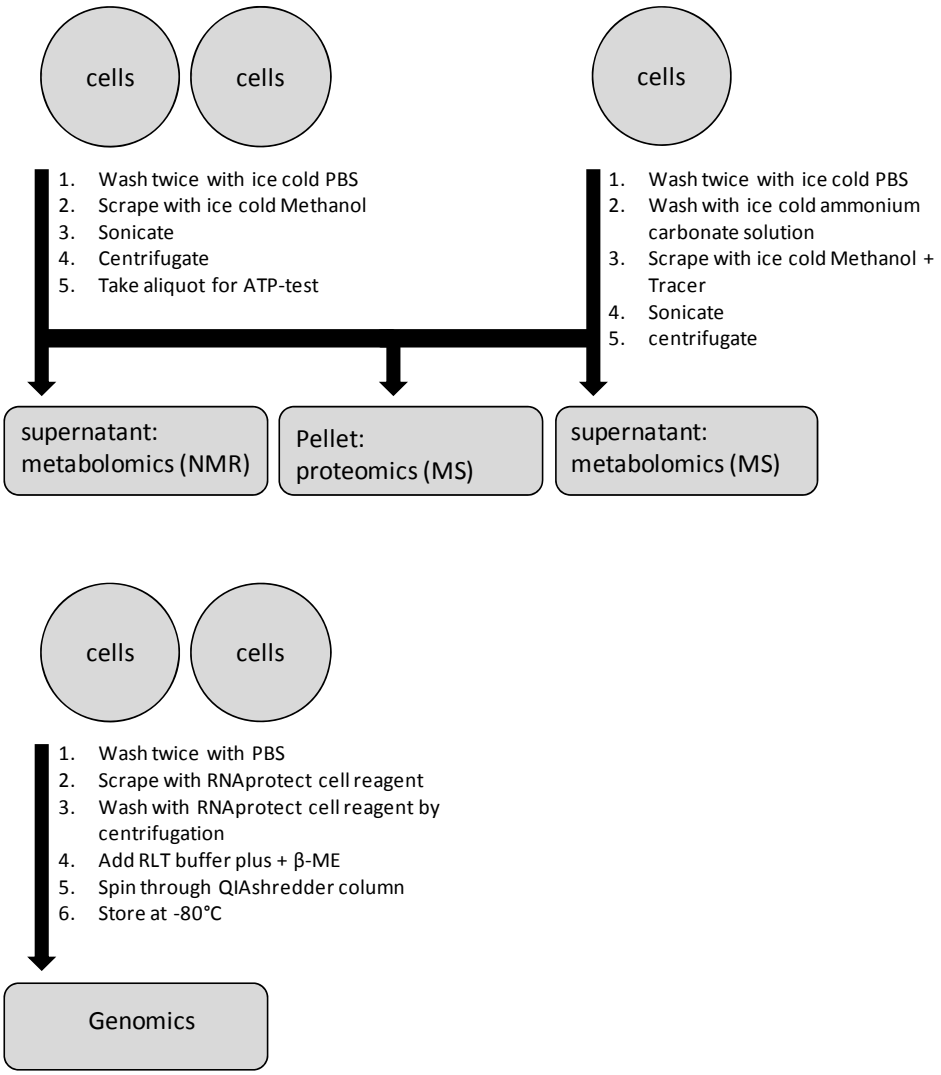

Figure 4.1: Schema of sample preparation for the different endpoint measurements.
[Predict-IV 2011a]

Preliminary sample preparation studies were conducted for all necessary endpoints. Before the final protocols for sample preparation (Figure 4.1) were fixed, draft protocols were developed in cooperation with the analytical laboratories and the following parameters were varied until satisfactory results could be measured:

- Solutions used for cell washing
- Solutions and liquid volumes used for cell scraping and lysis
- Time and strength of sonication
- Tubes used for sample preparation, transport and storage
- Number of technical replicates for test compounds and controls

The Predict-IV consortium decided that the kinetics data would be normalized to the DNA content of the treated cells, since sandwich cultured cells could not be detached and counted. The DNA was quantified with the Quant-iT™ PicoGreen® dsDNA Kit from Invitrogen™ which selectively stains double-stranded DNA with a fluorescent dye. The challenge during the establishment of this assay was the correct performance of the calibration curve. Since not all of the freshly isolated cells seeded onto a cell culture plate attached, the resulting adherent cell cultures contain a variable number of cells. Therefore, it was necessary to run the calibration curve using freshly isolated cells in suspension.

Test experiments showed that the solution used for cell lysis heavily influenced the DNA quantification. Therefore, defined numbers of fresh hepatocytes were mixed with the appropriate amount of collagen used for one well of the sandwich culture and the appropriate volume of methanol as used for the kinetics protocol. Then the mixture was sonicated according to the protocol for kinetics sampling and the DNA content was quantified. The resulting calibration curve was used for the calculation of the DNA content of the adherent cells, and included an optimal dilution.

4.2 Establishment of the CYP characterisation assays

For every donor the basal expression, as well as the inducibility of several phase-I, II, and III enzymes, was estimated using a mRNA assay (QuantiGene® Plex 2.0 Assay from Affymetrix, Figure 4.2). Additionally, the activity of two CYPs was measured by monitoring the metabolism of an appropriate, specific substrate. At the time of writing, these studies have not been finished. The samples from all donors have been collected and stored, but will only be measured in parallel after the last Predict-IV study is finished. Therefore, the establishment of these two methods is described herein in their entirety.

The QuantiGene® Plex 2.0 Assay was performed with a customized probe panel containing major CYPs, UGT, transporters and transcription factors involved in drug metabolism as well as three housekeeping genes. The housekeeping genes were selected out of a group of candidate genes tested in primary rat hepatocytes treated with the prototypical CYP inducers Dexamethasone (Dex; CYP3A), Pregnane

carbonitrile (PCN; CYP3A), Phenobarbital (PB; CYP3A/2C) and 3-Methylcholanthrene (3MC; CYP1A2) [Hewitt 2007, Richert 2009].

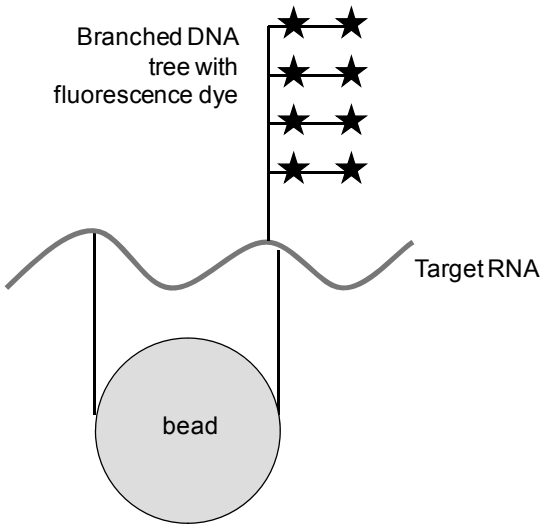

Figure 4.2: QuantiGene® Plex 2.0 Assay.
The QuantiGene® Plex 2.0 Assay was used for the expression and induction analysis of genes coding for enzymes, transporters, and transcription factors involved in drug metabolism. The target RNA was captured by target-specific beads and the signal is amplified by a tree built up with short DNA sequences which carried a fluorescent dye [Panomics 2008, modified].

The selection criteria were (1) stable expression over time, (2) no expression changes by cell treatment and (3) expression level similar to target genes of the customized panel. During the final studies, cells from every biological replicate in 96-well plate monolayer culture were treated daily for three days with Dex, PCN, 3MC or PB. Subsequently, the cells were lysed by incubation with an appropriate cell lysis mixture and stored at -80°C. The QuantiGene® Plex 2.0 assay started with an in situ hybridization of the target RNA in the cell lysate. The target RNA is captured by target-specific magnetic beads, followed by a signal amplification using the branched DNA technique. Finally, a fluorescent dye is bound and the signal intensity of the different targets is measured by a method similar to flow cytometry. A set of two lasers detect the target-specific beads as well as the signal intensity which is proportional to the number of bound target RNA molecules [Panomics 2008]. Using this assay, the donor-specific basal expression and inducibility of major drug-metabolizing enzymes as well as transporters and transcription factors involved in drug metabolism was estimated.

The enzyme activities of two major CYPs were measured for every donor. Cells in 6-well plate monolayer culture were treated for 30, 60, and 90 minutes with different

concentrations of CYP specific substrates: midazolam (CYP3A; 2, 10, and 20µM), testosterone (CYP3A; 50, 100, and 250µM) and phenacetin (CYP1A; 2, 20, and 80µM) [´t Hoen 2001, Kobayashi 2002, Hewitt 2007, Richert 2009]. The concentration of the the parent substrate and metabolites in the cell culture medium was measured by a cooperating group using specific HPLC methods. Based on the total protein content of the cells measured with the Bradford Assay, the amount of substrate metabolised per minute per milligram of protein was calculated. Although the measurement of the 6β-hydroxylation of testosterone is commonly used to calculate the activity of rat CYP3A [Richert 2009], the appropriate metabolite was not detected in any donor. Midazolam and phenacetin were metabolized into 1-hydroxymidazolam and acetaminophen, respectively. Based on this preliminary experiment an incubation time of 60 minutes and substrate concentrations for subsequent studies were fixed (Midazolam: 10µM; Phenacetin: 20µM).

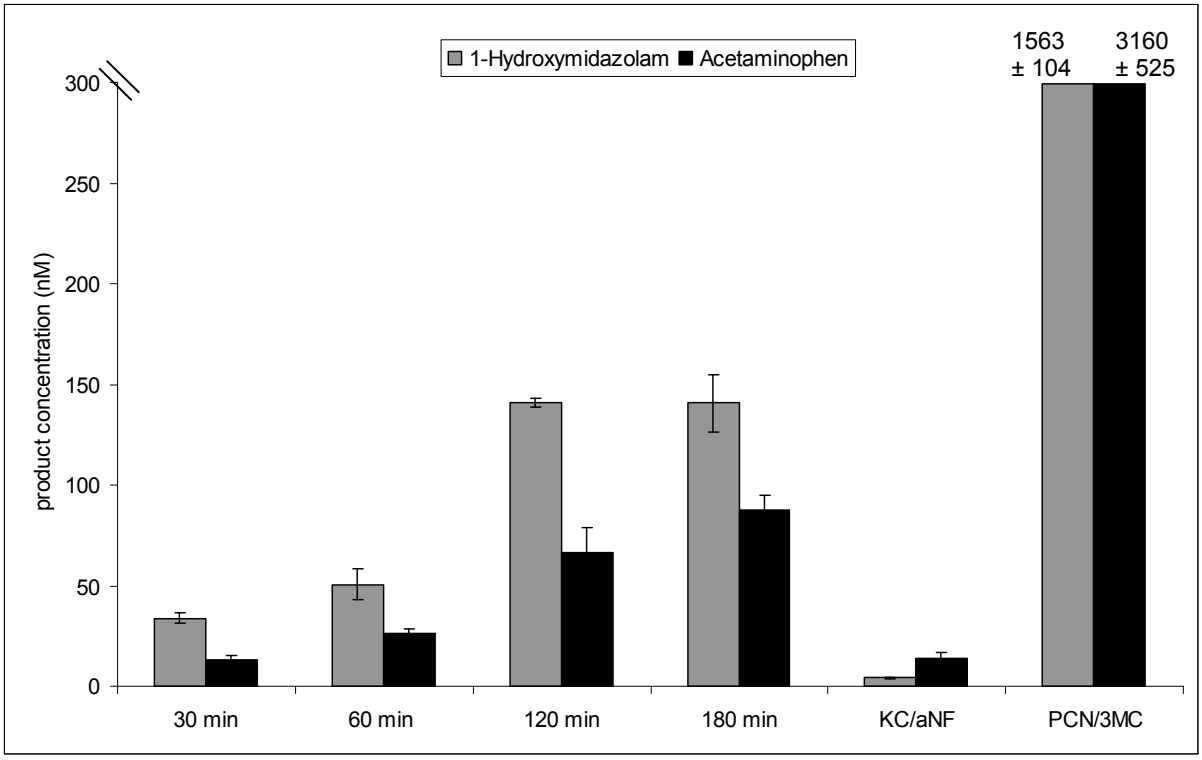

Figure 4.3: Preliminary study for the establishment of CYP activity measurement.
Primary rat hepatocytes were treated with 10µM midazolam and 20µM phenacetin. The concentration of the products 1-hydroxymidazolam and acetaminophen were measured by HPLC at different time points. CYP3A and CYP1A were inhibited by 30 minutes pre-treatment with 10µM ketoconazole (KC) and 1µM α-Naphthoflavone (aNF) which markedly decreased the detected product concentration after incubation for one hour. Pre-treatment with the CYP inducers pregnane carbonitrile (PCN; 10µM) and 3-Methylcholanthrene (3MC; 5µM) for three days heavily increased the product production after one hour incubation. n = 3.

The linearity of the CYP reaction over time was demonstrated throughout a range of cell treatments from 30 to 180 minutes. After 120 minutes the production of Acetaminophen increased less strongly while the synthesis of 1-Hydroxymidazolam reached a plateau (Figure 4.3). Thus, the most sensitive measurement was observed after a 60 minute incubation. Inhibition of CYP activity was shown after pre-treatment of the cells for 30 minutes with the CYP inhibitors ketoconazole (CYP3A; 1, 10, and 50µM) [Brown 2007, Hewitt 2007] and α-naphthoflavone (CYP1A; 1, 10, and 50µM) [Liu 2009, Shi 2011] followed by addition of the substrate and incubation for one hour. The metabolism of midazolam was markedly decreased, while the synthesis of Acetaminophen was slightly diminished. This suggests a less effective inhibition of CYP1A or the involvement of other enzymes or isoforms in the metabolism of Phenacetin. Finally, the cells were pre-incubated for three days with known CYP-inducers: PCN (CYP3A; 10µM), Dex (CYP3A; 50µM) and 3MC (CYP1A; 5µM), respectively. During this experiment the metabolism of both substrates was markedly increased. In conclusion, the CYP inhibition and induction studies indicated a specific metabolism of midazolam and phenacetin by CYP3A and CYP1A, respectively. Therefore, the established assays are well suited for the determination of the activities of these CYPs.

4.3 Dose finding

During the final studies, the cells were treated with two different doses of each reference compound. The high dose was defined to be the TC10 while the low dose was selected to be 1/10th of the high dose. In order to define the TC10 for the seven test compounds a dose finding study with three different steps was performed. Firstly, a pre-screening of a wide range of concentrations was conducted over a short time in 96-well plate monolayer culture. The large number of different compounds and doses could be only handled in the 96-well plate format which is incompatible with the sandwich culture. Based on the results of the pre-screening five to eight concentrations of each compound were selected for the subsequent long term study in a 24-well plate sandwich culture. This cell culture format enabled the use of the sandwich culture system as well as the measurement of several different doses and compounds in parallel. Finally, three doses around the TC10 were tested during the dose validation study in the 6-well plate sandwich format, the culture system which

was also used for the final studies (Figure 4.4). Finally, the high doses for the main studies were determined.

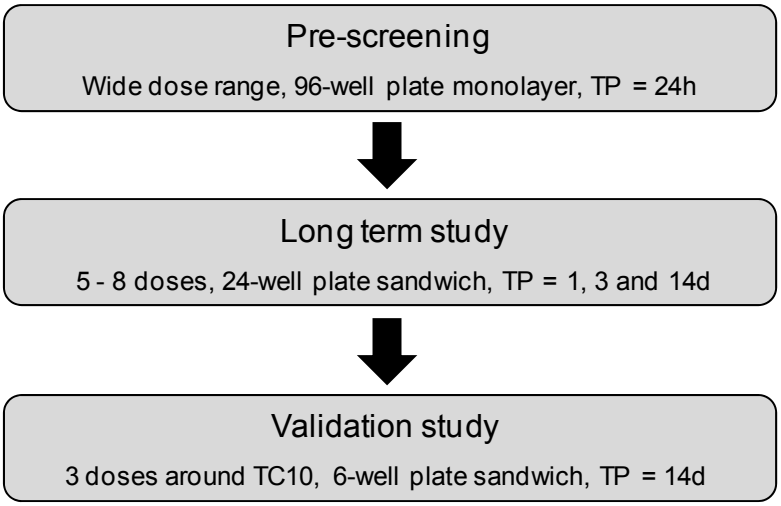

Figure 4.4: Schema of the different steps of the dose finding study.
TP = time point of cell viability measurement

4.3.1 Prescreening and dose selection for long-term dose finding study

In order to get an overview of the cytotoxic potential of the different test compounds the seven compounds were screened in a 96-well plate monolayer culture with one biological replicate and three technical replicates over a wide dose range (Table 4.1). This cell culture system was used since monolayer cultures are well suited for short term cytotoxicity tests and the 96-well plate format needs a smaller number of cells, media, and test compound than bigger formats. For this first screening the doses were selected based on historical unpublished in-house data. Stock solutions were prepared at 200-fold concentrations in DMSO and DMEM-F12; 0.5% DMSO was used as vehicle control to enable treatment with very high doses, since the highest doses of fenofibrate, valproic acid and acetaminophen were near to the limit of solubility in medium. The cells were treated once for 24 hours one day after cell seeding and cell viability was calculated by ATP quantification.

Based on the results of the 24h-pre-screening the doses for the long-term dose finding study were selected in order to cover the range of cell viability between 100% and 0% of vehicle control. For the generation of results which allow a robust definition of the TC10, it was necessary to choose enough doses spread uniformly over the entire cell vitality range. Furthermore, the increments between the individual concentrations had to be small enough to be able to recognize any rapid decrease in

Table 4.1: Results of the 24h-pre-screening.

Primary rat hepatocytes in 96-well plate monolayer cultures were treated with a wide dose range of the seven test compounds. After 24h the cell viability was calculated as percent of vehicle control by quantification of ATP. SD: standard deviation.

Acetaminophen												
dose/µM	20000	10000	5000	2000	1000	500	200	100	50	25	10	1
cell viability/%	2.4	27.1	42.4	61.0	70.9	76.2	73.8	82.3	89.8	90.8	82.9	84.1
SD/%	1.5	4.0	2.5	2.0	5.1	2.3	1.2	5.6	3.7	1.8	4.7	9.2
EMD 335823												
dose/µM	5000	4000	3000	2000	1500	1000	750	500	250	100		
cell vitality/%	26.7	63.3	61.4	64.6	76.3	84.4	96.5	108.9	114.1	110.4		
SD/%	3.6	1.8	3.8	3.0	0.7	4.7	3.1	5.4	1.9	4.7		
Fenofibrate												
dose/µM	5000	3000	2000	1500	1000	750	500	250	100			
cell viability/%	87.4	84.4	88.0	91.4	82.0	79.0	90.6	90.1	91.2			
SD/%	3.9	2.0	6.1	3.3	3.7	3.8	1.8	3.3	3.3			
Metformin												
dose/µM	5000	3500	2000	1000	500	100						
cell viability/%	1.6	1.3	59.3	81.0	78.9	95.8						
SD/%	0.0	0.3	1.5	5.2	4.8	3.8						
Rosiglitazone												
dose/µM	750	500	400	300	100	75	50	25	10	1		
cell viability/%	0.1	0.5	100.9	66.2	85.9	99.5	107.5	110.1	101.7	104.2		
SD/%	0.2	0.2	10.9	22.5	7.1	4.2	2.8	5.3	7.9	4.3		
Troglitazone												
dose/µM	250	200	150	100	80	70	60	50	20	10	1	
cell viability/%	0.4	0.0	0.0	0.0	0.6	30.8	93.5	97.5	106.4	102.8	105.7	
SD/%	0.1	0.1	0.1	0.2	0.4	12.8	4.9	3.2	5.5	5.2	4.4	
Valproic acid												
dose/µM	1000	750	500	250	200	150	100	50	10	1		
cell viability/%	89.9	94.1	84.6	105.2	115.1	120.2	118.7	110.3	118.1	114.0		
SD/%	6.1	4.8	28.2	5.8	4.7	3.4	8.1	11.9	3.8	3.3		

cell viability, an effect observed with troglitazone (Tro). In this case, the cell viability remained at around 100% up to a concentration of 60µM before rapidly decreasing to 30.8 ± 12.8% at 70µM; 80µM Tro killed nearly all of the cells.

Eight concentrations were chosen for the subsequent long-term dose finding study to enable the fine tuning of the TC10. For acetaminophen (APAP), fenofibrate (FF) and metformin (Met) 5000µM, 3000µM, and 2000µM, respectively, were chosen as the highest doses due to the low solubility of the compounds. These doses caused cytotoxicities of 42.4 ± 2.5%, 84.4 ± 2.0%, and 59.3 ± 1.5%, respectively, which was sufficient for the estimation of the TC10. APAP, Met, FF, EMD 335823 (EMD), and valproic acid (VA) showed cytotoxicity at relatively high doses compared to rosiglitazone (Rosi) and Tro. As a result, the gradations between the chosen doses for the latter two compounds were larger and the concentrations smaller.

4.3.2 Long term dose finding study and dose selection for validation study

The long term dose finding study was performed in the 24-well plate format. In contrast to 96-well plates, this format enables the application of the sandwich culture and therefore treatment for 14 days. Primary hepatocytes in monolayer cultures remain vital for only three to five days. The final studies had to be performed in 6-well plate sandwich cultures to enable the isolation of enough RNA for gene expression analysis. Since the historical data generated with primary hepatocytes cultured in 24- and 6-well plate sandwich cultures were comparable, the 24-well plate format was used for this dose finding study in order to decrease the demand for cells. The cells were treated daily for 14 days, starting on the third day after cell seeding, using 200-fold stock solutions for each compound and 0.5% DMSO as vehicle control. During the dose finding study a higher DMSO concentration was chosen than in the final studies (0.2%) to enable treatment with high doses without reaching the upper limit of solubility. Since the cytotoxicity of FF and APAP was relatively low and FF showed a low solubility, a higher DMSO concentration was needed for these two compounds. The doses for the long-term dose finding study (Table 4.2) were based on the results 24h-pre-screening test and selected to cover the viability range between 100% and 0% of vehicle control.

After one, three and 14 days the cell viability was calculated as a percentage of the vehicle control by quantification of ATP. Furthermore, the cells were photographed and checked for morphological alterations. The long term dose finding study was performed with three biological and three technical replicates and the results were visualized graphically. Since the aim of the project is the detection of very early substance specific changes in gene expression, the TC10 was estimated for all seven compounds. During the final studies the TC10 was used as a high dose and 1/10th of this as the low dose since cellular treatment with doses higher than the TC10 may trigger general unspecific effects related to apoptosis and necrosis.

Table 4.2: Doses (in µM) used for long term dose finding studies in 24-well plates.

	Dose 1	Dose 2	Dose 3	Dose 4	Dose 5	Dose 6	Dose 7	Dose 8
Acetaminophen	10	100	500	1000	2500	5000		
EMD 335823	100	500	750	1000	2500	5000		
Fenofibrate	10	100	500	1000	3000			
Metformin	10	100	500	1000	2000			
Rosiglitazone	1	10	50	100	200	300		
Troglitazone	1	10	20	50	60	65	70	100
Valproic acid	10	100	250	500	750	1000		

The TC10 was estimated based on the results for the cell viability as well as the cell morphology. For Tro, VA, APAP, and EMD both parameters were in agreement. However, the morphology of the cells treated with Rosi, Met, and FF appeared unaffected while the ATP content was markedly decreased (Figure 4.6, appendix Table 7.1). This effect was comparable in all three biological replicates, thus hypersensitivity in one donor could be ruled out as a possible explanation. Sandwich cultures treated with one of these three compounds seemed to react more sensitively to ATP quantification than the monolayer cultures. Therefore, the dose selection was mainly based on the cell morphology since these data were comparable with historical in-house data collected for the three compounds. For each of the seven compounds, the doses for the validation study were selected using the results of the 14 day timepoint, since cytotoxicity increased with both dose and time of treatment. Based on these results, three doses around the TC10 and the lowest concentration which seemed to affect the cell morphology were selected for a final validation study.

For APAP and VA, three doses over the complete dose range of the 24-well plate study were chosen, since the measured cell viability after treatment with the lowest

dose on day 14 was less than 100%. Only slight changes in cell viability were observed using higher doses; throughout treatment the cell morphology seemed to be unaffected. Furthermore, VA seemed to be more cytototoxic at earlier time points, an observation which was not validated in a subsequent test. The highest dose of FF for the validation study was 1000µM, since higher concentrations were very difficult to dissolve in the vehicle and precipitated out after the stock solution was added to the cell culture medium. Furthermore, neither the effects on the cell viability nor on the cell morphology were increased by higher concentrations than 1000µM. For EMD and Met, doses up to the TC50 were selected such that the results of the ATP test could be compared with the changes in cell morphology. The day 14 ATP results were below 100% at the lowest doses of Met with a smooth decrease as a result of increasing dose, while the lowest doses of EMD showed viabilities higher than the vehicle with a strong decrease with higher dose.

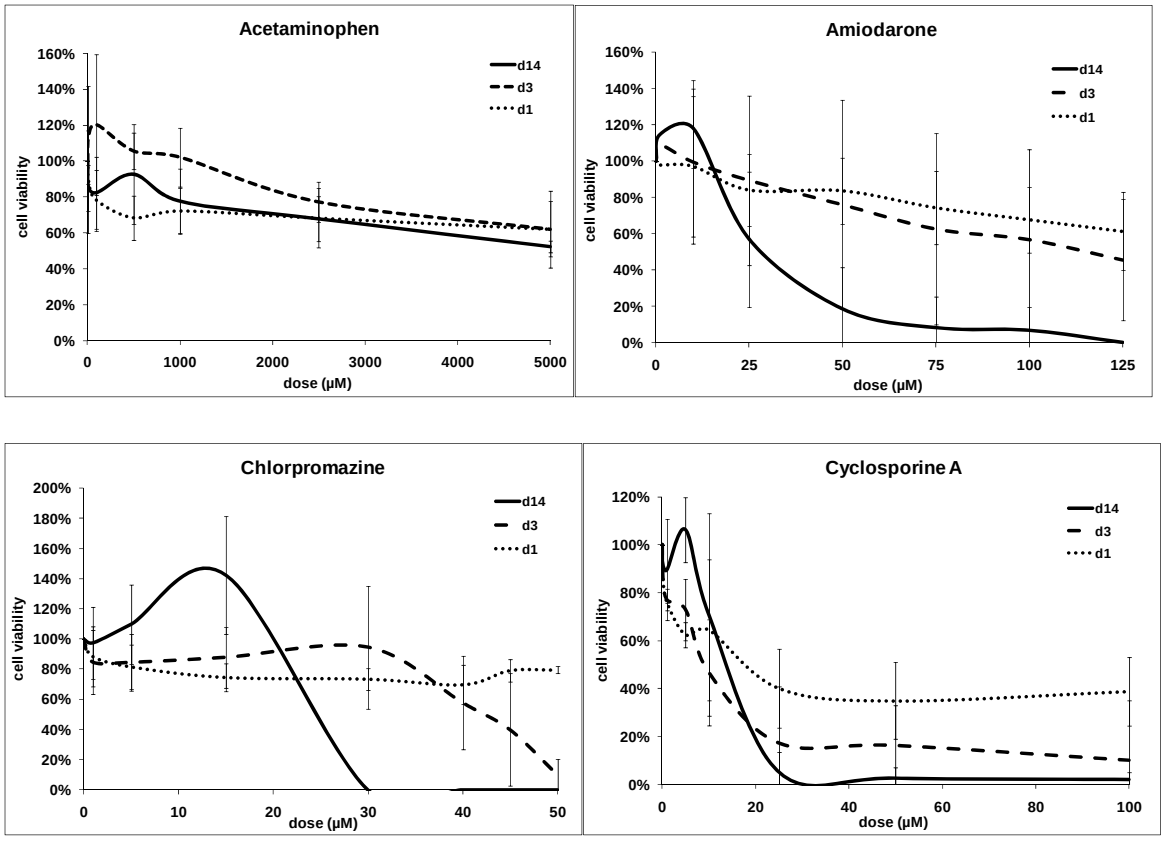

Figure 4.5: Results of the long term dose finding study in 24-well plate sandwich culture.
The cell viability was calculated as percentage of control and is plotted as the mean of the three biological replicates plus or minus the standard deviation as a function of the dose.

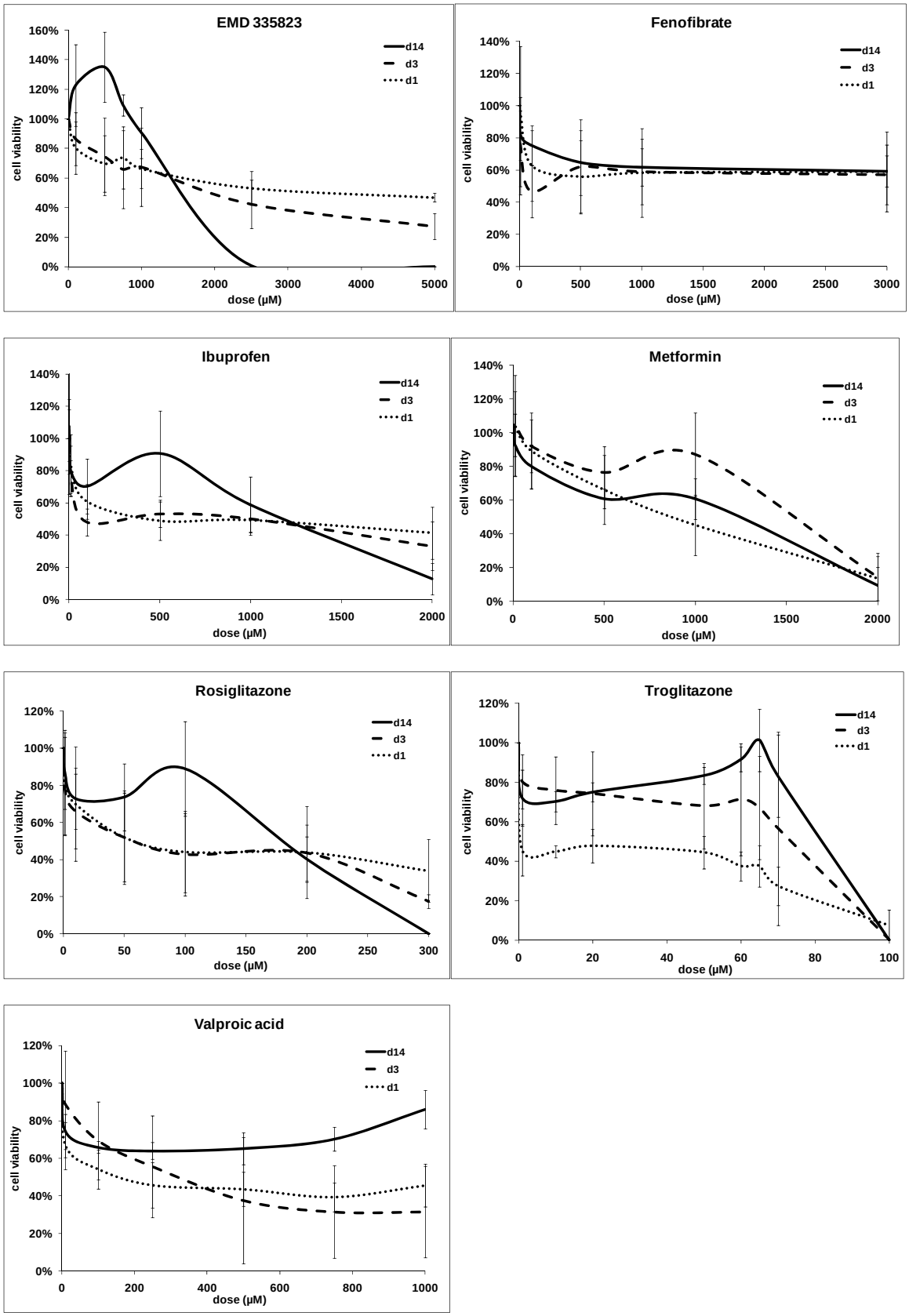

Figure 4.5 continued: Results of the long term dose finding study in 24-well plate sandwich culture.
The cell viability was calculated as percentage of control and is plotted as the mean of the three biological replicates plus or minus the standard deviation as a function of the dose.

Rosi and Tro showed a marked decrease in cell viability at doses higher than 100µM and 65µM, respectively. Therefore, doses around these critical points were chosen for further validation. EMD also showed a marked time dependent increase in cytotoxicity at doses above 1000µM. This observation underlined the previous decision to select the final doses based on the results of 14 day repeated treatment since the assumption is that any effects which become apparent on day 14 may be be preceeded by gene expression changes, which can be developed as early biomarkers in further studies.

4.3.3 Validation study and dose selection for final study

During the long term dose finding study, three doses around the TC10 of every compound were selected for the subsequent validation study using the cell culture format of the final studies. Here, cells of one biological donor in 6-well plate sandwich cultures were treated in order to investigate whether the TC10 calculated in the 24-well plate format could be transferred to the 6-well plate format. The cell viability was measured using the ATP test after 14 days of daily treatment. The results of the ATP quantification as well as the changes in cell morphology were comparable to the results of the study in 24-well plates. Based on these results the doses used during the final ‘omics and kinetics studies were selected (Table 4.3, Table 4.4).

It was agreed within the consortium, together with members of the advisory board, to use 1000µM as the highest dose for the final studies if the TC10 of a compound was higher than 1000µM. This decision was in line with the ICH Guidance on genotoxicity testing and data interpretation for pharmaceuticals intended for human use [ICH-S2 2008]. The cutoff was fixed in order to solve problems regarding the limit of solubility and to keep the discrepancy between doses used in cell culture and during in vivo studies as small as possible. So the high dose (HD) selected for APAP and FF was 1000µM. The HD for Met was also selected to be 1000µM since this dose caused slight changes in the cell morphology. For EMD 750µM were selected as the HD although this dose did not affect the cell viability during the long term dose finding study; in this test the TC10 was 1000µM, but this concentration damaged the cells (Figure 4.6). VA seemed to be less cytotoxic at day 14 when compared to earlier time points during the long-term dose finding study; the cell viability was not decreased dose-dependently in contrast to days one and three. During the validation study, a

dose dependent decrease in cell viability was seen; concentrations of 500µM and 1000µM affected the cell morphology and cells detached and died (Figure 4.6). Therefore, 100µM was selected as HD for VA. Tro showed cell viabilities around 80% at all of the three tested doses, but only 70µM changed the cell morphology to the effect that the cells began to round up. Therefore, 70µM was chosen as the HD. Rosi affected the cell morphology at 100µM, the critical dose during the long term dose finding study, but not at 10µM (Figure 4.6). Since the cell viability was markedly decreased by concentrations higher than 100µM the HD for Rosi was fixed at 80µM. With all treatments, this dose selection data correlated with that from another PhD project performed using the same cell culture system [Hrach 2008]. Accordingly, the low dose was fixed by the Predict-IV consortium and the advisory board to be 1/10th of the HD. This dose should represent a non-toxic dose (Figure 4.6), with no visible effect on cell morphology.

Table 4.3: Doses (in µM) used for the validation study.

	Dose 1	Dose 2	Dose 3
Acetaminophen	10	1000	5000
EMD 335823	500	1000	1500
Fenofibrate	10	500	1000
Metformin	100	1000	1500
Rosiglitazone	10	100	200
Troglitazone	1	50	70
Valproic Acid	10	500	1000

Table 4.4: Results of the validation study.
The cell viability is shown as mean of three technical replicates in percentage of the vehicle control ± standard deviation.

	Dose 1	Dose 2	Dose 3
Acetaminophen	84.4% ± 4.1%	84.1% ± 2.5%	69.1% ± 2.6%
EMD 335823	83.9% ± 1.4%	74.1% ± 1.2%	47.3% ± 4.5%
Fenofibrate	49.6% ± 1.2%	43.9% ± 0.8%	37.6% ± 0.7%
Metformin	65.6% ± 1.3%	45.3% ± 1.6%	12.9% ± 1.0%
Rosiglitazone	62.1% ± 2.7%	49.5% ± 2.4%	22.9% ± 0.9%
Troglitazone	81.9% ± 2.1%	77.8% ± 2.9%	82.9% ± 5.9%
Valproic Acid	86.7% ± 2.6%	68.0% ± 4.3%	59.2% ± 2.1%

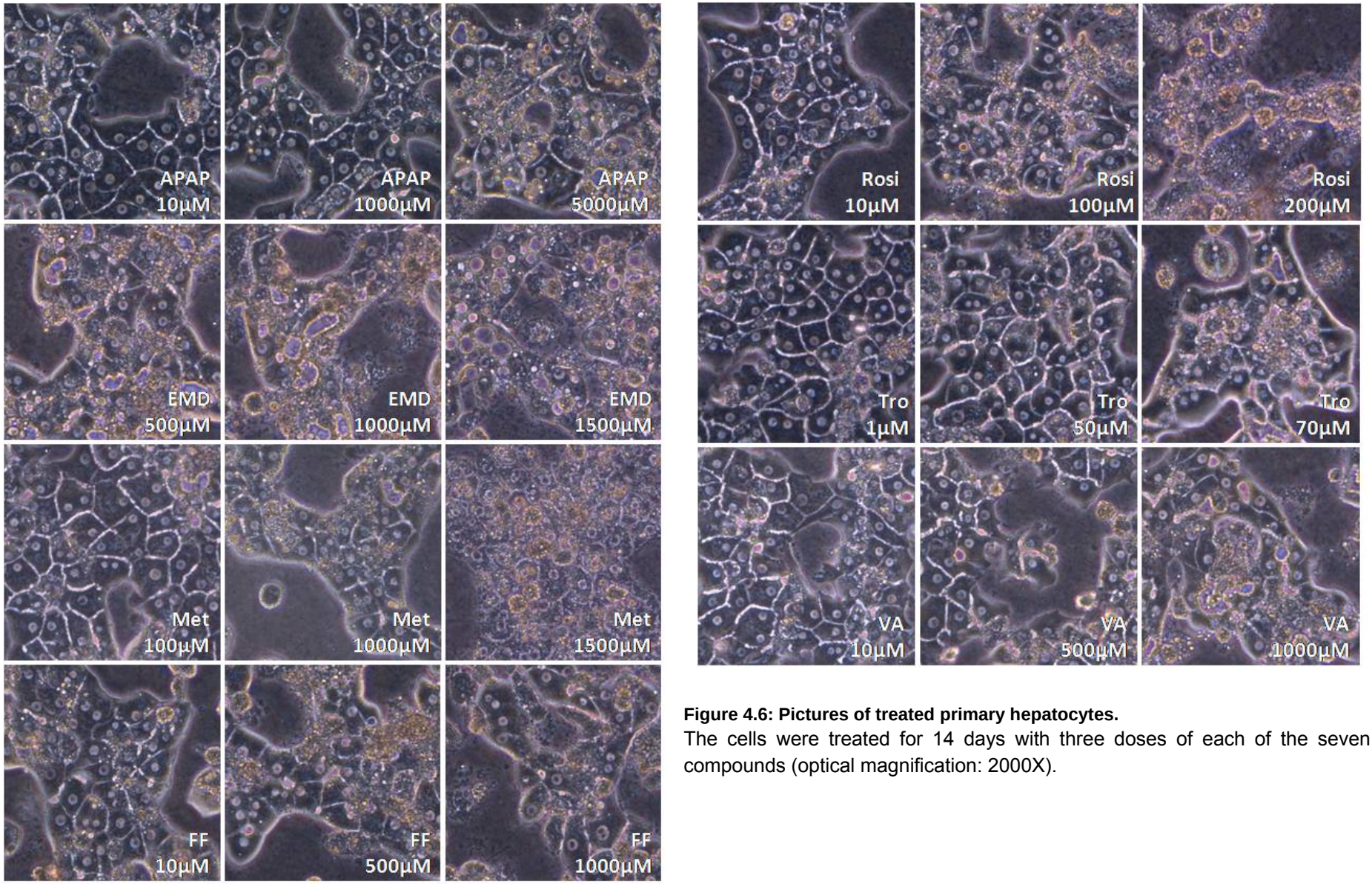

Figure 4.6: Pictures of treated primary hepatocytes.
The cells were treated for 14 days with three doses of each of the seven test compounds (optical magnification: 2000X).

4.4 Final studies

The final studies were performed with three biological replicates in 6-well plate sandwich cultures. The cells were treated daily for 14 days starting on day three after cell seeding with the doses selected and validated during the long term dose finding and the validation studies. Two technical replicates per time point were performed for each of the doses (Table 4.5). Two wells of vehicle control (DMSO) were treated per time point. After one, three and 14 days of treatment the cells were washed, lysed and frozen according to the protocol described in chapter 3.3.1.

Table 4.5: Doses (in µM) used for cell treatment during final studies.

	Low dose (µM)	High dose (µM)
Acetaminophen	100	1000
EMD 335823	75	750
Fenofibrate	100	1000
Metformin	100	1000
Rosiglitazone	8	80
Troglitazone	7	70
Valproic acid	10	100
Dimethyl-Sulfoxide	0.2%	0.2%

One technical replicate of each biological replicate was processed. The second technical replicate was stored at -80°C as a backup. The RNA was isolated, quantified and tested for quantity and quality. All RNA samples had a high purity with RIN values of nine to ten. A minimal RNA concentration of 150µg/ml was required for cDNA synthesis, which was fulfilled by all samples except one for which the backup replicate had to be substituted. The cDNA was used to synthesize biotin labeled cRNA. This cRNA was also quantified and the quality was checked. A cRNA concentration of at least 45.45µg/ml was needed for microarray hybridization, requirements which were met by all the processed samples. The biotin labled cRNA was then hybridized to Illumina® Sentrix Bead Chips (chapter 3.3.3). All raw data generated was analysed using Expressionist™ and IPA® as described in the Materials and Methods.

4.4.1 Gene expression analysis

The quality of the gene expression data was checked with the software GenomeStudio by assessing the response of the internal controls (chapter 3.4.1). No problems were observed for any of the measured samples. The visualization of the total number of detected genes did not show any outliers except in one array for which the scanning process failed. During the analysis with GenomeStudio no genes could be detected indicating a general problem during the hybridization process. Since the sample loaded onto this array was a fourth biological replicate, and for most of the substances only three replicates were measured, the hybridization and scanning for this single sample was not repeated and the array was excluded from all further analysis.

The gene expression data was uploaded into Expressionist to check the distribution of the raw data using scatter plots in order to choose the appropriate normalization method. The scatter plots for all the scanned gene chips showed a linear data distribution with minimal parallel shifts around the centre (Figure 4.7).

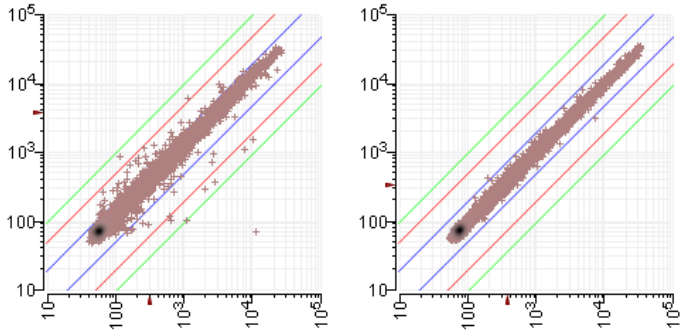

Figure 4.7: Data distribution before (left) and after (right) the Central Tendency Normalization.
The left scatter plot shows a linear data distribution as assumption for the Central Tendency Normalization with a data cloud slightly shifted parallel to the central line. In the right plot the data cloud is placed onto the central line without modification of the clouds shape.

Therefore, Central Tendency Normalization as a linear normalization method was performed. The non-normalized data were visualized in a box plot diagram (Figure 4.8) where the medians of the single arrays were found to scatter around the signal intensity 100 which was used as a median target value during normalization. Figure 4.7 shows the raw data in comparison to the normalized data. The data cloud which was slightly shifted from the central line before the normalization was then positioned on to the central line and the medians of the box plots were set to 100 (Figure 4.8).

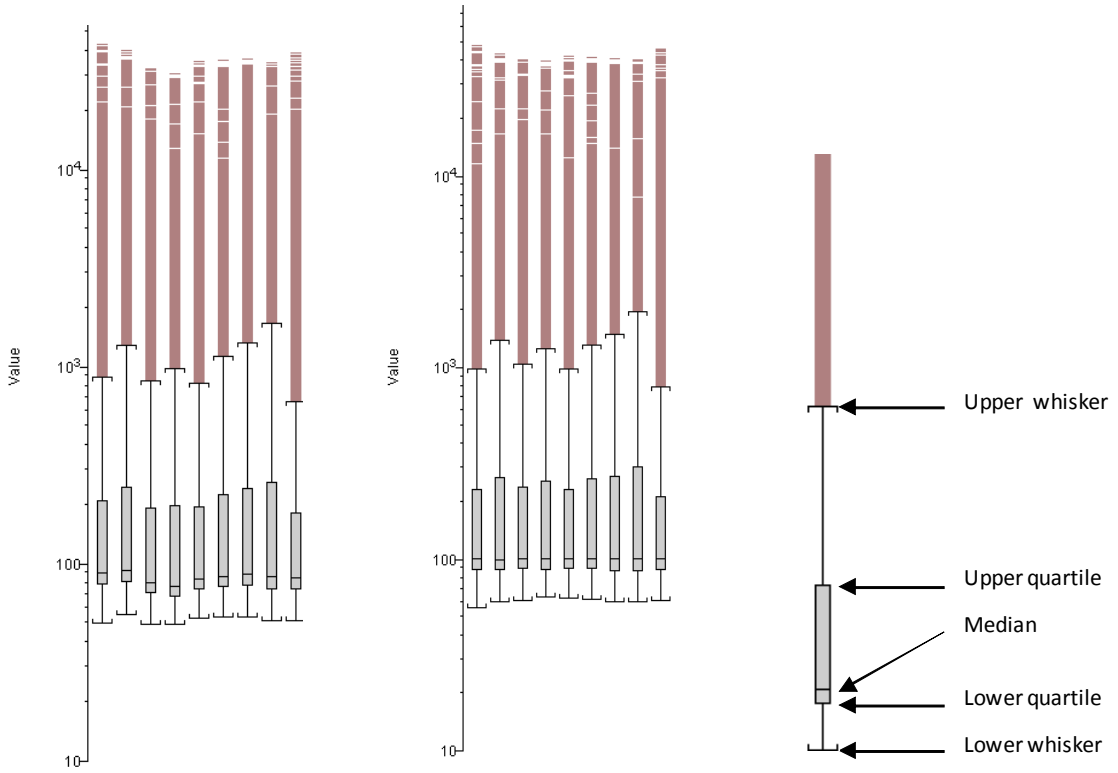

Figure 4.8: Data distribution before (left) and after (right) the Central Tendency Normalization.
The left box plot shows the medians of the different samples spread around a signal intensity of 100. The medians of all samples were shifted to a signal intensity of 100 by Central Tendency Normalization (right) without other modification of the data shown by unchanged shape of the boxes.

The fold-change, the p-value and the BH-Q-value were calculated (chapter 3.4.3) and the deregulated genes (Table 4.6) were filtered using the cutoff criteria: $p \leq 0.05$, BH Q ≤ 0.2, and fold-change ≤ -1.5 and ≥ 1.5. The biological interpretation of the gene expression data was performed using the IPA® (Ingenuity® Systems) software. Although the study reported here is focused on rat data, IPA®'s gene lists contained the gene symbols of the capitalized ortholog human genes. The precision of the orthology was spot-checked for several genes using the "BLAST" function provided by the National Center for Biotechnology Information [NCBI 2011]. For rat genes lacking a human ortholog the uncapitalized rodent gene symbols were used.

Table 4.6: Overview of the number of deregulated genes.
The data was filtered due to p ≤ 0.05, BH-Q ≤ 0.2, Fold change ≤-1.5 and ≥1.5, respectively. LD = low dose, HD = high dose, 1/3/14: treatment day 1, 3, and 14.

	LD1	LD3	LD14	HD1	HD3	HD14
Acetaminophen	-	-	-	-	1	-
EMD 335823	-	-	-	37	864	1063
Fenofibrate	1	92	13	2	46	21
Metformin	-	-	1	3243	3401	-
Rosiglitazone	-	-	-	3	466	857
Troglitazone	-	-	-	-	144	-
Valproic acid	-	-	-	-	-	-

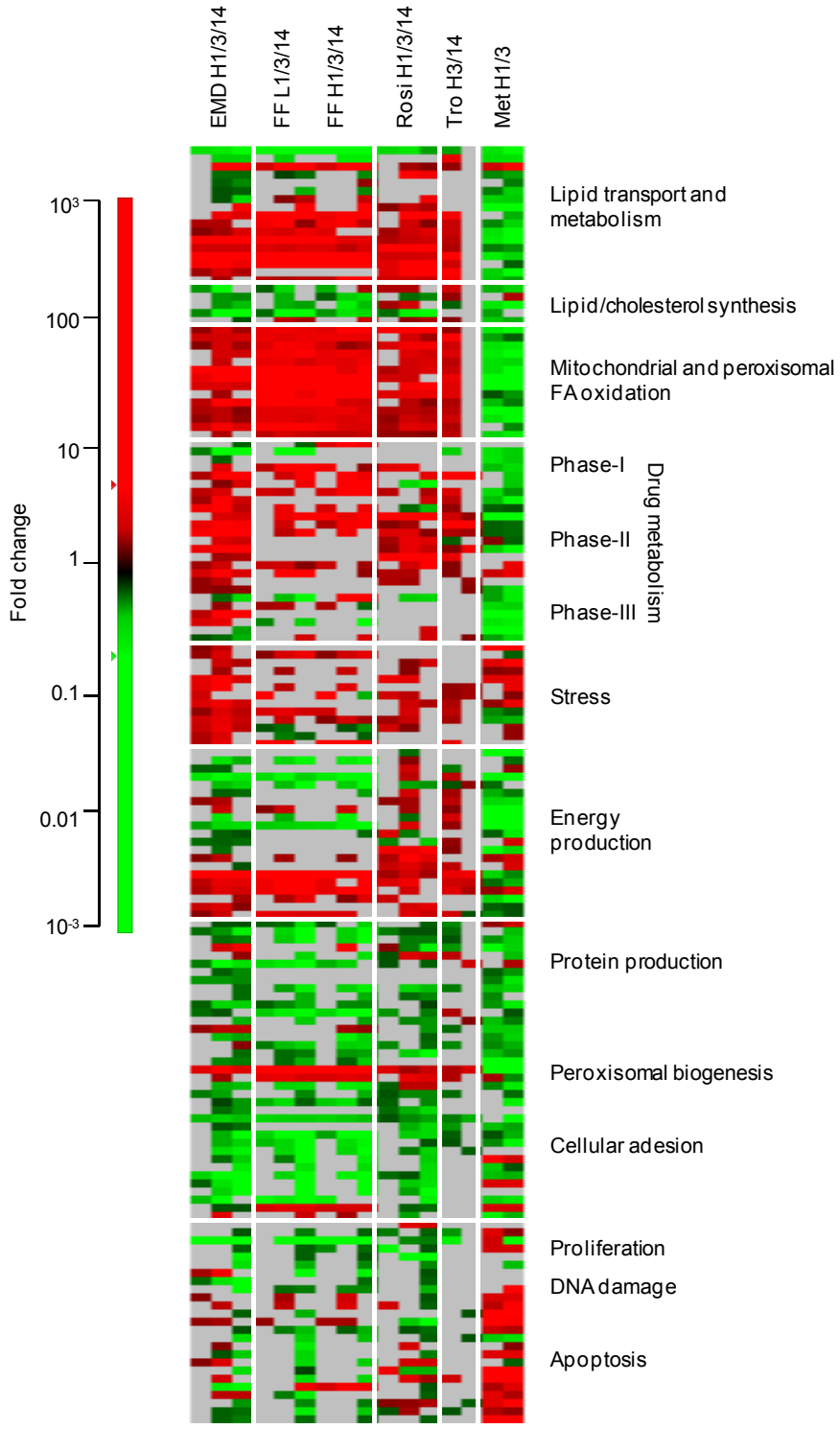

Figure 4.9: Gene expression results of EMD, FF, Rosi, Tro, and Met.
Up- (red) and downregulated (green) genes were divided into functional groups and visualized by a heatmap. H = high dose, L = low dose, 1/3/14 = treatment day 1, 3, and 14.

4.4.1.1 Acetaminophen

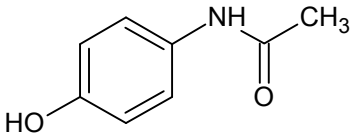

Acetaminophen (APAP), better known as Paracetamol, is a widely used analgesic drug. It has a weak anti-inflammatory effect and reduces fever by inhibiting cyclooxygenase 1 and 2, which are involved in the synthesis of prostaglandins [Botting 2000]. At therapeutic doses APAP is relatively non-toxic, but if consumed in very high doses the liver is is a major target for significant toxicity. The kidney can be considered to be a secondary target organ for toxicity [Botting 2000]. APAP is an over-the-counter-medication and nearly 50% of all the cases of acute liver failure in the USA are related to APAP exposure. APAP overdose, whether intentional (suicide) or unintentional, causes the death of many patients each year [Lee 2004]. APAP is oxidized mainly by CYP2E1 but also by CYP2A1, CYP2A6 and CYP3A4 to N-acetyl-p-benzoquinone imine, which is detoxified by conjugation with GSH. Once GSH is depleted by high doses of APAP, oxidative stress, damage of the mitochondria, liver inflammation, necrosis, and apoptosis occurs in human and rodent liver [James 2003, Kaplovitz 2005]. Since ethanol induces CYP2E1, long-term ethanol exposure increases the hepatoxicity of APAP and should therefore not be taken together with the drug [Lee 2003]. The results of gene expression analyses performed with livers of APAP-treated rats and in vitro-treated primary human and rat hepatocytes correlate with the in vivo effects and have helped our understanding of the molecular mechanisms of APAP-induced hepatotoxicity. For example, the induction of CYPs (CYP3A) leads to an increased production of reactive metabolites and induces stress-related genes (Hmox, Gadd45, Txnrd1) and pro-apoptotic factors like c-Myc [de Longueville 2003, Kikkawa 2006, Morishita 2006, Suzuki 2008, Tuschl 2008].

During the present study APAP deregulated a very small number of genes. The sole gene to be upregulated significantly was the oxidative stress marker alpha/beta hydrolase 1 (ABHD1) [Stoelting 2009]. This may be a consequence of the doses used. The high dose was fixed at 1000µM by the Predict-IV advisory board facing problems with the limit of solubility and in vitro concentrations far away from in vivo doses. This decision was upheld by the ICH “Guidance on genotoxicity testing and data interpretation for pharmaceuticals intended for human use” which recommends 1000µM as highest dose if the dosage is not limited by cytotoxicity or solubility [ICH-S2 2008]. However, this concentration did not affect cell viability during our dose

finding studies (chapter 4.1) and therefore was not expected to markedly change the gene expression level of treated cells. Research groups which published marked changes in cytotoxicity or gene expression treated their cells with concentrations starting at around 5000µM [Suzuki 2008, Jemnitz 2008].

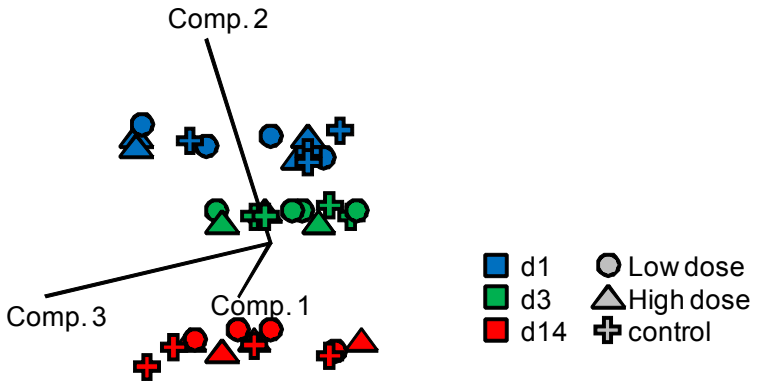

Figure 4.10: PCA of the Acetaminophen samples.
The treated samples cluster together with the time-matched controls indicating that the treatment with APAP did not alter the gene expression of the cells compared to the control cells.

The PCA, as a first overview of the data, underlined these expectations (Figure 4.10). All the samples of one time point - low and high dose and the time-matched control - clustered together, clearly showing that there are little differences in the gene expression of the treated cells related to the control. In addition to ABHD1, the high dose APAP-treatment after three and 14 days deregulated a small number of genes which met the defined cut-off criteria (Table 4.6, appendix Table 7.2). However, these genes possessed a BH Q-value ≥ 0.2 and have no relevant pharmacological or toxic associations.

The recommended dosage for adult human patients is 650 - 1000mg of APAP every four to six hours or 1300mg every eight hours; and not exceeding 4000mg per day [RX-APAP 2011]. The maximum human plasma concentration (c_{max}) after taking 1g APAP averages 12.6µg/ml [Stangier 2000]. Rats orally dosed with 250mg/kg showed a c_{max} of 139µg/ml [Van Kolfschoten 1985] without developing histopathological changes [Kikkawa 2006, Morishita 2006] or elevated ALT and AST levels [Kikkawa 2006]. The high dose used during the present study (1000µM = 151.16µg/ml) slightly exceeded rodent non-toxic plasma concentration. So while this in vitro study was performed with an in vivo relevant concentration, it was too low to investigate and predict hepatotoxic effects, since APAP causes in vivo and in vitro toxicities solely at very high doses.

4.4.1.2 Valproic acid

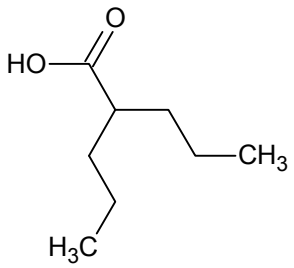

Valproic acid (VA) is a first generation anti-epileptic drug which is also used for the therapy of bipolar disorders and migraine by increasing the synthesis and release of the inhibitory neurotransmitter γ-aminobutyric acid (GABA). This relatively safe drug does however cause elevated serum aminotransferase levels in 30 – 50% of patients. These effects seem to be dose-dependent and are in most cases transient without consequences for further treatment. However, VA can cause severe idiosyncratic effects in the liver and is a teratogen. It is heavily metabolized to more than ten different metabolites which are conjugated with GSH and glucuronide before they are eliminated via bile or urine [Löscher 1999, Tong 2005]. After CYP oxidation, the metabolite 4-ene-VA is β-oxidized in the mitochondria and is then able to inhibit β-oxidation enzymes. The resulting disturbance of β-oxidation, as well as mitochondrial damage and a decrease in free Coenzyme A levels, can lead to hepatotoxic effects, including microvesicular steatosis, and has been reported in both rats and humans. Furthermore, this reactive metabolite can cause oxidative stress leading to GSH-depletion and necrosis [Chang 2006, Tang 2007].

During the present study VA deregulated a very small number of genes, but without statistical significance related to the BH Q-value (Table 4.6, appendix Table 7.3). Therefore, these gene changes were not considered biologically relevant. The small changes in the gene expression level of VA-treated cells could also be observed in the PCA (Figure 4.11), which showed results similar to APAP. The samples of the low and high dose clustered together with the appropriate time-matched control showing that the gene expression level of the compound treated cells did not markedly differ from the control. The very few alterations in gene expression may be a consequence of a too low concentration selected as the high dose (100μM). This dose decreased the cell viability during the dose finding study in the 24-well plate format to 54.1 ± 10.3%. During the subsequent validation study in 6-well plates the doses 10, 500, and 1000μM were tested. Here the cell viability was decreased to 68.0 ± 4.3% by 500μM VA and the cells had started to round up and detach. The next lower concentration (10μM) decreased the cell viability to 86.7 ± 2.6% but did not affect the cell morphology. Therefore, the slightly higher dose of 100μM was chosen in order to avoid a non-toxic dose that was too low. To validate the optimal

concentration of VA for gene expression analysis the validation study in 6-well plates should have been repeated with additional doses in the range between 10µM to 500µM. Furthermore, the cell viability should have been measured with a further cytotoxicity assay because of the discrepancy between the ATP data in monolayer and sandwich cultures. Since the ATP test quantifies ATP in living cells it may be more sensitive towards drug-induced effects in the mitochondria and therefore dependent on the test compound's mode of action. This assumption is corroborated by the low ATP amounts also measured for Met and FF - while the cell morphology was not affected. A cytotoxicity test which measures the loss of cell membrane integrity (e.g. LDH assay) could provide additional information to aid in dose selection.

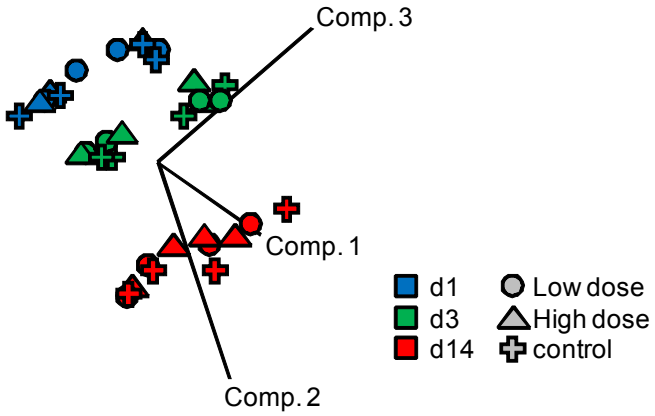

Figure 4.11: PCA of the Valproic acid samples.
The treated samples cluster together with the time-matched controls indicating that the treatment with VA did not alter the gene expression of the cells compared to the control cells.

For human use, an oral dose of 10 – 15mg/kg/day is recommended to reach the therapeutic plasma concentration of 50 – 100µg/ml [RX-VA 2011]. The acute hepatotoxicity of VA in human and animals is relatively low [Löscher 1999] and there is a lack of efficient animal and in vitro models for the investigation and prediction of idiosyncratic drug effects [Kaplovitz 2005, Uetrecht 2008]. However, VA induced liver necrosis and steatosis was shown in rats after intraperitoneal injection of 500mg/kg [Tong 2005] and also after coadministration of the CYP-inducer phenobarbital [Löscher 1993]. During a teratogenicity study, where doses which cause only minimum toxicities to the dams are recommended [ICH-S5 1993], pregnant rats were orally dosed with 200mg/kg/day. This resulted in a c_{max} of 340µg/ml [RX-VA 2011], which is equal to 3.4- to 6.8-times the human therapeutic dose. The high dose (100µM = 16.6µg/ml) used in the present study, reached neither human therapeutic

nor rodent minimum-toxic plasma concentrations. Kiang et al. investigated the cytotoxicity of VA as well as its potential to trigger oxidative stress production and GSH depletion in sandwich-cultured rat hepatocytes at doses of 1mM and higher [Kiang 2010, Kiang 2011]. A further study measuring gene and protein expression changes in in vitro cultured hepatocytes was performed with 1.2mM VA [Rogiers 1995]. During the present study, a concentration of 1mM VA decreased the cell viability in the 6-well plate format to 59.2 ± 2.1% and markedly affected the cell morphology (Figure 4.6). Since the determination of gene expression changes caused by slight toxic doses (TC10) was the goal of this study a concentration of 1mM VA would have been incompatible. However, the cytotoxicity caused by doses in the range of 10 to 500µM should have been further analysed in order to optimize the dose selection and for gene expression analysis. The performance of in vitro studies with in vivo relevant doses would not be possible in the present system due to marked cytotoxicity. Nevertheless, cellular treatment with higher doses of VA may deregulate genes which could be correlated to in vivo toxicities. This may enable the prediction of the dose-related mechanisms of VA's hepatotoxicity while the prediction of idiosyncratic effects remains complex and probably not possible to elucidate with these cell models.

4.4.1.3 Fenofibrate

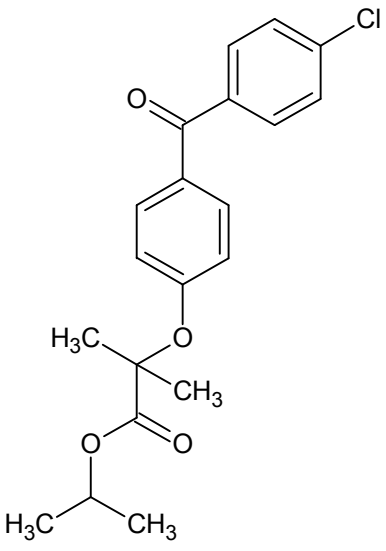

Fenofibrate (FF) belongs to the class of fibrates which are hypolipidemic drugs, are designed to lower the plasma triglyceride and cholesterol levels of patients with hypercholesterolemia or mixed dyslipidemia. As a prodrug fenofibrate is hydrolysed by esterases to its active form fenofibric acid which is an agonist of the peroxisome proliferator activated receptor alpha (PPARα). By PPARα signaling, FF activates lipoprotein lipase (LPL) a key enzyme in lipid metabolism which cleaves triglycerides into free fatty acids and glycerol. Furthermore, FF decreases the production of apolipoprotein B and C-III which are part of very low and low density lipoproteins (VLDL, LDL) and increases the expression of apolipoprotein A-I and A-II as part of high density lipoproteins (HDL).

The different lipoproteins enable the transport of the hydrophobic lipids in the blood while HDL has a higher affinity to cholesterol receptors in the liver and is therefore catabolized faster [DB-FF 2011]. PPARα is a type II nuclear receptor which is highly expressed in metabolically active tissues like liver, heart, kidney and muscle. It forms a heterodimer with the retinoid X receptor (RXR) after a ligand has bound. The activated PPARα/RXR heterodimer binds to peroxisome proliferator response elements (PRE) and acts as a transcription factor for several genes involved in lipid catabolism and glucose homeostasis. Its natural ligands include fatty acids, which activate their own metabolism, since PPARα activation increases fatty acid uptake and oxidation. This pharmacological effect was observed in preclinical studies with rodents as well as in human clinical trials [Corton 2000, Willson 2000]. However, PPARα activation also triggers several well described adverse effects. FF may cause dose-related elevation of ALT and AST levels, which are usually transient. After long-term usage, cholestatic hepatitis, as a consequence of the increased excretion of cholesterol as bile salts, can lead to chronic active hepatitis followed by cirrhosis in extremely rare cases [RX-FF 2011]. In rodents, FF acts as a non-genotoxic hepatocarcinogen. The rodent and the human PPARα are very similar at the DNA as well as protein level but its expression in rodent livers is approximately 10 fold higher than in humans. In rodents, PPARα activates the proliferation of peroxisomes and regulates their function [Corton 2000, Willson 2000]. One hypothesis for the mechanism of action of non-genotoxic hepatocarcinogens like fenofibrate is their ability to elevate peroxisomal ß-oxidation. This can cause the excessive generation of hydrogen peroxide (H_2O_2) which is the product of lipid oxidation. Catalases transform H_2O_2 into water and oxygen and other anti-oxidant enzymes like superoxide dismutases, and also detoxify reactive oxygen species like H_2O_2. If the cellular rescue mechanisms are overextended, hydrogen peroxide can cause oxidative stress by lipid peroxidation and the generation of other reactive oxygen species (ROS). ROS may lead to oxidative DNA damage and eventually lead to the formation of liver tumors in rodents. Tumor promotion and the regulation of peroxisomal function seem to be restricted to rodents because of differences in the PRE which are not conserved across species [Corton 2000, Nishimura 2007]. Nevertheless, species-specific intracellular factors may also influence PPARα signaling, since PPARα overexpression in human primary hepatocytes and HepG2 cells did not increase the expression of PPARα target genes after treatment with FF

[Lawrence 2001]. Furthermore, the transfection of human hepatocytes and HepG2 cells with rat PPARα and rat PRE could not induce peroxisome proliferation and PPARα activation after cellular treatment with peroxisome proliferators [Ammerschläger 2004]. Fenofibric acid is directly conjugated with glucuronate and excreted via the urine. Only a small amount is reduced at the carbonyl moiety to benzhydrol metabolite and is subsequently excreted in urine as a glucuronide conjugate. Therefore, the formation of reactive metabolites seems not to be involved in FF's hepatotoxicity [RX-FF 2011].

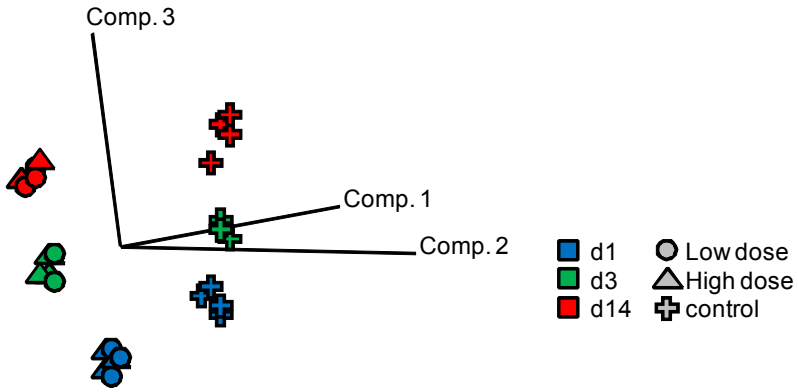

Figure 4.12: PCA of the Fenofibrate samples.
The treated samples (turquoise) cluster separated from the controls (gray to black) indicating a marked deregulation of genes in all samples by FF.

Fenofibrate markedly altered the gene expression of treated hepatocytes

The PCA (Figure 4.12) of FF showed a clear separation of the treated samples from the controls, while the high and the low dose of each time point clustered together. Thus, FF markedly altered the gene expression of the treated cells but the effects of the low dose were as prominent as those of the high dose treatment. This could indicate that the doses for treatment were too high to see dose-dependent effects. The major gene expression changes observed included deregulation of PPARα target genes. Since FF was reported to activate PPARα in a cell-based transactivation assay with an EC50 (concentration triggering 50% of an effect's strength) of 18μM [Willson 2000] cell treatment with 100μM and 1000μM FF may suggest the reason for strong PPARα effects, even at the lower concentration used in our studies. These effects may be already saturated after cellular treatment with 100μM so higher doses could not increase these effects any further.

During the short time screening in the monolayer culture FF showed nearly no cytotoxicity, up to a concentration of 5000µM. In contrast, concentrations of 500µM and higher decreased the cell viability after 14 days of treatment to values around 60%. The cell morphology was not altered after treatment with 500µM while 1000µM slightly affected the cell morphology and was therefore chosen as the high dose - independently from the results of the cytotoxicity tests. Compounds like FF, which directly affect the mitochondria, may also alter ATP synthesis and make our standard cytotoxicity test more sensitive. Thus, the dose finding study for FF should be repeated with additional doses between 500µM and 1000µM using cytotoxicity tests with other endpoints, such as loss of cell membrane integrity in order to correctly define the TC10.

Table 4.6 shows the number of significantly deregulated genes caused by FF exposure. Interestingly, treatment for three days altered the highest number of genes, independent of the dose. The genes selected for biological data interpretation are listed in the appendix (Table 7.4) and visualized in Figure 4.9. Genes with a BH Q-value > 0.2 were also discussed since they were involved in pathways known to be deregulated by FF or they are directly related to PPARα target genes containing a PRE within their promotor sequence.

Fenofibrate induced genes triggering cellular lipid uptake and catabolism

Cornwell et al. [Cornwell 2004] and Nishimura et al. [Nishimura 2007] showed that the pharmacological effects of FF, such as increasing lipid uptake and metabolism in the liver, can be reconstructed by gene expression profiling of rat livers after in vivo treatment of rats with FF and other fibrates. Their findings correlate well with the results of the gene expression profiling in primary rat hepatocytes described in this study. The gene encoding the very low density lipoprotein receptor (VLDLR), a cell surface protein that is responsible for the uptake of lipids from the blood, was upregulated in a dose- and time-related manner; up to 10.3-fold. Lipids are cleaved intracellularly by the PPARα target lipoprotein lipase (LPL) into glycerol and fatty acids (FA) [Mandard 2004]. LPL gene expression was induced by the low and the high dose of FF on day 14 (up to 60-fold) while the gene encoding apolipoprotein C-II (APOC2) which inhibits LPL was downregulated. Cornwell et al. described the downregulation of apolipoprotein C and A by FF in vivo which could also be shown in this in vitro study. However, the PPARα gene itself was not upregulated by FF during

the present study which also correlated well with previously reported gene expression studies with hepatocytes and livers of rats treated with PPARα agonists [Guo 2006, Tamura 2006].

The expression of the Aquaporin 9 (AGP9) gene was downregulated at all time points and by both doses. This water channel is located in the basolateral membrane and manages glycerol uptake into the liver [Huebert 2002, Hibuse 2006]. In contrast, the gene expression of Aquaporin 7 (AQP7) was heavily induced and correlated well with the results reported by Tamura et al. after the treatment of rats as well as hepatocytes with PPARα-agonists [Tamura 2006]. AQP7 is highly expressed in adipose tissue, and to a minor extent in the liver, and acts as an efflux channel of glycerol into the blood. It is upregulated during fasting when triglycerides are cleaved in adipocytes in order to provide glycerol for hepatic gluconeogensis. The expression of hepatic AQP9 is also induced in order to increase the take up of higher amounts of glycerol for energy production [Hibuse 2006]. During the present study AQP7 expression was upregulated, probably in order to release the increased levels of glycerol, produced by the enhanced lipid cleavage, back into the cell culture medium. In parallel, the uptake of further glycerol from the cell culture media was reduced by the downregulation of AQP9. Additionally, genes encoding proteins involved in the biosynthesis of cholesterol were repressed, especially after high dose treatment on days three and 14, which may be a consequence of a high break down rate of triacylglycerides and cholesterolesters (Figure 4.13). Sterol O-acyltransferase 1 (SOAT1) gene expression was upregulated after 14 days of treatment, independent of dose. This enzyme esterifies cholesterol enabling its storage as lipid droplets in the cell. The gene encoding Perilipin (PLIN2), which is involved in lipid storage, was also upregulated at all time points and doses.

Free FA’s are bound and transported intracellularly by fatty acid binding proteins (FABP), the gene expression of which were time- and dose-dependently upregulated up to 91-fold. FA’s are activated in the cytosol by acyl-CoA synthetase (ACSL) whose gene expression was upregulated relatively constantly by low and high dose at all time points. These results correlated well with other gene expression studies performed with primary rat and mouse hepatocytes treated with fenofibrate and other PPARα agonists [Guo 2006, Tamura 2006].

Fenofibrate enhanced expression of genes involved in mitochondrial and peroxisomal fatty acid degradation

Activated FA's are further oxidized in the mitochondria and transported into these by the PPARα target carnitin-palmitoyltransferase (CPT), the gene expression of which were upregulated up to 15-fold [Mandard 2004]. Carnitine O-acetyltransferase (CRAT) and carnitine O-octanoyltransferase (CROT) regulate the mitochondrial and peroxisomal concentration of FA-CoA and the expression of these genes were also induced. The expression of genes encoding enzymes involved in every step of mitochondrial β-oxidation of FA's were increased by low and high dose FF at all time points up to 8.1-fold. These gene expression changes were consistant with results obtained after treatment of rats in vivo and hepatocytes in vitro with PPARα-agonists [Cornwell 2004, Guo 2006, Tamura 2006].

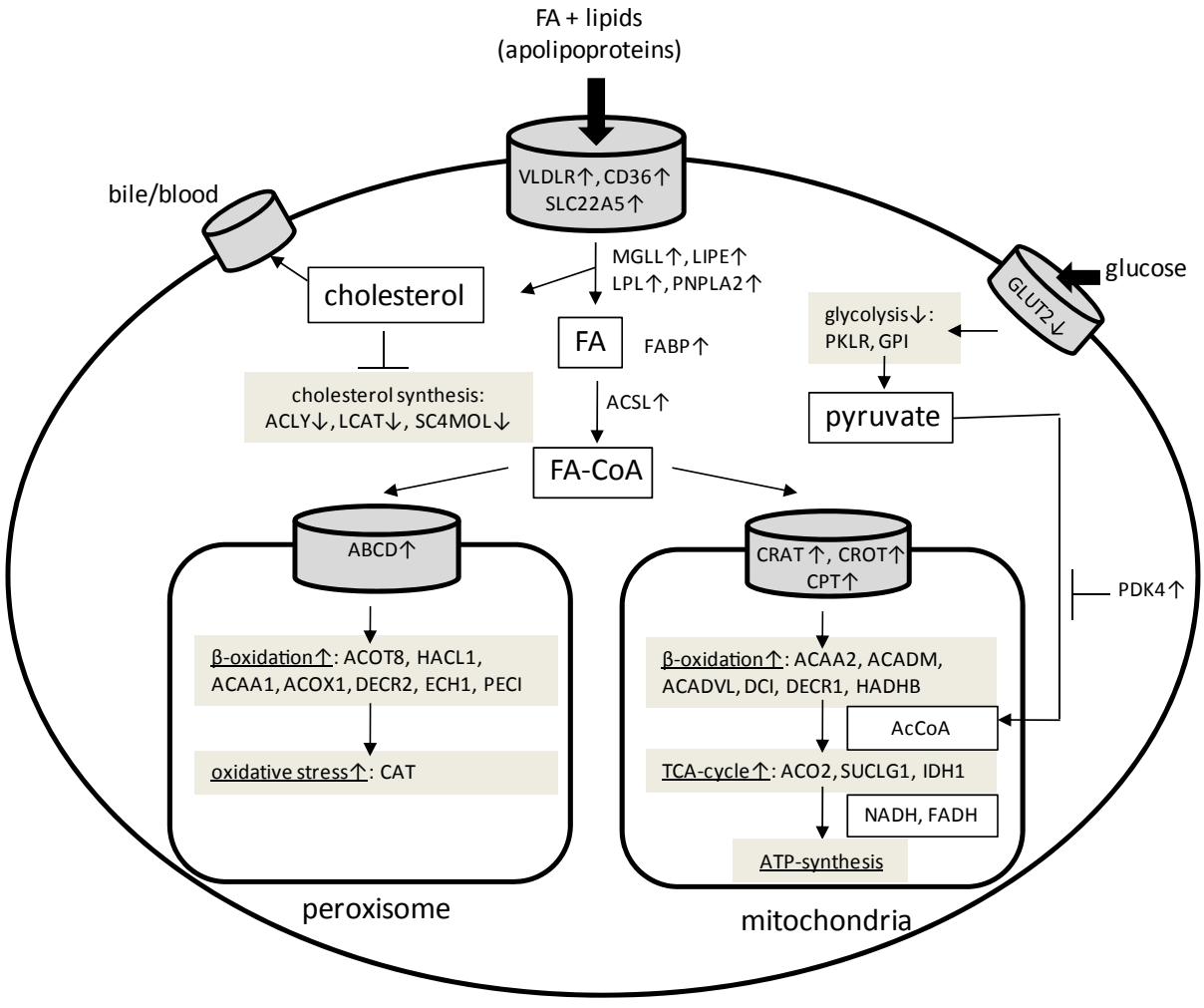

Figure 4.13: Alterations in lipid metabolism in FF treated cells.
FF induced lipid uptake and metabolism and decreased energy production from glucose.

In most cell types the breakdown of FA's is primarily performed in peroxisomes, small organelles surrounded by a single-layered membrane, while very long FA's with more than 20 C-atoms are only rarely oxidized in peroxisomes [Lodish 2001]. Genes encoding transporters for the uptake of FA's into peroxisomes were upregulated by both doses of FF. In addition, the gene expression of enzymes involved in the peroxisomal FA-oxidation (Acyl-CoA oxidase (ACOX1), acetyl-CoA acyltransferase (ACAA1), enoyl-CoA hydratase (ECH1) were increased independently from time and dose, up to 38.6-fold. Acyl-CoA oxidase (ACOX1) was identified as the first direct PPARα target and is used as a marker gene for PPARα-agonist action [Ammerschläger 2004, Mandard 2004].

FF deregulated genes related to glucose metabolism

The intensive breakdown of fatty acids seemed to saturate the cell's energy consumption, which was exacerbated by the hepatic glucose uptake transporter gene GLUT2 being suppressed. Furthermore, genes encoding enzymes involved in glycolysis, including pyruvate kinase (PKLR) and lactate dehydrogenase (LDHB), and gluconeogenesis, such as glucose-6-phosphatase (G6PC) and glucose-6-phosphate translocase (SLC37A4) were downregulated. Increased FA oxidation triggers the phosphorylation of the pyruvate dehydrogenase complex (PDC) which transforms the endproduct of glycolysis, pyruvate, into acetyl-CoA (AcCoA). The phosphorylation of PDC is catalysed by pyruvate dehydrogenase kinase (PDK) and inhibits PDC's activity [Sugden 2001]. FF induced the gene expression of PDK4, indicating a metabolic switch triggered by enhanced lipid catabolism. In addition, FF upregulated the gene expression of enzymes involved in the Krebs cycle, like aconitase (ACO2), isocitrate dehydrogenase (IGH1) and succinate-CoA ligase (SUCLG1). The gene encoding glycerol-3-phosphate dehydrogenase (GPD), which transfers electrons into the electron transport chain and builds up the mitochondrial transmembrane potential as basis for ATP production, was also induced.

In conclusion, the gene deregulations related to glucose metabolism and the induction of genes involved in the Krebs cycle seem to be a consequence of the increased lipid metabolism and do not indicate a response of the cells to toxic effects. The expression changes of genes involved in FA and glucose metabolism correlates well with Cornwell's findings of in vivo treated rats [Cornwell 2004] as well as with

other gene expression studies performed with in vitro treated rodent hepatocytes [Guo 2006, Tamura 2006].

Fenofibrate induced cellular markers of stress and DNA damage

One hypothesis for the hepatocarcinogenic action of FF in rodents is oxidative DNA damage by ROS as a consequence of enhanced lipid metabolism. In particular, peroxisomal lipid catabolism generates hydrogen peroxide which can be detoxified by antioxidant enzymes, but only up to a specific limit [Corton 2000]. Supporting this hypothesis, the formation of oxidative stress was indicated by the data in the present study by the upregulation of several genes coding for antioxidant enzymes. Catalase (CAT) reduces hydrogen peroxide produced by lipid oxidation in the peroxisomes. Superoxide dismutase 2 (SOD2) and glutathione peroxidase (GPX1) detoxify ROS in the mitochondria [Marquardt 2004]. Heme oxygenase 1 (HMOX1) [Keyse 1990], ferritin (FTL) [Cairo 1995, Vogt 1995, Orino 2001] and thioredoxin interacting protein (TXNIP) [Watanabe 2010] are general markers for oxidative stress. In addition, FF induced the gene expression of phase-II enzymes like UDP-glucuronosyltransferase (UGT), sulfotransferase (SULT) and glutathione-S-transferase (GSTA) indicating an enhanced cellular detoxification activity. However, FF downregulated the gene expression of glutamate-cysteine ligase (GCLC) and GSH synthetase (GSS), which are involved in GSH synthesis. These genes are upregulated if additional GSH is required, e.g., for defense against oxidative stress and reactive metabolites [Yuan 2009]. Therefore, FF seemed not to deplete cellular GSH during the present study. FF upregulated genes encoding enzymes involved in the repair of DNA damage, including growth arrest and DNA-damage-inducible alpha (GADD45A) [Smith 2000] and APEX nuclease (APEX1) which is induced by oxidative stress [Edwards 1998]. During a toxicogenomics study in rats treated with non-genotoxic hepatocarcinogens, APEX1 was also upregulated in the liver [Ellinger-Ziegelbauer 2005].

Fenofibrate did not induce genes involved in apoptosis and proliferation

The second hypothesis of FF's carcinogenesis in rodents is the induction of cell proliferation, without increasing apoptosis [Corton 2000]. The intrinsic apoptosis pathway is triggered by cytochrome c release from the mitochondria which activates caspases. This process can be inhibited by anti-apoptotic BCL2-family members [Matés 2008]. Pro-apoptotic factors like BAX, BAD and BAK can be activated by cellular stress [Hail 2006]. During the present study low and high dose treatment for

one and three days induced the expression of the pro-apoptotic member of the BCL2-family - BCL2-like 14 (BCL2L14). On day 14 genes encoding pro-apoptotic key factors like BCL2-antagonist/killer 1 (BAK1), BCL2-associated X protein (BAX) and BCL2-related ovarian killer (BOK) were downregulated and no caspases were deregulated. Furthermore, gene expression of the anti-apoptotic factor v-akt murine thymoma viral oncogene homolog 1 (AKT1) was downregulated. Hence, long term treatment with high and low doses of FF did not increase expression of genes encoding proteins which trigger apoptosis.

Cyclin D, Cyclin E and cyclin-dependent kinase inhibitor 1B (p27, Kip1) play a major role in cell cycle progression from the G1 to S phase [Ogawa 2009]. The Cyclin D gene was downregulated on day 14 after high and low dose treatment while genes encoding Cyclin E and p27 were not deregulated in the present study. Genes encoding polymerase delta 4 (POLD4) [Liu 2006] and topoisomerase II beta (TOP2B) [Osheroff 1998] which are involved in DNA replication as well as tubulin alpha 1a (TUBA1A) which participates in spindle formation [Hernández 2009] were also repressed. This did not correlate with the already mentioned study from Ellinger-Ziegelbauer et al. [2005] where tubulins and topoisomerase II alpha were upregulated by non-genotoxic hepatocarcinogens. Further indications that FF did not induce cell proliferation in the present study were the upregulation of genes G0/G1switch 2 (G0S2) and geminin (GMNN), which inhibit centrosome duplication [Lu 2009]. G0S2 is a PPARα target [Zandbergen 2005] which is upregulated during the re-entry from G0 into G1 phase of blood mononuclear cells [Russell 1991]. However, recent studies showed that G0S2 triggers apoptosis after DNA damage in human primary fibroblasts and acts as a tumor suppressor [Welch 2009]. In addition, FF repressed the annexin A5 gene (ANXA5), a calcium-dependent phospholipid binding protein whose induction is associated with many carcinomas in rats and humans [Glückmann 2007, Xue 2009]. Cimica et al. correlated the upregulation of serveral genes with liver regeneration in rats after partial hepatectomy [Cimica 2007]. Consistent with this study the angiotensinogen gene (AGT) and the serpin peptidase inhibitor clade E member 2 gene (SERPINE2) were induced while the genes encoding connective tissue growth factor (CTGF), syndecan 4 (SDC4) and alpha-2-macroglobulin (A2M) were downregulated during the present study. Further growth factor genes, like epidermal growth factor (EGF), transforming growth factor alpha/beta (TGFA/B) and early growth response 1 (EGR1), were also repressed

indicating that FF did not induce cell proliferation during the study presented here. One gene, the cell cycle promotor cell division cycle 25 homolog A gene (CDC25A) [Källström 2005], was induced which correlated with data published on livers from FF treated rats [Nishimura 2007].

Fenofibrate affected genes related to different cellular functions

Increased production of several enzymes involved in lipid and xenobiotic metabolism is hypothesised to trigger hepatomegaly in animal studies after exposure to FF [Cornwell 2004]. The peroxisomal biogenesis factors 11 alpha and 19 (PEX11A, PEX19) genes were time-dependently induced, indicating enhanced peroxisomal biogenesis and is a well known PPARα effect in rodents [Li 2002a]. This correlated with other in vitro and in vivo studies performed with FF and other PPARα agonists, respectively [Guo 2006, Tamura 2006]. The gene encoding uncoupling protein 2 (UCP2) was heavily upregulated during the present study. UCP2 controls the ratio of adenosine triphosphate/adenosine diphosphate, plays a role in the generation of ROS and was induced in other studies performed with primary hepatocytes treated with PPARα agonists [Mandard 2004]. This proton channel is able to uncouple the oxidative phosphorylation process leading to an uncontrolled decrease in the mitochondrial transmembrane potential which can ultimately cause ATP depletion and cell death [Chavin 1999].

FF downregulated the solute carrier family 10 member 1 gene (NTCP, SLC10A1). Decreased expression of NTCP was associated with human cholestasis in vivo but FF's cholestatic hepatitis is thought to be caused by increased cholesterol excretion into the bile [RX-FF 2011]. In addition, the biliary efflux transporter ATP-binding cassette sub-family G member 1 (ABCG2, BCRP) was induced at the early time points, but ATP-binding cassette sub-family B member 1B (Abcb1b, MDR1) and the basolateral efflux transporter ATP-binding cassette sub-family C member 3 (ABCC3, MRP3) were heavily downregulated at day 14.

Genes encoding different classes of proteins which are synthesized and excreted by hepatocytes were downregulated by FF, including the complement components C2, C6, and CFH, the chemokines CXCL11 and CXCL16, the acute phase proteins alpha-2-macroglobulin (A2M), alpha-2-HS-glycoprotein (AHSG), and fibrinogen (FGB) as well as the coagulation factors F5, F9, and F11. The expression of chemokines, complement factors and acute phase proteins is regulated by

intercellular signaling between hepatocytes and immune cells. Activated immune cells release mediators which bind to receptors on the hepatocyte membrane and trigger the synthesis and release of proteins related to the hepatic inflammatory response [Trautwein 1994, Dhainaut 2001, Tacke 2009]. Thus, the downregulation of genes related to inflammation and blood coagulation in the present study were probably associated with the toxic effects of FF since immune cells as essential initiators of inflammatory pathways were not present in the hepatocyte monoculture. Additional indications of drug-induced cytotoxic effects were the suppression of several genes involved in cellular adhesion and morphology, like laminin (LAMC2), E-cadherin (CDH1), fibulin (FBLN1), tubulin (TUBA1A), and vimentin (VIM) [Chen 2006, Malcos 2011, Vuoriluoto 2011]. The cells started detaching and downregulated further genes encoding enzymes related to key hepatic functions, such as CYP7A1, which synthesizes bile acids. Furthermore, the gene encoding Na-K-ATPase (ATP1A1) was downregulated which plays a role in the maintenance of the cellular membrane potential.

In conclusion, the whole genome gene expression data for the FF treated cells showed clear induction of lipid catabolism and corresponds to the compound's pharmacological effect [Nishimura 2007, Cornwell 2004]. A similar study performed with mouse primary hepatocytes transfected with a PPARα response element in order to increase the pharmacological effect of FF resulted in similar findings after treatment of cells for 24 hours [Guo 2006]. The study presented here was performed with non-transfected cells and was therefore closer to the in vivo situation and also showed the deregulation of several in vivo-relevant genes being increased over the time of treatment. The gene expression data indicated the formation of oxidative stress and DNA damage which are known mechanism of FF's hepatocarcinogenicty potential in rodents. However, the data did not support the hypothesis which assumes a disturbed balance of apoptosis and cell proliferation to be the reason for FF's carcinogenicity [Corton 2000]. Tamura et al. directly compared the PPARα agonist mediated gene expression changes in primary hepatocytes and livers of in vivo treated rats. Genes involved in cell proliferation were markedly induced in vivo but hardly in vitro [Tamura 2006]. Parzefall et al. also showed that PPARα agonists failed to increase proliferation in in vitro cultured rat hepatocytes while DNA replication was increased when Kupffer cells were co-cultured or hepatocytes were treated with Kupffer cell derived TNFα [Parzefall 2001]. This discrepancy between in

vivo and in vitro derived results highlights one of the limitations of hepatocyte monocultures. Primary hepatocytes are well suited for the investigation of effects which are restricted to mechanisms and pathways taking place solely in the hepatocyte itself. However, effects triggered by intercellular signaling of different hepatic cell types were not detectable in the present system. FF downregulated genes encoding proteins which are synthesized in the hepatocytes and excreted into the blood after activated immune cells induced the appropriate pathways by the release of pro-inflammatory mediators [Dhainaut 2001]. Since these cells were not present in the hepatocyte monoculture the downregulation of chemokines, complement components and acute phase proteins could be related to drug-induced cytotoxicity, which secondarily decreases cellular protein production. This hypothesis is strengthened by the downregulation of genes encoding coagulation factors as another class of proteins which are synthesized and excreted by hepatocytes, but which have no relation to inflammatory processes. Further indications of cytotoxic effects mediated by FF include the downregulation of several genes involved in cell adhesion, morphology and maintenance of the cellular membrane potential. Based on the present gene expression data FF would have been classified as slightly hepatotoxic, since compared to EMD, as a potential PPARα-agonist, FF induced fewer genes related to oxidative stress. In addition, EMD enhanced the deregulation of these marker genes to a higher extent and also showed expression changes related to mitochondrial and metabolic impairment.

FF's toxicity is species-specific and the pharmacological mode of action also slightly differs between rodents and humans. Plasma triglyceride and cholesterol levels are decreased in both species by induction of PPARα, while proxisome proliferation and the enhanced expression of peroxisomal lipid metabolizing enzymes are restricted to rodents. Humans, as well as cultured human primary hepatocytes, lack the activation of rodent PPARα key targets like acyl coenzyme A oxidase, peroxisome proliferation and hepatocarcinogenesis [Roglans 2002, Klauning 2003, Ammerschläger 2004]. In primary human hepatocytes FF induced apoptosis but did not enhance proliferation [Klauning 2003, Kubota 2005]. In humans FF is regarded as a well tolerated and safe drug [Moutzouri 2010]. Increased ALT and AST serum levels, which preceeds transient FF induced hepatocellular reactions and chronic active hepatitis, have been reported [Tolman 2000]. The relative risk for cholelithiasis associated with fibrate treatment was 1.7-fold (80% of patients taking FF and 20% other fibrate derivatives).

A further study (FIELD trial) compared FF with a placebo in 9,795 patients while no case of biliary disease was reported and there was no increased incidence of cancer [Davidson 2007]. Thus, FF was chosen as a human low toxic reference substance for the Predict-IV project and only slight changes in the gene expression of FF treated human primary hepatocytes were expected. Therefore, the FF derived data reported here show in vivo relevant drug induced mechanisms and can be used as a basis for the investigation of species differences in primary hepatocytes. It also strengthens the need for in vitro studies prior to regulatory animal studies. If these tests are conducted in cells of rodents, as a standard species in toxicology and in cells of humans, species differences could be detected and regulatory studies could be performed in more human relevant species.

During the present study the high dose used for cellular treatment with FF (1000µM) was approximately two times higher than the lowest in vivo dose causing liver damage in rodents. The rodent c_{max} after oral treatment with 100mg/kg was 381 ± 120µM [Hanafy 2007]. Rats developed liver carcinomas during a 24-month study after daily oral dosing of 200mg/kg [FDA-FF 2004] and liver damage after two months of daily oral treatment with 60mg/kg [Pierno 2006]. The human steady state plasma concentration is achieved after five days of daily treatment. Then the c_{max} amounts to 63.7µM after 200mg of FF were taken [Keating 2002], approximately 2/3th of the LD used in the present study (100µM).

4.4.1.4 Troglitazone and Rosiglitazone

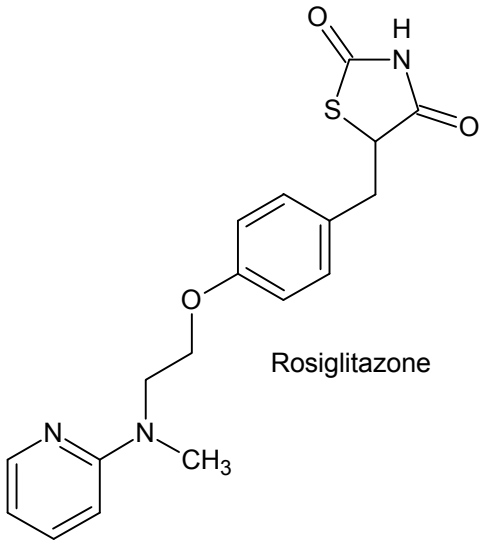

Rosiglitazone

Troglitazone (Tro) and Rosiglitazone (Rosi) belong to the class of thiazolidinedione drugs (TZDs) which were developed for the treatment of non-insulin dependent diabetes mellitus (NIDDM). This disease is based on insulin resistance of muscle and adipose tissue and is associated with hyperglycemia. TZDs increase the insulin sensitivity of muscle, liver and adipose tissue by activation of the peroxisome proliferator activated receptor γ (PPARγ), a ligand activated transcription factor of the nuclear hormone receptor super family [Tugwood 2002, Yokoi 2010]. PPARγ

dimerises, like PPARα, with the retinoid X receptor (RXR) after a ligand has bound. The activated PPARγ/RXR heterodimer binds to peroxisome proliferator response elements (PRE) and acts as a transcription factor for several genes involved in lipid and glucose homeostasis, adipocyte differentiation and inflammation. PPARγ is mainly expressed in adipose tissue, heart, intestine, colon, kidney, spleen and muscle cells. One of its main target genes is the glucose transporter GLUT4 which increases the uptake of glucose into muscle and adipose tissue and thereby lowers the blood glucose level [Corton 2000, Willson 2000].

Tro was the first TZD approved by the FDA in 1997. It was withdrawn from the market in March 2000 after 94 cases of severe drug-induced liver failure were associated with Tro treatment, including several liver transplantations and 65 deaths [Gale 2001, Tugwood 2002, Floyd 2009]. Preclinical tests with rodents showed no significant elevation of serum liver enzyme levels. Rats which received cardiotoxic doses of Tro developed liver necrosis and hepatocellular hypertrophy. Monkeys showed mild and tolerable hepatotoxic side effects, including bile duct hyperplasia [Smith 2003, Kaplowitz 2005]. During clinical studies 1.9% (48 persons) of the Tro treated patients (2510) had serum ALT levels greater than three times the upper limit of normal. Twenty patients were withdrawn from treatment and two patients developed reversible jaundice. The liver biopsies of two patients showed idiosyncratic hepatocellular damages while two others had also cholestatic effects. Tro's adverse hepatic effects occurred after long term treatment (three to seven months) and could not be linked to the dose. Thus, it was classified as idiosyncratic and approved due to a positive benefit/risk ratio [Watkins 1998, Lebovitz 2002]. Since then it has been heavily discussed if the findings during the clinical studies were interpreted in the right way and if Tro should have been approved [Gale 2001, Kaplowitz 2005]. After its withdrawal scientists all over the world have begun to investigate Tro's mechanisms of hepatotoxicity, which has not yet explained completely. In vitro Tro was found to be very cytotoxic, inducing depletion of GSH and damaging the mitochondria. Furthermore, Tro is a potent inducer of CYP1A, 2A, 2B6, 2D6, 2E1 and 3A4, especially in humans. After oral uptake Tro is transformed by several CYPs (Figure 4.14) especially CYP3A4 is involved in the formation of a very active quinone which can undergo redox cycling to generate ROS. This metabolite may be further transformed by ring opening to a bifunctional reactive intermediate which can bind covalently to DNA and proteins or undergo further redox

cycling to produce more ROS [Tuschl 2008]. Rachek et al. showed that the main mechanism of Tro's hepatotoxicity seemed to be the generation of oxidative stress, which damages mitochondrial DNA (mtDNA). This can lead to the depletion of ATP and the impairment of the electron transport chain, eventually triggering the production of further ROS. Finally, the mitochondria swell, their membrane depolarizes and cell necrosis or apoptosis is induced. This hypothesis is supported by a further experiment of this group where they showed that the co-treatment with an antioxidant diminishes the cytotoxicity of Tro [Rachek 2009].

Tro is excreted into the bile after sulfation and glucuronidation and inhibits the bile salt export pump (BSEP) in vitro in rat hepatocytes as well as in human clinical studies and therefore has the potential to induce cholestatic liver injury [Marion 2007, Yokoi 2010].

Compared to Tro, Rosi has a slightly modified molecular structure and shows a less cytotoxic potential at equimolar concentrations [Lloyd 2002, Guo 2006, Rachek 2009, Rogue 2011]. It was marketed in 1999 after clinical trials had been performed without any incidence of hepatotoxicity (but myocardial infarctions were observed). After its approval, Rosi was reported to be related to 11 cases of severe acute liver failure, including nine deaths [Floyd 2009]. This has been was challenged by other authors, who have stated Rosi's unsuspicious hepatic safety profile [Beiderbeck 2009, Osei 2009]. However, in September 2010 the EMA recommended the withdrawal of Rosi due to cardiovascular risks, whereupon Germany immediately stopped marketing the drug [press release 11/10 BfArM]. Rosi is extensively metabolized in the liver by CYP2C8 and CYP2C9. After N-demethylation and hydroxylation reactions the metabolites are conjugated with sulfate and glucuronic acid without the formation of reactive metabolites [DB-Rosi 2011, Kirchheiner 2005]. Rosi inhibits the mitochondrial respiration and induces apoptosis to a much lower extent than Tro, while ATP depletion and mtDNA damage have not been detected [Rachek 2009].

Several case studies of severe adverse hepatic effects in human patients who were treated with Rosi or Tro reported abrupt elevation of serum liver enzyme levels and poor general condition of patients who had been taking the drug for months or years and underwent regulary liver function tests. Biopsy and autopsy findings of patients which developed liver failure showed hepatomegaly, liver necrosis, bile duct proliferation, inflammation and cholestatic hepatitis. These effects were interpreted

as idiosyncratic side effects since they occurred independently from dosage and time of treatment [Li 2000, Murphy 2000, Gouda 2001, Bonkovsky 2002, Su 2006, Floyd 2009]. Since idiosyncratic reactions occur very rarely and are usually based on individual hypersensitivities or related to underlying diseases they are considered to be unpredictable with currently available in vitro and in vivo systems [Kaplowitz 2005, Uetrecht 2008].

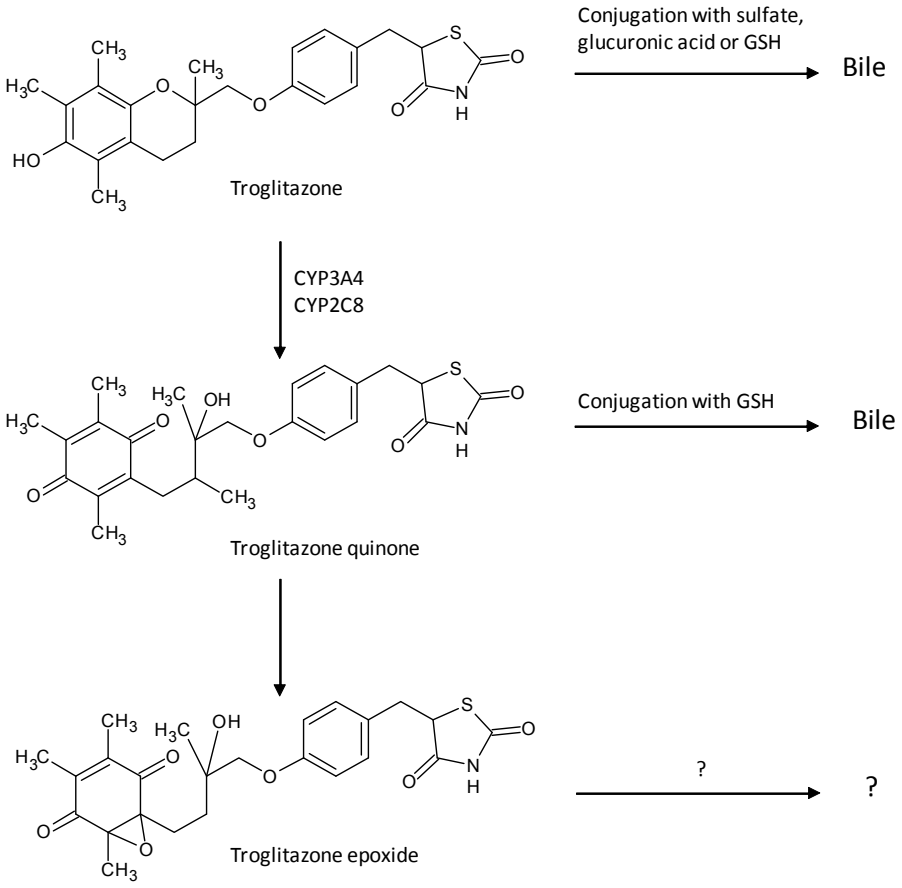

Figure 4.14: Metabolism of Troglitazone.
Tro is activated by different CYPs to active metabolites which can cause hepatotoxic effects when they are not detoxified by shown phase-II reactions [Tuschl 2008, modified].

Rosi but not Tro markedly altered gene expression of treated hepatocytes

During the study reported here Tro did not markedly alter the gene expression of the treated cells. This is visualized by the PCA (Figure 4.15) where the low and high dose of each time point clustered together with the time matched control. The dose finding for Tro was difficult since during the 24h screening assay the cell vitality seemed to be unaffected up to a dose of 60µM while 70µM decreased the vitality to 30.8 ± 12.8% and 80µM killed all the cells (Table 4.1). The cytotoxicity was expected

to increase with the time of treatment so the critical dose 70µM was tested again in the long term dose finding study but the cell vitality after 14 days of treatment was nearly unaffected up to 70µM and the next higher dose (100µM) killed all cells (Appendix Table 7.1). These effects were reproduced during the validation study in 6-well plates (Table 4.4). Thus, 70µM was chosen as the high dose since the morphology of the cells was slightly affected (Figure 4.6). In order to get better results in the gene expression study the dose range between 70µM and 100µM should have been investigated more precisely with small increments of the doses since these small changes in gene expression may be due to a high dose which was too low.

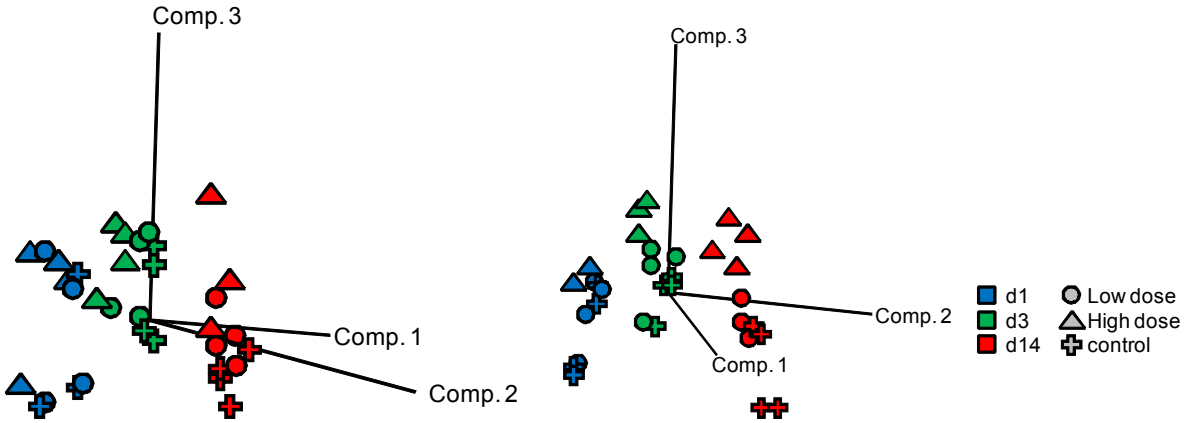

Figure 4.15: PCA of Troglitazone and Rosiglitazone samples.
The Tro treated samples (left figure) cluster together with the time matched controls indicating that Tro did not change the gene expression of the treated cells. Rosi changed the gene expression of the high dose treated cells since the high dose samples cluster separately from the low dose samples (right figure). The low dose did not affect the cell's expression level since the low dose clustered together with the time matched control.

Rosi notably changed the gene expression of the low and high dose treated cells. In the PCA (Figure 4.15) the samples of the low and the high dose of day three and 14 formed separate clusters while the samples of day one clustered together with the time matched control indicating that the gene expression after one day of treatment was similar to the gene expression level of the control cells. High dose treatment altered between three and 857 genes while the number of deregulated genes rose with the time of treatment (Table 4.6). Tro significantly deregulated 144 genes on day

three. However, some genes with a BH Q-value > 0.2 were also included into the biological data interpretation since they showed a trend correlating to the literature (Appendix Table 7.5, Table 7.6). The genes discussed in the following were also visualized using a heatmap (Figure 4.9).

Tro and Rosi enhanced the expression of genes involved in lipid metabolism

Tro and Rosi upregulated several genes involved in lipid metabolism, especially on day three (Appendix Table 7.5 and Table 7.6). In vivo the PPARγ agonists Tro and Rosi reduce the serum level of triglycerides and free FA's [Kumar 1996, Lebovitz 2001] by the activation of genes that lead to an increase in the differentiation of adipocytes and the fat storage in subcutaneous adipose depots. These tissues specifically highly express PPARγ, and especially the isoform PPARγ2 [Elbrecht 1996, Yanase 1997, Montague 2000, Schadinger 2005]. Although the adipose tissue is the major target of the TZDS, Memon et al. showed, that genes involved in hepatic lipid uptake and metabolism were induced in livers of Tro treated mice. Obese mice showed stronger effects than lean ones, while also the PPARγ gene itself was upregulated in the livers of obese mice compared to the lean control group. Therefore, the authors concluded that Tro's pharmacological effects are partly triggered by hepatic PPARγ [Memon 2000] and that especially PPARγ2 is upregulated in steatotic hepatocytes [Schadinger 2005]. Similar results were also obtained in Rosi treated mice [Watkins 2002]. Consistent with these data, in our in vitro study Tro and Rosi upregulated the genes encoding the low density lipoprotein receptor (LRP1) and the transporter CD36, which participates in hepatic lipid and FA uptake. Furthermore, the expression of genes involved in the breakdown of FA's in the cytosol, the mitochondria and the peroxisomes, such as monoglyceride lipase (MGLL), acyl-CoA thioesterase (ACOT1), acetyl-Coenzyme A acetyltransferase 1 (ACAT1) and peroxisomal acyl-CoA oxidase (ACOX1) were induced [Michael 1999]. Interestingly, the majority of these genes were deregulated to a higher extent by Rosi than by Tro (Appendix Table 7.5 and 7.6). In addition, genes encoding enzymes involved in fat storage, like perilipin 2 (PLIN2), were induced. Genes involved in the biosynthesis of cholesterol, for example sterol-C4-methyl oxidase-like (SC4MOL), were downregulated consistent with Wang et al. who showed the inhibition of cholesterol biosynthesis by Tro in HepG2 cells [Wang 1999].

Tro and Rosi altered the expression of genes involved in energy production

Apart from genes involved in lipid metabolism, PPARγ regulates genes involved in carbohydrate homeostasis. By activation of PPARγ TZDs increase peripheral glucose uptake while insulin resistance is decreased. This is mainly triggered by induction of the glucose transporters GLUT1 and GLUT4, which are expressed in adipose and muscle tissues. Yonemitsu et al. showed that Tro improves glucose transport in a rat muscle cell line by enhancement of the translocation of GLUT4 to the plasma membrane [Yonemitsu 2001]. Similar results were obtained in rat adipose tissue [Furuta 2002] and rat adipocytes in vitro [Shintani 2001] while gene expression of GLUT4 was also increased. In in vitro cultured primary human muscle cells Tro induced the expression of the glucose transporter GLUT1 while GLUT4 expression was not affected [Park 1998]. Furthermore, the GLUT4 gene was upregulated in subcutaneous adipose tissue of human patients during treatment with Tro [Ciaraldi 2002]. The hepatic glucose uptake and release is accomplished by GLUT2 while GLUT1 and GLUT4 are not expressed in hepatocytes [Uldry 2004]. GLUT2 was downregulated by Rosi during the present study on day three and 14 but not by Tro. Tro and Rosi also upregulated genes encoding enzymes which are involved in glycolysis, like phosphoglycerate kinase 1 (PGK1), phosphofructokinase (PFKL) and enolase (ENO1) [Michael 1999]. In addition, Rosi upregulated the gene expression of the glycolytic enzyme glucokinase (GCK), consistent with Kim et al. who detected a PPRE in the GCK gene [Kim 2004]. The decrease of hepatic gluconeogenesis by TZDs was shown in rodents in vivo [Fujiwara 1995, Aoki 1999] and in vitro [Davies 1999, Davies 2001] while the gene expression and/or the activity of enzymes like glucose-6-phosphatase (G6P) and phosphoenolpyruvate carboxykinase (PCK1) were found to be repressed. In the present study Rosi induced the PCK1 gene on day one while it was downregulated on day three and not deregulated after 14 days of treatment. Rosi decreased the gene expression of the catalytic subunit of G6P (G6PC) on day three while Tro had no effect on either gene. In contrast, Tro and Rosi induced the expression of the pyruvate carboxylase gene (PC) after three days of treatment. PC is also involved in gluconeogenesis and is hypothesised by Fulgencio et al. to be inhibited by TZDs [Fulgencio 1996]. The pyruvate dehydrogenase kinase (PDK4) gene was induced by Tro and Rosi. PDK4 inhibits the formation of acetyl-CoA from pyruvate, as the end product of glycolysis, and its

upregulation may be triggered by enhanced lipid catabolism, required to provide enough energy for the cell [Sugden 2001].

Uncoupling protein 2 (UCP2) gene expression was induced by Tro after three days and by Rosi after one and three days of treatment. UCPs are proton channels which are able to uncouple the oxidative phosphorylation in the mitochondria by proton influx, independent from the ATPase. This energy consumptive process is normally used to generate heat in the adipose tissue and can lead to ATP depletion and cell death by the uncontrolled decrease of the transmembrane potential [Chavin 1999, Voet 2002]. The upregulation of UCP2 gene expression was also detected in rodent livers after in vivo treatment with Tro [Memon 2000]. Impairment of mitochondrial respiration appears to be a major mechanism of Tro's hepatotoxicity. Nadanaciva et al. reported Tro, but not Rosi, to act as an uncoupler and inhibitor of oxidative phosphorylation [Nadanaciva 2007]. A further study showed that Tro induced mitochondrial permeability transition while Rosi did not [Masubuchi 2006a]. During the present study Tro and Rosi induced UCP2 to a similar extent, which was considered to be an indicator of drug-induced mitochondrial effects. Therefore, based on these gene expression changes it could not be shown whether Tro is more toxic than Rosi.

Tro and Rosi induced stress markers and genes involved in drug metabolism

Tro is a potent inducer of its own metabolism, via CYP3A4 induction [Sahi 2000], which was upregulated up to 39-fold by day 14. Rosi also induced CYP3A4 in a time-dependent manner up to 31-fold. Phase-II enzymes like UDP-glucuronosyltransferase (UGT), sulfotransferase (SULT) and glutathione-S-transferase (GSTA) were upregulated by both substances, indicating an active detoxification process. Tro heavily enhanced (12.4-fold) the gene expression of GSTA5 on day 14, which suggests the formation of reactive metabolites as they are usually detoxified via conjugation with GSH (Figure 4.14). These metabolites can then bind to cellular components and cause oxidative stress and DNA damage. Rosi lacks the chroman ring which is metabolized to form Tro's toxic metabolite. This may be the reason for Rosi's lower hepatototoxic potential [Smith 2003]. Interestingly, genes encoding antioxidant enzymes like glutathione peroxidase (GPX1; which detoxifies ROS in the mitochondria [Marquardt 2004]), ferritin (FTL) [Cairo 1995, Vogt 1995, Orino 2001] and thioredoxin interacting protein (TXNIP) [Watanabe 2010],

which are general markers for oxidative stress, were induced by both Tro and Rosi to a similar extent. The strong induction of genes related to the metabolism and transfer of GSH, like GSTA5 and GPX1, indicate a depletion of GSH in the Tro treated cells, and is a well described mechanism of Tro's hepatotoxicity [Smith 2003]. Masubuchi et al. showed that Tro is transformed into reactive metabolites faster than other TZDs and possesses a high GSH-conjugation rate in rats and humans [Masubuchi 2007]. Neither Tro nor Rosi induced the expression of genes related to DNA damage in the present study. However, oxidative stress can also be produced by extensive oxidation of FA's, especially in the peroxisomes. Enzymes like ACOX1, whose gene expression was induced during the present study, are known to produce hydrogen peroxide [Corton 2000]. Consistent with this, the gene encoding catalase (CAT), which reduces hydrogen peroxide, was induced by Tro and Rosi, and can be considered to be a compensatory mechanism.

Tro and Rosi suppressed proliferation-associated genes and induced pro-apoptotic factors

PPARγ agonists were shown to inhibit proliferation and to induce apoptosis in several human cancer cell lines [Morosetti 2004, Freudlsperger 2006, Lin 2007]. Rosi also reduced tumor incidence in a mouse model for hepatocarcinogenicity [Galli 2010]. In mouse hepatocytes the suppression of cyclin D1, as a key mechanism for cell cycle arrest in the G1 phase, is mediated by PPARγ2 activation [Sharma 2004]. However, in several clinical studies Rosi and Tro failed to inhibit tumor growth of the breast [Burstein 2003, Yee 2007], prostate [Smith 2004], thyroid [Kebebew 2009] and colon [Kulke 2002]. During one study, Tro stabilized the disease state of prostate cancer patients for up to 90 weeks [Mueller 2000]. Hepatocytes are differentiated cells which proliferate very rarely [Marquardt 2004] and are therefore not well suited for the study of cell cycle arrest.

However, after one day of high dose treatment Rosi upregulated the gene encoding cyclin D1 (CCND1), which is involved in the cell cycle progression from G0 to early G1 phase [Flatt 2000]. The cell cycle promotor cell division cycle 25 homolog A gene (CDC25A) was also induced on days one and three [Källström 2005]. Furthermore, the genes for the cell cycle inhibitors p21 (CDKN1A) and p27 (CDKN1B), which act during the G1 phase [Owa 2001], were downregulated on day 14. The G0/G1switch 2 (G0S2) gene expression was induced after three and 14 days. G0S2 is reported to

be upregulated during the re-entry from G0 into G1 phase in blood mononuclear cells [Russell 1991], while recent studies showed that G0S2 acts as tumor suppressor triggering apoptosis after DNA damage in human primary fibroblasts [Welch 2009]. Further genes which were associated with liver regeneration after partial hepatectomy in vivo, such as angiotensinogen (AGT) and serpin peptidase inhibitor clade E member 2 (SERPINE2), were also induced after three and 14 days [Cimica 2007]. In contrast, the genes encoding connective tissue growth factor (CTGF), syndecan 4 (SDC4) and alpha-2-macroglobulin (A2M) were downregulated in the present study while their induction has been correlated to liver regeneration and proliferation [Cimica 2007]. Genes encoding polymerase delta 4 (POLD4), which is involved in DNA replication [Liu 2006], and tubulin alpha 1a (TUBA1A), which participates in spindle formation [Hernández 2009], were also repressed. The annexin A5 gene (ANXA5), the induction of which has been associated with many carcinomas in rats and humans [Glückmann 2007, Xue 2009], was downregulated on day 14 as well as transforming growth factor alpha/beta (TGFA/B). The expression of the pro-apoptotic member of the BCL2-family BCL2-like 14 (BCL2L14) [Matés 2008] was induced on days 3 and 14, as was the cell death inducing DFFA-like effector A gene (CIDEA) [Valousková 2008], indicating the induction of apoptosis. However, genes encoding pro-apoptotic key factors, like BCL2-antagonist/killer 1 (BAK1) and BCL2-related ovarian killer (BOK) [Hail 2006], were downregulated on day 14 and no caspases were deregulated.

In conclusion, these results indicate that Rosi did not enhance proliferation but induced apoptosis in the treated cells. Since the present study was performed in primary hepatocytes, which are differentiated cells remaining in the G0 phase, any cell cycle arrest effects caused by Rosi could not be shown directly with this in vitro system. Although several publications have described Rosi's anti-proliferative action, the upregulation of the cyclin D1 gene on day one and the suppression of the cell cycle inhibitors p21 and p27 on day 14, together with the induction of genes associated with liver regeneration on days 3 and 14 indicate a re-entry of the hepatocytes into the cell cycle during the earlier time points. In contrast, the downregulation of genes encoding proteins and enzymes involved in later phases of the cell cycle, like POLD4, TUBA1A and ANXA5, indicate that after 3 and 14 days of treatment with Rosi cell cycle progression was inhibited. This hypothesis is supported by the gene expression profile of the cell cycle promotor CDC25A which was

upregulated at early time points but not on day 14. In addition, Rosi induced the gene expression of pro-apoptotic factors on day 14 while anti-apoptotic factors were not upregulated.

The gene expression profile of the Tro treated cells resembled the one of the Rosi treated hepatocytes, although Tro affected a smaller number of genes. Genes encoding cyclins or cell cycle inhibitors were not deregulated. Gene expression of SERPINE2 and AGT, which are associated with liver regeneration, was induced by high dose treatment on day three while genes encoding the growth factors CTGF and EGR1 were downregulated. On day three the G0G2 gene, which might be involved in cell cycle re-entry from the G0 phase or the induction of apoptosis, was induced as well as the gene encoding the cell cycle promotor CDC25A while on day 14 the polymerase TOP2B gene was repressed. In addition, gene expression of the pro-apoptotic factors, BCL2L14 and CIDEA, was upregulated indicating that Tro like Rosi did not activate cellular proliferation but apoptosis in the present study.

Tro and Rosi deregulated genes associated with different cell functions

Tro was shown to inhibit the bile salt export pump (BSEP) in rat hepatocytes as well as in human clinical trials while a decrease of bile salt excretion can lead to Tro-induced intrahepatic cholestatic liver injury [Marion 2007, Yokoi 2010]. Tro inhibits rodent BSEP protein with a K_i value of 1.3µM [Funk 2001]. During the present study the gene expression of BSEP was not affected by Tro and Rosi, agreeing with Rogue et al. [Rogue 2011] while Rosi downregulated the gene encoding the transporter MDR1 which is also involved in biliary excretion. On day 14 both compounds induced the gene expression of the basal uptake transporter OATP8 while Rosi also upregulated the gene encoding OAT2 - a transporter involved in the efflux of substances from the blood [Giacomini 2010].

Tro and Rosi induced the gene expression of PEX11A and PEX19 which are markers for peroxisomal biogenesis [Koch 2010]. The expression of the PPARγ gene was not significantly induced by Rosi or by Tro during this study. However, Davies et al. showed that Tro induces PPARγ on mRNA and protein levels in in vitro cultured rat hepatocytes, as well as in livers of in vivo treated rats [Davies 1999a, Davies 2002]. Rogue et al. detected a significant PPARγ induction in rat hepatocytes treated with 40µM Tro but not in Rosi treated cells [Rogue 2011]. The rodent EC50 for PPARγ was calculated to be 0.076µM for Rosi and 0.78µM for Tro [Willson 2000]. Thus, the

compound concentrations used during the present study were high enough to have activated PPARγ, which was confirmed by gene expression changes correlating with relevant PPARγ associated effects described in the literature.

Tro and Rosi downregulated genes involved in cell adhesion and morphology, for example E-cadherin (CDH1), fibronectin (FN1) and tubulin (TUBA1A) indicating that the cells started to detach due to cytotoxicity [Chen 2006, Malcos 2011]. Furthermore, genes encoding proteins which are synthesized and secreted by hepatocytes, such as the coagulation factors F5, F9, and F11, the complement components C6, CFH, and CFI, the chemokines CXCL9, CXCL11, and CXCL16 as well as the acute phase proteins alpha-2-macroglobulin (A2M) and fibrinogen (FGB), were all downregulated. Except for the coagulation factors these proteins are involved in hepatic inflammatory processes and are regulated by the intercellular signaling between hepatocytes and immune cells [Trautwein 1994, Dhainaut 2001]. Since this cell type was missing in the present system and the gene expression of other hepatic proteins like coagulation factors were also suppressed, these deregulations appear to be associated with drug-mediated toxic effects impairing cellular protein production.

In conclusion the pharmacological effects of Tro and Rosi could be only partly reconstructed by the whole-genome gene expression analysis in primary hepatocytes reported here. This was expected since the targets of TZDs are adipose and muscle tissue which highly express PPARγ [Grossman 1997]. Nevertheless, the upregulation of lipid metabolism associated genes and the downregulation of genes involved in hepatic gluconeogenesis could be shown, confirming what is known from the literature. The gene expression data presented here were consistent with a similar study performed by Rogue et al. [Rogue 2011] as well as with results of an in vivo study in mice [Memon 2000, Watkins 2002]. TZDs were shown also to have anti-proliferative effects [Freudlsperger 2006, Galli 2010]. Although hepatocytes, as differentiated cells, are not well suited for the study of cell cycle arrest our data indicated that genes related to cell cycle promotion were suppressed by Tro and Rosi while apoptotic factors were induced. However, the focus of the present study was the investigation of genes involved in any toxic effects. Both compounds are known to induce CYP3A4 which can transform Tro into reactive metabolites [Sahi 2000].

The CYP induction, as well as the upregulation of genes related to oxidative stress and uncoupling of the oxidative phosphorylation, could be clearly shown. Interestingly, Rosi deregulated a higher number of genes and triggered higher fold changes for genes involved in lipid and energy metabolism than Tro although the used concentration for cellular treatment was only slightly higher. In vivo Rosi possess a higher efficacy than Tro since the recommended daily doses for humans are 4 - 8mg for Rosi and 200 - 600mg for Tro [RX-Rosi 2011, RX-Tro 2011]. However, Tro was shown to be more cytotoxic than Rosi at equimolar doses in vitro [Lloyd 2002, Guo 2006, Rachek 2009, Rogue 2011] which was confirmed during the dose finding part of the present study. Furthermore, Tro induced the CYP3A4 gene and several genes encoding enzymes of the xenobiotic metabolism to a higher extent than Rosi but not marker genes of oxidative stress. This was not expected, since Rosi was assumed to be less hepatotoxic than Tro, based on the different molecular structures that can prevent the formation of reactive metabolites [Smith 2003, Kirchheiner 2005]. Nevertheless, Masubuchi et al. showed that Rosi can be conjugated to GSH. They concluded that Rosi is also transformed into reactive metabolites but to a lesser extent and at a much slower rate than Tro [Masubuchi 2007]. Tro and Rosi were also part of a set of reference compounds used for the development of an in vitro prediction model for hepatotoxicity based on gene expression changes in sandwich cultured primary rat hepatocytes [Hrach 2011]. In their study one of three biological replicates of Tro was misclassified as non-hepatotoxic while Rosi was rightly predicted to be non-hepatotoxic. The doses used for cellular treatment with Tro and Rosi were similar to these used in the present study. Based on the present gene expression data Rosi would have been classified as a weak hepatotoxic compound, since it upregulated marker genes for oxidative stress while there were no indications for mitochondrial impairment and DNA damage. Tro would have been classified as non- or weakly hepatotoxic due to minor expression changes of genes associated with oxidative stress and energy production.

The doses used for cellular treatment during the present study were in vivo relevant for Tro (LD = 7µM, HD = 70µM) but not for Rosi (LD = 8µM, HD = 80µM). Tro caused hepatomegaly during a 104 - week study where male rats were orally dosed with 400mg/kg/day or 800mg/kg/day, while the highest dose also caused liver necrosis. Interestingly, female rats seemed to absorb Tro more effective than males since they

possessed higher plasma levels and therefore showed greater adverse hepatic effects already after oral dosage of 200mg/kg. The c_{max} of male rats after the administrations of 400mg/kg amounted to 36.4 ± 24.9µM and was comparable to the c_{max} of rats which received 800mg/kg of Tro. The c_{max} of female rats after the administrations of 200mg/kg amounted to 166.8 ± 42.6µM [FDA-Tro 1997]. Female rats which received 400mg/kg/day of Rosi had a c_{max} of 350.3 ± 8.2µM and developed hepatomegaly during a four-week study [FDA-Rosi 1999]. Concentrations in the range of the rodent c_{max} of Rosi could not be used for the treatment of hepatocytes in the present in vitro system since a dose more than four times the present high dose was very cytotoxic. The human c_{max}, after taking recommended doses was 1.6 ± 0.9µM for Rosi [Cox 2000] and 2 - 4µM for Tro [Funk 2001]. Short term studies in primary human hepatocytes detected no or only slight cytotoxicity for Rosi with concentrations up to 200µM [Lloyd 2002, Rogue 2011a]. Thus, human hepatocytes can be treated with doses more than 100 times the safe human plasma concentration of Rosi, which is a good basis for the investigation of dose-dependent human cytotoxicity. Tro was found to be more cytotoxic in human than in rat hepatocytes [Lauer 2009, Rogue 2011 and 2011a]. Cellular treatment can be performed with doses which are several times the human safe plasma concentration, therefore enabling human in vitro investigations similar to Rosi. However, these tests can detect dose-related predictable toxicities while the idiosyncratic part of Tro's and Rosi's hepatotoxicity will remain unpredictable with our present system. Studies with primary human hepatocytes of different donors are suited better for the investigation of idiosyncratic effects since donors may express varying isoforms of drug-metabolizing enzymes possessing different activities. Furthermore, individual hypersensitivities and immunological parameters may be studied if co-cultures with Kupffer cells are implemented.

4.4.1.5 EMD 335823

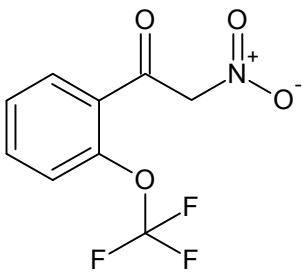

EMD 335823 (EMD) was a drug candidate developed by Merck KGaA for the treatment of diabetic complications. During phases of high intracellular glucose levels, for example due to diabetes mellitus, glucose is transformed via two steps into fructose (polyol pathway) in addition to normal glycolysis. The first and rate limiting reaction is the formation of sorbitol catalyzed by

aldose reductase (AR) [Lorenzi 2007], the target molecule of EMD 335823 [internal data]. Sorbitol is a very hydrophilic alcohol which cannot diffuse through cell membranes and therefore accumulates in the cell. The resulting osmotic changes are discussed to trigger common diabetic complications like retino-, nephro- and neuropathy. Another hypothesis assumes that these effects are caused by oxidative stress. Firstly, AR consumes NADPH which is also a co-factor for GSH-reductases. Reduced GSH is essential for the cellular defense against reactive metabolites. Secondly, the enzyme transforming sorbitol into fructose produces NADH. An altered NAD^+/NADH ratio affects several cell functions and increased levels of NADH may activate NADH oxidases which can cause oxidative stress [Lorenzi 2007, Cunha 2008, Matsumoto 2008].

During a preclinical two-week oral study EMD caused strong elevations of serum levels of liver enzymes in rats, indicating marked liver damage. Histopathological findings included bile duct necrosis and inflammation as well as liver cell necrosis after low (25mg/kg) and high dose (500mg/kg) treatment. Furthermore, EMD induced several PPARα target molecules, like members of fatty acid β-oxidation, and was therefore assumed to be a potential PPARα activator. It also induced enzymes involved in the detoxification of reactive metabolites, oxidative stress and damaged proteins, such as glutathione-S-transferase (GSTA2), UDP-glucuronosyltransferase (UGT1A6) and FK506 binding protein (FKBP11). EMD inhibited its pharmacological target AR. AR is furthermore involved in the transformation of toxic lipid metabolites like 4-hydroxy-trans-2-nonenal (HNE) into 1,4-dihydroxynonene (DHN). GSH-conjugates of HNE and DHN were found in liver, blood and urine of treated rats [internal data] indicating that EMD reduced the formation of DHN by inhibition of AR, which was shown also by Srivastava et al. for other AR inhibitors [Srivastava 2001]. The development of EMD was stopped prior to any clinical studies, since the preclinical findings showed a high risk of the formation of drug induced liver injuries in humans. In the context of the PredTox project, funded by the European Commission as part of the Sixth Framework Programme (FP6), EMD was re-tested in rats which developed similar adverse hepatic effects at high dose (350mg/kg) but not at low dose (15mg/kg) treatment [Adler 2010].

EMD markedly altered gene expression of treated cells

EMD markedly changed the gene expression level in the high dose treated cells during this study. This was shown in the PCA (Figure 4.16) where the high dose samples of all time points clustered separately, as well as by the large number of statistically significant deregulated genes (Table 4.6) which increased with the time of treatment. The low dose samples clustered very close to the time-matched controls illustrating that their gene expression levels were not markedly altered compared to the control samples. The PCA also showed the time-related difference between the gene expression level of the low and the high dose treated cells since the low and high dose of the first time point cluster closer together than the low and high dose samples of day three and 14. High dose treatment with EMD dose-dependently deregulated between 37 and 1063 genes (Table 4.6). The genes discussed in the following biological interpretation are listed in the appendix (Appendix Table 7.7) and are visualized by a heatmap (Figure 4.9).

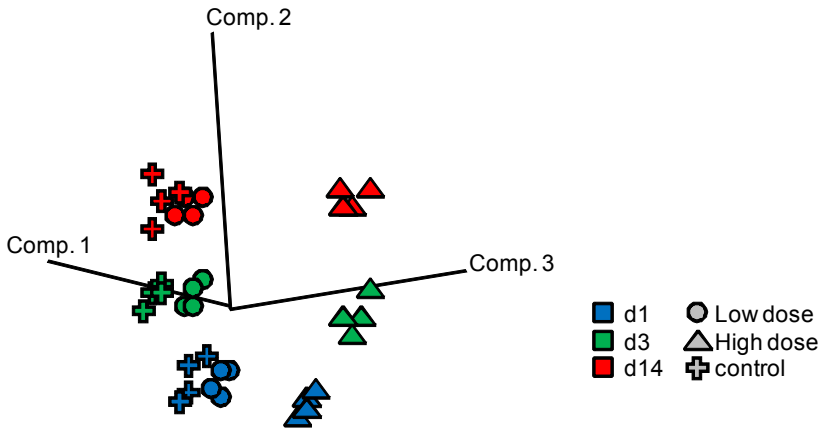

Figure 4.16: PCA of EMD samples.
The low dose treated samples of all three time points cluster very close to the time matched controls indicating a slight difference of the gene expression level of these sample groups. The high dose treated samples cluster completely separately as a consequence of a markedly altered gene expression profile compared to the control.

EMD induced genes involved in lipid metabolism

In agreement to the preclinical findings, EMD induced many genes involved in lipid metabolism, including direct PPARα target genes [Mandard 2004]. The genes encoding the very low density lipoprotein receptor (VLDLR) and the transporter CD36, which are involved in the uptake of lipids from the blood, as well as the PPARα target gene encoding lipoprotein lipase (LPL) which cleaves lipids into

glycerol and FA, were upregulated. In addition, the expression of genes involved in FA metabolism, including acyl-CoA thioesterase (Acot1), were enhanced up to 90-fold. Expressions of the PPARα target genes CYP4A11 and FA binding protein (FABP1) were induced, and are involved in catabolism and intracellular transport of FA. Genes involved in the import of FA into the mitochondria, like carnitine O-octanoyltransferase (CROT), carnitine O-acetyltransferase (CRAT) and carnitine palmitoyltransferase (CPT1B), were also induced as well as several genes involved in mitochondrial and peroxisomal FA catabolism. Interestingly, the strongest upregulations were observed on day three (Appendix Table 7.7), which correlates well with the gene expression study performed in livers of rats treated with EMD [Ellinger-Ziegelbauer 2011]. Cholesterol synthesis seemed to be downregulated since genes encoding lecithin-cholesterol acyltransferase (LCAT) and ATP citrate lyase (ACLY) were repressed while genes involved in fat storage, such as fat storage-inducing transmembrane protein (FITM2) and perilipin (PLIN2), were induced. Genes associated with peroxisome proliferation, a typical effect of PPARα agonists in rodents [Li 2002a], were upregulated up to 5.1-fold. These included genes involved in peroxisomal FA catabolism, for example acyl-CoA thioesterase (ACOT8) and the PPARα target gene acyl-CoA oxidase (ACOX1), as well as genes related to peroxisomal biogenesis and division (e.g., peroxisomal biogenesis factors 11 alpha and 19 (PEX11A, PEX19)). The expression changes of genes involved in lipid metabolism caused by EMD is consistent with gene expression results of hepatocytes and livers of rats treated with known PPARα agonists [Guo 2006, Tamura 2006] as well as with the gene expression profile of the FF treated cells reported in this study. Thus, these findings support the hypothesis of EMD being a potential PPARα agonist. However, the PPARα gene itself was not upregulated by EMD during the present study, but this is in agreement with previously published reports for FF and other PPARα agonists [Guo 2006, Tamura 2006, Ellinger-Ziegelbauer 2011, Sposny 2011].

EMD increased the expression of drug-metabolizing enzymes and stress markers

EMD upregulated genes encoding several phase-I enzymes, including alcohol dehydrogenase (ADH1C), aldehyde oxidase (AOX1) and epoxide hydrolase (EPHX) while CYP3A4 induction increased time-dependently up to 26.3-fold. EMD also upregulated the expression of genes encoding the phase-II enzymes glutathione-S-transferases (GSTA) and UDP-glucuronosyltransferases (UGT) at all time points,

indicating an enhanced activation of detoxification processes within these cells. Here the strongest inductions were observed for GSTA5, which conjugates reactive metabolites with GSH and was upregulated time-dependently up to 20.9-fold. EMD induced further genes encoding enzymes which are involved in GSH metabolism: GSH reductase (GSR) regenerates oxidized GSH, GSH peroxidase (GPX2) reduces and detoxifies peroxides while GSH is oxidized and glutamate-cysteine ligase (GCLC) catalyzes the first step of GSH synthesis. The enhanced gene expression of enzymes involved in the synthesis, regeneration and conjugation of GSH suggests the formation of reactive metabolites and ROS in the EMD treated cells followed by a possible GSH depletion [Yuan 2009]. This hypothesis is strengthened by the upregulation of genes encoding stress markers, like oxidative stress induced growth inhibitor (OSGIN1) and FK506 binding protein (FKBP8) as well as antioxidant enzymes like superoxide dismutase (SOD2), heme oxygenase (HMOX1), catalase (CAT), thioredoxin interacting protein (TXNIP) and NAD(P)H quinone dehydrogenase (NQO1). These changes clearly show that EMD induced oxidative stress and activated the NRF2 related stress defense [Kaspar 2009]. The results also support the effects found in preclinical studies and are consistent with a gene expression study in livers of rats treated with EMD [Ellinger-Ziegelbauer 2011, Sposny 2011].

EMD deregulated genes involved in energy production

EMD downregulated different genes involved in glycolysis, such as glucokinase (GCK), pyruvate kinase (PKLR) and lactate dehydrogenase B (LDHB), as well as gluconeogenesis like glucose-6-phosphate isomerase (GPI), glucose-6-phosphatase (G6PC) and glucose-6-phosphat translocase (SLC37A4). Furthermore, the glycogen synthase gene (GYS2) and the gene encoding the glucagon receptor (GCGR) were downregulated. GYS2 is involved in the storage of glucose by synthesizing glycogen while GCGR triggers the cellular signaling for the utilization of stored glycogen [Voet 2002]. In addition, the gene expression of pyruvate dehydrogenase (PDHB) and malate dehydrogenase 2 (MDH2), which are involved in the Krebs cycle, were repressed and the gene encoding pyruvate dehydrogenase kinase (PDK4), an inhibitor of PDHB, was induced. The downregulation of genes related to glycolysis, gluconeogensis, the Krebs cycle as well as the catabolism and the synthesis of glycogen indicated toxic effects leading to an impairment of cellular energy production, as well as effects on mitochondrial function. This is strengthened by the upregulation of the gene encoding malic enzyme (ME1) which transforms malate, an

intermediate of the Krebs cycle, into pyruvate [Heart 2009], as well as the increased gene expression of lactate dehydrogenase A (LDHA) which is involved in anaerobic glycolysis. In addition, gene expression of uncoupling protein (UCP2) was increased. UCP2 plays a role in the generation of ROS, sustains the ratio of adenosine triphosphate/adenosine diphosphate and is able to uncouple oxidative phosphorylation leading to an uncontrolled decrease of the mitochondrial transmembrane potential. This can cause ATP depletion and eventually cell death [Chavin 1999]. UCP2 was also induced in studies performed with primary hepatocytes treated with other PPARα agonists [Mandard 2004] but also in hepatocytes treated with the PPARγ agonist Tro which is known to cause mitochondrial damage [Memon 2000]. The upregulation of the glycerol-3-phosphate dehydrogenase gene (GPD1) on day 14 seemed to be an attempt by the cells to maintain mitochondrial function, since GPD1 mediates the entrance of electrons into the electron transport chain, thus building up the mitochondrial transmembrane potential.

Genes related to protein production and cellular adhesion were downregulated

EMD time-dependently downregulated genes involved in cellular adhesion, like laminin (LAMC2), cadherin (CDH1), vitronectin (VTN), as well as cell morphology such as vimentin (VIM), tubulin (TUBA1A) and filamin (FLNA) [Chen 2006, Malcos 2011, Vuoriluoto 2011]. The suppression of these genes indicates that the cells may have started to detach. Detaching of hepatocytes was associated with dedifferentiation and the loss of hepatic function, since primary hepatocytes in suspension retain their functional activity only for a few hours [Jouin 2006, Hewitt 2007]. Consistent with this, genes encoding proteins which are synthesized and released by hepatocytes like the coagulation factors F5, F11, and F12, the complement components C2, C5, C6, CFB and CFH, as well as the acute phase proteins alpha-2-macroglobulin (A2M) and alpha-2-HS-glycoprotein (AHSG) were downregulated. The excretion of complement factors and acute phase proteins, as part of the inflammatory response, is triggered by activated immune cells by the release of mediators which bind to receptors on the hepatocyte membrane [Tacke 2009]. Since these cell types are not present in a hepatocyte monoculture the deregulation of the appropriate genes can be assumed to be a toxic effect due to a diminished cellular protein production within the hepatocytes. In addition, the gene

expression of CYP7A1, which is involved in the synthesis of bile acids, as one of the hepatic key functions was downregulated as well as Na-K-ATPase (ATP1A1) which plays a central role in maintaining the cellular transmembrane potential.

EMD-treatment affected the gene expression of different transporters

The gene encoding the basolateral transporter SLCO2B1 (OATP-B) which imports substrates from the blood into the hepatocyte was time-dependently downregulated. Furthermore, the biliary efflux transporter encoded by the gene ABCG2 (BCRP) was induced on day three while the Abcb1b gene (MDR1) was time-dependently downregulated. The gene expression of basal transporters was also affected contrarily since MRP3 was upregulated on days one and three while MRP6 was downregulated on day 14. In summary, genes encoding efflux and influx transporters were deregulated without any obvious trend. While the apical cholesterol transporter encoded by the gene ABCG5 was upregulated up to 6.2-fold. An increased excretion of cholesterol into the bile has been reported to be associated with FF-mediated hepatitis [RX-FF 2011] and may also account for biliary adverse effects of EMD. However, whether EMD increases the biliary cholesterol efflux from treated hepatocytes has to be validated using other functional tests.

MRP3 inter alia transports conjugated bilirubin, the product of hemoglobin breakdown, back into the blood when the biliary excretion via MRP2 is disturbed. Thus, an increased expression of MRP3 can cause hyperbilirubinemia [Kamisako 2000]. Although MRP2 gene expression was not affected, the deregulation of the MRP3 gene may be a hint that there was an adverse effect of the bile ducts during preclinical studies. It has been shown that sandwich cultured primary hepatocytes form functional bile canaliculi-like structures [Tuschl 2006, Tuschl 2009]. However, these structures lack endothelial cells which coat the bile ducts in vivo and are involved in biliary adverse effects [Marquardt 2004]. During preclinical studies rats treated with EMD developed bile duct necrosis and inflammation. Effects like these can not be studied using monocultures of primary hepatocytes since this system lacks the affected endothelial cells. Furthermore, inflammation is usually triggered by the release of inflammatory mediators like cytokines by the Kupffer cells which can activate apoptosis in hepatocytes and recruit peripheral immune cells into the liver [Tacke 2009]. Thus, the deregulation of transporters in compound-treated hepatocytes can give only hints for biliary effects.

EMD induced the gene expression of its pharmacological target molecule

EMD upregulated the gene expression of its target molecule AR (AKR7A3) at all three time points, with the greatest induction seen on day 3 (13.5-fold). These results correlate well with the in vivo EMD rat data, where this molecule was induced on the gene and protein levels [Sposny 2011]. The induction of the gene could be a direct consequence of the inhibition of the AR enzyme as EMD's pharmacological effect. The blockade of the polyol pathway, as the alternative for glycolysis, should consequently lead to an increased rate of this catabolic pathway. However, genes involved in glycolysis were downregulated while the polyol pathway is only activated at high glucose levels and therefore difficult to study at physiological glucose concentrations [Lorenzi 2007].

EMD downregulated genes involved in apoptosis and proliferation

On day 14 EMD downregulated genes encoding pro-apoptotic key factors like BCL2-antagonist/killer 1 (BAK1) and BCL2-related ovarian killer (BOK), which can be activated by cellular stress [Hail 2006]. On day three gene expression of the pro-apoptotic member of the BCL2-family, BCL2-like 14 (BCL2L14) [Matés 2008] and the cell death-inducing DFFA-like effector gene (CIDEA) [Valousková 2008], were induced.

Gene expression of cyclin D1 (CCND1), which promotes cell cycle progression in early G1 phase, and cyclin-dependent kinase inhibitor 1B (p27, Kip1) which plays a role in cell cycle progression from G1 to S phase [Ogawa 2009], were downregulated on day 14, consistent with the findings in vivo [Ellinger-Ziegelbauer 2011]. Further indications that EMD did not induce cell proliferation were the upregulation of genes geminin (GMNN), which inhibits centrosome dublication [Lu 2009], and growth arrest and DNA-damage-inducible alpha (GADD45A), which triggers cell cycle arrest due to DNA damage. Genes encoding growth factors involved in cellular proliferation and growth, like transforming growth factor alpha (TGFA), connective tissue growth factor (CTGF) and early growth response 1 (EGR1), were repressed on day 14 while the cell cycle promotor cell division cycle 25 homolog A gene (CDC25A) was induced on day one and three [Källström 2005, Cimica 2007]. The downregulation of genes involved in proliferation and cell cycle progression indicate that EMD did not enhance cellular proliferation during this study. Pro-apoptotic genes were downregulated on day 14 but upregulated on day three in correlation with the induction of the

GADD45A gene which is involved in cell cycle arrest after DNA damage. However, no other genes associated with DNA damage were upregulated.

In conclusion, the gene expression profile of EMD treated hepatocytes was similar to the profile of FF as well as literature data of hepatocytes treated with other known PPARα agonists [Cornwell 2004, Guo 2006, Tamura 2006]. The induction of genes involved in lipid metabolism and peroxisomal biogenesis, as well as the upregulation of known PPARα targets, could be shown. However, PPARα agonists usually act as non-genotoxic hepatocarcinogens in rodents while the formation of oxidative stress and the disturbance of the balance between proliferation and apoptosis are discussed as molecular mechanisms [Corton 2000]. EMD induced the gene expression of different antioxidant proteins and enzymes involved in the detoxification of reactive metabolites indicating the formation of these as well as of oxidative stress. Except for the induction of the GADD45A gene there was no indication for DNA damage. EMD did not induce genes involved in proliferation and did not markedly suppress apoptosis during the present study. As already discussed in chapter 4.4.1.3 the induction of proliferation associated genes could be shown in livers of rats treated in vivo with PPARα agonist while these genes were unaffected in PPARα agonist treated hepatocytes in vitro [Tamura 2006]. Parzefall et al. showed that DNA replication in PPARα agonist treated hepatocytes was increased when Kupffer cells were co-cultured or by co-treatment of hepatocyte monocultures with Kupffer cell derived TNFα [Parzefall 2001]. Therefore, these effects triggered by intercellular signaling of different hepatic cell types are not detectable using hepatocyte monocultures. Primary hepatocytes are well suited for the investigation of effects which are restricted to mechanisms and pathways taking place solely in the hepatocyte itself.

The gene expression results also showed the activation of the pharmacological target while further pharmacological effects are difficult to explain with the present system since activation of the polyol pathway and the resulting changes in glycolysis only appear at high intracellular glucose levels [Lorenzi 2007]. Due to the dergulation of genes encoding basolateral and apical transporters the hepatic elimination of substrates seemed to be slightly shifted towards basolateral excretion which could be a hint for a disturbed biliary transport, as was also seen in vivo. EMD induced several

genes encoding phase-I and -II enzymes which indicates an active drug metabolism but not per se a toxic effect. However, in agreement to the preclinical findings EMD caused oxidative stress and possibly depleted GSH since genes related to these pathways were heavily upregulated. Furthermore, energy production and mitochondrial function appeared to be disturbed since anabolic and catabolic pathways of glucose and glycogen were downregulated. Other indications for EMD-mediated toxic effects were the suppression of genes involved in cellular adhesion and morphology as well as the production of different classes of hepatic proteins. Therefore, EMD would have been classified as potentially hepatotoxic based on the present data.

During the present study cells were treated with 750µM EMD as the high dose while rats which orally received a hepatotoxic dose of EMD (350mg/kg) had a c_{max} of 1,389 ± 287µM [internal data]. Thus, in vivo relevant doses could not be used with the present system since they would cause a very high cytotoxicity. The EMD derived results of the study presented here will be compared to gene expression data of EMD treated human hepatocytes in the context of Predict-IV. It was shown that humans in vivo as well as in in vitro cultured human primary hepatocytes lack the activation of rodent PPARα key targets like acyl coenzyme A oxidase, peroxisome proliferation, and hepatocarcinogenesis [Roglans 2002, Klauning 2003, Ammerschläger 2004]. Therefore, if EMD is a PPARα agonist, the gene expression profile of the human cells is expected to markedly differ from that of the rat hepatocytes regarding the induction of genes involved in lipid metabolism and peroxisomal biogenesis as well as PPARα target genes.

4.4.1.6 Metformin

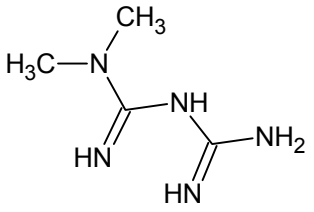

Metformin (Met) belongs to the class of biguanides and was approved in the 1950s for the treatment of type 2 diabetes [Strack 2008]. It activates the hepatic AMP-activated protein kinase (AMPK) which diminishes gluconeogenesis and enhances hepatic glucose uptake and catabolism. Additionally, the insulin sensitivity is improved by decreasing intestinal glucose uptake and increasing insulin binding to insulin receptors [DB-Met 2011]. However, in contrast to TZDs, Met does not increase peripheral glucose disposal but acts predominantly in the liver [Natali 2006].

Met is predominantly excreted renally without transformation by drug-metabolizing enzymes and is a very safe drug with very few side effects being reported [Strack 2008]. Nevertheless, Met's guanidium group gets positively charged under physiological conditions and binds to negatively charged cell surfaces. Thus, Met accumulates in mitochondria and can disturb cellular energy production. Met directly inhibits complex I of the mitochondrial respiratory chain and reduces ATP production. The resulting increase in glycolysis depicts the cell's attempt to compensate for the diminished stocks of ATP. Heavily increased rates of glycolysis enhance the production of lactate by anaerobic glycolysis and cause lactic acidosis, Met's rare but major adverse effect which could become life-threatening in rats and human [Dykens 2008, Strack 2008, Brando 2010].

During the present study Met was used as a negative control because of its rare side effects and low cytotoxicity in vitro [Lauer 2009]. The PCA (Figure 4.17) of the Met treated cells showed that the high dose samples clustered separately indicating a marked change in gene expression related to the control. The low dose samples clustered together with the time matched vehicle controls and showed only slight changes on days three and 14. These findings correlated with the number of statistically significant deregulated genes. Low dose treatment with Met altered only one gene on day 14 while high dose Met changed the gene expression level of more than 3000 genes on days one and three (Table 4.6). The genes discussed in the following are listed in the appendix (Table 7.8) and also visualized in a heatmap (Figure 4.9).

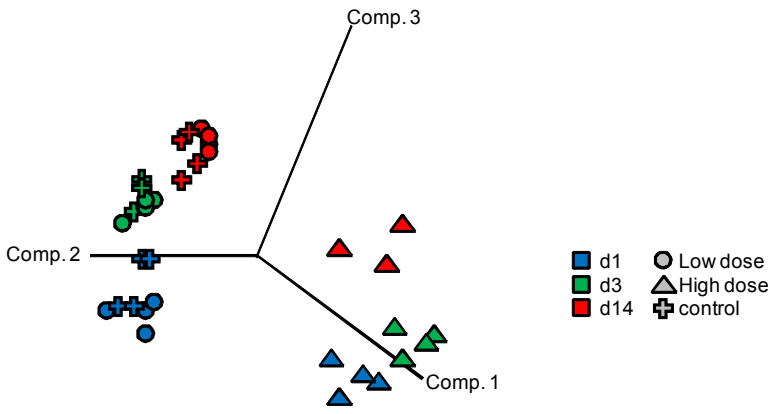

Figure 4.17: PCA of the Metformin samples.
The low dose treated samples cluster together with the time matched controls indicating a comparable gene expression level while high dose treatment markedly changed the gene expression level since the appropriate samples cluster separately.

Metformin downregulated genes related to lipid metabolism and energy production

The most affected pathway by Met was lipid metabolism. Here several genes involved in lipid transport, such as apolipoprotein A-V (APOA5) and low density lipoprotein receptor (LDLR), lipid catabolism like lipase (LIPC) and monoglyceride lipase (MGLL), fatty acid transport and catabolism including fatty acid binding protein (FABP1), members of the CYP4A family and acyl-CoA thioesterase (ACOT1), fat storage like fat storage-inducing transmembrane protein (FITM2) and cholesterol synthesis like lecithin-cholesterol acyltransferase (LCAT) and sterol-C4-methyl oxidase-like (SC4MOL) were downregualted. Genes encoding enzymes involved in peroxisomal fatty acid breakdown, such as acetyl-CoA acyltransferase (ACAA1) and peroxisomal enoyl CoA hydratase (ECH1) as well as mitochondrial β-oxidation like carnitine O-acetyltransferase (CRAT), long chain acyl-CoA dehydrogenase (ACADL) and acetyl-CoA acetyltransferase (ACAT1) were suppressed. The downregulation of these genes was stronger on day three than on day one of treatment. Several genes related to glycolysis and/or gluconeogenesis were also downregulated, except for the genes encoding phosphoglycerate kinase (PGK1) and phosphoenolpyruvate carboxykinase (PCK2) which were slightly induced on day three. In addition, the gene encoding glycerol-3-phosphate-dehydrogenase (GPD1), which is involved in the transport of electrons from cytosolic NADH to the mitochondrial respiratory chain, was downregulated [Michael 1999, Voet 2002]. Two genes encoding glycogen catabolizing enzymes were induced which could be related to the repression of genes involved in lipid and carbohydrate metabolism. The hepatocytes seemed to be no longer able to produce energy from fatty acids or glycolysis and therefore broke down glycogen for ATP production. This disturbance could be a hint for drug-induced impairment of the mitochondria where cellular energy production takes place.

Metformin induced genes associated with stress

Mitochondrial disturbance could be caused by the generation of ROS. During the present study Met induced genes encoding antioxidant enzymes like ferritin (FTL) [Cairo 1995, Vogt 1995, Orino 2001], thioredoxin (TXN) [Watanabe 2010] and heme oxygenase 1 (HMOX1) [Keyse 1990], which have been shown to be upregulated in response to oxidative stress. Nevertheless, the genes encoding the antioxidant enzymes superoxide dismutase (SOD2) and catalase (CAT) were downregulated which could be a consequence of the suppression of genes involved in lipid metabolism, since CAT detoxifies ROS produced via peroxisomal lipid oxidation

[Marquradt 2004]. While Met downregulated the genes of several phase-I, -II, and -III molecules the gene encoding the transporter MDR1, which excretes substrates into the bile, was induced. Additionally, the gene for UDP-glucuronosyltransferase (UGT1A6), which conjugates metabolites with glucuronides and the genes encoding the GSH-synthesizing enzymes glutamate-cystein ligase (GCLC) and hydroxyacylglutathione hydrolase (HAGH) were induced on day three. Since GSH plays a major role in the detoxification of reactive metabolites and ROS the upregulation of genes involved in the metabolism of GSH indicate the formation of oxidative stress in the cells [Yuan 2009].

Metformin deregulated genes involved in apoptosis and proliferation

Met upregulated genes induced by DNA damage, including APEX nuclease (APEX1), O-6-methylguanine-DNA methyltransferase (MGMT) and DNA-damage-inducible transcript (DDIT3) on day one and to greater extent on day three [Edwards 1998, Matés 2008]. p53 target genes, such as growth arrest DNA-damage-inducible (GADD45A), cyclin G1 (CCNG1) and p21 (CDKN1A) were upregulated. GADD45A induction is associated with the arrest of the cell cycle related to DNA damage while CCNG1 and p21 inhibit the cell cycle progression during the G1 phase [Smith 2000, Zhao 2003]. The induction of GADD45A was stronger on day one than on day three while p21 was upregulated only on day three. Since Met does not act as a genotoxicant, DNA damage could be caused by the suggested increase in ROS, indicated by the upregulation of genes encoding antioxidant enzmyes. In contrast, genes associated with proliferation and tumor formation, like lipocalin (LCN2) [Kim 2009, Jin 2011] and annexin (ANXA5) [Glückmann 2007, Xue 2009] as well as with DNA replication such as proliferating cell nuclear antigen (PCNA) and polymerase (POLD) were induced time-dependently on day one and three [Moldovan 2007]. However, genes encoding the pro-apoptotic key factors [Hail 2006] BCL2-antagonist/killer 1(BAK1), BCL2-associated X protein (BAX) and BH3 interacting domain death agonist (BID) were markedly upregulated while the induction of apoptosis was indicated by the enhanced gene expression of the effector caspases caspase-6 (CASP6) and -7 (CASP7) [Matés 2008]. The gene encoding caspase-2 (CASP2), which is involved in heat shock induced apoptosis [Tu 2006], was also upregulated as well as caspase-4 (CASP4) which is associated with ER stress [Hitomi 2004]. The induction of genes associated with proliferation, the upregulation

of pro-apoptotic genes and of genes encoding caspases were all stronger on day three than on day one. Therefore, the balance between apoptosis and proliferation seem to be slightly shifted towards cell death by treatment with Met.

Met downregulated genes related to different cellular functions

In correlation to the downregulation of genes encoding several peroxisomal proteins Met suppressed the gene expression of PEX11A and PEX19, which are markers for peroxisomal biogenesis [Koch 2010]. Met also downregulated genes involved in cell adhesion and morphology, like laminin (LAMC2), vimentin (VIM) and E-cadherin (CDH1) indicating that the cells are starting to detach due to cytotoxicity [Chen 2006, Malcos 2011, Vuoriluoto 2011]. Furthermore, genes encoding proteins which are synthesized and secreted by hepatocytes like the coagulation factors F10, 11, and F12, the complement components C5, C6, CFH, and CFB, the chemokines CXCL9, CXCL11, and CXCL16, as well as the acute phase proteins fibrinogen (FGB), afamin (AFM), and kallikrain (KLKB1) were downregulated. Except for the coagulation factors, these proteins are involved in the hepatic inflammatory response and are regulated by the intercellular signaling between hepatocytes and immune cells [Trautwein 1994, Dhainaut 2001]. In these experiments the gene changes are more likely to be associated with cytotoxic effects which impair cellular protein production since immune cells were missing in this cell system and the gene expression of other hepatic proteins like coagulation factors was also suppressed. In addition, Met downregulated the gene expression of several basal and apical transporters like NTCP, OATP8, OCT, MDR3, and MDR6, while MDR1, which mediates biliary excretion, was upregulated.

Taken together, high dose treatment with Met deregulated a large number of genes on day one and three but not on day 14. At a first glance this seemed to be unexpected for a compound which was used as negative control. However, the gene expression profile of the Met treated cells markedly differed from that of cells treated with known hepatotoxic substances. In contrast to FF, Tro and EMD, Met suppressed the expression of a large number of genes encoding enzymes which are involved in lipid metabolism. The downregulation of genes encoding regulatory enzymes of FA oxidation was also detected by Fulgencio et al. in Met treated rat primary hepatocytes [Fulgencio 2001]. However, this is not consistent with Met’s known

pharmacological action since it was shown to reduce serum level of triglycerides and free FA in humans and rats [Zhou 2001, Strack 2008]. The increase of FA oxidation seems to be triggered by the activation of Met's molecular target AMPK [Zhou 2001] the hepatic enzyme activity of which, but not its protein level, was found to be increased in Met treated mice [Huang 2008]. AMPK gene expression was not deregulated by Met during the present study. Met furthermore time-dependently upregulated genes involved in cellular proliferation while in parallel pro-apoptotic genes and cell cycle arrest related genes were induced. In total the balance between apoptosis and proliferation seemed to be shifted towards cell death since the gene expression of several caspases was also enhanced. Correspondingly, the gene expression of pathways generating energy from glucose and lipids was decreased. In addition, a small number of genes related to oxidative stress and cell cycle arrest, caused by DNA damage, were induced. This is consistent with results of a previous gene expression study [Lauer 2009] as well as with the study of Dykens et al. who detected the formation of ROS in primary rat hepatocytes treated with equimolar concentrations of Met for 24 hours [Dykens 2008]. They also showed that Met depleted cellular GSH after treatment with 2000µM, indicating a dose-dependent increase in the production of ROS until the cellular defense mechanisms are exhausted. The deregulation of genes involved in energy production from lipids and glucose, as well as the induction of genes related to oxidative stress, DNA damage and apoptosis may indicate mitochondrial impairment due to oxidative stress. It was shown that Met can accumulate in the mitochondria and cause adverse effects by inhibition of cellular respiration. This can lead to lactic acidosis, which is a known side effect of Met, but also to the formation of oxidative stress and cell death [Dykens 2008, Strack 2008]. In line with this, the media of the Met high dose treated cells started to change its colour from red to yellow during the first days in culture, suggesting a marked decrease of the pH-value. Lactic acidosis can be caused by increased hepatic production of lactic acid due to disturbed energy production in affected mitochrondria. In vivo lactic acid is released into the blood and excreted renally [Strack 2008]. In vitro, lactic acid is released into the media and subsequently decreasing the pH-value. Thus, the observed change in the medium's colour may indicate the development of lactic acidoses in the Met treated cells due to mitochondrial impairment and oxidative stress. Met very rarely causes lactic acidosis in humans [Strack 2008] and also preclinical studies with rats which received a daily

dose of 200mg/kg and possessed a c_{max} of 66.5 ± 2.5µM showed no increased incidence of lactic acidosis after 28 days treatment [Bando 2010]. The maximum recommended daily dose of Met for humans is 2550mg, while the resulting human c_{max} after taking 2000mg of Met amounts to 10.8µM [Strack 2008]. Hence, the concentration used as the high dose (1000µM) during the present study was many times higher than safe plasma concentrations of humans and rodents, which may explain the indications of adverse effects observed. The low dose (100µM), which was slightly higher than the safe rodent plasma concentration, did neither significantly change the gene expression of the treated cells (Figure 4.17) nor change the colour of the cell culture medium. This confirms the predictivity of rat primary hepatocytes for Met's toxic effects at in vivo relevant concentrations. Based on the gene expression data Met would not have been classified as hepatotoxic since the downregulation of several cell functions and the induction of apoptosis seemed to be related to general cytotoxicity. However, the gene expression changes triggered by treatment with high doses of per se non-hepatotoxic compounds have to be validated in order to investigate the robustness of the present system towards false positive results.

4.4.1.7 Common deregulated genes

The aim of the EU Predict-IV project is the development of a cell based in vitro system which enables the prediction of organ specific toxicities. Global gene expression analyses were performed in order to define a set of genes meeting these requirements. Although the data for the seven compounds described in this thesis are not sufficient to determine a predictive genomic model, the genes which were commonly deregulated by all the test compounds should be discussed. Therefore, the gene expression profiles of EMD, FF, Met, Rosi and Tro were compared while APAP and VA were not included due to the minor changes in gene expression observed. For this comparison the appropriate dose and time point was selected where the highest number of genes was deregulated (Table 4.6). Thus, the statistically significant ($p \leq 0.05$, BH-$Q \leq 0.2$) commonly deregulated genes for EMD high dose day 14 (EMD H14), Rosi high dose day 14 (Rosi H14), FF low dose day three (FF L3), Tro high dose day three (Tro H3) and Met high dose day three (Met H3) are disscussed (Table 4.7).

EMD, FF, Rosi and Tro induced genes mainly involved in lipid metabolism and energy production, while genes related to proliferation, inflammation and cellular transport were downregulated. The gene expression profile of Met clearly differed from that of the other compounds since Met downregulated the complete gene set except of the transporter SLC20A1. However, the induction of genes encoding lipid metabolizing genes by FF, EMD, Rosi and Tro seemed to be associated with the expected pharmacological mode of action of these reference compounds. The PPARγ agonists Tro and Rosi in vivo reduce the serum level of triglycerides and free FA [Kumar 1996, Lebovitz 2001] and have been shown to activate hepatic genes involved in lipid metabolism [Memon 2000, Watkins 2002].

Table 4.7: Overview of common deregulated genes by EMD, Rosi, FF, Met and Tro.
The statistically significant ($p \leq 0.05$, BH-Q ≤ 0.2) commonly deregulated genes by EMD high dose day 14 (EMD), Rosi high dose day 14 (Rosi), FF low dose day 3 (FF), Tro high dose day 3 (Tro) and Met high dose day 3 (Met) are listed. (+ = upregulation, - = downregulation, * = BH-Q > 0.2)

Symbol	Gene Name	Access. No.	Function	EMD	FF	Rosi	Tro	Met
ACADM	acyl-CoA dehydrogenase, C-4 to C-12 straight chain	NM_016986.1	lipid metabolism	+	+	+	+	-
Acot1	acyl-CoA thioesterase 1	NM_031315.1	lipid metabolism	+	+	+	+	-
CRAT	carnitine O-acetyltransferase	NM_001004085.2	lipid metabolism	+	+	+	+	-
Cyp4a14	cytochrome P450, family 4, subfamily a, polypeptide 14	XM_575886.1	lipid metabolism	+	+	+	+	-
DECR2	2,4-dienoyl CoA reductase 2, peroxisomal	NM_171996.2	lipid metabolism	+	+	+	+	-
LONP2	lon peptidase 2, peroxisomal	XM_214655.3	lipid metabolism	+	+	+	+	-
NUDT7	nudix (nucleoside diphosphate linked moiety X)-type motif 7	XM_341693.2	lipid metabolism	+	+	+	+	-
SLC22A5	solute carrier family 22 (organic cation/carnitine transporter), member 5	NM_019269.1	energy production	+	+	+	+	-
APOA5	apolipoprotein A-V	NM_080576.1	lipid metabolism	-	-	-*	-	-
CXCL16	chemokine (C-X-C motif) ligand 16	XM_573130.1	inflammation	-	-	-	-	-
PRICKLE1	prickle homolog 1 (Drosophila)	XM_235609.3	anti-proliferative	-	-	-	-	-
SLC20A1	solute carrier family 20 (phosphate transporter), member 1	NM_031148.1	cellular transport	-	-	-	-	+*

As a PPARα agonist FF acts directly on the liver and enhances expression of several genes involved in lipid catabolism, which has been shown in vitro and in vivo [Cornwell 2004, Guo 2006, Tamura 2006]. EMD was associated with several PPARα effects during preclinical studies [internal data] and its gene expression profile was very similar to that of FF in this study. The gene expression changes caused by EMD are comparable to a set of commonly deregulated genes by Tro, Rosi and FF. PPAR

agonists induce mitochondrial and peroxisomal lipid metabolism which was shown by the set of commonly deregulated genes, which encode mitochondrial enzymes such as acyl-CoA dehydrogenase (ACADM) and carnitine O-acetyltransferase (CRAT), peroxisomal enzymes like lon peptidase (LONP2) [Omi 2008] and 2,4-dienoyl CoA reductase (DECR2). The transport of FA into the mitochondria requires carnitin. In line with the increased expression of mitochondrial, genes encoding FA oxidizing enzymes, the induction of the gene encoding the solute carrier family 22 (organic cation/carnitine transporter) member 5 (SLC22A5) indicates an increased cellular uptake of carnitin [Michael 1999]. In addition, the PPAR agonists induced the gene encoding the peroxisomal enzyme NUDIX hydrolase 7 (NUDT7) which is involved in the homeostasis of coenzyme A and therefore also in lipid metabolism and energy production [Reilly 2008]. During the present study EMD, FF, Met, Rosi and Tro deregulated genes related to proliferation and cell death whereas none of them seemed to activate proliferation of the treated cells. PPARγ agonists were shown to trigger anti-proliferative effects in several human tumor cell lines [Morosetti 2004, Freudlsperger 2006, Lin 2007] and a mouse model for hepatocarcinogenicity [Galli 2010]. In contrast, PPARα agonists act as non-genotoxic hepatocarcinogens in rodents but not in humans. However, this adverse effect of PPARα agonists can not be shown in hepatocyte monocultures since the proliferation of hepatocytes is thought to be activated by cellular signaling of Kupffer cells [Parzefall 2001]. Met is not associated with carcinogenicity or with anti-proliferative effects [Strack 2008, DB-Met 2011]. EMD, FF, Met, Rosi and Tro commonly repressed the expression of the gene encoding Prickle homolog (PRICKLE1) which is hypothesized to act as a putative tumor suppressor in human hepatocellular carcinoma by inhibiting cellular proliferation [Chan 2006]. EMD, FF, Rosi, and Tro, but not Met, downregulated the gene encoding the solute carrier family 20 member 1 (SLC20A1), a basolateral transporter which manages the uptake of phosphate from the blood. Phosphate is essential for the synthesis of ATP and nucleic acids as well as for cellular signaling. In addition, the depletion of SLC20A1 resulted in reduced proliferation in HepG2 cells [Beck 2009]. A further commonly downregulated gene was chemokine (C-X-C motif) ligand 16 (CXCL16). The protein encoded by this gene is associated with cancer progression [Deng 2010] but also with liver inflammation [Heydtmann 2005]. Whether genes involved in proliferation and inflammation play a role in a prediction model based on a hepatocyte monoculture has to be further investigated since these

complex pathways usually incorporate additional hepatic cell types. As already mentioned the activation of proliferation by PPARα agonists require intercellular signaling of Kupffer with parenchymal cells [Parzefall 2001]. Kupffer cells and liver-infiltrating macrophages also play a major role in the triggering of inflammation by the release of mediators like cytokines which activate different pathways in hepatocytes [Tacke 2009]. Furthermore, hepatocytes, as terminally differentiated cells, remain in the G0 phase and proliferate very rarely [Marquardt 2004]. Cell cultures possessing an inactive cell cycle are not suited for the prediction of cell cycle arresting drug effects, for example triggered by PPARγ agonists. The gene encoding apolipoprotein A-V (APOA5) was also repressed by all of the five compounds. APOA5 is produced in the liver and secreted into the blood where it is involved in lipid transport and the regulation of plasma triglyceride levels. It was shown to be a direct PPARα target gene and to be induced by fibrates [Vu-Dac 2003]. The downregulation of the APOA5 gene by all of the five compounds, including PPARα agonists, indicates cytotoxicity is affecting hepatic protein production.

In conclusion, the commonly deregulated genes caused by EMD, FF, Rosi and Tro were mainly associated with the pharmacological mode of action of these substances and not with any toxicicity effects. In contrast, Met downregulated the majority of these genes clearly indicating the induction of apoptosis. However, the downregulation of the APOA5 gene by all of the compounds did not correlate with their pharmacological mode of actions and therefore is probably related to a toxic effect and indicating the impairment of cellular protein production. Nevertheless, the present set of commonly deregulated genes is neither suited for the prediction of toxic effects in vivo nor for the classification of the tested drugs as hepatotoxic or non-hepatotoxic. On the one hand the number of commonly deregulated genes was too small in order to classify the tested compounds while on the other hand the genes correlated with the pharmaceutical but not with the toxic effects of the reference compounds. However, the definition of a predictive gene set was not the major aim of this study. It was rather the question whether the data of the present study, representing interim findings of the project Predic-IV, were suited to give first hints for the final results. The gene expression profiles of only five out of the seven tested compounds could be compared, since treatment with VA and APAP changed only a few genes. Furthermore, the remaining drugs possessed very similar pharmaceutical mode of actions since Tro and Rosi belong to the class of TZDs

which are PPARγ agonists while FF and also likely EMD are PPARα agonists. PPARγ and PPARα act as transcription factors for several genes involved in lipid and energy metabolism. The final analysis at the end of the project Predict-IV will include further compounds with different pharmaceutical mode of actions and diverse toxicity profiles. The comparison of compounds with various modes of actions and different hepatotoxic mechanisms should better enable the identification of genes associated with toxic effects, independent of the pharmaceutical actions of the tested compounds, as basis for the identification of predictive transcriptomic markers.

5 Concluding remarks and future perspectives

During the present study sandwich cultured primary rat hepatocytes were treated for 14 days with a non-toxic and a toxic dose of seven hepatotoxicity reference compounds. After one, three and 14 days whole-genome gene expression analyses were performed in order to investigate whether drug-induced in vivo toxicities could be predicted based on the gene expression profiles of cells treated in vitro.

5.1 Dose selection

The selection of the right dose for in vitro models is one of the most important challenges at the beginning of a gene expression study. Treatment with very low concentrations of a compound may hardly change the gene expression profile of the treated cells or affect genes associated with pharmacological but not toxic effects. In contrast, the treatment of cells with very high concentrations causing marked cytotoxicity may affect genes mainly related to cell death. Both regimes can lead to false positive classifications of drug candidates. Currently, there are no guidelines available for the choice of the correct dosing-scheme for toxicogenomic studies. The "ICH Guidance on genotoxicity testing and data interpretation for pharmaceuticals intended for human use for genotoxicity testing" recommends doses causing not more than 30% reduction in growth of the used cell line in order to avoid false positive results of genotoxicity tests due to high cytotoxic effects [ICH-S2 2008]. However, several different approaches are described in the literature. Roth et al. used the highest rodent c_{max} measured during in vivo studies with the test compound as the high dose for comparative in vitro tests [Roth 2011]. Further toxicogenomics studies were performed with the TC10 or the TC20 of the appropriate compound as high dose while the low dose was defined as the highest dose causing no cytotoxicity or as one fifth of the TC20, respectively [Barros 2008, Hrach 2011].

The Predict-IV consortium decided to use the TC10 as the highest dose and 1/10 of it as the low dose. The cell viability was calculated based on the ATP content of living cells but there was a discrepancy between the assays' results and the cell morphology as well as with historical in house data for Met, FF and, Rosi. The ATP test seemed to be too sensitive, maybe due to mitochondrial effects disturbing the

production of ATP. Thus, the ATP test should have been supported by a further assay measuring second, different functional endpoint. However, the integration of assays with different endpoints like cell membrane integrity or metabolic and functional activity often creates the problem that these assays possess varying sensitivities and the calculated TC10s differ from each other and have to be interpreted carefully [Limonciel 2011].

During the study described here primary hepatocytes were treated with APAP (100µM, 1000µM), EMD (75µM, 750µM) Met (100µM, 1000µM), FF (100µM, 1000µM), Rosi (8µM, 80µM), Tro (7µM, 70µM) or VA (10µM, 100µM). APAP, Tro and VA deregulated either no or only very few genes, which may be a consequence of the concentration used being too low. In addition, other gene expression studies described in the literature were performed with higher concentrations of these substances [Rogiers 1995, Suzuki 2008, Jemnitz 2008, Lauer 2009, Rogue 2011]. However, the high dose of APAP was set to 1000µM based on the “ICH Guidance on genotoxicity testing and data interpretation for pharmaceuticals intended for human use for genotoxicity testing” [ICH-S2 2008] which recommends 1000µM as the highest dose if the dosage is not limited by cytotoxicity or solubility. Consequently, few gene deregulations were expected for APAP which causes hepatotoxic effects in vivo (and in vitro) only at very high concentrations. Responsive concentrations of VA reported in the literature exceed the TC10 used in the present study and could therefore not be applied using the present study design. The doses used for APAP and VA were also lower than the toxic in vivo c_{max} concentrations reported for rodents, strengthening the usefulness of the used in vitro system. However, the dose finding study for Tro should be repeated integrating the measurement of further toxic endpoints since toxicogenomic investigations for Tro were described in the literature at doses feasible to use in the present in vitro system. In contrast, the dose selection for EMD and Rosi was appropriate since the high dose triggered marked gene expression changes which enabled the reconstruction of known pharmaceutical and toxic mechanisms. Nevertheless, both doses selected for treatment with FF caused similar effects indicating that the low dose already exhausted the responsiveness of the cells. Here the dose finding could also be improved by the integrated measurement of different cytotoxicity endpoints.

In general, treatment with very high doses could lead to effects related to cell death caused by unspecific cytotoxicity rather than by compound-specific toxicity mechanisms [ICH-S2 2008]. This seemed to be especially true for the Met treated cells, since the high dose induced genes involved in the activation of apoptosis, while genes related to metabolic pathways and several cellular functions were repressed.

Except for FF, the low doses of the reference compounds had very little effect on gene expression in the treated cells and were therefore not included into the biological data interpretation. Since the low dose was defined as a non-toxic dose, which was not expected to markedly change the gene expression profiles of the treated cells, these results underline the predictive power of the present in vitro system and study design.

5.2 The predictive power of gene expression analyses in drug treated primary rat hepatocytes

During the present study treatment with multiple reference compounds affected several different molecular pathways. Cells treated with the PPARα-agonist FF and the PPARγ-agonists Rosi and Tro gave very similar gene expression profiles. These results are in agreement with a study comparing the cellular response of primary rat hepatocytes to PPARγ and PPARα/γ agonists [Rogue 2011]. Consistent with the fibrates' pharmacological mode of action which was shown in rodent and human in vivo studies [Corton 2000, Wilson 2000] as well as by hepatic gene expression changes of in vivo treated rats [Cornwell 2004], FF heavily upregulated several genes involved in the cellular uptake and catabolism of lipids as well as mitochondrial and peroxisomal fatty acid oxidation. This also correlated with gene expression changes triggered by EMD, strengthening the hypothesis of EMD being a potential PPARα-agonist [internal data]. While fibrates directly act on hepatic lipid metabolism, related to their lipid lowering action, the antidiabetic drugs Tro and Rosi enhance insulin sensitivity by the activation of PPARγ which mainly triggers the increased uptake of glucose into muscle tissue [Grossman 1997]. However, Tro and Rosi have been also shown to activate the hepatic isoform PPARγ2 and to enhance several hepatic genes which were originally found to be PPARα-target genes in adipose tissue [Memon 2000, Mandard 2004, Schadinger 2005]. Therefore, the induction of

genes related to hepatic lipid uptake and catabolism detected during our study can be considered to be a pharmacological effect of Rosi and Tro. While lipid metabolism related genes were upregulated by FF and EMD, genes involved in glycolysis as well as the synthesis of cholesterol and lipids were downregulated, which may be a consequence of the increased lipid catabolism providing enough energy for the cells. Consistent with this, the pyruvate dehydrogenase kinase gene (PDK4) was upregulated. PDK4 blocks the entrance of glucose-derived pyruvate into the Krebs cycle [Sugden 2001]. In addition, EMD activated the gene encoding aldo-keto reductase (AKR7A3) which was assumed to be EMD's pharmacological target. These findings are in line with genomic and proteomic profiling in livers of EMD-treated rats reported recently [Sposny 2011].

EMD, FF, Rosi and Tro induced genes encoding phase-I and -II drug metabolizing enzymes. This indicates an active induction of xenobiotic metabolism as a consequence of drug treatment and could not per se considered to be a toxic effect. Nevertheless, the induction of phase-I enzymes, e.g., CYPs, could trigger adverse effects based on drug-drug-interactions and are therefore required to be tested during drug development [FDA 2004, Guengerich 2008, Walsky 2008]. The four compounds heavily induced CYP3A4 which is responsible for the metabolism of a large number of drugs and effects on CYP3A4 expression often have consequences for drug-drug-interactions. A toxic pathway affected by all of the four reference compounds was the NRF2 mediated stress response. The upregulation of different NRF2 regulated genes indicates the formation of reactive metabolites or oxidative stress and this effect was strongest in the EMD treated cells. Furthermore, EMD heavily induced genes involved in GSH conjugation, reduction and synthesis and therefore seemed to deplete cellular GSH [Yuan 2009], which is consistent with preclinical findings [internal data]. While EMD was stopped due to hepatic adverse effects during animal studies, FF seldom causes hepatotoxic effects in humans but acts as non-genotoxic hepatocarcinogen in rodents [Corton 2000, Moutzouri 2010]. During the present study FF upregulated genes encoding antioxidant and GSH-conjugating enzymes to a lesser extent than EMD and did not induce genes related to GSH synthesis. However, the gene expression profile of the FF treated cells indicated oxidative DNA damage since genes involved in DNA repair and DNA damage related cell cycle arrest were upregulated. This supports the hypothesis that FF's hepatocarcinogenic mechanism may be based on oxidative DNA damage.

Cellular proliferation could not be shown since genes related to proliferation and cancer, as well as to the inhibition of apoptosis, were downregulated, which is in agreement with other published in vitro studies [Tamura 2006]. Based on the present data EMD would have been rightly classified as hepatotoxic while FF appears to have a low toxic potential. The c_{max} of in vivo treated rats developing hepatotoxicity was twice as high as the high dose used for cellular treatment with EMD and would have caused marked hepatotoxicity [internal data]. The high dose used for cellular treatment with FF was two times the rodent toxic c_{max} [Hanafy 2007]. Thus, FF could be tested at in vivo relevant doses since the low dose caused gene expression changes similar to the high dose.

Both Rosi and Tro were withdrawn from the market, although only Tro was associated with drug-induced hepatotoxicity [Kaplowitz 2005, Beiderbeck 2009, Osei 2009]. Tro is heavily metabolized in the liver and its reactive intermediates can trigger the formation of oxidative stress, GSH depletion and mitochondrial impairment [Rachek 2009]. In contrast, Rosi was shown to be less cytotoxic which seems to be a consequence of its slightly different molecular structure preventing the formation of reactive metabolites [Kirchheiner 2005]. Consistent with the literature, Tro showed a greater cytotoxicity at equimolar doses during the dose finding studies of the present work [Lloyd 2002, Guo 2006, Rachek 2009, Rogue 2011]. However, the difference in the hepatotoxic potential of both drugs could not be explained based on the gene expression data. Genes associated with oxidative stress and conjugation reactions of GSH with ROS or reactive metabolites were induced by both compounds, and Rosi affected a higher number of genes. Therefore, Rosi would have been classified as having a low toxic potential based on the present data while Tro probably would have been classified as a non- or low toxic compound. The concentrations used for treatment were in vivo relevant for Tro but not for Rosi, since the c_{max} in rats developing adverse effects was four times as high as the high dose Rosi used here [FDA-Rosi 1999]. Nevertheless, treatment with doses in this concentration range would cause marked cytotoxicity. Tro and Rosi furthermore downregulated genes related to cellular growth, proliferation and cell cycle progression while pro-apoptotic factors were induced. Rosi upregulated genes involved in glycolysis and Krebs cycle while genes encoding enzymes of gluconeogenesis were suppressed indicating an active energy production without toxic effects on the mitochondria. In contrast, Tro

deregulated genes involved in glycolysis, gluconeogenesis and the Krebs cycle lacking any clear link to drug-induced mitochondrial impairment.

The gene expression profile of the Met treated cells clearly differed from those derived from EMD, FF, Rosi and Tro, which seemed to be mainly based on the compound's different mode of action since the gene expression profiles of the PPARα and PPARγ agonists were highly characterized by their pharmacological effects. Met, like Rosi and Tro, is used as a glucose lowering drug for the therapy of type II diabetes and does not cause hepatotoxic side effects [Strack 2008]. However, its pharmacological mode of action is not based on the activation of PPARγ but on the direct enhancement of hepatic glycolysis [Natali 2006]. In contrast to the other four compounds, Met downregulated several genes involved in lipid and glucose metabolism as well as apical and basolateral transporters. Furthermore, it affected genes related to cell death and proliferation while the upregulation of different effector caspases indicated the induction of apoptosis. In addition, Met induced the gene expression of few antioxidant enzymes. These deregulations seemed to be related to Met induced lactic acidosis. Met is able to accumulate in the mitochondria and to inhibit cellular respiration. Subsequently, the cells increase aerobic and anaerobic glycolysis in order to produce ATP which leads to increased amounts of lactate and can cause oxidative stress and cell death. Lactate is released into the blood and decreases the pH [Dykens 2008, Strack 2008] while in vitro lactate is excreted into the cell culture medium. During our study the color of the cell culture medium of the Met treated cells changed from red to yellow during the first days of treatment, indicating a decreased pH which may have been due to the release of lactate. The high dose of Met used was many times higher than the c_{max} of rats which developed lactic acidosis. Thus, it seems very likely that this adverse effect also accurred in the treated hepatocytes. Based on the present gene expression data, Met would not have been classified as hepatotoxic since the downregulation of several cellular functions as well as the induction of apoptosis seemed to be related to general cytotoxicity due to cellular treatment with high doses of a compound. However, the robustness of the present system towards false positive results has to be further investigated since Rosi would have been incorrectly classified as hepatotoxic.

The genes and pathways deregulated during the present study correlated well with gene expression changes used for the classification of substances during similar studies. Roth et al. predicted the hepatotoxicity of test compounds based on expression changes of genes related to cellular stress, growth and proliferation after the treatment of primary hepatocytes for 24 hours [Roth 2011]. Hrach et al. defined a gene set which enabled the hepatotoxicity related classification of different pharmaceutical compounds and the top ranked genes were associated with energy and drug metabolism, as well as cellular growth, proliferation and cell adhesion. This set of top ranked genes included lactate dehydrogenase B (LDHB) and triosephosphate isomerase (TPI1) which are involved in glucose metabolism as well as junctional adhesion molecule (JAM3) which plays a role in the functionality of the canaliculi [Hrach 2011]. During the present study LDHB and JAM3 were repressed by EMD, FF, Rosi and Tro, but induced by Met. TPI1 was not deregulated by Met but induced by the other four compounds indicating once more the specificity of the appropriate gene expression profiles.

The majority of hepatotoxicity prediction systems published during the last decade were based on gene expression studies in livers of in vivo treated animals. Since these data were obtained using the genomic material of the complete liver, they also identified changes in pathways requiring the signaling between different hepatic cell types, e.g., inflammation [Thomas 2001, Kier 2004, Zidek 2007]. During the present study EMD, FF, Met, Rosi and Tro downregulated several genes encoding proteins which are synthesized and released by hepatocytes which are related to inflammation, such as chemokines, acute phase proteins, members of the complement system and proteins used for the antigen presentation onto the cell surface. These proteins are regulated by immune cells releasing pro-inflammatory factors which bind to receptors of the hepatocyte membrane [Trautwein 1994, Dhainaut 2001, Tacke 2009, Oo 2010]. Since immune cells were not present in the hepatocyte monoculture, the downregulation of these genes indicated cytotoxic effects due to a diminishing of cellular protein production. This hypothesis was strengthened by the repression of genes encoding coagulation factors which are also produced by hepatocytes but are not associated with inflammation [Dhainaut 2001].

5.3 Limitations of sandwich cultured rat hepatocytes

The whole genome gene expression analysis of drug treated primary rat hepatocytes enabled the reconstruction of pharmacological as well as toxic mechanisms of the different reference compounds. However, the predictive power of hepatocyte monocultures is limited to those mechanisms solely related to hepatocytes. Hepatocytes make up 78% of the liver's mass and maintain the hepatic key functions like xenobiotic metabolism, production of diverse proteins and bile, as well as glucose homeostasis [Schmidt 2005]. However, the various functions of hepatocytes are regulated by intercellular signaling with other hepatic cell types. Kupffer cells, the resident hepatic macrophages, secrete inflammatory factors like cytokines which can induce extrinsic apoptosis or proliferation of the hepatocytes [Tacke 2009]. In addition, Parzefall et al. showed that PPARα-agonists fail to induce cellular proliferation in hepatocyte monocultures since Kupffer cells stimulate this mechanism by the release of TNFα [Parzefall 2001]. Hepatocyte proliferation can also be caused by an impaired activity of pit cells which are resident hepatic lymphocytes killing tumor cells [Kmieć 2001]. Monocultures of hepatocytes lack other hepatic cell types and are therefore not predictive for mechanisms requiring intercellular communication like inflammation or Kupffer cell-mediated proliferation. Inflammatory processes can be triggered by hepatocytes presenting adducts of, e.g., proteins and drug metabolites on their surface. These adducts activate lymphocytes which trigger an immune response as well as the lysis of the antigen presenting cells [Kmieć 2001]. Effects like these are associated with idiosyncratic hepatotoxicity which can be only investigated using co-cultures of hepatocytes with immune cells [Kaplowitz 2005]. The immune response includes the activation of hepatocytes to release acute phase proteins, chemokines or complement factors [Dhainaut 2001]. Since the present system lacked immune cells, the deregulation of genes encoding these protein classes seemed to be related to drug-mediated cytotoxicity.

Hepatotoxicity is not only restricted to hepatocytes but also affects other hepatic cell types like, e.g., endothelial cells of the bile ducts. Hence, cell death or inflammation of the biliary system can not be detected with the present cell model system since it lacks these cell types. However, the deregulation of genes encoding hepatic transporters can give hints for in vivo effects. FF mediated cholestasis was associated with an increased excretion of cholesterol into the bile [RX-FF 2011]. The upregulation of genes encoding the apical transporters BCRP and ABCG5 by FF and

EMD, respectively, indicate a potentially increased biliary excretion which may be correlated to in vivo toxicities in the bile ducts. Another hepatic cell type involved in adverse effects are the stellate cells, which play a major role in the development of liver cirrhosis and fibrosis by the over-production of collagen [Blouin 1977, Friedmann 1997]. Stellate cells are also involved in hepatocyte proliferation, caused by the release of growth factors like transforming growth factor alpha and beta [Kmieć 2001].

5.4 Impact on drug development and future perspectives

The present study describes a gene expression study using primary rat hepatocytes treated for 14 days with different hepatotoxic reference compounds. Based on the present gene expression data, pharmacological and toxic effects of the test compounds could be reconstructed and correlated to in vivo effects. However, in vivo relevant concentrations could not be used for all of the reference compounds since the concentration used for treatment was limited by cytotoxicity. The present study represents an advancement in the field of in vitro prediction systems since the data include three different time points based on the long-term, repeat-dose treatment of primary hepatocytes. Related studies published so far compared histopathological findings with the hepatic gene expression profile of in vivo treated rats or with gene expression changes of hepatocytes after short-time treatment in vitro [Thomas 2001, Kier 2004, Zidek 2007, Roth 2011]. In contrast to these studies investigating acute drug effects, the aim of the work in hand was the study of long-term drug-mediated toxic effects based on the repeated treatment of hepatocytes in vitro. Therefore, time-dependend changes in gene expression of the treated cells were detected specifically for every test compound while the changes on day one often suggested the findings of the later time points but with lower statistical significance. This was consistent with a recently reported pilot study demonstrating the possibility to classify drugs related to their hepatotoxicity based on in vitro derived gene expression data. In their study the lowest misclassification rate was achieved by the usage of data from later time points [Hrach 2011].

The present work is part of the EU-funded project Predict-IV whose aim is the development of an in vitro model for the prediction of human in vivo toxic effects by

the combination of genomic, proteomic and metabolomic markers. Therefore, the genomic data derived from the seven reference compounds of the present study will be compared with the gene expression data of another four reference substances. These compounds expand the range of hepatotoxic mechanisms and pharmacological mode of actions since they belong to different chemical classes and cause different toxic effects in vivo, for example, steatosis and cholestasis. By defining marker genes and pathways of high relevance for the prediction of in vivo toxicities, this project provided a sound basis for the analysis of the additional compounds. During the next steps of data analysis, the whole genome gene expression data of all eleven test compounds has to be condensed to a small set of genes enabling the prediction of the test compounds' hepatotoxic potential. The resulting gene set then has to be validated using another method for gene expression analysis. Nowadays specific gene sets can be analyzed relatively quickly with methods such as multiplexed branched DNA assays or quantitative polymerase chain reaction (qPCR). The further phases of data analysis will be based on the integration of proteomic and metabolomic results in order to define the most relevant biomarkers for the prediction of in vivo toxicities from in vitro data. In addition, the data obtained from rat primary hepatocytes will be compared with gene expression data obtained from the human hepatoma cell line HepaRG as well as primary human primary hepatocytes treated with the same eleven reference compounds. The focus during this comparison will be the investigation of species-specific differences of pharmaceutical and toxic effects since, for example, PPARα-agonists like FF act as non-genotoxic hepatocarcinogens in rodents but not in humans [Willson 2000].

Predict-IV's aim is the establishment of a non-animal based prediction model. However, rat hepatocytes have to be freshly isolated for every experiment so animals are still needed. Nevertheless, the results of the Predict-IV project will give new insights into the predictive power of rat hepatocytes related to human toxicities. Potentially new genomic, proteomic and/or metabolomic biomarkers will be defined which may support the preclinical and clinical phases of drug development in two different ways: Firstly, the detection of a new drug's hepatotoxic potential can refine the selection of drug candidates prior to preclinical testing and may reduce the attrition rates. Secondly, a multiple endpoint in vitro prediction model provides additional mechanistic information of a new drugs' toxicity mechanisms which can support the interpretation of findings during animal studies as well as clinical trials.

Thus, the use of primary rat hepatocytes, as a well known and unconditionally available in vitro model of high in vivo relevance, is an essential tool for the validation of rat and human cell lines and the investigation of species-differences.

During the work reported here the concentrations of the test compounds in the cell culture medium at time of treatment were compared to plasma concentrations derived from animal studies in order to estimate the in vivo relevance of the doses used for in vitro treatment. However, during in vitro studies the medium concentrations of the test compounds may not correlate with the real exposure of the cells since an unknown amount of the compound may bind to the cell culture plastic or the extracellular matrix. Furthermore, the compound may evaporate or remain in the cell culture medium without affecting the cells. Therefore, the Predict-IV kinetics team will determine the intracellular concentration of the reference compounds in order to optimize the correlation to in vivo plasma concentrations. Finally, these data will be used for the calculation of the margins of safety by physiologically based pharmacokinetic modeling as a basis for the extrapolation of in vitro derived data to the in vivo situation.

6 References

Adler M., Hoffmann D., Ellinger-Ziegelbauer H., Hewitt P., Matheis K., Mulrane L., Gallagher W. M., Callanan J. J., Suter L., Fountoulakis M. M., Dekant W. and Mally A., Assessment of candidate biomarker of drug-induced hepatobiliary injury in preclinical toxicity studies, *Toxicol Lett* (2010) 196:1-11

Agilent RNA 6000Nano Kit Guide, edition 08/2006, Agilent Technologies, Waldbronn/Germany

Agilent, http://www.genomics.agilent.com/GenericA.aspx?PageType=Custom&SubPageType=Custom&PageID=2181, assessed 1st August 2011

Amacher D. E., The discovery and development of proteomic safety biomarkers for the detection of drug-induced liver toxicity, *Toxicol Apppl Pharmacol* (2010) 245:134-142

Ammerschläger M., Beigel J., Klein K.-U. and Müller S. O., Characterization of the species-specificity of peroxisome proliferators in rat and human hepatocytes, *Toxicol Sci* (2004) 78:229-240

Ames B. N., Lee F. D. and Durston W. E., An improved bacterial test system for the detection and classification of mutagens and carcinogens, *Proc. Natl. Acad. Sci. USA* (1973) 70:782-786

Aninat C., Piton A., Glaise D., Dumont J., Le Charpentier T., Langouët S., Morel F., Guguen-Guillouzo C. and Giullouzo A., Expression of Cytochrome P450, conjugating enzymes and nuclear receptors in human hepatoma HepaRG cells, *Drug Metab Dispos* (2006) 34(1):75-83

Anthérieu S., Chesné C., Li R., Camus S., Lahoz A., Picazo L., Turpeinen M., Tolonen A., Uusitalo J., Guguen-Guillouzo C. and Guillouzo A., Stable Expression, Activity, and Inducibility of Cytochrome P450 in Differentiated HepaRG Cells, *Drug Metab Despos* (2010) 38(3):516-525

Aoki K., Saito T., Satoh S., Mukasa K., Kaneshiro M., Kawasaki S., Okamura A. and Sekihara H., Dehydroepiandrosterone suppresses the elevated hepatic glucose-6-phosphatase and fructose-1,6-bisphosphatase activities in C57BL/Ksj-db/db mice: comparison with troglitazone, *Diabetes* (1999) 48(8):1579-1585

Avery S. V., Molecular targets of oxidative stress, *Biochem. J.* (2011) 434:201-210

Bando K., Ochiai S., Kunimatsu T., Deguchi J., Kimura J., Funabashi H. and Seki T., Comparison of potential risks of lactic acidosis induction by biguanides in rats, *Regul Toxicol Pharmacol* (2010) 58:155-160

Barros S. A. and Martin R. B., Predictive toxicogenomics in preclinical discovery, *Methods Mol Biol* (2008) 460:89-112

Barth A., Braun J. and Müller D., Bile acid transport and metabolism in rat liver slices, *Exp Toxicol Pathol* (2006) 57:313-319

Beck L., Leroy C., Salaün C., Margall-Ducos G., Desdouets C. and Friedlander G., Identification of a novel function of PiT1 critical for cell proliferation and independent of its phosphate transport activity, *J Biol Chem* (2009) 284(45):31363-31374

Beiderbeck A. B. and Sakaquchi M., Commentary on 'Case series of liver failure associated with rosiglitazone and pioglitazone' by James Floyd et al., *Phramacoepidemiol Drug Saf* (2009) 18(12):1247-1249

Benjamini Y., Drai D., Kafkafi N. and Golani I., Controlling the false discovery rate in behavior genetics research, *Behav Brain Res* (2001) 125(1-2):279-284

Blouin A., Bolender R. P. and Weibel E. R., Distribution of organelles and membranes between hepatocytes and nonhepatocytes in the rat liver parenchyma, *J Cell Biol* (1977) 72:441-455

Boehme K., Dietz Y., Hewitt P. and Mueller S. O., Activation of p53 in HepG2 cells as surrogate to detect mutagens and promutagens in vitro, *Toxicol Lett* (2010) 198(2): 272-281

Boehme K., Dietz Y., Hewitt P. and Mueller S. O., Genomic profiling uncovers molecuar pattern for toxicological characterization of mutagens and pro-mutagens in vitro, *Toxicol Sci* (2011) [Epub ahead of print]

Boehmer A. E., Mendes Ribeiro Corréa A., de Souza D. G., Knorr L., Hansel G., Corbellini L. G., Driemeier D., Portela L. V. and Souza D. O., Long-term cyclosporine treatment: evaluation of serum biochemical parameter and histopathological alterations in Wistar rats, *Exp Toxicol Pathol* (2011) 63(1-2):119-123

Bonkovsky H. L., Azar R., Bird S., Szabo G. and Banner B., Severe cholestatic hepatitis caused by thiazolidinediones: risks associated with substituting rosiglitazone for troglitazone, *Dig Dis Sci* (2002) 47(7):1632-1637

Bort R., Castell J. V., Pfeifer A., Gómez-Lechón M. J. and Macé K., High Expression of Human CYP2C in Immortalized Human Liver Epithelial Cells, *Toxicol In Vitro* (1999) 13:633-638

Botting R. M., Mechanism of action of acetaminophen: is there a cyclooxygenase 3?, *CID* (2000) 31(Suppl. 5):202-210

Brando K., Ochiai S., Kunimatsu T., Dequchi J., Kimura J., Funabashi H. and Seki T., Comparison of potencial risks of lactic acidosis induction by biguanides in rats, *Regul Toxicol Pharmacol* (2010) 58(1):155-160

Brown H. S., Chadwick A. and Houston J. B., Use of Isolated Hepatocyte Preparations for Cytochrome P450 Inhibition Studies; Comparison with Microsomes for K_i Determination, *Drug Metab Dispos* (2007) 35:2119-2126

Burstein H. J., Demetri G. D., Mueller E., Sarraf P., Spiegelman B. M. and Winer E. P., Use of peroxisome proliferator-activated receptor (PPAR) gamma ligand troglitazone as treatment for refractory breast cancer: a phase II study. *Breast Cancer Res Treat* (2003) 79(3):391-397

Butcher E. C., Can cell systems biology rescue drug discovery?, *Nat Rev Drug Discov* (2005) 4:461-467

Cairo G., Tacchini L., Pogliaghi G., Anzon E., Tomasi A. and Bernelli-Zazzera A., Induction of ferritin synthesis by oxidative stress, *J Biol Chem* (1995) 270(2):700-703

Callander R. D., Mackay J. M., Clay P., Elcombe C. R. and Elliott B. M., Evaluation of Phenobarbital/ beta-naphthoflavone as an alternative S9-induction regime to Arcolor 1254 in the rat for use in in vitro genotoxic assays, *Mutagenesis* (1995) 10(6):517-522

CellTiter-Glo® Assay Manual, edition 06/2009, Promega Corporation, Madison/USA

Chan D. W., Chan C. Y., Yam J. W., Ching Y. P. and Nq I. O., Prickle-1 negatively regulates Wnt/beta-catenin pathway by promoting Dishevelled ubiquitination/ degradation in liver cancer, *Gastroenterology* (2006) 131(4):1218-1227

Chang T. K. H. and Abbott F. S., Oxidative stress as mechanism of valproic acid-associated hepatotoxicity, *Drug Metab Rev* (2006) 38:627-639

Chavin K. D., Yang S., Lin H. Z., Chatham J., Chacko V. P., Hoek J. B., Walajtys-Rode E., Rashid A., Chen C.-H., Huang C.-C., Wu T.-C., Lane M. D. and Diehl A. M., Obesity induces expression of uncoupling protein-2 in hepatocytes and promotes liver ATP depletion, *J Biol Chem* (1999) 274:5692-5700

Chen X. and Gumbiner B. M., Crosstalk between different adhesion molecules, *Curr Opin Cell Biol* (2006) 18(5):572-578

Ciaraldi T. P., Kong A. P., Chi N. V., Kim D. D., Baxi S., Loviscach M., Plodkowski R., Reitz R., Caulfield M., Mudaliar S. and Henry R. R., Regulation of glucose transport and insulin signaling by troglitazone or metformin in adipose tissue of type 2 diabetic subjects, *Diabetes* (2002) 51(1):30-36

Cimica V., Batusic D., Haralanova-Ilieva B., Chen Y., Hollemann T., Pieler T. and Ramadori G., Serial analysis of gene expression (SAGE) in rat liver regeneration, *Biochem Biophys Res Commun* (2007) 360(3):545-552

Clayton D. F., Weiss M. and Darnell J. E. Jr, Liver-specific RNA metabolism in hepatoma cells: variations in transcription rates and mRNA levels, *Mol Cell Biol* (1985) 5(10): 2633-2641

Cornwell P. D., De Souza A. T. and Ulrich R. G., Profiling of hepatic gene expression in rats treated with fibric acid analogs, *Mutat Res* (2004) 549:131-145

Corton J. C., Anderson S. P. and Stauber A., Central role of peroxisome proliferator-activated receptors in the actions of peroxisome proliferators, *Annu. Rev. Pharmacol. Toxicol*. (2000) 40:491-518

Cox P. J., Ryan D. A., Hollis F, J., Harris A.-M., Miller A. K., Vousden M. and Cowley H., Absorption, disposition, and metabolism of rosiglitazone, a potent thiozolidinedione insulin sensitizer, in humans, *Drug Metab Dispos* (2000) 28(7):772-780

C-Path, 13 June 2008, http://c-path.org/pdf/PSTC_nephro_VXDS_summary_final.pdf, downloaded at 10 June 2011

Cunha J. M., Jolivalt C. G., Ramos K. M., Gregory J. A., Calcutt N. A. and Mizisin A. P., Elevated lipid peroxidation and DNA oxidation in nerve from diabetic rats: Effects of aldose reductase inhibition, insulin and neuropathic factors, *Metabolism* (2008) 57(7):873-881

Daly A. K., Drug-induced liver injury: past, present and future, *Pharmacogenomics* (2010) 11 (5):607-611

Dash A., Inman W., Hoffmaster K., Sevidal S., Kelly J., Obach R. S., Griffith L. G. and Tannenbaum S. R., Liver tissue engeneering in the evaluation of drug safety, *Exper Opin. Drug Metab. Toxicol*. (2009) 5(10):1159-1174

Davidson M. H., Armani A., McKenney J. M. and Jacobson T. A., Safety considerations with fibrate therapy, *Am J Cardiol* (2007) 99(Suppl):3C-18C

Davies G. F., Khandelwal R. L. and Roesler W. J., Troglitazone inhibits expression of the phosphoenolpyruvate carboxykinase gene by an insulin-independent mechanism, *Biochim Biophys Acta* (1999) 1451(1):122-131

Davies G. F., Khandelwal R. L. and Roesler W. J., Troglitazone induces expression of PPARgamma in liver, *Mol Cell Biol Res Commun* (1999a) 2(3):202-208

Davies G. F., Khandelwal R. L., Wu L., Juurlink B. H. J. and Roesler W. J., Inhibition of phosphoenolpyruvate carboxykinase (PEPCK) gene expression by troglitazone: a peroxisome proliferator-activated receptor-γ (PPARγ)-independent, antioxidant-related mechanism, *Biochem Pharmacol* (2001) 62:1071-1079

Davies G. F., McFie P. J., Khandelwal R. L. and Roesler W. J., Unique ability of troglitazone to up-regulate peroxisome proliferator-activated receptor-gamma expression in hepatocytes, *J Pharmacol Exp Ther* (2002) 300(1):72-77

DB-Met: www.drugbank.ca/drugs/DB00331, accessed 1st August 2011

DB-FF: www.drugbank.ca/drugs/DB01039, assessed 12 August 2011

DB-Rosi: www.drugbank.ca/drugs/DB00412, assessed 12 August 2011

De Longueville F., Atienzar F. A., Marcq L., Dufrane S., Evrard S., Wouters L., Leroux F., Bertholet V., Gerin B., Whomsley R., Arnould T., Remacle J. and Canning M., Use of Low-Density Microarrays for studying gene expression patterns induced by hepatotoxicants on primary cultures of rat hepatocytes, *Toxicol Sci* (2003) 75:378-392

Deng L., Chen N., Li Y., Zheng H. and Lei Q., CXCR6/CXCL16 as a regulator in metastasis and progression of cancer, *Biochim Biophys Acta* (2010) 1806:42-49

Dieterle F. and Marrer E., New technologies around biomarkers and their interplay with drug development, *Anal Bioanal Chem* (2008) 390:141-154

DiMasi J. A., Hansen R. W. and Grabowski H. G., The price of innovation: new estimates of drug development costs, *J Health Econ* (2003) 22:151-185

Donato M. T., Lahoz A., Castell J. V. and Gómez-Lechón M. J., Cell lines: A tool for In Vitro Metabolism Studies, *Curr Drug Metab* (2008) 9:1-11

Dykens J. A. and Will Y., The significance of mitochondrial toxicity testing in drug development, *Drug Discov Today* (2007) 12(17/18):777-785

Dykens J. A., Jamieson J., Marroquin L., Nadanaciva S., Billis P. A. and Will Y., Biguanide-induced mitochondrial dysfunction yields increased lactate production and cytotoxicity of aerobically-poised HepG2 cells and human hepatocytes in vitro, *Toxicol Appl Pharmacol* (2008) 233:203-210

ECHA, About REACH, accessed at 10 June 2011 from http://echa.europa.eu/reach_en.asp

Edwards M., Rassin D. K., Izumi T., Mitra S. and Perez-Polo J. R., APE/Ref-1 response to oxidative stress in aged rats, *J Neurosci Res* (1998) 54(5):635-638

Elashoff M., Role of Statistics in Toxicogenomics, Essential Concepts in Toxicogenomics, Humana Press (2008), Mendrick D. L. and Mattes W. B. (editors)

Elbrecht A., Chen Y., Cullinan C. A., Hayes N., Leibowitz M. D., Moller D. E. and Berger J., Molecular Cloning Expression and Characterization of Human Peroxisome Proliferator Activated Receptor γ1 and γ2, *Biochem Biophys Res Commun* (1996) 224:431-437

Ellinger-Ziegelbauer H., Stuart B., Wahle B., Bomann W., Ahr H. J., Comparison of the expression profiles induced by genotoxic and non-genotoxic carcinogens in rat liver, *Mutat Res* (2005) 575:61-84

Ellinger-Ziegelbauer H., Adler M., Amberg A., Brandenburg A., Callanan J. J., Connor S., Fountoulakis M., Gmuender H., Gruhler A., Hewitt P., Hodson M., Matheis K. A., McCarthy D., Raschke M., Riefke B., Schmitt C. S., Sieber M., Sposny A., Suter L., Sweatman B. and Mally A., The enhanced value of combining conventional and "omics" analysis in early assessment of drug-induced hepatobiliary injury, *Toxicol Appl Phramacol* (2011) 252(2):97-111

EMA 2010, Reflection paper on co-development of pharmacogenomic biomarkers and Assays in the context of drug development, 24 June 2010, downloaded at 10 June 2011 from http://www.ema.europa.eu/docs/en_GB/document_library/Scientific_guideline/2010/07/WC500094445.pdf

Engesser H. (ed.), Schülerduden Die Mathematik II, Bibliographisches Institut & F. A. Brockhaus AG, Mannheim, 3. ed. (1991)

Expressionist™ online help, assessed on 20 Juli 2011

Farkas D., New toxicogenomics tools accelerate early-stage safety assessment in drug development, *Bio IT World* (2010) 6:24-29

FDA 2004, Concept paper: Drug Interaction Studies – Study Design, Data Analysis, and Implications for Dosing and Labeling, 01 October 2004, downloaded at 10 June 2011 from http://www.fda.gov/ohrms/dockets/ac/04/briefing/2004-4079B1_04_ Topic2-TabA.pdf

FDA 2005, Guidance for Industry Pharmacogenomic Data Submission, March 2005, downloaded at 10 June 2011 from http://www.fda.gov/downloads/Drugs/GuidanceComplianceRegulatoryInformation/Guidances/ucm079849.pdf

FDA-FF: FDA Approval Package for Fenofibrate, Pharmacological Review 021656/S-000, 13 July 2004, downloaded from www.pharmapendium.com

FDA-Rosi: FDA Approval Package for Rosiglitazone, Pharmacological Review 021071/S-000 Part 02, 11 May 1999, downloaded from www.pharmapendium.com

FDA-Tro: FDA Approval Package for Troglitazone, Pharmacological Review 020720 9 January 1997, downloaded from www.pharmapendium.com

Fielden M. R. and Kolaja K. L., The state-of-the-art in predictive toxicogenomics, *Curr Opin Drug Discov Devel* (2006) 9(1):84-91

Flatt P. M. and Pietenpol J. A., Mechanisms of cell-cycle checkpoints: At the crossroads of carcinogenesis and drug discovery, *Drug Metab Rev* (2000) 32(3&4):283-305

Floyd J. S., Barbehenn E., Lurie P. and Wolfe S. M., Case series of liver failure associated with rosiglitazone and pioglitazone, *Pharmacoepidemiol Drug Saf* (2009) 18:1238-1243

Freudlsperger C., Moll I., Schuhmacher U. and Thies A., Anti-proliferative effect of peroxisome proliferator-activated receptor gamma agonists on human malignant melanoma cells in vitro, *Anticancer Drugs* (2006) 17(3):352-332

Friedmann S. L., Molecular mechanisms of hepatic fibrosis and principles of therapy, *J Gastroenterol* (1997) 32:424-430

Fujimura H., Murakami N., Miwa S., Aruga C. and Toriumi W., The suitability of rat hematoma cell line H4IIE for evaluating the potentials of compounds to induce CYP3A23 expression, *Exp Toxicol Pathol* (2010) Epub ahead of print

Fujiwara T., Okuno A., Yoshioka S. and Horikoshi H., Suppression of hepatic gluconeogenesis in long-term Troglitazone treated diabetic KK and C57BL/KsJ-db/db mice, *Metabolism* (1995) 44(4):486-490

Fulgencio J. P., Kohl C., Girard J. and Pégorier J. P., Troglitazone inhibits fatty acid oxidation and esterification, and gluconeogenesis in isolated hepatocytes from starved rats, *Diabetes* (1996) 45(11):1556-1562

Fulgencio J. P., Kohl C., Girard J. and Pégorier J. P., Effect of metformin on fatty acid and glucose metabolism in freshly isolated hepatocytes and on specific gene expression in cultured hepatocytes, *Biochem Pharmacol* (2001) 62:439-446

Funk C., Ponelle C., Scheuermann G. and Pantze M., Cholestatic potential of troglitazone as a possible factor contributing to troglitazone-induced hepatotoxicity: In vivo and in vitro interactions at the canalicular bile salt export pump (Bsep) in the rat, *Mol Pharmacol* (2001) 59(3):627-635

Furuta M., Yano Y., Gabazza E. C., Araki-Sasaki R., Tanaka T., Hori Y., Nakatani K., Sumida Y. and Adachi Y., Troglitazone improves GLUT4 expression in adipose tissue in an animal model of obese type 2 diabetes mellitus, *Diabetes Res Clin Pract* (2002) 56(3):159-171

Gale E. A., Lessons from the glitazones: a story of drug development, *Lancet* (2001) 357(9271):1870-1875

Galli A., Ceni E., Mello T., Polvani S., Tarocchi M., Buccoliero F., Lisi F., Cioni L., Ottanelli B., Foresta V., Mastrobuoni G., Moneti G., Pieraccini G., Surrenti C. and Milani S., Thiazolidinediones inhibit hepatocarcinogenesis in hepatitis B virus-transgenic mice by peroxisome proliferator-activated receptor gamma-independent regulation of nucleophosmin, *Hepatology* (2010) 52(2):493-505

Ganey P. E., Luyendyk J. P., Maddox J. F. and Roth R. A., Adverse hepatic drug reactions: inflammatory episodes as consequence and contributor, *Chem Biol Interact* (2004) 150:35-51

Genedata: Website of the company Genedata, accessed at 26 July 2011, www.genedata.com/products/expressionist.html

GeneGo: Website of the company GeneGo, www.genego.com/metatox.php, accessed at 26 July 2011

Giacomini K. M., Huang S-W., Tweedie D. J., Benet L. Z., Brouwer K. L., Chu X., Dahlin A., Evers R., Fischer V., Hillgren K. M., Hoffmaster K. A., Ishikawa T., Keppler D., Kim R. B., Lee C. A., Niemi M., Polli J. W., Sugiyama Y., Swaan P. W., Ware J. A., Wright S. H., Yee S. W., Zamek-Gliszczynski M. J., and Zhang L., Membrane transporters in drug development, *Nat Rev Drug Discov* (2010) 9:215-236

Glückmann M., Fella K., Waidelich D., Merkel D., Kruft V., Kramer P. J., Walter Y., Hellmann J., Karas M. and Kröger M., Prevalidation of potential protein biomarkers in toxicology using iTRAQ reagent technology, *Preoteomics* (2007) 7(19):1564-1574

Gómez-Lechón M. J., Lahoz A., Jiménez N., Vicente Castell J. and Donato M. T., Cryopreservation of rat, dog and human hepatocytes: influence of preculture and cyroprotectants on recovery, cytocchrome P450 activities and induction upon thawing, *Xenobiotica* (2006) 36(6):457-472

Gómez-Léchon M. J., Castell J. V and Donato M. T, The use of hepatocytes to investigate drug toxicity, *Methods Mol Biol* (2010) 640:389-415

Goodsaid F. M., Frueh F. W. and Mattes W., The Predictive Safety Testing Consortium: A synthesis of the goals, challenges and accomplishments of the Critical Path, *Drug Discov Today Technol* (2007) 4(2):48-50

Goodwin B., Moore L. B., Stoltz C. M., McKee D. D. and Kliewer S. A., Regulation of the human CYPsB6 gene by the nuclear pregnane X receptor, *Mol Pharmacol* (2001) 60:427-431

Gordon E. M., Douglas M. C., Jablonski P., Owen J. A., Sali A. and Watts J. M., Gastroduodenal hormones and bile-secretion studies in the isolated perfused pig liver, *Surgery* (1972) 72(5):708-721

Gouda H. E., Khan A., Schwartz J. and Cohen R. I., Liver failure in a patient treated with long-term rosiglitazone therapy, *Am J Med* (2001) 111(7):584-585

Grossman S. L. and Lessem J., Mechanisms and clinical effects of thiazolidinediones, *Expert Opin Investig Drugs* (1997) 6(8):1025-1040

Guengerich F. P., Cytochrome P450 and chemical toxicology, *Chem. Res. Toxicol*. (2008) 21:70-83

Gunderson K. L., Kruglyak S., Graige M. S., Garcia F., Kermani B. G., Zhao C., Che D., Dickinson T., Wickham E., Bierle J., Doucet D., Milewski M., Yang R., Siegmund C., Haas J., Zhou L., Oliphant A., Fan J.-B., Barnard S. and Chee M. S., Decoding randomly ordered DNA arrays, *Genome Res* (2004) 14(5):870-877

Guo L., Fang H., Collins J., Fan X.-H., Dial S., Wong A., Mehta K., Blann E., Shi L., Tong W. and Dragan Y. P., Differential gene expression in mouse primary hepatocytes exposed to the peroxisome proliferator-activated receptor α agonists, *BMC Bioinformatics* (2006) 7(Suppl 2):18-29

Guo L., Zhang L., Sun Y., Muskhelishvili L., Blann E., Dial S., Shi L., Schroth G. and Dragan Y. P., Differences in hepatotoxicity and gene expression profiles by anti-diabetic PPARγ agonists on rat primary hepatocytes and human HepG2 cells, *Mol Divers* (2006) 10:349-360

Guo L., Dial S., Shi L., Branham W., Liu J., Fang J.-L., Green B., Deng H., Kaput J. and Ning B., Similarities and differences in the expression of drug-matabolozing enzymes between human hepatic cell lines and primary human hepatocytes, *Drug Metab Dispos* (2011) 39:528-538

Hagenbuch B. and Meier P. J., The superfamily of organic anion transporting polypeptides, *Biochim Biophys Acta* (2003) 1-18

Hagenbuch B. and Dawson P., The sodium bile salt cotransport family SLC10, *Pflugers Arch – Eur J Physiol* (2004) 447:566-570

Hail N. Jr., Carter B. Z., Konopleva M. and Andreeff M., Apoptosis effector mechanisms: A requiem performed in different keys, *Apoptosis* (2006) 11:889-904

Hanafy A., Spahn-Langguth H., Vergnault G., Grenier P., Grozdanis M. T., Lenhardt T. and Langguth P., Pharmacokinetic evaluation of oral fenofibrate nanosuspension and SLN in comparison to conventional suspension of micronized drug, *Adv Drug Deliv Rev* (2007) 59:419-426

Halegoua-De Marzio D. and Navarro V. J., Drug-induced hepatotoxicity in humans, *Curr Opin Drug Discov Devel* (2008) 11(1):53-59

Hashizume T., Yoshitomi S., Asahi S., Uematsu R., Matsumura S., Chatani F. and Oda H., Advantages of human hepatocyte-derived transformats expressing a series of human cytochrome p450 isoforms for genotoxicity examination, *Toxicol Sci* (2010) 116(2):488-497

Heart E., Cline G. W., Collis L. P., Pongratz R. L., Gray J. P. and Smith P. J. S., Role of malic enzyme, pyruvate carboxylation, and mitochondrial malate import in glucose-stimulated insulin secretion, *Am J Physiol Endocrinol Metab* (2009) 296:E1354-1362

Heidebrecht F., Schulz I., Keller M., Behrens S. E. and Bader A., Improved protocols for protein and DNA isolation from three-dimensional collagen sandwich cultures of primary hepatocytes, *Anal Biochem* (2009) 393(1):141-144

Hernández L. G., van Steeg H., Luijten M. and van Benthem J., Mechanisms of non-genotoxic carcinogens and importance of a weight of evidence approach, *Mutat Res* (2009) 682(2-3):94-109

Heydtmann M., Lalor P. F., Eksteen J. A., Hübscher S. G., Briskin M. and Adms D. H., CXC chemokine ligand 16 promotes integrin-mediated adhesion of liver-infiltrating lymphocytes to cholangiocytes and hepatocytes within the inflammed liver, *J Immunol* (2005) 174:1055-1062

Hewitt N. J., Gómez-Lechón M. J., Houston J. B., Hallifax D., Brown H. S., Maurel P., Kenna J. G., Gustavsson L., Lohmann C., Skonberg C., Guillouzo A., Tuschl G., Li A. P., LeClyse E., Groothuis G. M. M. and Hengstler J. G., Primary hepatocytes: Current understanding of the regulation of metabolic enzymes and transporter proteins, and pharmaceutical practice for the use of hepatocytes in metabolism, enzyme induction, transporter, clearance, and hepatotoxicity studies, *Drug Metab Rev* (2007) 39:159-234

Hewitt P. and Walijew A., Toxicogenomics in drug safety assessment, *Pharmacogenomics* (2008) 9(4):379-382

Hibuse T., Maeda N., Nagasawa A. and Funahashi T., Aquaporins and glycerol metabolism, *Biochim Biophys Acta* (2006) 1758:1004-1011

Hirode M., Ono A., Miyagishima T., Nagao T., Ohno Y. and Urushidani T., Gene expression profiling in rat liver treated with compounds inducing phospholipidosis, *Toxicol Appl Pharmacol* (2008) 229:290-299

Hitomi J., Katayama T., Equchi Y., Kudo T., Taniquchi M., Koyama Y., Manabe T., Yamaqishi S., Bando Y., Imaizumi K., Tsujimoto Y. and Tohyama M., Involvement of caspase-4 in endoplasmic reticulum stress-induced apoptosis and Abeta-induced cell death, *J Cell Biol* (2004) 165(3):347-356

Hoebe K. H. N., Witkamp R. F., Fink-Gremmels J., Van Miert A. S. J. P. M., and Monshouwer M., Direct cell-to-cell contact between Kupffer cells and hepatocytes augments endotoxin-induced hepatic injury, *Am J Physiol Gastrointest Liver Physiol* (2001) 280:G720-G728

Hrach J., Toxicogenomics approaches for the prediction of hepatotoxicity in vitro, PhD thesis (2008), Ruperto-Carola University of Heidelberg/Germany

Hrach J., Mueller S. O. and Hewitt P., Development of an in vitro liver prediction model based on longer term primary rat hepatocyte culture, *Toxicol Lett* (2011) 206:189-196

Huang X., Wullschleger S., Shpiro N., McGuire V. A., Sakamoto K., Woods Y. L., McBurnie W., Fleming S. and Alessi D. R., Important role of the LKB1-AMPK pathway in suppressing tumorigenesis in PTEN-deficient mice, *Biochem J* (2008) 412:211-221

Huebert R. C., Splinter P. L., Garcia F., Marinelli R. A. and LaRusso N. F., Expression and localization of aquaporin water channels in rat hepatocytes, *J Biol Chem* (2002) 277(26):22710-22717

Hussaini S. H. and Farrington E. A., Idiosyncratic drug-induced liver injury: an overview, *Expert Opin. Drug Saf.* (2007) 6(6):673-684

Hwa A. J., Fry R. C., Sivaraman A., So P. T., Samson L. D., Stolz D. B. and Griffith L. G., Rat liver sinusoidal endothelial cells survive without exogenous VEGF in 3D perfused co-cultures with hepatocytes, *FASEB J* (2007) 21:2564-2579

ICH M3, Guidance on nonclinical safety studies for the conduct of human clinical trials and marketing authorization for pharmaceuticals M3(R2), International Conference on Harmonisation of technical requirements for registration of pharmaceuticals for human use (ICH), Current Step 4 version, 11 June 2009

ICH S2, Guidance on genotoxicity testing and data interpretation for pharmaceuticals intended for human use S2(R1), International Conference on Harmonisation of technical requirements for registration of pharmaceuticals for human use (ICH), Current Step 2 version, 06 March 2008

ICH S5, Detection of toxicity to reproduction for medical products & toxicity to male fertility S5(R2), International Conference on Harmonisation of technical requirements for registration of pharmaceuticals for human use (ICH), Current Step 4 version, 24 June 1993

Illumina® TotalPrep™ - Assay Manual, edition 09/2010, Life Technologies Corporation, Carlsbad/USA

Illumina-TN, Technical Note: Gene expression microarray data quality control, edition 22 Januar 2010, downloaded on 1st August 2011 from http://www.illumina.com /Documents/products/technotes/technote_gene_expression_data_quality_control .pdf

Illumina, http://www.illumina.com/technology/direct_hybridization_assay.ilmn, assessed 1st August 2011

Ingenuity: Website of the company Ingenuity, accessed at 26 July 2011, www.ingenuity.com

IPA online help, assessed on 20 Juli 2011

Jaeschke H., Reactive oxygen and mechanisms of inflammatory liver injury, *J Gastroenterol Hepatol* (2000) 15:718-724

James L. P., Mayeux P. R. and Hinson J. A., Acetaminophen-induced hepatotoxicity, *Drug Metab Dispos* (2003) 31:1499-1506

Jemnitz K., Veres Z., Monostory K., Kóbori K. and Vereczkey L., Interspecies differences in acetaminophen sensitivity of human, rat, and mouse primary hepatocytes, *Toxicol In Vitro* (2008) 22:961-967

Jin D., Zhang Y. and Chen X., Lipocalin 2 deficiency inhibits cell proliferation, autophagy, and mitochondrial biogenesis in mouse embryonic cells, *Mol Cell Biochem* (2011) 351(1-2):165-172

Jossé R., Aninat C., Glaise D., Dumont J., Fessard V., Morel F., Poul J.-M., Guguen-Guillouzo C. and Giullouzo A., Long-term functional stability of human HepaRG hepatocytes and use for chronic toxicity and genotoxicity studies, *Drug Metab Dispos* (2008) 36(6):1111-1118

Jouin D., Blanchard N., Alexandre E., Delobel F., David-Pierson P., Lavé T., Jaeck D., Richert L. and Coassolo P., Cryopreserved human hepatocytes in suspension are a convenient high throughput tool for the prediction of metabolic clearance, *Eur J Pharm Biopharm* (2006) 63:347-355

Källström H., Lindqvist A., Pospisil V., Lundgren A. and Rosenthal C. K., Cdc24A localisation ans shutteling: characterisation of sequences mediating nuclear export and import, *Exp Cell Res* (2005) 303(1):89-100

Kamisako T., Kaobayashi Y., Ishihara T., Hiquchi K., Tanaka Y., Gabazza E. C. and Adachi Y., Recent advances in bilirubin metabolism research: the molecular mechanism of hepatocyte bilirubin transport and its clinical relevance, *J Gastroenterol* (2000) 35(9):659-664

Kaplowitz N., Mechanisms of liver cell injury, *J Hepatol* (2000) 32(Suppl. 1):39-47

Kaplowitz N., Drug induced liver injury, *CID* (2004) 38(Suppl. 2):44-48

Kaplowitz N., Idiosyncratic drug hepatotoxicity, *Nat Rev Drug Discov* (2005) 4:489-499

Kaspar J. W., Niture S. K. and Jaiswal A. K., Nrf2:INrf2(Keap1) signaling in oxidative stress, *Free Radic Biol Med* (2009) 47(9):1304-1309

Kassianides C., Nussenblatt R., Palestine A. G., Mellow S. D. and Hoofnagle J. H., Liver injury from cyclosporine A, Dig Dis Sci (1990) 35(6):693-697

Keating G. M. and Ormrod D., Micronized Fenofibrate: An updated review of its clinical efficacy in the management of dyslipidaemia, *Drugs* (2002) 62(13):1909-1944

Kebebew E., Lindsay S., Clark O. H., Woeber K. A., Hawkins R. and Greenspan F. S., Results of rosiglitazone therapy in patients with thyroglobulin-positive and radioiodine-negative advanced differentiated thyroid cancer, *Thyroid* (2009) 19(9):953-956

Kenny J. R., Chen L., McGinnity D. F., Grime K., Shakesheff K. M., Thomson B. and Riley R., Efficient assessment of the utility of immortalized Fa2N-4 cells for cytochrome P450 (CYP) induction studies using multiplex quantitative reverse transcriptase-polymerase chain reaction (qRT-PCR) and substrate cassette methodologies, *Xenobiotica* (2008) 38(12): 1500-1517

Keyse S. M., Applegate L. A., Tromvoukis Y. and Tyrrell R. M., Oxidant stress leads to transcriptional activation of the human heme oxygenase gene in cultured skin fibroblasts, *Mol Cell Biol* (1990) 10(9):4967-4969

Kiang T. K. L., Teng X. W., Karagiozov S., Surendradoss J., Chang T. K. H. and Abbott F. S., Role of oxidative metabolism in the effect of valproic acid on markers of cell viability, necrosis, and oxidative stress in sandwich-cultured rat hepatocytes, *Toxicol Sci* (2010) 118(2):501-509

Kiang T. K. L., Teng X. W., Surendradoss J., Karagiozov S., Abbott F. S. and Chang T. K. H., Glutathione depletion by valproic acid in sandwich-cultured rat hepatocytes: Role of biotransformation and temporal relationship with onset of toxicity, *Toxicol Appl Pharamcol* (2011) 252:318-324

Kier L. D., Neft R., Tang L., Suizu R., Cook T., Onsurez K., Tiegler K., Sakai Y., Oritz M.,Nolan T., Sankar U. and Li A. P., Applications of microarrays with toxicologically relevant genes (tox genes) for the evaluation of chemical toxicants in Sprague Dawley rats in vivo and human hepatocytes in vitro, *Mutat Res* (2004) 549:101-113

Kikkawa R., Fujikawa M., Yamamota T., Hamada Y., Yamada H. and Horii I., In vivo hepatotoxicity study of rats in comparison with in vitro hepatotoxicity screening systems, *J Toxicol Sci* (2006) 31(1):23-34

Kim S.-y., Kim H.-i., Park S.-K., Im S.-S., Li T., Cheon H. G. and Ahn Y.-h., Liver Glucokinase Can Be Activated by Peroxisome Proliferator-Activated Receptor-γ, *Diabetes* (2004) 53(Suppl. 1):66-70

Kim J. W., Lee S. H., Park Y. S., Jeong S. H., Kim N., Lee D. H. and Lee H. S., Transcriptome analysis of hepatitis B virus-associated small hepatocellular carcinoma by serial analysis of gene expression, *Int J Oncol* (2009) 35(1):129-137

Kirchheiner J., Roots I., Goldammer M., Rosenkranz B. and Brockmöller J., Effect of genetic polymorphisms in cytochrome p450 (CYP) 2C9 and CYP2C8 on the pharmacokinetics of oral antidiabetic drugs: clinical relevance, *Clin Pharmacokinet* (2005) 44(12):1209-1225

Klaassen C. D. and Aleksunes L. M., Xenobiotic, bile acid, and cholesterol transporters: Function and regulation, *Pharmacol Rev* (2010) 62:1-96

Klauning J. E., Babich M. A., Baetcke K. P., Cook J. C., Corton J. C., David R. M., DeLuca J. G. Lai D. Y., McKee R. H., Peters J. M., Roberts R. A. and Fenner-Crisp P. A., PPARalpha agonist-induced rodent tumors: modes of action and human relevance, *Crit Rev Toxicol* (2003) 33(6):655-780

Kmieć Z., Cooperation of liver cells in health and disease, *Adv Anat Embryol Cell Biol* (2001) 161(III-XIII):1-151

Kobayashi K., Urashima K., Shimada N and Chiba K., Substrate specificity for rat cytochrome P450 (CYP) isoforms: screening with cDNA-expressed systems of the rat, *Biochem Pharmacol* (2002) 63:889-896

Koch J., Pranjic K., Huber A., Ellinger A., Hartig A., Kragler F. and Brocard C., PEX11 family members are membrane elongation factors that coordinate peroxisome proliferation and maintenance, *J Cell Sci* (2010) 123(Pt 19):3389-400

Kola I. and Landis J., Can the pharmaceutical industry reduce attrition rates?, *Nat Rev Drug Discov* (2004) 3:711-715

Koo S. H. and Lee E. J. D, Pharmacogenetics approach to therapeutics, *Clin Exp Pharmacol Physiol* (2006) 28(1):19-24

Kubota T., Yano T., Fujisaki K., Itoh Y. and Oishi R., Fenofibrate induces apoptotic injury in cultured human hepatocytes by inhibiting phosphorylation of Akt, *Apoptosis* (2005) 10:349-358

Kulke M. H., Demetri G. D., Sharpless N. E., Ryan D. P., Shivdasani R., Clark J. S., Spiegelman B. M., Kim H., Mayer R. J. and Fuchs C. S., A phase II study of troglitazone, an activator of the PPARgamma receptor, in patients with chemotherapy-resistant metastatic colorectal cancer, *Cancer J* (2002) 8(5):395-399

Kumar S., Boulton A. J., Beck-Nielsen H., Berthezene F., Muggeo M., Persson B., Spinas G. A., Donoghue S., Lettis S. and Steward-Long P., Troglitazone, an insulin action enhancer, improves metabolic control in NIDDM patients. Troglitazone Study Group, *Diabetologia* (1996) 39(6):701-709

Labbe G., Pessayre D. and Fromenty B., Drug-induced liver injury through mitochondrial dysfunction: mechanism and detection during preclinical safety studies, *Fundam Clin Pharmacol* (2008) 22:335-353

Lauer B., Tuschl G. and Mueller S. O., Species-specific toxicity of diclofenac and troglitazone in primary human and rat hepatocytes, *Chem Biol Interact* (2009) 179(1):17-24

Lawrence J. W., Li Y., Chen S., DeLuca J. G., Berger J. P., Umbenhauer D. R., Moller D. E. and Zhou G., Differential gene regulation in human versus rodent hepatocytes by peroxisome proliferator-activated receptor (PPAR) α, *J Biol Chem* (2001) 276(34):31521-31527

Lebovitz H. E., Dole J. F., Patwardhan R., Rappaport E. B. and Freed M. I., Rosiglitazone monotherapy is effective in patients with type 2 diabetes, J Clin *Endocrinol Metab* (2001) 86(1):280-288

Lebovitz H. E., Differentiating members of the thiazolidinedione class: a focus on safety, *Diabetes Metab Res Rev* (2002) 18(2):23-29

Lee W. M., Drug-induced hepatotoxicity, *N Engl J Med* (2003) 349:474-485

Lee M. W., Acetaminophen and the U. S. Acute Liver Failure Study Group: Lowering the risk of hepatic failure, *Hepatology* (2004) 40:6-9

Lee W. M. and Senior J. R., Recognizing drug-induced liver injury: Current problems, possible solutions, *Toxicol Pathol* (2005) 33:155-164

Lehmann J. M., McKee D. D., Watson M. A., Willson T. M., Moore J. T. and Kliewer S. A., The orphan nuclear receptor PXR is activated by compounds that regulate CYP3A4 gene expression and cause drug interactions, *J. Clin. Invest.* (1998) 102(5):1016-1023

Li H., Heller D. S., Leevy C. B., Zierer K. G. and Klein K. M., Troglitazone-induced fulminant hepatitis: report of a case with autopsy findings, *J Diabetes Complications* (2000) 14(3):175-177

Li A. P., A review of the common properties of drugs with idiosyncratic hepatotoxicity and the “multiple determinant hypothesis” for the manifestation of idiosyncratic drug toxicity, *Chem Biol Interact* (2002) 142:7-23

Li X., Baumgart E., Dong G.-X., Morrell J. C., Jimenez-Sanchez G., Valle D., Smith K. D. and Gould S. J., PEX11α is required for peroxisome proliferation in response to 4-phenylbutyrate but is dispensible for peroxisome proliferator-activated receptor alpha-mediated peroxisome proliferation, *Mol Cell Biol* (2002a) 22(23):8226-8240

Li A. P., Evaluation of drug metabolism, drug-drug interactions, and in vitro hepatotoxicity with cryopreserved human hepatocytes, *Methods Mol Biol* (2010) 640:281-294

Limonciel A., Aschauer L., Wilmes A., Prajczer S., Leonard M. O., Pfaller W. and Jennings P., Lactate is an ideal non-invasive marker of evaluating temporal alterations in cell stress and toxicity in repeat dose testing regimes, Toxicol In Vitro (2011) [Epub ahead of print]

Lin M. S., Chen W. C., Bai X. and Wang Y. D., Activation of peroxisome proliferator-activated receptor gamma inhibits cell growth via apoptosis and arrest of the cell cycle in human colorectal cancer, *J Dig Dis* (2007) 8(2):82-88

Lin J., Schyschka L., Mühl-Benninghaus R., Neumann J., Hao L., Nussler N., Dooley S., Liu L., Stöckle U., Nussler A. K. and Ehnert S., Comparative analysis of phase I and II enzyme activities in 5 hepativ cell lines identifies Huh-7 and HCC-T cells with the highest potential to study drug metabolism, *Arch Toxicol* (2011) [Epub ahead of print]

Little Dipper™ Manual, edition 09/2008, SciGene, Sunnyvale/USA

Liu G. and Warbrick E., The p66 and p12 subunits of DNA polymerase δ are modified by ubiquitin and ubiquitin-like proteins, *Biochem Biophys Res Commun* (2006) 349(1):360-366

Liu Z. H. and Zeng S., Cytotoxicity of ginkgolic acid in HepG2 cells and primary rat hepatocytes, *Toxicol Lett* (2009) 187(3):131-136

Lloyd S., Hayden M. J., Sakai Y., Fackett A., Silber P. M., Hewitt N. J. and Li A. P., Differential in vitro hepatotoxicity of troglitazone and rosiglitazone among cryopreserved human hepatocytes from 37 donors, *Chem Biol Interact* (2002) 142:57-71

Lodish H., Berk A., Zipursky S. L., Matsudaira P., Baltimore D. and Darnell J. E. (ed.), Molekulare Zellbiologie, Spektrum Akademischer Verlag GmbH Heidelberg/Germany (2001) 4. edition

Lord P. G., Nie A. and McMillian M., Applications of Genomics in PreclinicalDrug Safety Evaluation, *Basic Clin. Pharmacol. Toxicol*. (2006) 98:537-546

Lorenzi M., The polyol pathway as a mechanism for diabetic retinopathy: Attractive, elusive, and resilient, *Exp Diabetes Res* (2007) 2007:61038

Löscher W., Nau H., Wahnschaffe U., Hönack D., Rundfeldt C., Wittfoht W. and Bojic U., Effects of valproate and E-2-en-valproate on functional and morphological parameters of rat liver. II. Influence of phenobarbital comedication, *Epilepsy Res* (1993) 15(2):113-131

Löscher W., Valprate: A reappraisal of its pharmacodynamic properties and mechanism of action, *Prog Neurobiol* (1999) 58:31-59

Lu F., Lan R., Zhang H., Jiang Q. and Zhang C., Geminin is partially localized to the centrosome and plays a role in proper centrosome dublication, *Biol Cell* (2009) 101(5):273-285

Lupp A., Danz M. and Müller D., Morphology and cytochrome P450 isoforms expression in precision-cut rat liver slices, *Toxicology* (2001) 161(1-2):53-66

Malcos J. L. and Hancock W. O., Engineering tubulin: microtubule functionalization approaches for nanoscale device application, *Appl Microbiol Biotechnol* (2011) 90:1-10

Mandard S., Müller M. and Kersten S., Peroxisome proliferator-activated receptor alpha target genes, *Cell Mol Life Sci* (2004) 61(4):393-416

Marion T. L., Leslie E. M. and Brouwer K. L. R., Use of sandwich-cultured hepatocytes to evaluate impaired bile acid transport as a mechanism of drug-induced hepatotoxicity, *Mol Pharm* (2007) 4(6):911-918

Marquard H. and Schäfer S. (editors), Lehrbuch der Toxikologie, Wissenschaftliche Verlagsgesellschaft mbH, Stuttgart, (2004)

Masubuchi Y., Metabolic and non-metabolic factors determining troglitazone hepatotoxicity: A review, *Drug Metab. Pharmacokinet*. (2006) 21(5):347-356

Masubuchi Y., Kano S. and Horie T., Mitochondrial permeability transition as a potential determinant of hepatotoxicity of antidiabetic thiazolidinediones, *Toxicology* (2006a) 222:233-239

Masubuchi N., Makino C. and Murayama N., Prediction of in vivo potential for metabolic activation of drugs into chemically reactive intermediates: Correlation of in vitro and in vivo generation of reactive intermediates and in vitro glutathione conjugate formation in rats and human, *Chem Res Toxicol* (2007) 20:455-464

Matés J. M., Segura J. A., Alonso F. J. and Márquez J., Intracellular redox status and oxidative stress: implications for cell proliferation, apoptosis, and carcinogenesis, *Arch Toxicol* (2008) 82:273-299

Matsumoto T., Ono Y., Kuromiya A., Toyosawa K., Ueda Y. and Bril V., Long –term treatment with Renirestat (AS-3201), a potent aldose reductase inhibitor, suppresses diabetic neuropathy and cataract formation in rats, *J Pharmacol Sci* (2008) 107:340-348

Mattes W. B., Public Consortium Efforts in Toxicogenomics, Essential Concepts in Toxicogenomics, Humana Press (2008), Mendrick D. L. and Mattes W. B. (editors)

Memon R. A., Tecott L. H., Nonogaki K., Beigneux A., Moser A. H., Grunfeld C. and Feingold K. R., Up-regulation of peroxisome proliferator-activated receptors (PPAR-alpha) and PPAR-gamma messenger ribonucleic acid expression in the liver in murine obesity: troglitazone induces expression of PPAR-gamma-responsive adipose tissue-specific genes in the liver of obese diabetic mice, *Endocrinology* (2000) 141(11):4021-4031

Mendrick D. L., Genomic and genetic biomarkers of toxicity, *Toxicology* (2008) 245:175-181

Michael G. (ed.), Biochemical Pathways, Spektrum Akademischer Verlag GmbH Heidelberg; Berlin/Germany (1999) 1st edition

Miyamoto S., Matsumoto A., Mori I. and Horinouchi A., Relationship between in vitro phospholipidosis assay using HepG2 cells and 2-week toxicity studies in rats, *Toxicol Mech Methods* (2009) 19(8):477-485

Moldovan G. L., Pfander B. and Jentsch S., PCNA, the meastro of the replication fork, *Cell* (2007) 129(4):665-679

Montague C. T. and O'Rahilly S., The perils of portliness: Causes and consequences of visceral adiposity, *Diabetes* (2000) 49:883-888

Morishita K., Mizukawa Y., Kasahara T., Okuyama M., Takashima K., Toritsuka N., Miyagishima T., Nagao T. and Urushidani T., Gene expression profile in liver of differing ages of rats after single oral administration of acetaminophen, *J Toxicol Sci* (2006) 31(5):491-507

Morosetti R., Servidei T., Mirabella M., Rutella S., Mangiola A., Maira G, Mastrangelo R. and Koeffler H. P., The PPARgamma ligands PGJ2 and rosiglitazone show a differential ability to inhibit proliferation and to induce apoptosis and differentiation of human glioblastoma cell lines, *Int J Oncol* (2004) 25(2):493-502

Moutzuori E., Kei A., Elisaf M. S. and Milionis H. J., Management of dyslipidemias with fibrates, alone and in combination with statins: role of delayed-release fenofibric acid, *Vasc Health Risk Manag* (2010) 9(6):525-539

Mueller E., Smith M., Kroll T. Aiyer A., Kaufman D. S., Demetri G., Figg W. D., Zhou X. P., Eng C., Spiegelman B. M. and Kantoff P. W., Effects of ligand activation of peroxisome proliferator-activated receptor gamma in human prostate cancer, *Proc Natl Acad Sci U S A* (2000) 97(20):10990-10995

Mueller S. O., Tuschl G. and Kling M., Alternatives in pharmaceutical toxicology: global and focussed approaches—two case studies, *ALTEX* (2007) 24(2):117-124

Mullard A., 2010 FDA drug approvals, *Nat Rev Drug Discov* (2011) 10:82-85

Muller P. Y. and Dieterle F., Tissue-specific, non-invasive toxicity biomarker: translation fom preclinical safety assessemnt to clinical safety monitoring, Expert Opin. *Drug Metab. Toxicol.* (2009) 5(9):1023-1038

Murphy E. J., Davern T. J., Shakil A. O., Shick L., Masharani U., Chow H., Freise C., Lee W. M. and Bass N. M., Troglitazone-induced fulminant hepatic failure. Acute Liver Failure Study Group, *Dig Dis Sci* (2000) 45(3):549-553

Nadanaciva S., Dykens J. A., Bernal A., Capaldi R. A. and Will Y., Mitochondrial impairment by PPAR agonists and statins identified via immunocaptured OXPHOS complex activities and respiration, *Toxicol Appl Pharmacol* (2007) 223:277-287

NanoDrop 1000 V3.7 user's manual, edition 07/2008, Thermo Fisher Scientific, Wilmington/USA

Natali A. and Ferrannini E., Effects of metformin and thiazolidinediones on suppression of hepatic glucose production and stimulation of glucose uptake in type 2 diabetes: a systematic review, *Diabetologica* (2006) 49:434-441

NCBI: http://blast.ncbi.nlm.nih.gov/Blast.cgi, assessed on 31 Januar 2011

NIH, Homepage of the U. S. National Institutes of Health (NIH), retrieved 9 April 2011, www.clinicaltrials.gov/ct2/info/glossary, last update: 18 March 2008

Nishimura J., Dewa Y., Muguruma M., Kuroiwa Y., Yasuno H., Shima T., Jin M., Takahashi M., Umemura T. and Mitsumori K., Effect of fenofibrate on oxidative DNA damage and on gene expression related to cell proliferation and apoptosis in rats, *Toxicol Sci* (2007) 97(1):44-54

OECD 431, Guideline for the testing of chemicals, In vitro skin corrosion: Human skin model test, Organisation for Economic Co-operation and Development (OECD), 13 April 2004

OECD 432, Guideline for the testing of chemicals, In vitro 3T3 NRU phototoxicity test, Organisation for Economic Co-operation and Development (OECD), 13 April 2004

OECD 438, Guideline for the testing of chemicals, Isolated chicken eye test method for identifying ocular corrosives and severe irritants, Organisation for Economic Co-operation and Development (OECD), 07 September 2009

OECD 439, Guideline for the testing of chemicals, In vitro skin irritation: Reconstructed human epidermis test method, Organisation for Economic Co-operation and Development (OECD), 22 July 2010

Ogawa K., Molecular pathology of early stage chemically induced hepatocarcinogenesis, *Pathol Int* (2009) 59(9):605-622

Olsaysky Goyak. K. M., Laurenzana E. M. and Omiecinski C. J., Hepatocyte differentiation, *Methods Mol Biol* (2010) 640:115-138

Olson A. L. and Pessin J. E., Structure, function, and regulation of the mammalian facilitative glucose transporter gene family, *Annu Rev Nutr* (1996) 16:235-256

Olson H., Betton G., Stritar J. and Robinson D., The predictivity of the toxicity of pharmaceuticals in humans from animal data – an interim assessment, *Toxicol Lett* (1998) 1021103:535-538

Omi S., Nakata R., Okamura-Ikeda K., Konishi H. and Taniguchi H., Contributing of peroxisome-specific isoform of lon protease in sorting PTS1 proteins to peroxisomes, *J Biochem* (2008) 143:649-660

Oo Y. H., Shetty S. and Adams D. H., The role of chemokines in the recruitment of lymphocytes to the liver, *Dig Dis* (2010) 28(1):31-44

Orino K., Lehmann L., Tsuji Y., Ayaki H., Torti S. V. and Torti F. M, Ferritin and the response to oxidative stress, *Bicohem J* (2001) 357:241-247

Osei S. Y., Koro C. E., Cobitz A. R., Kolatkar N. S. and Stender M., Commentary on 'Case series of liver failure associated with rosiglitazone and pioglitazone' by Floyd et al., *Pharmacoepidemiol Drug Saf* (2009) 18(12):1244-1246

Osheroff N., DNA topoisomerases, *Biochim Biophys Acta* (1998) 1400(1-3):1-2

Otto M., Hansen S. H., Dalgaard L., Dubois J. and Badalo L., Development of an in vitro assay for the investigation of metabolism-induced drug hepatotoxicity, *Cell Biol Toxicol* (2008) 24:87-99

Owa T., Yoshino H., Yoshimatsu K. and Nagasu T., Cell cycle regulation in the G1 phase: A promising target of the development of new chemotherapeutic anticancer agents, *Curr Med Chem* (2001) 8:1487-1503

Ozer J., Ratner M., Shaw M., Bailey W. and Schomaker S., The current state of serum biomarkers of hepatotoxicity, *Toxicology* (2008) 245:194-205

Panomics Inc., Fremont/USA, QuantiGene® Plex 2.0 Reagent System User Manual 2008

Park K. S., Ciaraldi T. P., Abrams-Carter L., Mudaliar S., Nikoulina S. E. and Henry R. R., Troglitazone regulation of glucose metabolism in human skeletal muscle cultures from obese type II diabetic subjects, *J Clin Endocrinol Metab* (1998) 83(5):1636-1643

Parzefall W., Berger W., Kainzbauer E., Teufelhofer O., Schulte-Hermann R. and Thurman R. G., Peroxisome proliferators do not increase DNA synthesis in purified rat hepatocytes, *Carcinogenesis* (2001) 22(3):519-523

Pascussi J. M., Gerbal-Chaloin S., Drocourt L., Maurel P. and Vilarem M. J., The expression of CYP2B6, CYP2C9 and CYP3A4 genes: a tangle of networks of nuclear and steroid receptors, *Biochim Biophys Acta* (2003) 1619:243-253

Patel R. D., Hollingshead B. D., Omniecinski C. J., and Perdew G. H., Aryl-Hydrocarbon receptor activation regulates the constitutive androstane receptor levels in murine and human liver, *Hepatology* (2007) 46(1):209-218

Pennie W. D., Tugwood J. D., Oliver G. J. A. and Kimber I., The principles and practice of toxicogenomics: Application and opportunities, *Toxicol Sci* (2000) 54:277-283

Pfeifer A. M. A., Cole K. E., Smoot D. T., Weston A., Groopman J. D., Shields P. G., Vignaud J.-M., Juillerat M., Lipsky M. M., Trump B. F., Lechner J. F. and Harris C. C., Simian virus 40 large tumor antigen-immortalized normal human epithelial cells express hepatocyte chracteristics and metabolize chemical carcinogens, *Proc. Natl. Acad. Sci. USA* (1993) 90:5123-5127

Pierno S., Didonna M. P., Cippone V., De Luca A., Pisoni M., Friferi A., Nicchia G. P., Svelto M., Chiesa G., Sirtori C., Scanziani E., Rizzo C., De Vito D. and Conte Camerino D., Effects of chronic teatment with statins and fenofibrate on rat skeletal muscle: a biochemical, histological and electrophysical study, *Br J Pharmacol* (2006) 149(7):909-919

Pollak P. T. and Shafer S. L., Use of population modeling to define rational monitoring of amiodarone hepatic effects, *Clin Pharmacol Ther* (2004) 311(3):864-873

Predict-IV (2011): Official homepage of the EU-project Predict-IV: http://www.predict-iv.toxi.uni-wuerzburg.de

Predict-IV (2011a): Standard operation procedure of the project, unpublished data

Preziosi P., Science, pharmacoeconomics and ethics in drug R&D: a sustainable future scenario?, *Nat Rev Drug Discov* (2004) 3:521-526

Rachek L. I., Yuzefovych L. V., LeDoux S. P., Julie N. L. and Wilson G. L., Troglitazone, but not Rosiglitazone, damages mitochondrial DNA and induces mitochondrial dysfunction and cell death in human hepatocytes, *Toxicol Appl Pharmacol* (2009) 240:348-354

Rainsford K. D., Ibuprofen: pharmacology, efficacy and safety, *Inflammopharmacology* (2009) 17:275-342

Rawlins M. D., Cutting the costs of drug development?, *Nat Rev Drug Discov* (2004) 3:360-364

Raychaudhuri S., Stuart J. M., and Altman R. B., Principal Component Analyis to summarize microarray experiments: Application to sporulation time series, *Pac Symp Biocomput.* (2000) 455-466

Reed J. C., Apoptosis-regulating proteins as targets for drug discovery, *Trends Mol Med* (2001) 7(7):314-319

Reilly S.-J., Tillander V., Ofman R., Alexson S. E. H. and Hunt M. C., The Nudix hydrolase 7 is an acyl-CoA diphosphatase involved in regulation of peroxisomal coenzyme A homeostasis, *J Biochem* (2008) 144:655-663

Richert L., Alexandre E., Lloyd T., Orr S., Viollon-Abadie C., Patel R., Kingston S., Berry D., Dennison A., Heyd B., Mantion G. and Jeak D., Tissue collection, transport and isolation procedure required to optimize human hepatocyte isolation from wate liver surgical resections. A multilaboratory study, *Liver Int* (2004) 24:371-378

Richert L., Tuschl G., Abadie C., Blanchard N., Pekthong D., Mantion G., Weber J.-C. and Mueller S. O., Use of mRNA expression to detect the induction of drug metabolising enzymes in rat and human hepatocytes, *Toxicol Appl Pharmacol* (2009) 235:68-96

RNAprotect Cell Reagent Handbook, edition 10/2010, Qiagen, Hilden/Germany

Robin M. A., Descatoire V., Pessayre D. and Berson A., Steatohepatitis-inducing drugs trigger cytokeratin cross-links in hepatocytes. Possible contribution to Mallory-Denk body formation, *Toxicol In Vitro* (2008) 22(6):1511-1519

Rodríguez-Antona C., Donato M. T., Boobis A., Edwards R. J., Watts P. S., Castell J. V. and Gómez-Lechón M.-J., Cytochrome P450 expression in human hepatocytes and hepatoma cell lines: molecular mechanisms that determine lower expression in cultured cells, *Xenobiotica* (2002) 32(6):505-520

Rogiers V., Akrawi M., Vercruysse A., Phillips I. R. and Shephard A., Effect of the anticonvulsant, valproate, on the expression of components of the cytochrome-P-450-mediated monooxygenase system and glutathione S-transferases, *Eur. J. Biochem.* (1995) 231:337-343

Roglans N., Bellido A., Rodríguez C., Cabrero A., Novell F., Ros E., Zambón D. and Laguna J. C., Fibrate treatment does not modify the expression of acyl coenzyme A oxidase in human liver, *Clin Pharmacol Ther* (2002) 72(6):692-701

Rogue A., Renaud M. P., Claude N. Guillouzo A. and Spire C., Comparative gene expression profiles induced by PPARγ and PPARα/γ agonists in rat hepatocytes, *Toxicol Appl Pharmacol* (2011) 254:18-31

Rogue A., Lambert C., Jossé R., Antherieu S., Spire C., Claude N. and Guillouzo A., Comparative gene expression profiles induced by PPARγ and PPARα/γ agonists in human hepatocytes, *PloS ONE* (2011a) 6(4):e18816

Roth A., Boess F., Landes C., Steiner G., Freichel C., Plancher J. M., Raab S., de Vera Mudry C., Weiser T. and Suter L., Gene expression-based in vivo and in vitro prediction of liver toxicity allows compound selection at early stages of drug development, *J Biochem Mol Toxicol* (2011) 25(3):183-194

Russel W. and Burch R., The principles of human experimental technique, (1959) Methuen, London

Russell L. and Forsdyke D. R., A human putative lymphocyte G0/G1 switch gene containing a CpG-rich island encodes a small basic protein with the potential to be phosphorylated, *DNA Cell Biol* (1991) 19(8):581-591

RX-APAP: www.rxlist.com/tylenol-drug.htm, assessed 9 August 2011

RX-FF: www.rxlist.com/antara-drug, accessed 1st August 2011

RX-Rosi: www.rxlist.com/avandia-drug.htm, accessed 4 September 2011

RX-Tro: www.rxlist.com/rezulin-drug.htm, accessed 4 September 2011

RX-VA: www.rxlist.com/depakene-drug-patient.htm, assessed 9 August 2011

Sahi J., Hamilton G., Sinz M., Barros S., Huang S. M., Lesko L. J. and LeClyse E. L., Effect of troglitazone on cytochrome P450 enzymes in primary cultures of human and rat hepatocytes, *Xenobiotica* (2000) 30:273-284

Sahu S. C. (Editor), Hepatotoxicity: From Genomics to in vitro and in vivo Models, John Wiley & Sons. Ltd (2007)

Saito K., Kobayashi K., Mizuno Y., Fukuchi Y., Furihata T. and Chiba K., Peroxisome proliferator-activated receptor alpha (PPARα) agonists induce constitutive androstane receptor (CAR) and cytochrome P450 2B in rat primary hepatocytes, *Drug Metab. Pharmacokinet*. (2010) 25(1):108-111

Sandimmune: http://www.rxlist.com/sandimmune-drug.htm, accessed 1st August 2011

Schadinger S. E., Bucher N. L. R., Schreiber B. M. and Farmer S. R., PPARγ2 regulates lipogenesis and lipid accumulation in steatotic hepatocytes, *Am J Physiol Endocrinol Metab* (2005) 288:E1195-E1205

Schmidt R. F., Lang F. and Thews G., Physiologie des Menschen mit Pathopysiologie, Springer Medizin Verlag Heidelberg, 29. ed.,(2005)

Schmitz S., Der Experimentator Zellkultur, Elsevier GmbH, Spektrum Akademischer Verlag, Heidelberg/Germany, 1. edition 2007

Schoonen W. G. E. J., Westerink W. M. A. and Horbach G. J., High-throughput screening for analysis of in vitro toxicity, *EXS* (2009) 99:401-452

Schroeder A., Mueller O., Stocker S., Salowsky R., Leiber M., Gassmann M., Lightfoot S., Menzel W., Granzow M. and Ragg T., The RIN: an RNA integrity number for assigning integrity values to RNA measurements, *BMC Mol Biol* (2006) 7(3)

Schug M., Heise T., Bauer A., Storm D., Blaszkewicz M., Bedawy E., Brulport M., Geppert B., Hermes M., Föllmann W., Rapp K., Maccoux L., Schormann W., Appel K. E., Oberemm A., Gundert-Remy U. and Hengstler J. G., Primary rat hepatocytes as in vitro system for gene expression studies: comparison of sandwich, Matrigel and 2D cultures, *Arch Toxicol* (2008) 82:923-931

Seglen P. O., Preparation of isolated rat liver cells, *Methods Cell Biol* (1976) 13:29-83

Sharma C., Pradeep A., Pestell R. and Rana B., Peroxisome proliferator-activated receptor γ activation modulates cyclin D1 transcription via β-catenin-independent and cAMP-response element-binding protein-dependent pathways in mouse hepatocytes, *J Biol Chem* (2004) 279(17):16927-16938

Shi Q., Yang X., Greenhaw J. and Salminen W., Hepatic cytochrome P450s attenuate the cytotoxicity induced by leflunomide and its active metabolite A77 1726 in primary cultured rat hepatocytes, *Toxicol Sci* (2011) [Epub ahead of print]

Shintani M., Nishimura H., Yonemitsu S., Ogawa Y., Hayashi T., Hosada K., Inoue G. and Nakao K., Troglitazone not only increases GLUT4 but also induces its translocation in rat adipocytes, *Diabetes* (2001) 50(10):2296-2300

Smith M. L., Ford J. M., Hollander M. C., Bortnick R. A., Amundson S. A., Seo Y. R., Deng C. X., Hanawalt P. C. and Fornace A. J. Jr., p53-mediated DNA repair responses to UV radiation: studies of mouse cells lacking p53, p21, and/or gadd45 genes, *Mol Cell Biol* (2000) 20(10):3705-3714

Smith M. T., Mechanism of Troglitazone Hepatotoxicity, *Chem Res Toxicol* (2003) 16(6):679-687

Smith M. R., Manola J., Kaufman D. S., George D., Oh W. K., Mueller E., Slovin S., Spiegelman B., Small E. and Kantoff P. W., Rosiglitazone versus placebo for men with prostate carcinoma and a rising serum prostate-specific antigen level after radical prostatectomy and/or radiation therapy, *Cancer* (2004) 101(7):1569-1574

Soars M. G., McDinnity D. F., Grime K. and Riley R. J., The pivotal role of hepatocytes in drug discovery, *Chem Biol Interact* (2007) 168:2-15

Sposny A., Schmitt C. S. and Hewitt P. G., Mechanistic investigation of EMD335823s hepatotoxicity using multiple omics profiling technologies. Handbook of Systems Toxicology, Volume 1 (2011) 25:389-405, John Wiley & Sons, Ltd. West Sussex/UK Casciano D. A. and Sahu S. C. (ed.)

Srivastava S., Conklin D. J., Liu S-Q., Prakash N., Boor P. J., Srivastava S. K., and Bhatnagar A., Identification of biochemical pathways for the metabolism of oxidized low-density lipoprotein derived aldehyde-4-hydroxy trans-2-nonal in vascular smooth muscle cells, *Atherosclerosis* (2001) 158:339-350

Stangier J., Su C.-A. P. F., Fraunhofer A. and Tetzloff W., Pharmacokinetics of Acetaminophen and Ibuprofen when coadministered with Telmisartan in healthy volunteers, *J Clin Pharmacol* (2000) 40:1338-1346

Stoelting M., Geyer M., Reuter S., Reichelt R., Bek M. J. and Pavenstädt H., Alpha(beta hydrolase 1 ia upregulated in D5 dopamine receptor knockout mice and reduces O2-production of NADPH oxidase, *Biochem Biophys Res Commun* (2009) 379(1):81-85

Strack T., Metformin: A review, Drugs of Today (2008) 44(4):303-314

Su D. H., Lai M. Y. and Wu H. P., Liver failure in a patient receiving rosiglitazone therapy, *Diabet Med* (2006) 23(1):105-106

Sugden M. C., Bulmer K. and Holness M. J., Fuel-sensing mechanisms integrating lipid and carbohydrate utilization, *Biochem Soc Trans* (2001) 29(Pt2)272-278

Sunman J. A., Hawke R. L., LeClyse E. L. and Kashuba A. D. M., Kupffer cell-mediated IL-2 suppression of CYP3A activity in human hepatocytes, *Drug Metab Dispos* (2004) 32(3):359-363

Suzuki H., Inoue T., Matsushita T., Kobayashi K., Horii I., Hirabayashi Y. and Inoue T., In vitro gene expression analysis of hepatotoxic drugs in rat primary hepatocytes, *J. Appl. Toxicol.* (2008) 28:227-236

Suter L., Schroeder S., Meyer K., Gautier J. C., Amberg A, Wendt M., Gmuender H., Mally A., Boitier E., Ellinger-Ziegelbauer H., Matheis K. and Pfannkuch F., EU framework 6 project: predictive toxicology (PredTox)—overview and outcome, *Toxicol Appl Pharmacol* (2011) 252(2):73-84

Tacke F., Luedde T. and Trautwein C., Inflammatory pathways in liver homeostasis and liver injury, *Clinic Rev Allerg Immunol* (2009) 36:4-12

Tamura K., Ono A., Miyagishima T., Nagao T. and Urushidani T., Profiling of gene expression in rat liver and rat primary cultured hepatocytes treated with peroxisome proliferators, *J Toxicol Sci* (2006) 31(5):471-490

Tang W., Drug metabololite profiling and elucidation of drug-induced hepatotoxicity, *Expert Opin. Drug Metab. Toxicol*. (2007) 3(3):407-420

Technical Note: RNA Analysis, Gene expression microarray data quality control, Illumina, Inc. (2010), downloaded from www.illumina.com on April 28, 2011

Tennant R. W., The National Center for Toxicogenomics: Using new technologies to inform mechanistic toxicology, *Environ Health Perspect* (2002) 110(1):A8-10

TGPJ, Website of the Toxicogenomics Project in Japan, accessed at 26 July 2011, http://wwwtgp.nibio.go.jp/index-e.html

´t Hoen P. A. C., Bijsterbosch M. K., Van Berkel T. J. C., Vermuelen N. P. E. and Commandeur J. N. M., Midazolam Is a Phenobarbital-like Cytochrome P450 Inducer in Rats, *J Pharmacol Exp Ther* (2001) 299:921-927

Tirona R. G. Lee W., Leake B. F., Lan L.-B., Cline C. B., Lamba V., Parviz F., Duncan S. A., Inoue Y., Gonzales F. J., Schuetz R. G. and Kim R. B., The orphan nuclear receptor HNF4α determines PXR- and CAR-mediated xenobiotic induction of CYP3A4, *Nat Med* (2003) 9(2):220-224

Tolman K. G., Defining patient risk from expanded preventive therapies, *Am J Cardiol* (2000) 85:15E-19E

Tong V., Teng X. W., Chang T. K. and Abbott F. S., Valproic acid I: time course of lipid peroxidation biomarkers, liver toxicity, and valproic acid metabolite levels in rats, *Toxicol Sci* (2005) 86(2):427-435

Trautwein C., Böker K. and Manns M. P., Hepatocyte and immune system: acute phase reaction as a contribution to early defence mechanisms, *Gut* (1994) 35(9):1163-1166

Tu S., McStay G. P., Boucher L. M., Mak T., Beere H. M. and Green D. R., In situ trapping of activated initiator caspases reveals a role for caspase-2 in heat shock-induced apoptosis, *Nat Cell Biol* (2006) 8(1):72-77

Tugwood J. D. and Montague C. T., Biology and toxicology of PPARγ ligands, *Hum Exp Toxicol* (2002) 21:429-437

Tuschl G. and Mueller S. O., Effects of cell culture conditions on primary rat hepatocytes – Cell morphology and differential gene expression, *Toxicology* (2006) 218:205-215

Tuschl G., Lauer B. and Mueller S. O., Primary hepatocytes as a model to analyze species-specific toxicity and drug metabolism, *Exper Opin. Drug Metab. Toxicol*. (2008) 4(7):855-870

Tuschl G., Hrach J., Walter Y., Hewitt P. G. and Mueller S. O., Serum-free collagen sandwich cultures of adult rat hepatocytes maintain liver-like properties long term: A valuable model for in vitro toxicity and drug-drug interaction studies, *Chem Biol Interact* (2009) 181:124-137

Uetrecht J., Idiosyncratic drug reactions: Past, present, and future, *Chem. Res. Toxicol.* (2008) 21:84-92

Ukelis U., Kramer P.-J., Olejniczak K. and Mueller S. O., Replacement of in vivo acute oral toxicity studies by in vitro cytotoxicity methods: opportunities, limits and regulatory status, *Regul Toxicol Pharmacol* (2008) 51:108-118

Uldry M. and Thorens B., The SLC2 family of faciliated hexose and polyol transporters, *Pflugers Arch* (2004) 447(5):480-489

Urquhart B. L., Tirona R. G. and Kim R. B., Nuclar receptors and the regulation of drug-metabolizing enzymes and drug transporters: Implications of interindividual variability in response to drugs, *J Clin Pharmacol* (2007) 47:566-578

Valousková E., Smolková K., Santorová J., Jezek P. and Modrianský M., Redistribution of cell death-inducing DNA fragmentation factor-like effector-a (CIDEa) from mitochondria to nucleus is associated with apoptosis in HeLa cells, *Gen Physiol Biophys* (2008) 27(2):92-100

Van Hummelen P. and Saski J., State-of-the-art genomics approaches in toxicology, Mutat Res (2010) 705(3):165-171

Van Kolfschoten A. A., Olling M. and Van Noordwijk J., Pharmacokinetic interactions between indomethacin and paracetamol in the rat, *Pharm Weekbl Sci* (1985) 7(1):15-19

Vassallo P. and Trohman R. G., Prescribing amiodarone: an evidence-based review of clinical indications, *JAMA* (2007) 298(11):1312-1322

Vickers A. E. M. and Fisher R. L., Organ slices for the evaluation of human drug toxicity, *Chem Biol Interact* (2004) 150:87-96

Vidales L., Ricardo J., New L., Pearson C. I., Roter A. H., Naughton B. and Applegate D. R., 3D liver co-cultures maintain phase I, II and III metabolism activity in long-term culture, Poster presentation #534-329, SOT's 50th Annual Meeting, 2011 March 6-10, Washington D.C./USA

Voet D., Voet J. G. and Pratt C. W. (ed.), Fundamentals of Biochemistry, *John Wiley & Sons, Inc.* (2002) 1. edition

Vogt B. A., Alam J., Croatt A. J., Vercellotti G. M. and Nath K. A., Acquired resistance to acute oxidative stress. Possible role of heme oxygenase and ferritin, *Lab Invest* (1995) 72(4):474-483

Vu-Dac N., Gervois P., Jakel H., Nowak M., Bauge E., Dehondt H., Pennacchio L. A., Rubin E. M., Fruchart-Najib J. and Fruchart J. C., Apolipoprotein A5, a crucial determinant of plasma triglyceride levels, is highly responsive to peroxisome proliferator-activated receptor alpha activators, *J Biol Chem* (2003) 278(20):17982-17985

Vuoriluoto K., Haugen H., Kiviluoto S., Mpindi J.-P., Nevo J., Gjerdrum C., Tiron C., Lorens J. B. And Ivaska J., Vimentin regulates EMT induction by Slug and oncogenic H-Ras and migration by governing Axl expression in breast cancer, *Oncogene* (2011) 30:1436-1448

Walsky R. L. and Boldt S. E., In vitro Cytochtomr P450 inhibition and induction, *Curr Drug Metab* (2008) 9:928-939

Wang M., Wise S. C., Leff T. and Su T. Z., Troglitazone, an antidiabetic agent, inhibits cholesterol biosynthesis through a mechanism independent of peroxisome proliferator-activated receptor-gamma, *Diabetes* (1999) 28(2):254-260

Watanabe R., Nakamura H., Masutani H. and Yodoi J., Anti-oxidative, anti-cancer and anti-inflammatory actions by thioredoxin 1 and thioredoxin-binding protein-2, Pharmacol Ther (2010) 127(3):261-270

Watkins P. B. and Whitcomb R. W., Hepatic dysfunction associated with troglitazone, *N Engl J Med* (1998) 338(13):916-917

Watkins S. M., Reifsnyder P. R., Pan H.-J., German J. B. and Leiter E. H., Lipid metabolome-wide effects of the PPARγ agonist rosiglitazone, *J Lipid Res* (2002) 43:1809-1817

Watkins P. B., Drug safety sciences and the bottleneck in drug development, *Clin Pharmacol Ther* (2011) 89(6):788-790

Waxman D. J., P450 gene induction by structurally diverse xenochemicals: Central role of nuclear receptors CAR, PXR, and PPAR, *Arch Biochem Biophys* (1999) 369(1):11-23

Welch C., Santra M. K., El-Assaad W., Zhu X., Huber R. A., Keys R. A., Teodoro J. G. and Green M. R., Identification of a protein, G0S2, that lacks Bcl-2 homology domains and interacts with and antagonizes Bcl-2, *Cancer Res* (2009) 69(17):6782-6789

Westerink W. M. A. and Schoonen W. G. E. J., Phase II enzyme levels in HepG2 cells and cryopreserved primary human hepatocytes and their induction in HepG2 cells, *Toxicol In Vitro* (2007) 21:1592-1602

Willson T. M., Brown P. J., Sternbach D. D. and Henke B. R., The PPARs: From orphan receptors to drug discovery, *J Med Chem* (2000) 43(4):527-550

Wissenmedia, downloaded at 10 June 2011 from http://www.wissen.de/wde/generator/material/gesundheit/KOERPER/leber_1xl.html

Xie W., Uppal H., Saini S. P. S., Mu Y., Little J. M., Radominska-Pandya A. and Zemaitis M. A., Orphan nuclear receptor-mediated xenobiotic regulation in drug metabolism, *DDT* (2004) 9(10):442-448

Xu J. J., Diaz D. and O'Brien P. J. O., Application of cytotoxicity assays and pre-lethal mechanistic assays for assessment of human hepatotoxicity potential, *Chem Biol Interact* (2004) 150:115-128

Xue G., Hao L. Q., Ding F. X., Mei Q., Huang J. J., Fu C. G. and Sun S. H., Expression of annexin a5 is associated with higher tumor stage and poor prognosis in colorectal adenocarcinomas, *J Clin Gastroenterol* (2009) 43(9):831-837

Yanase T., Yashiro T., Takitani K., Kato S., Taniguchi S., Takayanagi R. and Nawata H., Differential Expression of PPARγ1 and γ2 Isoforms in Human Adipose Tissue, *Biochem Biophys Res Commun* (1997) 233:320-324

Yee L. D., Williams N., Wen P., Young D. C., Lester J., Johnson M. V., Farrar W. B., Walker M. J., Povoski S. P., Suster S. and Eng C., Pilot study of rosiglitazone therapy in women with breast cancer: effects of short-term therapy on tumor tissue and serum markers, *Clin Cancer Res* (2007) 13(1):246-252

Yonemitsu S., Nishimura H., Shintani M., Inoue R., Yamamoto Y., Masuzaki H., Ogawa Y., Hosoda K., Inoue G., Hayashi T. and Nakao K., Troglitazone induces GLUT4 translocation in L6 myotubes, *Diabetes* (2001) 50(5):1093-1101

Yokoi T., Troglitazone, *Handb Exp Pharmacol* (2010) 196:419-435

Yuan L. and Kaplowitz N., Glutathione in liver disease and hepatotoxicity, *Mol Aspects Med* (2009) 30(1-2):29-41

Zandbergen F., Mandard S., Escher P., Tan N. S., Patsouris D., Jatkoe T., Rojas-Caro S., Madore S., Wahli W., Tafuri S., Müller M. and Kersten S., The G_0/G_1 switch gene 2 is a novel PPAR target gene, *Biochem J* (2005) 392:313-324

ZEBET25, The Hen's Egg Test – Chorio-Allantoic Membrane (HET-CAM) in vivo assay for Identification of Ocular Corrosive and Severe Irritants, last update 27 March 2009, downloaded from AnimAlt-ZEBET database of the German Bundesamt für Risikobewertung on 09 June 2011

ZEBET133, The Limulus amoebocytes lysate (LAL) test – a replacement for the rabbit pyrogen test, last update 05 January 2001, downloaded from AnimAlt-ZEBET database of the German Bundesamt für Risikobewertung on 09 June 2011

ZEBET169, Screening for embryotoxic and teratogenic hazard potential of chemical substances using the Embryonic Stem Cell Test, last update 14 June 2000, downloaded from AnimAlt-ZEBET database of the German Bundesamt für Risikobewertung on 09 June 2011

Zhao L., Samuels T., Winckler S., Korgaonkar C., Tpmpkins V., Horne M. C. and Quelle D. E., Cyclin G1 has growth inhibitory activity linked to the ARF-Mdm2-p53 and pRb tumor suppressor pathway, *Mol Cancer Res* (2003) 1(3):195-206

Zhou G., Myers R., Li Y., Chen Y., Shen X., Fenky-Melody J., Wu M., Ventre J., Doebber T., Fujii N., Musi N., Hirshman M. F., Goodyear L. J. and Moller D. E., *J Clin Invest* (2001) 108:1167-1174

Zhou S.-F., Drugs behave as substrates, inhibitors and inducers of human Cytochrome P450 3A4, *Curr Drug Metab* (2008) 9:310-322

Zidek N., Hellmann J., Kramer P.-J. and Hewitt P. G., Acute hepatotoxicity: A predictive model based on focused Illumina microarrays, *Toxicol Sci* (2007) 99(1):289-302

7 Appendix

Table 7.1: Results of the long term dose finding study in 24 well plate sandwich culture.
The cell viability is shown as percentage of control and mean of the three biological replicates ± standard deviation in percent.

compound	dose1	dose2	dose3	dose4	dose5	dose6	dose7	dose8
day 1								
Acetaminophen	88.4 ± 28.4	78.0 ± 17.0	68.5 ± 12.3	72.3 ± 12.5	68.3 ± 16.7	62.2 ± 15.4		
EMD 335823	80.4 ± 17.6	69.8 ± 19.1	73.7 ± 21.0	66.3 ± 13.2	53.1 ± 11.4	46.8 ± 2.8		
Fenofibrate	93.3 ± 43.6	62.6 ± 21.9	55.8 ± 22.4	58.3 ± 27.5	58.9 ± 24.9			
Metformin	104.3 ± 29.8	89.4 ± 22.5	66.2 ± 20.6	45.3 ± 17.9	13.6 ± 13.1			
Rosigliatazone	80.8 ± 27.4	70.0 ± 30.8	52.0 ± 23.8	44.1 ± 21.9	43.9 ± 24.9	33.9 ± 17.0		
Troglitazone	45.8 ± 13.0	44.8 ± 3.0	47.8 ± 8.4	44.5 ± 8.3	37.5 ± 7.5	37.6 ± 10.4	27.4 ± 9.7	7.4 ± 7.9
Valproic acid	66.5 ± 12.6	54.1 ± 10.3	45.6 ± 12.1	43.5 ± 9.1	39.3 ± 7.7	45.5 ± 11.3		
day 3								
Acetaminophen	114.4 ± 27.1	120.1 ± 39.2	105.5 ± 10.1	102.1 ± 16.5	77.2 ± 11.2	62.0 ± 21.5		
EMD 335823	86.4 ± 17.9	74.3 ± 26.1	65.9 ± 26.4	67.4 ± 26.5	42.3 ± 16.4	27.3 ± 8.7		
Fenofibrate	75.1 ± 30.3	46.8 ± 16.3	62.0 ± 29.3	59.0 ± 20.4	57.1 ± 18.6			
Metformin	105.3 ± 19.2	92.0 ± 15.6	76.5 ± 15.4	87.2 ± 24.8	14.2 ± 14.5			
Rosigliatazone	79.4 ± 26.7	66.1 ± 20.2	51.9 ± 25.3	42.7 ± 22.2	43.5 ± 15.1	17.4 ± 3.7		
Troglitazone	80.4 ± 13.8	75.9 ± 17.1	74.2 ± 21.3	68.1 ± 21.7	71.3 ± 28.4	67.0 ± 26.2	56.6 ± 49.0	0.1 ± 0.2
Valproic acid	88.7 ± 28.4	69.4 ± 20.8	55.6 ± 27.0	37.5 ± 33.5	31.4 ± 24.7	31.5 ± 24.4		
day 14								
Acetaminophen	84.9 ± 12.8	82.3 ± 20.0	92.5 ± 27.8	77.5 ± 18.1	67.7 ± 12.4	52.3 ± 3.3		
EMD 335823	122.7 ± 27.5	135.0 ± 23.7	109.1 ± 7.2	90.5 ± 17.1	0.6 ± 0.3	0.0 ± 0.0		
Fenofibrate	81.6 ± 15.3	75.3 ± 12.3	64.6 ± 20.1	61.7 ± 11.6	59.1 ± 9.7			
Metformin	92.8 ± 18.6	80.0 ± 12.8	60.9 ± 5.9	60.8 ± 12.2	9.5 ± 10.8			
Rosigliatazone	88.4 ± 21.2	72.9 ± 16.4	73.7 ± 18.1	88.9 ± 25.5	40.2 ± 12.2	0.0 ± 0.0		
Troglitazone	72.1 ± 14.3	70.3 ± 5.3	75.0 ± 5.0	83.4 ± 4.4	91.7 ± 6.2	101.4 ± 15.8	83.1 ± 20.9	0.0 ± 0.0
Valproic acid	74.1 ± 9.4	65.8 ± 3.2	63.9 ± 4.4	65.2 ± 8.6	70.2 ± 6.4	86.0 ± 10.3		

Table 7.2: Genes deregulated by Acetaminophen.
FC: fold change, Q: BH Q-value, LD: low dose, HD: high dose, 1/3/14: day 1/3/14, grayed out numbers: significantly deregulated genes.

		LD1		HD1		LD3		HD3		LD14		HD14	
Access. No.	**gene name and symbol**	**FC**	**Q**	**FC**	**Q**	**FC**	**Q**	**FC**	**Q**	**FC**	**Q**	**FC**	**Q**
lipid metabolism													
XM_576485.1	acetyl-CoA acyltransferase 1 (ACAA1)							1.61	0.39				
NM_013112.1	apolipoprotein A-II (APOA2)							-1.55	0.37				
NM_053995.3	3-hydroxybutyrate dehydrogenase 1 (BDH1)											-1.55	0.52
NM_031841.1	stearoyl-CoA desaturase 2 (Scd2)							-1.77	0.36			-2.63	0.52
NM_024143.1	solute carrier family 27 member 5 (SLC27A5)							-1.71	0.35			-1.61	0.51
drug metabolism													
NM_019363.2	aldehyde oxidase 1 (AOX1)							1.70	0.26				
NM_031543.1	cytochrome P450, family 2, subfamily E, polypeptide 1 (CYP2E1)							-1.53	0.31				
XM_579318.1	glutathione S-transferase alpha 3 (GSTA3)									-1.72	0.81		
NM_001007718.2	sulfotransferase family 1E, member 1 (SULT1E1)							-1.62	0.37				
stress													
NM_001008520.1	alpha/beta hydolase 1 (ABHD1)							1.52	0.03				
NM_022500.2	ferritin, light polypeptide (FTL)							1.66	0.26				
energy production													
NM_013215.1	aldo-keto reductase family 7, member A3 (AKR7A3)							1.51	0.26				
NM_172030.1	ectonucleoside triphosphate diphosphohydrolase 2 (ENTPD2)											-1.55	0.54
NM_012565.1	glucokinase (hexokinase 4) (GCK)			1.51	0.67								
NM_031039.1	glutamic-pyruvate transaminase (GPT)											-1.66	0.51
inflammation													
NM_012488.1	alpha-2-macroglobulin (A2M)							1.65	0.26				
NM_176074.2	complement component 6 (C6)											-1.76	0.53
NM_139089.1	chemokine (C-X-C motif) ligand 10 (CXCL10)											1.53	0.52
NM_173123.1	cytochrome P450, family 4, subfamily F, polypeptide 2 (CYP4F2)											-1.73	0.51

		LD1		HD1		LD3		HD3		LD14		HD14	
Access. No.	**gene name and symbol**	**FC**	**Q**	**FC**	**Q**	**FC**	**Q**	**FC**	**Q**	**FC**	**Q**	**FC**	**Q**
cell function													
NM_001001505.1	hyaluronan binding protein 2 (HABP2)											-1.56	0.52
NM_053469.1	hepcidin antimicrobial peptide (Hamp)											10.11	0.51
NM_012584.1	hydroxysteroide (3-beta) dehydrogenase 4 (Hsd3b4)							-1.51	0.33				
NM_031620.1	phosphoglycerate dehydrogenase (PHGDH)							1.55	0.28				
NM_013044.2	tropomodulin 1 (TMOD1)											-1.56	0.52
XM_237288.3	villin 1 (VIL1)									-1.57	0.81		
NM_019156.1	vitronectin (VTN)											-2.05	0.51
NM_012942.1	cytochrome P450, family 7, subfamily A, polypeptide 1 (CYP7A1)							-1.90	0.31			-2.16	0.55
NM_145782.1	cytochrome P450, family 3, subfamily A, polypeptide 43 (CYP3A43)											-2.09	0.54
growth, proliferation, cell death													
NM_012551.1	early growth response 1 (EGR1)							1.62	0.26				
NM_130752.1	fibroblast growth factor 21 (FGF21)							1.83	0.26				
NM_001009632.1	G0/G1switch 2 (G0S2)							1.63	0.30				
NM_053453.1	regulator of G-protein signaling 2, 24kDa (RGS2)											-2.33	0.51
XM_343479.2	sema domain, immunoglobulin domain (Ig), short basic domain, secreted, (semaphorin) 3B (SEMA3B)											-1.58	0.51
XM_342920.2	splicing factor proline/glutamine-rich (SFPQ)											-1.61	0.52

Table 7.3: Genes deregulated by Valproic acid.
FC: fold change, Q: BH Q-value, LD: low dose, HD: high dose, 1/3/14: day 1/3/14, grayed out numbers: significantly deregulated genes.

		LD1		HD1		LD3		HD3		LD14		HD14	
Access. No.	**gene name and symbol**	**FC**	**Q**	**FC**	**Q**	**FC**	**Q**	**FC**	**Q**	**FC**	**Q**	**FC**	**Q**
XM_576485.1	acetyl-CoA acyltransferase (ACAA1)	1.62	1.00										
NM_053515.1	solute carrier family 25, member 4 (SLC25A4)							-1.65	0.81				
NM_031543.1	cytochrome P450, family 2, subfamily E, polypeptide 1 (CYP2E1)							-1.63	0.81			-1.79	0.42
NM_001007718.2	sulfotransferase family 1E, member 1 (SULT1E1)			1.76	0.84			1.64	0.87				
NM_053453.1	regulator of G-protein signaling 2, 24kDa (RGS2)							-1.54	0.84				
NM_198780.2	phosphoenolpyruvate carboxykinase 1 (soluble) (PCK1)							-1.55	0.85				
NM_031783.1	neurofilament, light peptide (NEFL)											-1.62	0.39
NM_053469.1	hepcidin antimicrobial peptide (Hamp)											-2.44	0.38
NM_022298.1	tubulin, alpha 1a (TUBA1A)							-1.59	0.81				
NM_130741.1	lipocalin 2 (LCN2)											-1.69	0.37
NM_017259.1	BTG family meber 2 (BTG2)							-1.52	0.86				

Table 7.4: Genes deregulated by Fenofibrate.
The table contains the gene assession numbers, the gene names and symbols, as well as the fold changes for genes deregulated with $p < 0.05$.
Grayed out numbers: BH $Q \leq 0.2$, FF: Fenofibrate, L: low dose, H: high dose, 1/3/14: treatment day 1/3/14.

Access. No.	**gene name and symbol**	**FF L1**	**FF L3**	**FF L14**	**FF H1**	**FF H3**	**FF H14**
lipid metabolism							
NM_080576.1	apolipoprotein A-V (APOA5)	-5.00	-12.97	-8.17	-10.36	-24.24	-8.84
XM_214872.2	apolipoprotein C-II (APOC2)	-	-2.83	-	-	-4.19	-4.16
NM_019373.1	apolipoprotein M (APOM)	-	-1.52	-2.07	-	-1.75	-2.35
NM_175762.2	low density lipoprotein receptor (LDLR)	-	-1.50	-1.74	-	-	-1.93
XM_243524.3	low density lipoprotein receptor-related protein 1 (LRP1)	-	-	-	-	-	1.66
NM_032616.1	lipolysis stimulated lipoprotein receptor (LSR)	-	-	-2.24	-	-	-1.93
NM_013155.1	very low density lipoprotein receptor (VLDLR)	2.24	7.87	7.57	2.44	9.96	10.39

Access. No.	gene name and symbol	FF L1	FF L3	FF L14	FF H1	FF H3	FF H14
NM_019157.2	aquaporin 7 (AQP7)	5.04	20.27	11.21	3.55	17.07	10.41
NM_022960.1	aquaporin 9 (AQP9)	-1.93	-1.72	-1.69	-1.76	-1.80	-1.69
XM_575339.1	CD36 molecule (CD36)	3.83	5.45	1.59	3.78	5.16	1.93
NM_012556.1	fatty acid binding protein 1 (FABP1)	2.91	2.35	3.42	2.81	2.34	3.59
NM_024162.1	fatty acid binding protein 3 (FABP3)	3.55	45.26	59.58	3.25	47.67	91.05
NM_138502.1	monoglyceride lipase (MGLL)	3.75	4.98	3.34	2.90	4.29	3.86
NM_012859.1	lipase, hormone-sensitive (LIPE)	-	1.57	1.95	-	-	1.99
NM_012598.1	lipoprotein lipase (LPL)	-	-	40.56	-	-	60.03
XM_341960.2	patatin-like phospholipase domain containing 2 (PNPLA2)	2.36	2.19	2.78	2.17	1.93	2.54
NM_012820.1	acyl-CoA synthetase long-chain family member 1 (ACSL1)	2.81	2.30	2.70	2.63	2.30	2.66
NM_057107.1	acyl-CoA synthetase long-chain family member 3 (ACSL3)	3.65	4.58	3.77	4.33	5.42	4.22
NM_175837.1	cytochrome P450, family 4, subfamily A, polypeptide 11 (CYP4A11)	29.96	38.86	21.20	28.05	34.96	17.69
XM_575886.1	cytochrome P450, family 4, subfamily a, polypeptide 14 (Cyp4A14)	7.54	11.15	12.21	8.35	10.76	10.63
NM_053477.1	malonyl-CoA decarboxylase (MLYCD)	2.91	3.18	3.10	2.80	3.02	3.13
NM_031315.1	acyl-CoA thioesterase 1 (ACOT1)	266.20	163.83	51.25	271.11	161.81	55.08
NM_001007144.1	perilipin 2 (PLIN2)	1.90	1.84	1.88	1.89	1.84	2.04
NM_031118.1	sterol O-acyltransferase 1 (SOAT1)	-	-	1.81	-	-	1.79
NM_016987.1	ATP citrate lyase (ACLY)	-1.64	-3.06	-	-2.30	-5.04	-2.50
XM_216452.3	24-dehydrocholesterol reductase (DHCR24)	-	-2.03	-2.52	-	-2.63	-3.32
NM_017024.1	lecithin-cholesterol acyltransferase (LCAT)	-	-2.30	-	-1.61	-4.59	-2.33
NM_080886.1	sterol-C4-methyl oxidase-like (SC4MOL)	-	-2.20	-2.16	-	-3.71	-3.08
NM_024143.1	solute carrier family 27 (fatty acid transporter), member 5 (SLC27A5)	-1.74	-7.46	-29.30	-2.01	-10.90	-46.59

Access. No.	gene name and symbol	FF L1	FF L3	FF L14	FF H1	FF H3	FF H14
peroxisomal lipid metabolism							
NM_033352.1	ATP-binding cassette, sub-family D (ALD), member 2 (ABCD2)	-	-	-	-	-	2.03
NM_012804.1	ATP-binding cassette, sub-family D (ALD), member 3 (ABCD3)	-	1.87	1.69	-	1.63	1.81
NM_130756.2	acyl-CoA thioesterase 8 (ACOT8)	2.75	4.10	3.78	2.34	3.65	3.22
NM_053493.1	2-hydroxyacyl-CoA lyase 1 (HACL1)	3.95	3.89	7.01	3.19	2.88	5.06
XM_576485.1	acetyl-CoA acyltransferase 1 (ACAA1)	38.64	33.42	36.39	33.80	31.55	34.88
NM_017340.1	acyl-CoA oxidase 1 (ACOX1)	8.12	6.05	5.74	8.04	5.94	6.81
NM_171996.2	2,4-dienoyl CoA reductase 2 (DECR2)	3.29	3.69	3.35	3.01	3.39	3.15
NM_022594.1	enoyl CoA hydratase 1 (ECH1)	3.55	3.00	3.54	3.40	2.99	3.81
NM_001006966.1	peroxisomal D3,D2-enoyl-CoA isomerase (PECI)	3.37	3.55	2.39	3.32	3.57	2.57
mitochondrial lipid metabolism							
NM_130433.1	acetyl-CoA acyltransferase 2 (ACAA2)	3.01	2.74	2.98	3.25	2.58	2.91
NM_016986.1	acyl-CoA dehydrogenase, C-4 to C-12 straight chain (ACADM)	2.92	3.03	2.57	3.08	2.97	2.69
NM_012891.1	acyl-CoA dehydrogenase, very long chain (ACADVL)	2.01	2.47	2.32	2.06	2.59	2.51
NM_017075.1	acetyl-CoA acetyltransferase 1 (ACAT1)	4.54	7.71	8.14	3.88	6.28	7.12
NM_017306.3	dodecenoyl-CoA isomerase (DCI)	1.99	-	-	2.03	1.57	1.67
NM_057197.1	2,4-dienoyl CoA reductase 1 (DECR1)	2.17	2.13	2.09	1.98	1.94	2.05
NM_133618.1	hydroxyacyl-CoA dehydrogenase/3-ketoacyl-CoA thiolase/enoyl-CoA hydratase (trifunctional protein), beta subunit (HADHB)	1.90	2.32	2.01	1.93	2.34	2.30
NM_013200.1	carnitine palmitoyltransferase 1B (CPT1B)	5.26	13.11	15.53	4.57	14.60	15.09
NM_001004085.2	carnitine O-acetyltransferase (CRAT)	6.20	6.43	6.34	6.02	5.86	6.03
NM_031987.1	carnitine O-octanoyltransferase (CROT)	4.39	6.24	3.57	4.52	6.28	3.56

Access. No.	gene name and symbol	FF L1	FF L3	FF L14	FF H1	FF H3	FF H14
drug metabolism							
NM_012541.2	cytochrome P450, family 1, subfamily A, polypeptide 2 (CYP1A2)	-	-	-1.63	2.59	-	-
NM_019184.1	cytochrome P450, family 2, subfamily C, polypeptide 9 (CYP2C9)	-	-22.99	-25.73	-	-10.22	-18.81
XM_217906.3	cytochrome P450, family 2, subfamily C, polypeptide 18 (CYP2C18)	-	-	1.52	-	-	1.67
NM_031543.1	cytochrome P450, family 2, subfamily E, polypeptide 1 (CYP2E1)	1.89	4.45	5.45	3.83	5.57	3.43
NM_153312.2	cytochrome P450, family 3, subfamily A, polypeptide 4 (CYP3A4)	-	2.08	27.87	-	6.24	97.28
NM_019286.2	alcohol dehydrogenase 1C (class I), gamma polypeptide (ADH1C)	-	-	3.72	-	-	3.46
NM_012844.1	epoxide hydrolase 1 (EPHX1)	-	3.56	-	2.38	5.03	-
NM_022936.1	epoxide hydrolase 2 (EPHX2)	3.55	4.27	5.32	3.37	4.01	4.89
XM_579318.1	glutathione S-transferase alpha 3 (GSTA3)	-	2.29	-	1.81	3.60	-
NM_001010921.1	glutathione S-transferase alpha 5 (GSTA5)	-	1.96	4.00	-	5.19	8.58
NM_022407.3	aldehyde dehydrogenase 1 family, member A1 (ALDH1A1)	2.28	2.04	-	2.63	-	-
XM_214478.3	aldehyde dehydrogenase 5 family, member A1 (ALDH5A1)	-	2.44	2.33	-	-	1.75
NM_012683.1	UDP glucuronosyltransferase 1 family, polypeptide A1 (UGT1A1)	2.04	2.18	1.56	2.04	-	1.65
NM_001007718.2	sulfotransferase family 1E, member 1 (SULT1E1)	-	15.53	34.74	-	16.90	27.14
NM_012623.2	ATP-binding cassette, sub-family B, member 1B (Abcb1b, MDR1)	-	-2.32	-14.58	-	-	-7.66
NM_080581.1	ATP-binding cassette, sub-family C, member 3 (ABCC3, MRP3)	-1.93	-	-2.87	-	-	-1.73
NM_181381.2	ATP-binding cassette, sub-family G (WHITE), member 1 (ABCG2, BCRP)	1.76	1.79	-	1.78	-	-
NM_017047.1	solute carrier family 10, member 1 (SLC10A1, NTCP)	-	-	-	-1.97	-	-3.10
NM_053537.1	solute carrier family 22, member 7 (SLC22A7, OAT2)	-	-	2.74	-	-	2.51
NM_031650.1	solute carrier organic anion transporter family, member 1B3 (SLCO1B3, OATP8)	-	-	2.27	-	-	-

Access. No.	gene name and symbol	FF L1	FF L3	FF L14	FF H1	FF H3	FF H14
stress							
NM_012520.1	catalase (CAT)	2.45	3.13	2.29	2.18	-	-
NM_030826.2	glutathione peroxidase 1 (GPX1)	1.53	2.43	3.42	1.55	2.12	3.04
NM_012580.1	heme oxygenase (decycling) 1 (HMOX1)	-	1.90	-	-	2.77	-
NM_017051.2	superoxide dismutase 2 (SOD2)	-	1.69	-	-	2.00	-
NM_001008767.1	thioredoxin interacting protein (TXNIP)	7.98	-	-	7.10	-	-2.22
XM_577041.1	ferritin, light polypeptide (FTL)	-	2.05	-	1.53	2.25	1.71
NM_012815.2	glutamate-cysteine ligase, catalytic subunit (GCLC)	-1.57	-1.70	-	-	-1.52	-2.00
NM_012962.1	glutathione synthetase (GSS)	-	-1.77	-1.61	-	-	-1.63
energy metabolism							
NM_012879.1	solute carrier family 2, member 2 (GLUT2) (SLC2A2)	-	-3.09	-4.96	-	-4.11	-8.31
NM_012624.2	pyruvate kinase, liver and RBC (PKLR)	-3.23	-5.46	-2.85	-4.09	-9.83	-5.60
NM_012595.1	lactate dehydrogenase B (LDHB)	-	-2.32	-6.85	-	-2.59	-5.38
NM_207592.1	glucose-6-phosphate isomerase (GPI)	-	-	-	-	-	-2.08
XM_576370.1	triosephosphate isomerase 1 (TPI1)	1.51	2.02	-	-	2.13	-
XM_233688.3	hexose-6-phosphate dehydrogenase (glucose 1-dehydrogenase) (H6PD)	-	-	-	-	-1.54	-1.78
NM_031589.2	solute carrier family 37 (glucose-6-phosphate transporter), member 4 (SLC37A4)	-2.46	-2.86	-3.13	-3.21	-4.88	-6.23
NM_013098.1	glucose-6-phosphatase, catalytic subunit (G6PC)	-	-2.20	-	-	-4.83	-
NM_012744.2	pyruvate carboxylase (PC)	2.12	-	-	-	-	-
NM_198780.2	phosphoenolpyruvate carboxykinase 1 (soluble) (PCK1)	4.16	-	-	2.71	-	-
NM_053551.1	pyruvate dehydrogenase kinase, isozyme 4 (PDK4)	22.76	21.68	19.05	24.35	24.40	20.82
NM_024398.2	aconitase 2, mitochondrial (ACO2)	1.92	1.91	-	1.78	1.67	-
NM_053752.1	succinate-CoA ligase, alpha subunit (SUCLG1)	-	1.82	-	-	1.78	-
NM_031510.1	isocitrate dehydrogenase 1 (NADP+), soluble (IDH1)	-	1.73	-	-	1.62	-
NM_012600.1	malic enzyme 1, NADP(+)-dependent, cytosolic (ME1)	3.42	5.73	4.96	3.19	5.85	5.43

Access. No.	gene name and symbol	FF L1	FF L3	FF L14	FF H1	FF H3	FF H14
NM_022215.2	glycerol-3-phosphate dehydrogenase 1 (soluble) (GPD1)	-	1.80	3.12	-	1.55	2.61
NM_012736.1	glycerol-3-phosphate dehydrogenase 2 (mitochondrial) (GPD2)	3.87	3.33	3.58	2.88	2.37	2.47
NM_019269.1	solute carrier family 22 (organic cation/carnitine transporter), member 5 (SLC22A5)	3.89	4.25	3.18	3.80	4.42	2.92
NM_019354.1	uncoupling protein 2 (mitochondrial, proton carrier) (UCP2)	7.46	17.29	-	6.52	19.10	5.68
NM_017025.1	lactate dehydrogenase A (LDHA)	3.10	2.90	2.55	2.59	2.51	-
NM_013089.1	glycogen synthase 2 (liver) (GYS2)	-	-	-	-	-	-1.74
XM_341693.2	nudix (nucleoside diphosphate linked moiety X)-type motif 7 (NUDT7)	3.68	4.84	6.31	3.32	-	5.70
cell function							
XM_344194.2	interferon regulatory factor 6 (IRF6)	-1.65	-1.69	-3.31	-1.51	-	-2.87
NM_053373.1	peptidoglycan recognition protein 1 (PGLYRP1)	-	-2.91	-7.52	-	-2.82	-6.52
XM_341957.2	interferon induced transmembrane protein 3 (1-8U) (IFITM3)	-	-2.52	-15.01	-	-2.64	-11.77
NM_207604.1	toll-like receptor 6 (TLR6)	-2.29	-2.33	-2.19	-	-2.54	-2.06
NM_017020.1	interleukin 6 receptor (IL6R)	-1.97	-2.00	-1.72	-2.35	-2.42	-1.94
NM_012747.2	signal transducer and activator of transcription 3 (acute-phase response factor) (STAT3)	-1.58	-1.96	-3.01	-	-1.84	-2.54
NM_145672.3	chemokine (C-X-C motif) ligand 9 (CXCL9)	-	-	-	-	4.34	-
NM_182952.2	chemokine (C-X-C motif) ligand 11 (CXCL11)	-	-	-3.07	-	-	-3.75
XM_573130.1	chemokine (C-X-C motif) ligand 16 (CXCL16)	-3.07	-4.13	-15.49	-2.31	-2.83	-
NM_176074.2	complement component 6 (C6)	-	-2.10	-4.49	-	-2.81	-4.50
NM_172222.2	complement component 2 (C2)	-	-	-2.28	-	-	-2.21
NM_130409.1	complement factor H (CFH)	-1.66	-1.91	-2.27	-	-1.93	-1.93
NM_012898.2	alpha-2-HS-glycoprotein (AHSG)	-	-	-	-	-4.64	-2.63
NM_020071.1	fibrinogen beta chain (FGB)	-1.79	-2.36	-2.89	-	-2.71	-2.93
NM_012488.1	alpha-2-macroglobulin (A2M)	-	-	-2.55	-	-	-2.10
NM_017096.1	C-reactive protein, pentraxin-related (CRP)	-	-	-	-	1.74	1.63
NM_012681.1	transthyretin (TTR)	-	-1.68	-1.82	-	-2.05	-2.18

Access. No.	gene name and symbol	FF L1	FF L3	FF L14	FF H1	FF H3	FF H14
NM_172320.1	afamin (AFM)	1.52	2.09	2.79	-	1.69	1.62
NM_012725.1	kallikrein B, plasma (Fletcher factor) 1 (KLKB1)	-	-2.35	-1.78	-	-2.21	-1.53
NM_022519.2	serpin peptidase inhibitor, clade A (alpha-1 antiproteinase, antitrypsin), member 1 (SERPINA1)	-	-1.81	-1.54	-	-1.87	-1.55
XM_215303.3	major histocompatibility complex, class I, E (HLA-E)	-2.49	-4.34	-5.02	-2.94	-5.57	-5.82
NM_053487.1	peroxisomal biogenesis factor 11 alpha (PEX11A)	6.95	6.05	6.90	7.21	6.22	6.48
XM_213930.3	peroxisomal biogenesis factor 19 (PEX19)	2.90	3.20	2.39	2.33	2.99	2.65
XM_222831.3	coagulation factor V (proaccelerin, labile factor) (F5)	-	-2.88	-3.13	-	-4.26	-3.81
XM_346365.2	coagulation factor IX (F9)	-	-	-1.96	-	-	-2.29
XM_224872.3	coagulation factor XI (F11)	-2.27	-3.30	-1.62	-2.49	-3.48	-1.65
NM_031334.1	cadherin 1, type 1, E-cadherin (epithelial) (CDH1)	-2.36	-2.94	-5.78	-	-3.26	-4.80
NM_019143.1	fibronectin 1 (FN1)	-	-2.93	-10.43	-	-2.95	-8.91
NM_001004269.1	junctional adhesion molecule 3 (JAM3)	-	-1.81	-5.83	-	-	-4.22
NM_019156.1	vitronectin (VTN)	-	-2.89	-20.59	-	-4.63	-29.07
XM_213902.3	laminin, gamma 2 (LAMC2)	-	-	-3.77	-	-	-3.33
XM_243637.3	fibulin 1 (FBLN1)	-3.19	-2.83	-2.71	-2.89	-2.56	-2.42
NM_022298.1	tubulin, alpha 1a (TUBA1A)	-	-	-31.65	-	-	-17.85
XM_238167.3	filamin A, alpha (FLNA)	-	-	-9.96	-	-	-5.89
NM_031140.1	vimentin (VIM)	-2.82	-7.53	-48.09	-2.09	-5.70	-31.31
NM_012504.1	ATPase, Na+/K+ transporting, alpha 1 polypeptide (ATP1A1)	-	-1.69	-2.32	-	-1.60	-2.54
NM_012942.1	cytochrome P450, family 7, subfamily A, polypeptide 1 (CYP7A1)	-5.71	-3.98	-8.99	-4.47	-	-
XM_341151.2	retinoid X receptor, gamma (RXRG)	2.25	2.79	2.77	2.09	2.33	2.26
NM_022941.2	nuclear receptor subfamily 1, group I, member 3 (NR1I3)	-	-	2.01	-	1.73	-
growth, proliferation, cell death							
NM_013132.1	annexin A5 (ANXA5)	-	-1.53	-6.76	-	-	-2.99
XM_576514.1	serum response factor (c-fos serum response element-binding transcription factor) (SRF)	-	-	-1.78	-	-	-1.67

Access. No.	gene name and symbol	FF L1	FF L3	FF L14	FF H1	FF H3	FF H14
NM_022266.1	connective tissue growth factor (CTGF)	-	-45.41	-146.28	-9.16	-53.21	-95.46
NM_012551.1	early growth response 1 (EGR1)	-	-	-3.17	-	-	-2.76
XM_341981.2	polymerase (DNA-directed), delta 4 (POLD4)	-	-1.66	-1.94	-	-1.69	-
XM_341386.2	topoisomerase (DNA) II beta 180kDa (TOP2B)	-	-	-1.61	-	-	-1.56
NM_012671.1	transforming growth factor, alpha (TGFA)	-	-	-2.20	-	-	-1.92
NM_031131.1	transforming growth factor, beta 2 (TGFB2)	-	-	-6.00	-	-	-4.62
XM_216492.3	cAMP responsive element binding protein 3 (CREB3)	-	-	-	-	-	-1.76
NM_012842.1	epidermal growth factor (EGF)	-	-1.76	-1.81	-	-1.93	-1.95
NM_024148.1	APEX nuclease (multifunctional DNA repair enzyme) 1 (APEX1)	-	1.75	-	-	2.12	-
NM_024127.1	growth arrest and DNA-damage-inducible, alpha (GADD45A)	-	1.96	-	-	2.46	-
NM_012861.1	O-6-methylguanine-DNA methyltransferase (MGMT)	-	-	-2.31	-	-	-
XM_214477.2	geminin, DNA replication inhibitor (GMNN)	1.65	-	-	1.72	1.68	-
NM_171992.2	cyclin D1 (CCND1)	-	-	-2.67	-	-	-2.39
XM_342632.2	cyclin-dependent kinase 14 (CDK14)	-	-	-4.01	-	-	-
NM_012923.1	cyclin G1 (CCNG1)	-	-	-2.95	-	-	-
NM_012524.1	CCAAT/enhancer binding protein (C/EBP), alpha (CEBPA)	-	-	1.71	-	-	1.65
NM_139087.1	cell growth regulator with EF-hand domain 1 (CGREF1)	-	-1.77	-2.37	-	-1.65	-2.30
XM_574454.1	growth arrest-specific 2 (GAS2)	-	-	-1.88	-	-1.62	-2.04
NM_053812.1	BCL2-antagonist/killer 1 (BAK1)	-	-	-3.18	-	-	-2.60
NM_017059.1	BCL2-associated X protein (BAX)	-	-	-1.50	-	-	-
NM_017312.2	BCL2-related ovarian killer (BOK)	-	-	-3.34	-	-	-3.13
XM_214551.3	cell death-inducing DFFA-like effector a (CIDEA)	-	-	3.75	2.34	4.12	3.82
NM_012935.2	crystallin, alpha B (CRYAB)	-	-2.94	-20.72	-	-2.66	-14.78
NM_022526.1	death-associated protein (DAP)	-	-1.86	-4.30	-	-	-
NM_139194.1	Fas (TNF receptor superfamily, member 6) (FAS)	-	-	-1.87	-	-	-1.83
NM_181086.2	tumor necrosis factor receptor superfamily, member 12A (TNFRSF12A)	-	-	-4.31	-	-	-2.57
XM_575700.1	BCL2-like 14 (apoptosis facilitator) (BCL2L14)	-	-	2.12	-	2.70	2.86

Access. No.	gene name and symbol	FF L1	FF L3	FF L14	FF H1	FF H3	FF H14
NM_021835.2	jun proto-oncogene (JUN)	-	-	-2.66	-	-	-2.60
NM_133571.1	cell division cycle 25 homolog A (S. pombe) (CDC25A)	2.31	2.15	1.54	2.26	2.12	1.54
NM_012603.2	v-myc myelocytomatosis viral oncogene homolog (avian) (MYC)	-	-	-2.43	-	-	-
XM_342470.2	apoptosis inhibitor 5 (API5)	-	-	-1.76	-	-	-1.61
NM_033230.1	v-akt murine thymoma viral oncogene homolog 1 (AKT1)	-	-	-1.85	-	-	-1.52
NM_001007732.1	serpin peptidase inhibitor, clade B (ovalbumin), member 9 (SERPINB9)	-	-	-12.52	-	-	-7.22
NM_131914.2	caveolin 2 (CAV2)	-	-	-4.32	-	-	-4.30
NM_001009632.1	G0/G1switch 2 (G0S2)	1.86	4.38	10.96	1.79	3.96	8.02
NM_134432.2	angiotensinogen (serpin peptidase inhibitor, clade A, member 8) (AGT)	-	1.90	1.62	-	-	-
NM_012649.1	syndecan 4 (SDC4)	-1.54	-1.83	-1.61	-	-1.82	-1.84
XM_343604.2	serpin peptidase inhibitor, clade E (nexin, plasminogen activator inhibitor type 1), member 2 (SERPINE2)	2.12	7.89	13.28	2.09	7.56	12.76

Table 7.5: Genes deregulated by Rosiglitazone.

The table contains the the gene assession numbers, the gene names and symbols as well as the fold changes of genes deregulated with $p < 0.05$. Grayed out numbers: BH $Q \leq 0.2$, Rosi: Rosiglitazone, H: high dose, 1/3/14: treatment day 1/3/14.

Access. No.	gene name and symbol	Rosi H1	Rosi H3	Rosi H14
lipid metabolism				
NM_080576.1	apolipoprotein A-V (APOA5)	-2.94	-3.82	-2.11
XM_243524.3	low density lipoprotein receptor-related protein 1 (LRP1)	-	1.69	1.56
NM_013155.1	very low density lipoprotein receptor (VLDLR)	-	5.03	3.75
NM_012598.1	lipoprotein lipase (LPL)	-	-	3.61
NM_138502.1	monoglyceride lipase (MGLL)	1.51	2.07	1.85
NM_019157.2	aquaporin 7 (AQP7)	-	4.88	6.40

Access. No.	gene name and symbol	Rosi H1	Rosi H3	Rosi H14
XM_575339.1	CD36 molecule (thrombospondin receptor) (CD36)	-	2.26	1.52
NM_012556.1	fatty acid binding protein 1, liver (FABP1)	1.68	2.14	2.81
NM_053477.1	malonyl-CoA decarboxylase (MLYCD)	1.82	2.00	2.14
NM_031315.1	acyl-CoA thioesterase 1 (Acot1)	20.98	91.35	38.81
NM_012820.1	acyl-CoA synthetase long-chain family member 1 (ACSL1)	2.21	2.31	2.35
NM_175837.1	cytochrome P450, family 4, subfamily A, polypeptide 11 (CYP4A11)	3.03	12.22	7.38
XM_575886.1	cytochrome P450, family 4, subfamily a, polypeptide 14 (Cyp4a14)	2.77	5.24	5.08
XM_230827.3	fat storage-inducing transmembrane protein 2 (FITM2)	2.09	2.13	2.00
NM_001007144.1	perilipin 2 (PLIN2)	1.82	1.84	-
NM_080886.1	sterol-C4-methyl oxidase-like (SC4MOL)	-	-1.72	-1.91
NM_017274.1	glycerol-3-phosphate acyltransferase, mitochondrial (GPAM)	1.73	2.28	-
NM_031841.1	stearoyl-Coenzyme A desaturase 2 (Scd2)	3.07	7.74	2.57
NM_024143.1	solute carrier family 27 (fatty acid transporter), member 5 (SLC27A5)	-1.73	-4.63	-7.24
peroxisomal lipid metabolism				
NM_012804.1	ATP-binding cassette, sub-family D (ALD), member 3 (ABCD3)	-	1.61	1.84
XM_576485.1	acetyl-CoA acyltransferase 1 (ACAA1)	10.67	21.14	19.75
NM_130756.2	acyl-CoA thioesterase 8 (ACOT8)	-	2.35	1.71
NM_017340.1	acyl-CoA oxidase 1, palmitoyl (ACOX1)	2.46	3.94	3.91
NM_171996.2	2,4-dienoyl CoA reductase 2, peroxisomal (DECR2)	-	2.86	2.30
NM_022594.1	enoyl CoA hydratase 1, peroxisomal (ECH1)	-	2.30	2.51
NM_053493.1	2-hydroxyacyl-CoA lyase 1 (HACL1)	1.81	2.29	2.86
NM_001006966.1	peroxisomal D3,D2-enoyl-CoA isomerase (PECI)	2.11	2.12	-
mitochondrial lipid metabolism				
NM_013200.1	carnitine palmitoyltransferase 1B (muscle) (CPT1B)	-	4.00	4.79
NM_001004085.2	carnitine O-acetyltransferase (CRAT)	2.85	3.29	3.25
NM_031987.1	carnitine O-octanoyltransferase (CROT)	-	1.87	1.54

Access. No.	gene name and symbol	Rosi H1	Rosi H3	Rosi H14
NM_130433.1	acetyl-CoA acyltransferase 2 (ACAA2)	1.80	1.88	1.84
NM_016986.1	acyl-CoA dehydrogenase, C-4 to C-12 straight chain (ACADM)	1.65	2.18	1.96
NM_017075.1	acetyl-CoA acetyltransferase 1 (ACAT1)	1.73	2.94	2.57
NM_017306.3	dodecenoyl-CoA isomerase (DCI)	1.66	1.63	1.50
NM_057197.1	2,4-dienoyl CoA reductase 1, mitochondrial (DECR1)	-	1.73	1.57
NM_057186.1	hydroxyacyl-CoA dehydrogenase (HADH)	1.96	2.38	1.78
drug metabolism				
NM_012540.2	cytochrome P450, family 1, subfamily A, polypeptide 1 (CYP1A1)	3.01	3.50	-
NM_173294.1	cytochrome P450, family 2, subfamily b, polypeptide 9 (Cyp2b9)	-	-	3.08
NM_019184.1	cytochrome P450, family 2, subfamily C, polypeptide 9 (CYP2C9)	-	-3.19	-5.64
XM_217906.3	cytochrome P450, family 2, subfamily C, polypeptide 18 (CYP2C18)	1.88	-	1.82
XM_215255.3	cytochrome P450, family 2, subfamily C, polypeptide 19 (CYP2C19)	-	-	2.24
NM_031543.1	cytochrome P450, family 2, subfamily E, polypeptide 1 (CYP2E1)	-	-1.69	-2.32
NM_153312.2	cytochrome P450, family 3, subfamily A, polypeptide 4 (CYP3A4)	6.13	4.78	30.76
NM_022407.3	aldehyde dehydrogenase 1 family, member A1 (ALDH1A1)	1.58	1.68	-
NM_012844.1	epoxide hydrolase 1, microsomal (xenobiotic) (EPHX1)	2.65	2.81	1.52
NM_022936.1	epoxide hydrolase 2, cytoplasmic (EPHX2)	1.73	3.10	2.75
XM_579318.1	glutathione S-transferase alpha 3 (GSTA3)	1.60	3.12	2.00
NM_001010921.1	glutathione S-transferase alpha 5 (GSTA5)	4.10	5.65	6.85
NM_001007718.2	sulfotransferase family 1E, estrogen-preferring, member 1 (SULT1E1)	-	2.27	5.53
NM_012683.1	UDP glucuronosyltransferase 1 family, polypeptide A1 (UGT1A1)	1.79	1.78	-
NM_130407.1	UDP glucuronosyltransferase 1 family, polypeptide A7C (Ugt1a7c)	1.79	1.72	-
NM_012623.2	ATP-binding cassette, sub-family B (MDR/TAP), member 1B (Abcb1b, MDR1)	-	-2.70	-2.92
NM_031650.1	solute carrier organic anion transporter family, member 1B3 (SLCO1B3, OATP8)	-	-	2.21
NM_053537.1	solute carrier family 22 (organic anion transporter), member 7 (SLC22A7, OAT2)	-	-	2.25
stress				
NM_012520.1	catalase (CAT)	-	2.44	-

Access. No.	gene name and symbol	Rosi H1	Rosi H3	Rosi H14
NM_030826.2	glutathione peroxidase 1 (GPX1)	-	1.56	2.20
NM_053906.1	glutathione reductase (GSR)	2.15	1.57	-
NM_012580.1	heme oxygenase (decycling) 1 (HMOX1)	3.50	2.88	-
NM_017051.2	superoxide dismutase 2, mitochondrial (SOD2)	-	1.51	-
NM_001008767.1	thioredoxin interacting protein (TXNIP)	2.27	1.90	-
XM_215293.3	vanin 1 (VNN1)	-	2.17	1.80
XM_576192.1	ferritin, light polypeptide (FTL)	1.72	1.99	-
energymetabolism				
NM_012879.1	solute carrier family 2 (facilitated glucose transporter), member 2 (SLC2A2)	-	-1.71	-
NM_012565.1	glucokinase (hexokinase 4) (GCK)	-	1.55	-
NM_013190.2	phosphofructokinase, liver (PFKL)	-	2.08	-
NM_053291.2	phosphoglycerate kinase 1 (PGK1)	-	1.87	-
NM_012595.1	lactate dehydrogenase B (LDHB)	-	-2.09	-2.07
XM_576370.1	triosephosphate isomerase 1 (TPI1)	-	2.32	-
NM_012495.1	aldolase A, fructose-bisphosphate (ALDOA)	1.66	1.74	-
NM_012554.1	enolase 1, (alpha) (ENO1)	-	1.70	-
NM_013098.1	glucose-6-phosphatase, catalytic subunit (G6PC)	-	-1.70	-
NM_012744.2	pyruvate carboxylase (PC)	-	2.53	-
NM_198780.2	phosphoenolpyruvate carboxykinase 1 (soluble) (PCK1)	2.65	-1.79	-
NM_031589.2	solute carrier family 37 (glucose-6-phosphate transporter), member 4 (SLC37A4)	-1.96	-	-2.52
NM_053551.1	pyruvate dehydrogenase kinase, isozyme 4 (PDK4)	3.58	3.48	6.29
NM_012600.1	malic enzyme 1, NADP(+)-dependent, cytosolic (ME1)	1.79	5.02	2.89
NM_012736.1	glycerol-3-phosphate dehydrogenase 2 (mitochondrial) (GPD2)	2.08	2.88	1.97
NM_019269.1	solute carrier family 22 (organic cation/carnitine transporter), member 5 (SLC22A5)	1.69	2.21	1.69
NM_019354.1	uncoupling protein 2 (mitochondrial, proton carrier) (UCP2)	2.52	3.67	-
XM_576370.1	triosephosphate isomerase 1 (TPI1)	-	2.32	-
NM_017025.1	lactate dehydrogenase A (LDHA)	1.98	2.88	2.05
XM_341693.2	nudix (nucleoside diphosphate linked moiety X)-type motif 7 (NUDT7)	-	2.41	2.99

Access. No.	gene name and symbol	Rosi H1	Rosi H3	Rosi H14
cell function				
NM_017020.1	interleukin 6 receptor (IL6R)	-1.93	-	-1.62
NM_012747.2	signal transducer and activator of transcription 3 (acute-phase response factor) (STAT3)	-	-1.53	-1.52
NM_207604.1	toll-like receptor 6 (TLR6)	-1.81	-1.84	-1.83
XM_341957.2	interferon induced transmembrane protein 3 (1-8U) (IFITM3)	-	-1.83	-4.47
NM_145672.3	chemokine (C-X-C motif) ligand 9 (CXCL9)	1.54	2.71	1.97
NM_182952.2	chemokine (C-X-C motif) ligand 11 (CXCL11)	-1.53	-	-1.59
XM_573130.1	chemokine (C-X-C motif) ligand 16 (CXCL16)	-1.57	-3.00	-2.41
NM_176074.2	complement component 6 (C6)	-	-1.70	-1.91
NM_130409.1	complement factor H (CFH)	-	-	-1.50
NM_024157.1	complement factor I (CFI)	-	-	-1.82
XM_215303.3	major histocompatibility complex, class I, E (HLA-E)	-2.06	-1.93	-2.08
NM_012488.1	alpha-2-macroglobulin (A2M)	-	-	-2.04
NM_022519.2	serpin peptidase inhibitor, clade A (alpha-1 antiproteinase, antitrypsin), member 1 (SERPINA1)	-	-	-1.61
NM_020071.1	fibrinogen beta chain (FGB)	-	-	-1.74
NM_053373.1	peptidoglycan recognition protein 1 (PGLYRP1)	-1.94	-2.61	-5.65
NM_172320.1	afamin (AFM)	-	1.71	2.06
NM_053487.1	peroxisomal biogenesis factor 11 alpha (PEX11A)	2.67	3.33	2.62
XM_213930.3	peroxisomal biogenesis factor 19 (PEX19)	-	1.96	1.87
XM_222831.3	coagulation factor V (proaccelerin, labile factor) (F5)	-1.64	-1.95	-1.95
XM_346365.2	coagulation factor IX (F9)	-1.53	-	-1.95
NM_031753.1	activated leukocyte cell adhesion molecule (ALCAM)	-1.66	-2.31	-3.14
NM_031334.1	cadherin 1, type 1, E-cadherin (epithelial) (CDH1)	-1.75	-1.92	-2.13
NM_019143.1	fibronectin 1 (FN1)	-1.51	-2.20	-3.10
NM_001001505.1	hyaluronan binding protein 2 (HABP2)	-	-2.68	-3.17
NM_012967.1	intercellular adhesion molecule 1 (ICAM1)	-	-	-1.58
NM_001004269.1	junctional adhesion molecule 3 (JAM3)	-	-1.86	-2.81
XM_213902.3	laminin, gamma 2 (LAMC2)	-	-	-2.56
NM_019156.1	vitronectin (VTN)	-	-	-3.15

Access. No.	gene name and symbol	Rosi H1	Rosi H3	Rosi H14
XM_238167.3	filamin A, alpha (FLNA)	-	-1.58	-3.32
NM_013044.2	tropomodulin 1 (TMOD1)	-1.71	-2.45	-3.49
NM_022298.1	tubulin, alpha 1a (TUBA1A)	-	-2.16	-7.23
NM_031140.1	vimentin (VIM)	-	-	-4.47
NM_012504.1	ATPase, Na+/K+ transporting, alpha 1 polypeptide (ATP1A1)	-	-1.64	-1.76
NM_012942.1	cytochrome P450, family 7, subfamily A, polypeptide 1 (CYP7A1)	-	-2.16	-
XM_341151.2	retinoid X receptor, gamma (RXRG)	-	2.73	2.27
growth, proliferation, cell death				
NM_013132.1	annexin A5 (ANXA5)	-	-	-1.61
NM_013144.1	insulin-like growth factor binding protein 1 (IGFBP1)	-1.79	-1.94	-1.85
XM_576514.1	serum response factor (c-fos serum response element-binding transcription factor) (SRF)	-	-	-1.57
NM_022266.1	connective tissue growth factor (CTGF)	-5.37	-14.78	-7.46
NM_012671.1	transforming growth factor, alpha (TGFA)	-	-	-1.89
XM_341981.2	polymerase (DNA-directed), delta 4 (POLD4)	-	-	-1.54
NM_012861.1	O-6-methylguanine-DNA methyltransferase (MGMT)	-	-	-1.63
NM_012923.1	cyclin G1 (CCNG1)	-	-	-2.27
NM_080782.2	cyclin-dependent kinase inhibitor 1A (p21, Cip1) (CDKN1A)	-	-	-1.53
NM_031762.2	cyclin-dependent kinase inhibitor 1B (p27, Kip1) (CDKN1B)	-	-	-1.65
NM_171992.2	cyclin D1 (CCND1)	2.26	-	-
NM_053453.1	regulator of G-protein signaling 2, 24kDa (RGS2)	-	-2.48	-12.03
NM_012801.1	platelet-derived growth factor alpha polypeptide (PDGFA)	-	-1.53	-1.72
NM_053812.1	BCL2-antagonist/killer 1 (BAK1)	-	-	-1.59
NM_053420.2	BCL2/adenovirus E1B 19kDa interacting protein 3 (BNIP3)	-	2.39	-
NM_017312.2	BCL2-related ovarian killer (BOK)	-	-	-1.84
XM_214551.3	cell death-inducing DFFA-like effector a (CIDEA)	-	2.28	2.21
NM_012935.2	crystallin, alpha B (CRYAB)	-	-2.31	-2.25
XM_225138.3	death-associated protein kinase 1 (DAPK1)	3.39	3.00	1.74

Access. No.	gene name and symbol	Rosi H1	Rosi H3	Rosi H14
NM_139194.1	Fas (TNF receptor superfamily, member 6) (FAS)	-	-	-1.54
NM_181086.2	tumor necrosis factor receptor superfamily, member 12A (TNFRSF12A)	-	-	-1.64
XM_575700.1	BCL2-like 14 (apoptosis facilitator) (BCL2L14)	-	1.59	1.79
NM_133571.1	cell division cycle 25 homolog A (S. pombe) (CDC25A)	1.51	1.72	-
NM_021835.2	jun proto-oncogene (JUN)	-1.51	-	-1.65
NM_012603.2	v-myc myelocytomatosis viral oncogene homolog (avian) (MYC)	-	-	-1.82
NM_212505.1	immediate early response 3 (IER3)	-	-	-2.79
NM_001007732.1	serpin peptidase inhibitor, clade B (ovalbumin), member 9 (SERPINB9)	-	-	-1.89
NM_134432.2	angiotensinogen (AGT)	-	1.88	-
NM_012649.1	syndecan 4 (SDC4)	-	-	-1.50
XM_343604.2	serpin peptidase inhibitor, clade E member 2 (SERPINE2)	-	1.94	4.24
NM_001009632.1	G0/G1switch 2 (G0S2)	-	4.23	4.57

Table 7.6: Genes deregulated by Troglitazone.
The table contains the gene assession numbers, the gene names and symbols, as well as the fold changes of genes deregulated with $p < 0.05$. Grayed out numbers: BH Q ≤ 0.2, Tro: Troglitazone, H: high dose, 3/14: treatment day 3/14.

Access. No.	gene name and symbol	Tro H3	Tro H14
lipid metabolism			
NM_080576.1	apolipoprotein A-V (APOA5)	-2.11	-
NM_013155.1	very low density lipoprotein receptor (VLDLR)	3.27	-
XM_243524.3	low density lipoprotein receptor-related protein 1 (LRP1)	1.63	1.56
NM_019157.2	aquaporin 7 (AQP7)	3.81	3.93
NM_012556.1	fatty acid binding protein 1, liver (FABP1)	1.99	2.12
XM_575339.1	CD36 molecule (thrombospondin receptor) (CD36)	2.06	-
NM_138502.1	monoglyceride lipase (MGLL)	1.94	1.54
NM_053477.1	malonyl-CoA decarboxylase (MLYCD)	1.84	1.63

Access. No.	gene name and symbol	Tro H3	Tro H14
NM_031315.1	acyl-CoA thioesterase 1 (ACOT1)	53.19	18.33
NM_012820.1	acyl-CoA synthetase long-chain family member 1 (ACSL1)	2.17	1.88
NM_175837.1	cytochrome P450, family 4, subfamily A, polypeptide 11 (CYP4A11)	7.37	2.73
XM_575886.1	cytochrome P450, family 4, subfamily a, polypeptide 14 (CYP4A14)	3.66	2.76
XM_230827.3	fat storage-inducing transmembrane protein 2 (FITM2)	2.19	-
NM_001007144.1	perilipin 2 (PLIN2)	1.65	-
NM_080886.1	sterol-C4-methyl oxidase-like (SC4MOL)	-1.59	-
peroxisomal lipid metabilism			
NM_012804.1	ATP-binding cassette, sub-family D (ALD), member 3 (ABCD3)	1.62	-
XM_576485.1	acetyl-CoA acyltransferase 1 (ACAA1)	15.72	14.86
NM_171996.2	2,4-dienoyl CoA reductase 2, peroxisomal (DECR2)	2.15	1.68
NM_053493.1	2-hydroxyacyl-CoA lyase 1 (HACL1)	2.62	-
NM_022594.1	enoyl CoA hydratase 1, peroxisomal (ECH1)	1.93	-
NM_001006966.1	peroxisomal D3,D2-enoyl-CoA isomerase (PECI)	1.98	-
NM_017340.1	acyl-CoA oxidase 1, palmitoyl (ACOX1)	3.30	2.96
mitochondrial lipid metabolism			
NM_013200.1	carnitine palmitoyltransferase 1B (muscle) (CPT1B)	2.83	-
NM_001004085.2	carnitine O-acetyltransferase (CRAT)	2.82	-
NM_031987.1	carnitine O-octanoyltransferase (CROT)	1.82	-
NM_130433.1	acetyl-CoA acyltransferase 2 (ACAA2)	1.87	-
NM_057186.1	hydroxyacyl-CoA dehydrogenase (HADH)	2.09	-
NM_133618.1	hydroxyacyl-CoA dehydrogenase/3-ketoacyl-CoA thiolase/enoyl-CoA hydratase (trifunctional protein), beta subunit (HADHB)	1.77	-
NM_016986.1	acyl-CoA dehydrogenase, C-4 to C-12 straight chain (ACADM)	1.92	1.61
NM_017075.1	acetyl-CoA acetyltransferase 1 (ACAT1)	2.01	1.54
NM_012891.1	acyl-CoA dehydrogenase, very long chain (ACADVL)	1.54	-
NM_017306.3	dodecenoyl-CoA isomerase (DCI)	1.59	-

Access. No.	gene name and symbol	Tro H3	Tro H14
drug metabolism			
NM_019363.2	aldehyd oxidase (AOX1)	1.95	-
NM_022407.3	aldehyddehydrogenase 1 family member A1 (ALDH1A1)	1.62	-
NM_019184.1	cytochrome P450, family 2, subfamily C, polypeptide 9 (CYP2C9)	-2.71	
NM_153312.2	cytochrome P450, family 3, subfamily A, polypeptide 4 (CYP3A4)	8.24	39.08
NM_012844.1	epoxide hydrolase 1, microsomal (xenobiotic) (EPHX1)	2.09	1.67
NM_022936.1	epoxide hydrolase 2 (EPHX2)	2.65	-
NM_001010921.1	glutathione S-transferase alpha 5 (GSTA5)	4.81	12.38
NM_181371.2	glutathione S-transferase kappa 1 (GSTK1)	1.84	1.69
NM_177426.1	glutathione S-transferase mu 1 (GSTM1)	-1.66	-
XM_341791.2	sulfotransferase family 2A, dehydroepiandrosterone (DHEA)-preferring, member 6 (Sult2a6)	1.55	3.77
NM_001007718.2	sulfotransferase family 1E, estrogen-preferring, member 1 (SULT1E1)	3.18	-
NM_012683.1	UDP glucuronosyltransferase 1 family, polypeptide A1 (UGT1A1)	1.56	-
NM_130407.1	UDP glucuronosyltransferase 1 family, polypeptide A7C (Ugt1a7c)	1.58	-
NM_173295.1	UDP glucuronosyltransferase 2 family, polypeptide B4 (UGT2B4)	-	1.64
XM_223299.3	UDP glucuronosyltransferase 2 family, polypeptide B10 (UGT2B10)	-	1.53
NM_031650.1	solute carrier organic anion transporter family, member 1B3 (SLCO1B3, OATP8)	-	1.54
NM_022287.1	solute carrier falily 26 (sulfate transporter), member 1 (SLC26A1)	-1.56	-
stress			
NM_030826.2	glutathione peroxidase 1 (GPX1)	1.63	1.71
XM_574282.1	vanin 2 (VNN2)	1.64	1.73
NM_001008767.1	thioredoxin interacting protein (TXNIP)	1.84	-
NM_012520.1	catalase (CAT)	1.89	-
XM_577041.1	ferritin, light polypeptide (FTL)	1.68	-
energy production			
NM_013190.2	phosphofructokinase (PFKL)	1.89	-
NM_012624.2	pyruvate kinase, liver and RBC (PKLR)	-1.78	-

Access. No.	gene name and symbol	Tro H3	Tro H14
NM_012595.1	lactate dehydrogenase B (LDHB)	-1.52	1.59
NM_053291.2	phosphoglycerate kinase 1 (PGK1)	1.74	-
XM_576370.1	triosephosphate isomerase (TPI1)	1.93	-
NM_012554.1	enolase 1, (alpha) (ENO1)	1.50	-
NM_012744.2	pyruvate carboxylase (PC)	2.20	-
XM_341319.2	phosphoenolpyruvate carboxykinase 2 (PEPCK) (PCK2)	1.60	-
NM_001008282.1	galactokinase 1 (GALK1)	1.66	-
XM_216372.3	galactose-1-phosphate uridylyltransferase (GALT)	1.51	-
NM_053551.1	pyruvate dehydrogenase kinase, isozyme 4 (PDK4)	3.21	3.78
NM_012736.1	glycerol-3-phosphate dehydrogenase 2 (mitochondrial) (GPD2)	1.89	-
NM_019269.1	solute carrier family 22 (organic cation/carnitine transporter), member 5 (SLC22A5)	1.88	-
NM_012600.1	malic enzyme, NADP(+) dependent, cytosolic (ME1)	2.78	1.83
NM_019354.1	uncoupling protein 2 (mitochondrial, proton carrier) (UCP2)	3.27	-
NM_017025.1	lactate dehydrogenase A (LDHA)	2.31	-1.52
XM_341693.2	nudix (nucleoside diphosphate linked moiety X)-type motif 7 (NUDT7)	2.14	2.06
cell function			
NM_031531.1	serpin peptidase inhibitor, clade A (alpha-1 antiproteinase, antitrypsin), member 3 (SERPINA3)	-1.87	-
XM_341957.2	interferon induced transmembrane protein 3 (IFITM3)	-1.74	-
NM_207604.1	toll-like receptor 6 (TLR6)	-1.58	-
NM_030845.1	chemokine (C-X-C motif) ligand 2 (CXCL2)	-2.00	-
NM_022177.2	chemokine (C-X-C motif) ligand 12 (CXCL12)	1.92	-
NM_145672.3	chemokine (C-X-C motif) ligand 9 (CXCL9)	-	2.09
NM_017096.1	C-reactive protein, pentraxin-related (CRP)	-	1.52
NM_012516.1	complement component 4 binding protein, beta (C4BPB)	-1.79	-
NM_172320.1	afamin (AFM)	1.85	-
XM_215303.3	major histocompatibility complex, class I, E (HLA-E)	-1.87	-
NM_176074.2	complement component 6 (C6)	-1.71	-

Access. No.	gene name and symbol	Tro H3	Tro H14
NM_053487.1	peroxisomal biogenesis factor 11 alpha (PEX11A)	1.82	2.56
XM_213930.3	peroxisomal biogenesis factor 19 (PEX19)	1.82	-
NM_013044.2	tropomodulin 1 (TMOD1)	-1.81	-2.24
NM_022298.1	tubulin, alpha 1a (TUBA1A)	-2.07	-
NM_019143.1	fibronectin 1 (FN1)	-1.59	-
NM_031334.1	cadherin 1, type 1, E-cadherin (epithelial) (CDH1)	-1.57	-
NM_031699.1	claudin 1 (CLDN1)	-	-1.65
XM_224872.3	coagulation factor XI (F11)	-1.68	-
XM_341151.2	retinoid X receptor, gamma (RXRG)	2.21	-
growth, proliferation, cell death			
NM_022266.1	connective tissue growth factor (CTGF)	-4.49	-
NM_012861.1	O-6-methylguanine-DNA methyltransferase (MGMT)	-	-1.54
XM_214551.3	cell death-inducing DFFA-like effector a (CIDEA)	2.13	-
XM_575700.1	BCL2-like 14 (BCL2L14)	-	1.79
NM_139194.1	Fas (TNF receptor superfamily, member 6) (FAS)	-	-1.59
NM_181086.2	tumor necrosis factor receptor superfamily, member 12A (TNFRSF12A)	-1.55	-
NM_133571.1	cell division cycle 25 homolog A (S. pombe) (CDC25A)	1.61	-
NM_053458.1	RAB9A, member RAS oncogen family (RAB9A)	1.64	-
NM_001007732.1	serpin peptidase inhibitor, clade B (ovalbumin), member 9 (SERPINB9)	-1.59	-
NM_012551.1	early growth response 1 (EGR1)	-2.06	-
XM_341386.2	topoisomerase (TOP2B)	-	-1.53
XM_343604.2	serpin peptidase inhibitor, clade E (SERPINE2)	1.68	-
NM_134432.2	angiotensinogen (AGT)	1.69	-
NM_001009632.1	G0/G1switch 2 (G0S2)	2.87	-

Table 7.7: Genes deregulated by EMD335823.
The table contains the gene assession numbers, the gene names and symbols, as well as the fold changes of genes deregulated with $p < 0.05$. Grayed out numbers: BH Q ≤ 0.2, EMD: EMD335823, H: high dose, 1/3/14: treatment day 1/3/14,

Access. No.	gene name and symbol	EMD H1	EMD H3	EMD H14
lipid metabolism				
NM_080576.1	apolipoprotein A-V (APOA5)	-3.48	-11.26	-6.37
XM_214872.2	apolipoprotein C-II (APOC2)	-	-2.64	-2.59
NM_013155.1	very low density lipoprotein receptor (VLDLR)	-	5.39	5.22
NM_175762.2	low density lipoprotein receptor (LDLR)	-	-1.68	-1.73
NM_053541.1	low density lipoprotein receptor-related protein 3 (LRP3)	-	-1.61	-1.92
NM_032616.1	lipolysis stimulated lipoprotein receptor (LSR)	-	-1.58	-1.66
NM_012597.2	lipase, hepatic (LIPC)	-	-1.52	-3.14
NM_012598.1	lipoprotein lipase (LPL)	-	-	6.87
NM_019157.2	aquaporin 7 (AQP7)	-	3.72	2.87
XM_575339.1	CD36 molecule (thrombospondin receptor) (CD36)	1.84	1.81	-
NM_012556.1	fatty acid binding protein 1, liver (FABP1)	1.57	1.75	2.45
NM_031315.1	acyl-CoA thioesterase 1 (Acot1)	19.31	90.77	29.98
NM_012820.1	acyl-CoA synthetase long-chain family member 1 (ACSL1)	2.26	2.14	2.20
NM_175837.1	cytochrome P450, family 4, subfamily A, polypeptide 11 (CYP4A11)	8.80	14.85	4.95
XM_575886.1	cytochrome P450, family 4, subfamily a, polypeptide 14 (Cyp4a14)	4.13	4.79	3.46
XM_230827.3	fat storage-inducing transmembrane protein 2 (FITM2)	1.74	2.39	1.82
NM_001007144.1	perilipin 2 (PLIN2)	-	1.69	-
NM_022193.1	acetyl-CoA carboxylase alpha (ACACA)	-1.55	-2.65	-1.98
NM_016987.1	ATP citrate lyase (ACLY)	-2.01	-5.72	-
NM_017024.1	lecithin-cholesterol acyltransferase (LCAT)	-	-1.99	-1.93
NM_080886.1	sterol-C4-methyl oxidase-like (SC4MOL)	-	-2.01	-2.34
NM_024143.1	solute carrier family 27 (fatty acid transporter), member 5 (SLC27A5)	-1.94	-7.33	-15.08

Access. No.	gene name and symbol	EMD H1	EMD H3	EMD H14
peroxisomal lipid metabolism				
NM_012804.1	acyl-CoA binding domain containing 3 (ACBD3)	-	-	-1.54
NM_171996.2	2,4-dienoyl CoA reductase 2, peroxisomal (DECR2)	1.60	2.60	1.69
NM_022594.1	enoyl CoA hydratase 1, peroxisomal (ECH1)	2.11	2.28	2.35
NM_130756.2	acyl-CoA thioesterase 8 (ACOT8)	1.51	2.41	1.75
NM_053493.1	2-hydroxyacyl-CoA lyase 1 (HACL1)	-	2.44	2.12
NM_001006966.1	peroxisomal D3,D2-enoyl-CoA isomerase (PECI)	-	2.01	-
XM_576485.1	acetyl-CoA acyltransferase 1 (ACAA1)	15.10	26.03	24.11
NM_017340.1	acyl-CoA oxidase 1, palmitoyl (ACOX1)	3.32	4.65	5.17
mitochondrial lipid metabolism				
NM_001004085.2	carnitine O-acetyltransferase (CRAT)	2.53	2.64	2.28
NM_031987.1	carnitine O-octanoyltransferase (CROT)	-	1.72	-
NM_013200.1	carnitine palmitoyltransferase 1B (muscle) (CPT1B)	1.94	4.65	3.93
NM_130433.1	acetyl-CoA acyltransferase 2 (ACAA2)	1.83	1.90	1.54
NM_016986.1	acyl-CoA dehydrogenase, C-4 to C-12 straight chain (ACADM)	1.60	1.91	1.63
NM_017075.1	acetyl-CoA acetyltransferase 1 (ACAT1)	2.20	4.13	2.67
NM_133618.1	hydroxyacyl-CoA dehydrogenase/3-ketoacyl-CoA thiolase/enoyl-CoA hydratase (trifunctional protein), beta subunit (HADHB)	-	1.77	-
drug metabolism				
NM_012541.2	cytochrome P450, family 1, subfamily A, polypeptide 2 (CYP1A2)	-	-	-1.66
NM_019184.1	cytochrome P450, family 2, subfamily C, polypeptide 9 (CYP2C9)	-1.78	-13.31	-10.58
NM_138515.1	cytochrome P450, family 2, subfamily D, polypeptide 6 (CYP2D6)	-	-1.63	-
NM_031543.1	cytochrome P450, family 2, subfamily E, polypeptide 1 (CYP2E1)	-	3.02	-
NM_153312.2	cytochrome P450, family 3, subfamily A, polypeptide 4 (CYP3A4)	1.79	6.40	26.34
NM_019286.2	alcohol dehydrogenase 1C (class I), gamma polypeptide (ADH1C)	-	1.52	2.52

Access. No.	gene name and symbol	EMD H1	EMD H3	EMD H14
NM_022407.3	aldehyde dehydrogenase 1 family, member A1 (ALDH1A1)	1.97	2.48	-
NM_019363.2	aldehyde oxidase 1 (AOX1)	1.70	4.97	2.10
NM_012844.1	epoxide hydrolase 1, microsomal (xenobiotic) (EPHX1)	3.59	4.95	1.93
NM_022936.1	epoxide hydrolase 2, cytoplasmic (EPHX2)	-	2.71	2.35
XM_579318.1	glutathione S-transferase alpha 3 (GSTA3)	3.33	8.96	4.09
NM_001010921.1	glutathione S-transferase alpha 5 (GSTA5)	4.18	17.05	20.93
NM_181371.2	glutathione S-transferase kappa 1 (GSTK1)	-	2.48	2.11
NM_138974.1	glutathione S-transferase pi 1 (GSTP1)	3.46	17.81	8.22
NM_053293.2	glutathione S-transferase theta 1 (GSTT1)	-	1.70	1.80
NM_012683.1	UDP glucuronosyltransferase 1 family, polypeptide A1 (UGT1A1)	1.67	2.09	-
NM_057105.2	UDP glucuronosyltransferase 1 family, polypeptide A6 (UGT1A6)	2.35	4.47	2.52
NM_130407.1	UDP glucuronosyltransferase 1 family, polypeptide A7C (Ugt1a7c)	1.64	1.93	-
NM_173295.1	UDP glucuronosyltransferase 2 family, polypeptide B4 (UGT2B4)	1.65	1.50	1.62
NM_012623.2	ATP-binding cassette, sub-family B (MDR/TAP), member 1B (Abcb1b, MDR1)	-	-1.74	-3.32
NM_181381.2	ATP-binding cassette, sub-family G (WHITE), member 2 (ABCG2, BCRP)	-	1.67	-
NM_053754.2	ATP-binding cassette, sub-family G (WHITE), member 5 (ABCG5)	1.96	6.20	5.00
NM_080581.1	ATP-binding cassette, sub-family C (CFTR/MRP), member 3 (ABCC3, MRP3)	2.46	3.07	-
NM_031013.1	ATP-binding cassette, sub-family C (CFTR/MRP), member 6 (ABCC6, MRP6)	-	-	-2.10
NM_080786.1	solute carrier organic anion transporter family, member 2B1 (SLCO2B1, OATP-B)	-1.57	-1.74	-2.22
stress				
NM_030835.2	stress-associated endoplasmic reticulum protein 1 (SERP1)	1.57	1.90	-
NM_138504.2	oxidative stress induced growth inhibitor 1 (OSGIN1)	1.60	2.56	-
XM_214316.3	FK506 binding protein 8, 38kDa (FKBP8)	-	2.18	1.80
NM_017051.2	superoxide dismutase 2, mitochondrial (SOD2)	-	1.69	-
NM_017000.2	NAD(P)H dehydrogenase, quinone 1 (NQO1)	3.08	5.27	2.53
NM_012580.1	heme oxygenase (decycling) 1 (HMOX1)	3.03	11.60	-
NM_001008767.1	thioredoxin interacting protein (TXNIP)	2.16	-	-

Access. No.	gene name and symbol	EMD H1	EMD H3	EMD H14
NM_031614.1	thioredoxin reductase 1 (TXNRD1)	2.61	3.74	2.19
NM_012520.1	catalase (CAT)	1.64	2.70	1.89
XM_577041.1	ferritin, light polypeptide (FTL)	2.17	3.13	2.00
NM_053906.1	glutathione reductase (GSR)	1.98	3.55	1.87
NM_012815.2	glutamate-cysteine ligase, catalytic subunit (GCLC)	1.82	2.63	-
NM_019354.1	uncoupling protein 2 (mitochondrial, proton carrier) (UCP2)	1.84	3.14	-
energy production				
NM_012879.1	solute carrier family 2 (facilitated glucose transporter), member 2 (SLC2A2)	-	-3.63	-2.30
NM_012565.1	glucokinase (hexokinase 4) (GCK)	-1.64	-1.62	-
NM_012624.2	pyruvate kinase, liver and RBC (PKLR)	-3.58	-10.88	-4.10
NM_012595.1	lactate dehydrogenase B (LDHB)	-	-2.36	-2.99
NM_207592.1	glucose-6-phosphate isomerase (GPI)	-	-1.63	-1.77
NM_012495.1	aldolase A, fructose-bisphosphate (ALDOA)	1.63	1.86	-
XM_576370.1	triosephosphate isomerase 1 (TPI1)	-	2.00	-
NM_013098.1	glucose-6-phosphatase, catalytic subunit (G6PC)	-	-3.86	-
NM_031589.2	solute carrier family 37 (glucose-6-phosphate transporter), member 4 (SLC37A4)	-2.17	-3.20	-3.28
NM_013089.1	glycogen synthase 2 (liver) (GYS2)	-	-1.66	-1.54
NM_172091.1	glucagon receptor (GCGR)	-1.76	-1.67	-1.69
NM_001007620.1	pyruvate dehydrogenase (lipoamide) beta (PDHB)	-	-1.71	-
NM_031510.1	isocitrate dehydrogenase 1 (NADP+), soluble (IDH1)	1.54	1.91	-
NM_031151.2	malate dehydrogenase 2, NAD (mitochondrial) (MDH2)	-	-	-1.51
NM_053551.1	pyruvate dehydrogenase kinase, isozyme 4 (PDK4)	4.88	7.64	6.48
XM_341693.2	nudix (nucleoside diphosphate linked moiety X)-type motif 7 (NUDT7)	1.97	3.12	2.89
NM_012600.1	malic enzyme 1, NADP(+)-dependent, cytosolic (ME1)	1.78	2.74	2.21
NM_022215.2	glycerol-3-phosphate dehydrogenase 1 (soluble) (GPD1)	-	-	1.69
NM_019269.1	solute carrier family 22 (organic cation/carnitine transporter), member 5 (SLC22A5)	2.00	2.60	1.57
NM_013215.1	aldo-keto reductase family 7, member A3 (aflatoxin aldehyde reductase) (AKR7A3)	6.83	13.46	6.13

Access. No.	gene name and symbol	EMD H1	EMD H3	EMD H14
NM_017025.1	lactate dehydrogenase A (LDHA)	1.54	2.00	-
cell function				
XM_344194.2	interferon regulatory factor 6 (IRF6)	-	-1.58	-1.55
NM_053373.1	peptidoglycan recognition protein 1 (PGLYRP1)	-1.75	-2.02	-4.60
NM_207604.1	toll-like receptor 6 (TLR6)	-	-1.71	-1.80
NM_145672.3	chemokine (C-X-C motif) ligand 9 (CXCL9)	-	2.30	3.84
NM_139089.1	chemokine (C-X-C motif) ligand 10 (CXCL10)	-	-	1.61
XM_573130.1	chemokine (C-X-C motif) ligand 16 (CXCL16)	-1.80	-5.22	-3.42
NM_012747.2	signal transducer and activator of transcription 3 (acute-phase response factor) (STAT3)	-	-1.61	-1.93
NM_017020.1	interleukin 6 receptor (IL6R)	-2.05	-2.04	-1.91
NM_172222.2	complement component 2 (C2)	-	-	-1.76
XM_345342.2	complement component 5 (C5)	-	-	-1.69
NM_176074.2	complement component 6 (C6)	-1.61	-2.92	-2.84
NM_212466.2	complement factor B (CFB)	-	-1.69	-3.96
NM_130409.1	complement factor H (CFH)	-	-1.55	-1.78
NM_024157.1	complement factor I (CFI)	-	-	-1.74
XM_215303.3	major histocompatibility complex, class I, E (HLA-E)	-1.76	-1.54	-
NM_012488.1	alpha-2-macroglobulin (A2M)	-	-	-2.30
NM_017096.1	C-reactive protein, pentraxin-related (CRP)	1.66	1.90	1.91
NM_012898.2	alpha-2-HS-glycoprotein (AHSG)	-	-2.32	-2.17
NM_012725.1	kallikrein B, plasma (Fletcher factor) 1 (KLKB1)	-	-	1.57
NM_012681.1	transthyretin (TTR)	-	-	-1.74
NM_012504.1	ATPase, Na+/K+ transporting, alpha 1 polypeptide (ATP1A1)	-	-1.88	-1.77
NM_053487.1	peroxisomal biogenesis factor 11 alpha (PEX11A)	2.79	4.66	2.79
XM_213930.3	peroxisomal biogenesis factor 19 (PEX19)	-	1.76	-
XM_222831.3	coagulation factor V (proaccelerin, labile factor) (F5)	-	-2.22	-2.32
XM_224872.3	coagulation factor XI (F11)	-1.86	-2.09	-
XM_225172.3	coagulation factor XII (Hageman factor) (F12)	-	-1.50	-2.02

Access. No.	gene name and symbol	EMD H1	EMD H3	EMD H14
NM_012548.1	endothelin 1 (EDN1)	-	-1.77	-1.99
XM_243637.3	fibulin 1 (FBLN1)	-2.33	-2.68	-2.35
XM_216386.3	catenin (cadherin-associated protein), alpha-like 1 (CTNNAL1)	-	-1.51	-1.72
NM_019156.1	vitronectin (VTN)	-	-2.23	-13.92
NM_031334.1	cadherin 1, type 1, E-cadherin (epithelial) (CDH1)	-	-2.29	-2.78
NM_019143.1	fibronectin 1 (FN1)	-	-3.21	-4.65
NM_001004269.1	junctional adhesion molecule 3 (JAM3)	-	-1.75	-2.67
XM_213902.3	laminin, gamma 2 (LAMC2)	-	-	-3.99
NM_031140.1	vimentin (VIM)	-2.97	-5.34	-11.55
NM_022298.1	tubulin, alpha 1a (TUBA1A)	-1.63	-3.71	-16.30
XM_238167.3	filamin A, alpha (FLNA)	-	-2.74	-8.61
NM_012942.1	cytochrome P450, family 7, subfamily A, polypeptide 1 (CYP7A1)	-2.36	-5.40	-
NM_021745.1	nuclear receptor subfamily 1, group H, member 4 (NR1H4)	-	-1.56	-1.56
NM_022941.2	nuclear receptor subfamily 1, group I, member 3 (NR1I3)	-	2.74	-
growth, proliferation, cell death				
XM_576514.1	serum response factor (c-fos serum response element-binding transcription factor) (SRF)	-	-	-1.53
NM_022266.1	connective tissue growth factor (CTGF)	-6.82	-43.57	-17.94
NM_012671.1	transforming growth factor, alpha (TGFA)	-	-	-1.60
NM_031131.1	transforming growth factor, beta 2 (TGFB2)	-	-	-4.63
NM_012551.1	early growth response 1 (EGR1)	-	-	-3.53
NM_212505.1	immediate early response 3 (IER3)	1.77	3.60	-
NM_001007732.1	serpin peptidase inhibitor, clade B (ovalbumin), member 9 (SERPINB9)	-1.68	-3.72	-5.68
NM_130741.1	lipocalin 2 (LCN2)	-	-	-14.33
NM_024148.1	APEX nuclease (multifunctional DNA repair enzyme) 1 (APEX1)	1.56	-	-
NM_024127.1	growth arrest and DNA-damage-inducible, alpha (GADD45A)	-	1.91	-
NM_012861.1	O-6-methylguanine-DNA methyltransferase (MGMT)	-	-	-1.65

Access. No.	gene name and symbol	EMD H1	EMD H3	EMD H14
XM_214477.2	geminin, DNA replication inhibitor (GMNN)	1.62	1.69	-
NM_031762.2	cyclin-dependent kinase inhibitor 1B (p27, Kip1) (CDKN1B)	-	-	-1.53
NM_171992.2	cyclin D1 (CCND1)	-	-	-3.26
XM_575700.1	BCL2-like 14 (apoptosis facilitator) (BCL2L14)	-	1.51	-
NM_053812.1	BCL2-antagonist/killer 1 (BAK1)	-	-1.52	-2.50
NM_053420.2	BCL2/adenovirus E1B 19kDa interacting protein 3 (BNIP3)	1.55	2.48	-
NM_017312.2	BCL2-related ovarian killer (BOK)	-	-	-3.31
XM_214551.3	cell death-inducing DFFA-like effector a (CIDEA)	-	2.29	-
NM_012935.2	crystallin, alpha B (CRYAB)	-	-4.20	-6.94
NM_022526.1	death-associated protein (DAP)	-	1.87	1.89
NM_139194.1	Fas (TNF receptor superfamily, member 6) (FAS)	-	-	-2.02
NM_181086.2	tumor necrosis factor receptor superfamily, member 12A (TNFRSF12A)	-	-1.67	-1.75
NM_021835.2	jun proto-oncogene (JUN)	-	-1.63	-1.81
NM_133571.1	cell division cycle 25 homolog A (S. pombe) (CDC25A)	1.53	1.75	-

Table 7.8: Genes deregulated by Metformin.
The table contains the gene assession numbers, the gene names and symbols, as well as the fold changes of genes deregulated with $p < 0.05$. Grayed out numbers: BH $Q \leq 0.2$, Met: Metformin, H1/3: high dose at treatment day 1/3.

Access. No.	gene name and symbol	Met H1	Met H3
lipid metabolism			
NM_080576.1	apolipoprotein A-V (APOA5)	-3.66	-12.60
XM_214872.2	apolipoprotein C-II (APOC2)	-3.35	-3.40
NM_013155.1	very low density lipoprotein receptor (VLDLR)	2.12	8.44
XM_243524.3	low density lipoprotein receptor-related protein 1 (LRP1)	-1.94	-2.13
NM_175762.2	low density lipoprotein receptor (LDLR)	-	-1.82
NM_012597.2	lipase, hepatic (LIPC)	-1.80	-2.87

Access. No.	gene name and symbol	Met H1	Met H3
NM_138502.1	monoglyceride lipase (MGLL)	-2.74	-2.56
NM_012556.1	fatty acid binding protein 1, liver (FABP1)	-5.28	-26.22
XM_575339.1	CD36 molecule (thrombospondin receptor) (CD36)	-	-2.30
NM_053477.1	malonyl-CoA decarboxylase (MLYCD)	-1.94	-2.98
NM_175837.1	cytochrome P450, family 4, subfamily A, polypeptide 11 (CYP4A11)	-3.64	-5.97
XM_575886.1	cytochrome P450, family 4, subfamily a, polypeptide 14 (Cyp4a14)	-4.15	-9.21
NM_031315.1	acyl-CoA thioesterase 1 (Acot1)	-1.82	-2.07
NM_012820.1	acyl-CoA synthetase long-chain family member 1 (ACSL1)	-4.26	-3.00
NM_057107.1	acyl-CoA synthetase long-chain family member 3 (ACSL3)	-	-1.67
XM_230773.3	acyl-CoA synthetase short-chain family member 2 (ACSS2)	-2.87	-6.28
XM_230827.3	fat storage-inducing transmembrane protein 2 (FITM2)	-2.53	-2.13
NM_016987.1	ATP citrate lyase (ACLY)	-2.21	-2.87
NM_013134.2	3-hydroxy-3-methylglutaryl-CoA reductase (HMGCR)	-	1.78
NM_017024.1	lecithin-cholesterol acyltransferase (LCAT)	-3.89	-12.16
NM_022193.1	acetyl-CoA carboxylase alpha (ACACA)	-2.17	-
NM_080886.1	sterol-C4-methyl oxidase-like (SC4MOL)	-	-3.08
NM_024143.1	solute carrier family 27 (fatty acid transporter), member 5 (SLC27A5)	-6.70	-48.94
peroxisomal lipid metabolism			
NM_012804.1	ATP-binding cassette, sub-family D (ALD), member 3 (ABCD3)	-2.57	-2.21
XM_576485.1	acetyl-CoA acyltransferase 1 (ACAA1)	-4.14	-7.45
NM_017340.1	acyl-CoA oxidase 1, palmitoyl (ACOX1)	-2.18	-1.62
NM_001006966.1	enoyl-CoA delta isomerase 2 (PECI)	-3.65	-4.15
NM_057197.1	2,4-dienoyl CoA reductase 1, mitochondrial (DECR1)	-4.19	-6.41
NM_171996.2	2,4-dienoyl CoA reductase 2, peroxisomal (DECR2)	-3.47	-3.18
NM_022389.2	7-dehydrocholesterol reductase (DHCR7)	-3.40	-8.46
XM_216452.3	24-dehydrocholesterol reductase (DHCR24)	-9.10	-10.12
NM_022594.1	enoyl CoA hydratase 1, peroxisomal (ECH1)	-5.50	-5.30

Access. No.	gene name and symbol	Met H1	Met H3
NM_053493.1	2-hydroxyacyl-CoA lyase 1 (HACL1)	-7.11	-5.07
mitochondrial lipid metabolism			
NM_031559.1	carnitine palmitoyltransferase 1A (liver) (CPT1A)	-7.14	-12.61
NM_001004085.2	carnitine O-acetyltransferase (CRAT)	-1.52	-2.06
NM_031987.1	carnitine O-octanoyltransferase (CROT)	-2.32	-1.81
NM_057186.1	hydroxyacyl-CoA dehydrogenase (HADH)	-5.37	-5.02
NM_130433.1	acetyl-CoA acyltransferase 2 (ACAA2)	-3.59	-5.17
NM_012819.1	acyl-CoA dehydrogenase, long chain (ACADL)	-	-1.91
NM_016986.1	acyl-CoA dehydrogenase, C-4 to C-12 straight chain (ACADM)	-3.00	-4.33
NM_022512.1	acyl-CoA dehydrogenase, C-2 to C-3 short chain (ACADS)	-2.53	-2.69
NM_012891.1	acyl-CoA dehydrogenase, very long chain (ACADVL)	-2.09	-2.38
NM_017075.1	acetyl-CoA acetyltransferase 1 (ACAT1)	-2.54	-3.47
drug metabolism			
NM_022407.3	aldehyde dehydrogenase 1 family, member A1 (ALDH1A1)	-3.70	-2.72
NM_012540.2	cytochrome P450, family 1, subfamily A, polypeptide 1 (CYP1A1)	-3.87	-2.46
NM_138515.1	cytochrome P450, family 2, subfamily D, polypeptide 6 (CYP2D6)	-2.35	-3.33
NM_031543.1	cytochrome P450, family 2, subfamily E, polypeptide 1 (CYP2E1)	-	-2.64
NM_153312.2	cytochrome P450, family 3, subfamily A, polypeptide 4 (CYP3A4)	-	-2.53
NM_022936.1	epoxide hydrolase 2, cytoplasmic (EPHX2)	-3.37	-1.99
NM_177426.1	glutathione S-transferase mu 1 (GSTM1)	-2.41	-14.57
NM_053293.2	glutathione S-transferase theta 1 (GSTT1)	-1.63	-1.51
NM_031834.1	sulfotransferase family, cytosolic, 1A, phenol-preferring, member 1 (SULT1A1)	-5.22	-24.47
XM_214935.3	sulfotransferase family, cytosolic, 2B, member 1 (SULT2B1)	-1.61	-1.68
NM_012683.1	UDP glucuronosyltransferase 1 family, polypeptide A1 (UGT1A1)	-1.62	-1.69
NM_130407.1	UDP glucuronosyltransferase 1 family, polypeptide A7C (Ugt1a7c)	1.51	-1.61
NM_173295.1	UDP glucuronosyltransferase 2 family, polypeptide B4 (UGT2B4)	-2.60	-7.11

Access. No.	gene name and symbol	Met H1	Met H3
NM_057105.2	UDP glucuronosyltransferase 1 family, polypeptide A6 (UGT1A6)	-	3.38
NM_012623.2	ATP-binding cassette, sub-family B (MDR/TAP), member 1B (Abcb1b, MDR1)	2.06	3.04
NM_012690.1	ATP-binding cassette, sub-family B (MDR/TAP), member 4 (ABCB4, MDR3)	-2.13	-4.03
NM_031013.1	ATP-binding cassette, sub-family C (CFTR/MRP), member 6 (ABCC6, MDR6)	-2.13	-4.00
NM_053537.1	solute carrier family 22 (organic anion transporter), member 7 (SLC22A7, OAT2)	-3.10	-2.78
NM_017047.1	solute carrier family 10 (sodium/bile acid cotransporter family), member 1 (SLC10A1, NTCP)	-14.09	-31.43
NM_031650.1	solute carrier organic anion transporter family, member 1B3 (SLCO1B3, OATP8)	-3.96	-4.64
NM_080786.1	solute carrier organic anion transporter family, member 2B1 (SLCO2B1, OATP-B)	-5.82	-8.65
NM_012697.1	solute carrier family 22 (organic cation transporter), member 1 (SLC22A1, OCT1)	-2.17	-3.08
stress			
NM_012912.1	activating transcription factor 3 (ATF3)	10.04	4.43
NM_138504.2	oxidative stress induced growth inhibitor 1 (OSGIN1)	-	-1.63
NM_031970.1	heat shock 27kDa protein 1 (HSPB1)	2.81	4.24
NM_175761.2	heat shock protein 90kDa alpha (cytosolic), class A member 1 (HSP90AA1)	1.58	1.59
NM_012580.1	heme oxygenase (decycling) 1 (HMOX1)	2.97	3.18
NM_017000.2	NAD(P)H dehydrogenase, quinone 1 (NQO1)	-	3.36
NM_053800.2	thioredoxin (TXN)	-	1.57
XM_577041.1	ferritin, light polypeptide (FTL)	1.66	3.35
NM_017051.2	superoxide dismutase 2, mitochondrial (SOD2)	-1.88	-1.61
NM_012520.1	catalase (CAT)	-2.09	-2.27
NM_012815.2	glutamate-cysteine ligase, catalytic subunit (GCLC)	-	1.65
NM_033349.1	hydroxyacylglutathione hydrolase (HAGH)	-	1.64
energy production			
NM_031741.1	solute carrier family 2 (facilitated glucose/fructose transporter), member 5 (SLC2A5)	-6.99	-6.49
NM_013190.2	phosphofructokinase, liver (PFKL)	-	-1.71
NM_053291.2	phosphoglycerate kinase 1 (PGK1)	-	1.63
NM_012624.2	pyruvate kinase, liver and RBC (PKLR)	-5.05	-6.64

Access. No.	gene name and symbol	Met H1	Met H3
NM_012565.1	glucokinase (GCK)	-1.68	-
NM_207592.1	glucose-6-phosphate isomerase (GPI)	-2.31	-1.81
XM_233688.3	hexose-6-phosphate dehydrogenase (glucose 1-dehydrogenase) (H6PD)	-3.15	-3.41
NM_031589.2	solute carrier family 37 (glucose-6-phosphate transporter), member 4 (SLC37A4)	-6.78	-8.26
NM_013098.1	glucose-6-phosphatase, catalytic subunit (G6PC)	-34.93	-31.68
NM_012744.2	pyruvate carboxylase (PC)	-6.95	-8.44
NM_198780.2	phosphoenolpyruvate carboxykinase 1 (soluble) (PCK1)	-1.67	-4.10
XM_341319.2	phosphoenolpyruvate carboxykinase 2 (mitochondrial) (PCK2)	-	2.44
NM_012621.3	6-phosphofructo-2-kinase/fructose-2,6-biphosphatase 1 (PFKFB1)	-5.68	-2.89
XM_214047.3	phosphoglucomutase 2 (PGM2)	1.69	2.23
NM_199118.1	glucosidase, alpha; acid (GAA)	-	2.48
NM_013089.1	glycogen synthase 2 (liver) (GYS2)	-3.01	-1.89
NM_053551.1	pyruvate dehydrogenase kinase, isozyme 4 (PDK4)	-1.69	-2.31
XM_225729.3	malic enzyme 2, NAD(+)-dependent, mitochondrial (ME2)	1.66	2.48
NM_022215.2	glycerol-3-phosphate dehydrogenase 1 (soluble) (GPD1)	-3.02	-5.70
NM_019269.1	solute carrier family 22 (organic cation/carnitine transporter), member 5 (SLC22A5)	-1.62	-1.57
NM_033235.1	malate dehydrogenase 1, NAD (soluble) (MDH1)	-1.94	-1.51
XM_237203.3	malate dehydrogenase 1B, NAD (soluble) (MDH1B)	1.71	1.53
NM_017025.1	lactate dehydrogenase A (LDHA)	-1.75	-
NM_012595.1	lactate dehydrogenase B (LDHB)	1.57	2.93
XM_341693.2	nudix (nucleoside diphosphate linked moiety X)-type motif 7 (NUDT7)	-3.06	-2.21
cell function			
NM_207604.1	toll-like receptor 6 (TLR6)	1.66	2.08
NM_017020.1	interleukin 6 receptor (IL6R)	-	-2.40
NM_145672.3	chemokine (C-X-C motif) ligand 9 (CXCL9)	-2.03	-2.72
NM_182952.2	chemokine (C-X-C motif) ligand 11 (CXCL11)	-5.61	-2.76
XM_573130.1	chemokine (C-X-C motif) ligand 16 (CXCL16)	-	-2.33
XM_230854.3	CD40 molecule, TNF receptor superfamily member 5 (CD40)	-	1.78

Access. No.	gene name and symbol	Met H1	Met H3
XM_345342.2	complement component 5 (C5)	-1.59	-2.05
NM_176074.2	complement component 6 (C6)	-1.81	-3.89
NM_130409.1	complement factor H (CFH)	-2.42	-2.74
NM_024157.1	complement factor I (CFI)	-1.95	-
NM_212466.2	complement factor B (CFB)	-2.07	-4.38
NM_017096.1	C-reactive protein, pentraxin-related (CRP)	-3.57	-6.57
XM_215303.3	major histocompatibility complex, class I, E (HLA-E)	-3.46	-10.25
NM_020071.1	fibrinogen beta chain (FGB)	-5.00	-4.18
NM_012582.1	haptoglobin (HP)	-	-1.52
NM_012725.1	kallikrein B, plasma (Fletcher factor) 1 (KLKB1)	-2.33	-1.82
NM_012681.1	transthyretin (TTR)	-2.45	-2.56
NM_172320.1	afamin (AFM)	-2.05	-2.87
NM_053487.1	peroxisomal biogenesis factor 11 alpha (PEX11A)	-1.92	-2.30
XM_213930.3	peroxisomal biogenesis factor 19 (PEX19)	-2.36	-2.00
NM_012942.1	cytochrome P450, family 7, subfamily A, polypeptide 1 (CYP7A1)	-7.24	-14.26
NM_017300.1	bile acid CoA: amino acid N-acyltransferase (glycine N-choloyltransferase) (BAAT)	-14.16	-10.37
NM_012548.1	endothelin 1 (EDN1)	1.68	-1.95
NM_019156.1	vitronectin (VTN)	-1.90	-4.17
XM_213902.3	laminin, gamma 2 (LAMC2)	-	-1.68
NM_031334.1	cadherin 1, type 1, E-cadherin (epithelial) (CDH1)	-	-4.59
NM_024351.1	heat shock 70kDa protein 8 (HSPA8)	-	1.91
NM_022298.1	tubulin, alpha 1a (TUBA1A)	4.36	2.22
NM_001004269.1	junctional adhesion molecule 3 (JAM3)	2.57	2.85
NM_031140.1	vimentin (VIM)	-	-8.79
NM_017143.2	coagulation factor X (F10)	-2.33	-2.13
XM_224872.3	coagulation factor XI (F11)	-1.55	-2.20
XM_225172.3	coagulation factor XII (Hageman factor) (F12)	-1.95	-4.93
NM_021745.1	nuclear receptor subfamily 1, group H, member 4 (NR1H4)	-2.56	-1.57
NM_052980.1	nuclear receptor subfamily 1, group I, member 2 (NR1I2)	-2.35	-2.21

Access. No.	gene name and symbol	Met H1	Met H3
NM_022941.2	nuclear receptor subfamily 1, group I, member 3 (NR1I3)	-2.85	-3.80
NM_013124.1	peroxisome proliferator-activated receptor gamma (PPARG)	2.30	2.23
XM_341151.2	retinoid X receptor, gamma (RXRG)	-4.44	-2.31
growth, proliferation, cell death			
XM_576514.1	serum response factor (c-fos serum response element-binding transcription factor) (SRF)	2.81	1.52
NM_013132.1	annexin A5 (ANXA5)	5.12	4.52
NM_022381.2	proliferating cell nuclear antigen (PCNA)	3.02	2.42
XM_214079.3	polymerase (DNA directed), delta 2, regulatory subunit 50kDa (POLD2)	2.37	2.68
XM_341981.2	polymerase (DNA-directed), delta 4 (POLD4)	-1.51	-
XM_236934.3	polymerase (DNA directed), eta (POLH)	-	1.82
NM_022266.1	connective tissue growth factor (CTGF)	2.18	-16.82
NM_130741.1	lipocalin 2 (LCN2)	-	8.26
NM_031131.1	transforming growth factor, beta 2 (TGFB2)	2.24	2.36
NM_024148.1	APEX nuclease (multifunctional DNA repair enzyme) 1 (APEX1)	2.47	2.83
NM_012861.1	O-6-methylguanine-DNA methyltransferase (MGMT)	1.93	4.31
NM_024134.1	DNA-damage-inducible transcript 3 (DDIT3)	10.30	12.22
NM_024127.1	growth arrest and DNA-damage-inducible, alpha (GADD45A)	4.80	4.12
XM_214477.2	geminin, DNA replication inhibitor (GMNN)	1.98	1.84
NM_012524.1	CCAAT/enhancer binding protein (C/EBP), alpha (CEBPA)	-2.58	-3.55
NM_080782.2	cyclin-dependent kinase inhibitor 1A (p21, Cip1) (CDKN1A)	-	1.52
XM_342812.2	cyclin C (CCNC)	2.82	2.99
NM_171992.2	cyclin D1 (CCND1)	-	-1.60
NM_012923.1	cyclin G1 (CCNG1)	4.72	4.78
XM_342632.2	cyclin-dependent kinase 14 (CDK14)	8.49	5.86
NM_053812.1	BCL2-antagonist/killer 1 (BAK1)	2.02	2.08
NM_181086.2	tumor necrosis factor receptor superfamily, member 12A (TNFRSF12A)	3.07	-1.71
NM_012935.2	crystallin, alpha B (CRYAB)	-	-2.40

Access. No.	gene name and symbol	Met H1	Met H3
XM_214551.3	cell death-inducing DFFA-like effector a (CIDEA)	-2.01	-1.88
XM_575641.1	cell death-inducing DFFA-like effector c (CIDEC)	-4.21	-3.45
NM_017059.1	BCL2-associated X protein (BAX)	2.62	2.91
NM_021850.2	BCL2-like 2 (BCL2L2)	2.54	1.68
NM_022684.1	BH3 interacting domain death agonist (BID)	-	1.51
NM_053420.2	BCL2/adenovirus E1B 19kDa interacting protein 3 (BNIP3)	1.83	2.73
NM_022522.2	caspase 2, apoptosis-related cysteine peptidase (CASP2)	2.91	1.84
NM_053736.1	caspase 4, apoptosis-related cysteine peptidase (CASP4)	2.80	7.38
NM_031775.2	caspase 6, apoptosis-related cysteine peptidase (CASP6)	1.82	1.65
NM_022260.2	caspase 7, apoptosis-related cysteine peptidase (CASP7)	4.25	4.39
NM_022277.1	caspase 8, apoptosis-related cysteine peptidase (CASP8)	-	1.71
XM_235169.3	Mdm2 p53 binding protein homolog (mouse) (MDM2)	4.36	3.33
XM_231692.3	v-raf murine sarcoma viral oncogene homolog B1 (BRAF)	2.25	1.90
NM_021835.2	jun proto-oncogene (JUN)	-	-2.65
NM_053720.1	apoptosis antagonizing transcription factor (AATF)	3.26	2.44
NM_001007732.1	serpin peptidase inhibitor, clade B (ovalbumin), member 9 (SERPINB9)	-	-3.07
NM_131914.2	caveolin 2 (CAV2)	-	-1.60
NM_012551.1	early growth response 1 (EGR1)	-	-2.43
XM_235169.3	Mdm2 p53 binding protein homolog (mouse) (MDM2)	4.36	3.33

Curriculum Vitae

AKADEMISCHE AUSBILDUNG

10/2003 – 10/2007 **Studium der Biologischen Chemie an der Hochschule Mannheim**

Diplomarbeit: Aufklärung molekularer Mechanismen in der Hepatotoxizität (Merck Serono R&D Darmstadt, Abteilung: Molecular and Cellular Toxicology)
Abschluss: Diplom Ingenieur (FH)

9/2005 – 2/2006 **Praxissemester am Institut für Transfusionsmedizin und Immunologie der Ruprecht-Karls-Universität Heidelberg**

Thema: Quantifizierung der Differenzierung mesenchymaler Stammzellen

PROMOTION

11/2007 - 09/2011 **Technische Universität Darmstadt und Merck Serono R&D Darmstadt, Abteilung: Molecular and Cellular Toxicology**

Thema: Gene expression profiling in primary rat hepatocytes for the prediction of hepatotoxicity

PUBLIKATIONEN

- B. Lauer, G. L. Truisi, P. G. Hewitt, Frühe Biomarker-basierte Risikobewertung der Leber- und Nierentoxizität, Laborwelt (2010) 4:10-12
- B. Lauer et al., Species-specific toxicity of diclofenac and troglitazone in primary human and rat hepatocytes, Chem. Biol. Interact. (2009) 179:17-24
- G. Tuschl et al., Primary hepatocytes as a model to analyze species-specific toxicity and drug metabolism, Expert Opin. Drug Metab. Toxicol. (2008) 4(7):855-870